Technical Report
TR-23-28
Februari 2024

The late Quaternary of Fennoscandia revisited

15 years of collaborative research at Sokli in northern Finland – a complete overview

Karin F Helmens
Stefan Engels
J Sakari Salonen
Minna Väliranta

SVENSK KÄRNBRÄNSLEHANTERING AB

SWEDISH NUCLEAR FUEL
AND WASTE MANAGEMENT CO

Box 3091, SE-169 03 Solna
Phone +46 8 459 84 00
skb.se

SVENSK KÄRNBRÄNSLEHANTERING

ISSN 1404-0344
SKB TR-23-28
ID 2027447

Februari 2024

The late Quaternary of Fennoscandia revisited

15 years of collaborative research at Sokli in northern Finland – a complete overview

Karin F Helmens[1], Stefan Engels[2],
J Sakari Salonen[3], Minna Väliranta[4]

1 Past Q
2 Department of Geography, Birkbeck University of London
3 Department of Geosciences and Geography, University of Helsinki
4 Ecosystems and Environment Research Programme, ECRU,
Faculty of Biological and Environmental Sciences, University of Helsinki

Keywords: Fennoscandia, Late Quaternary, Sokli geological proxy record, Lake/wetland histories, Vegetation developments, Quantitative climate reconstructions, Glaciation.

This report concerns a study which was conducted for Svensk Kärnbränslehantering AB (SKB). The conclusions and viewpoints presented in the report are those of the authors. SKB may draw modified conclusions, based on additional literature sources and/or expert opinions.

This report is published on www.skb.se

© 2024 Svensk Kärnbränslehantering AB

Summary

Few sediment/fossil records in northern Europe have escaped the widespread erosion by the Fennoscandian Ice Sheet during the Quaternary. Mostly due to non-typical bedrock conditions, a unique sediment record in the Sokli basin in northern Finland has survived multiple glaciations during the late Quaternary (last 130 kyr (thousand years)). The thick fossil-bearing lacustrine and fluvial deposits, which are found interlayered with glacial till beds, occur in a sheltered position in a steep depression formed in deeply weathered rocks of a magma intrusion (the Sokli Carbonatite Massif) in the Fennoscandian Precambrian Shield.

This report brings together 15 years of collaborative research in the Sokli and adjacent Loitsana basins. The latter forms part of a subglacially formed meltwater corridor with eskers and holds a thick lake deposit of Holocene age (present interglacial; last c. 11 kyr). The research was performed in the period 2006–2021 and was mainly funded by the Swedish Nuclear Fuel and Waste Management Company (SKB), with substantial additional funding from POSIVA (Finland), the Academy of Finland and the Bolin Center of Climate Change Studies at Stockholm University (Sweden).

Sediments have been recovered in a series of percussion drilling operations (Sokli basin) and by manual coring using a Russian peat corer (Loitsana basin) and are dated by means of a combination of radiocarbon and luminescence dating techniques. The lacustrine and fluvial deposits, and thick sediment layers of glacio-lacustrine origin, are studied using multiple environmental and climate proxies following the newest developments in these fields. These include analyses of a large variety of fossil remains: pollen/spores, non-pollen palynomorphs (NPP's), conifer stomata, macrofossils, diatoms, chironomids; diverse biogeochemical data: loss-on-ignition (LOI), carbon/nitrogen rations (C/N), elementary data inferred from X-ray fluorescence (XRF) core scanning, biogenic silica (BSi) measured by Fourier-transform infrared spectroscopy (FTIRS), stable isotopes from lipid biomarkers; and core lithology. Based on this multi-proxy data, detailed reconstructions have been made of 1) depositional environments and associated changes in aquatic and telmatic (shallow water (littoral)/ wetland/moist shore) ecosystems; 2) developments in regional vegetation; and 3) climate evolution. The detailed reconstruction of local (azonal) changes within the Sokli and Loitsana basins (1) facilitates the discrimination between local drivers (acting at the catchment scale) from regional climate, thereby increasing the accuracy of the regional vegetation and climate reconstructions. Furthermore, the combination of classic pollen analysis (which may suffer from long-distance transport) with conifer stomata and plant macrofossils (which originate from the lake/river surroundings), and by comparing the response of terrestrial and aquatic taxa (the latter of which do not depend on soil formation), have provided a solid basis for the interpretations of the regional vegetation and climate. Climate parameters are quantified based on pollen and chironomid assemblages, and from macrofossils/pollen of climate indicator plant species, using both classical multivariate regression methods and a new family of nonparametric machine-learning approaches adopted in paleoclimatology over the last decade.

Results from the Sokli and Loitsana studies have been published in 33 peer-reviewed scientific papers in international journals, four PhD theses, and three peer-reviewed SKB technical reports. The present report brings these data together in a concise and consistent way and brings in some new data. The multi-proxy data were earlier spread over many diagrams but are here combined coherently. Climate reconstructions based on pollen and indicator plant species have been re-run using the most recent protocols. Additionally, new detailed vegetation and climate records for the entire late Quaternary at Sokli and Loitsana are presented. The vegetation record is placed on an approximate timescale that makes use of, among others, a recently published speleothem record from a cave in northern Sweden (Korallgrottan). This report presents the first detailed comparison of the vegetation developments and climate evolution during the various ice-free time-periods at Sokli. Furthermore, sediment logs of all boreholes in the Sokli and Loitsana basins are presented and all dating results are discussed and evaluated. The latter applies as well to the quantitatively inferred climate estimates.

The multi-proxy analyses on the Sokli and Loitsana sediments provide an unprecedented wealth of environmental data for the late Quaternary of Fennoscandia. Most importantly, it has resulted in an environmental/climate record that significantly revises earlier concepts of glaciation, vegetation, and climate in Fennoscandia over the last 130 kyr. The Sokli sequence reveals a highly dynamic Fennoscandian Ice Sheet with significantly less ice-cover over Fennoscandia in both time and space. New data for the Tulppio Interstadial shows that, even under full glacial conditions (Marine Isotope Stage (MIS) 4-2 between c. 70–15 kyr BP, or the Pleniglacial in the NW European mainland stratigraphy), the Sokli basin was deglaciated twice in the middle part of MIS 3 around c. 40 kyr BP (Greenland Interstadials (GIS) 11/12 and 8). A glacier re-advance close to the basin, which is recorded during the oldest of the two ice-free periods in MIS 3 (Tulppio 1 Interstadial), and the glaciation (here defined as the Saariselkä glaciation) that separates the Tulppio 1 and 2 Interstadials, probably had their origin in the Saariselkä low-mountain range at c. 100 km north of Sokli. Ice build-up that led to the MIS 6 (before 130 kyr BP), MIS 5b (centered at c. 85 kyr BP), MIS 4-early 3 (c. 70–50 kyr BP) and MIS late 3-2 glaciations (c. 35–15 kyr BP), in contrast, are thought to have started mostly in the Scandinavian mountains. Ice-free conditions during parts of MIS 3, in the period between c. 50–35 kyr BP, are now reported from various key sites in Fennoscandia as well as in the central areas of Laurentide and Cordilleran glaciation in North America. Furthermore, in contrast to classical views of a harsh and unproductive ice-marginal environment, Sokli and Loitsana reconstruct warm insolation-forced summers and rich biota both in the Sokli Ice Lake and on the surrounding newly deglaciated terrain during the various deglaciation stages, in-line with studies in Canada. The Sokli basin was not glaciated during the cold MIS 5d stage (centered at c. 110 kyr BP). Instead, steppe-tundra vegetation, a braided river pattern and relatively high summer temperatures indicate a strong continental climate regime with the possibility of deep continuous permafrost.

Results from Sokli also show that warm interglacial conditions prevailed during all three warm stages of MIS 5. MIS 5 is defined as the Last Interglacial Complex at Sokli, in agreement with data covering large parts of the European mainland. The Nuortti warm stage in the Sokli basin corresponds to MIS 5e (centered at c. 125 kyr BP) or the Eemian Interglacial in the NW European mainland stratigraphy; the Sokli I warm stage corresponds to MIS 5c (c. 95 kyr BP; Brørup Interstadial); and the Sokli II warm stage to MIS 5a (c. 80 kyr BP; Odderade Interstadial). The interglacial developments in vegetation during MIS 5e, 5c and 5a were remarkably like that of the present interglacial (Holocene), although important and interesting differences are recorded. During all warm periods (MIS 5e, 5c, 5a and the Holocene) there were periods when mean July temperatures reached at least several degrees higher than the Late Holocene interglacial conditions. The Nuortti warm stage (MIS 5e) stands out by the local occurrence of temperate hazel (*Corylus*), winter temperatures probably higher than today, and substantial millennial-scale climate variability superimposed on the long-term orbital-forced climate evolution. Severe cooling and drying during the early MIS 5e Tunturi event between c. 127–126 kyr BP show the potential of major climate instability in a warm climate. A similar early MIS 5e cooling perturbation is recently depicted at high sediment accumulation rate sites in the northern North Atlantic Ocean, in the famous high-resolution speleothem record from Corchia, Italy, and the newly published speleothem record from Korallgrottan in northern Sweden. In the marine record, the cooling occurs associated with reductions in North Atlantic Deepwater formation. Finally, the environmental/climate conditions at Sokli reconstructed for MIS 5c and 5a preclude the persistence of any significant ice mass in Fennoscandia during these periods, in agreement with e.g. relative sea-level estimates from tectonically stable locations around the world. In summary, the Sokli archive does not only show a highly dynamic Fennoscandian Ice Sheet during the late Quaternary (Early and Mid-Weichselian), but it also reveals a much higher climate variability than previously reconstructed. Earlier environmental/climatic reconstructions for the late Quaternary were mostly based on long-distance correlation of highly fragmented and often poorly dated litho- and bio(pollen)-stratigraphic data, and comparison with the global ice volume record inferred from the marine oxygen-isotope stratigraphy. According to these reconstructions, Sokli was glaciated for nearly 100 kyr, from the start of MIS 5d to the start of the Holocene. MIS 5c and possibly MIS 5a were the only periods considered, within this time interval (Last Glacial), with ice-free conditions and arctic tundra vegetation.

As a final note, the Holocene vegetation and climate record from Loitsana Lake, which has the same detail as the older records from the Sokli basin, is very similar to that obtained for other sites in northern Fennsocandia, including newly studied Kuutsjärvi at c. 10 km east of Sokli in the crystalline low mountains of the Värriö Tunturit. This shows a negligible influence, if any, of the non-typical bedrock geochemistry at Sokli on the paleo-records of regional vegetation and climate.

Sammanfattning

Få sediment och fossila fynd i norra Europa har undgått den utbredda erosionen av den fennoskandiska inlandsisen under kvartär. På grund av icke-typiska berggrundsförhållanden har en unik sedimentsekvens i Sokli-bäckenet i norra Finland överlevt flera glaciationer under sena kvartär (senaste 130 000 åren). De tjocka fossilbärande lakustrina och fluviala avlagringarna som finns mellanlagrade i glaciala moränbäddar förekommer i en brant sänka bildad i djupt vittrade bergarter tillhörande en magmaintrusion (”the Sokli Carbonatite Massif”) i den fennoskandiska urbergsskölden.

Denna rapport sammanställer 15 års forskningssamarbete i Sokli- och angränsande Loitsana-bäckenet. Den senare utgör del av en subglacialt bildad smältvattenkorridor med åsar och tillhandahåller en tjock sjöavlagring av holocen ålder (nuvarande interglacial; senaste 11 000 åren). Forskningen utfördes under perioden 2006–2021 och finansierades huvudsakligen av SKB, med betydande bidrag från POSIVA (Finland), Finlands Akademi och Bolin Center of Climate Change Studies vid Stockholms universitet (Sverige).

Sediment har erhållits i en serie slagborrningsoperationer (Sokli-bäckenet) och genom manuell kärnborrning (Loitsana-bäckenet). Sedimenten har daterats med hjälp av en kombination av kol-14- och luminescensdateringstekniker. Lakustrina och fluviala avlagringar, samt tjocka sedimentlager av glacio-lakustrint ursprung, används för att rekonstruera miljö- och klimatförhållanden under sena kvartär enligt den senaste metodiken inom området. Dessa inkluderar analyser av ett stort antal fossila avlagringar: pollen/sporer, icke-pollen palynomorfer (NPP), barrstomata, makrofossiler, kiselalger, chironomider; olika biogeokemiska data: ”loss-on-ignition” (LOI), kol/kväve-relationer (C/N), data härledda från röntgenfluorescens (XRF) skanning, biogen kiseldioxid (BSi) mätt med infraröd spektroskopi (FTIRS), isotoper från lipidbiomarkörer; samt kärnlitologi. Baserat på dessa multi-proxydata har detaljerade rekonstruktioner gjorts av 1) avlagringssmiljöer och tillhörnade förändringar i akvatiska och telmatiska (grunt vatten/våtmark/fuktig strand) ekosystem; 2) utveckling av lokal vegetation; och 3) klimatutveckling. Den detaljerade rekonstruktionen av lokala (azonala) förändringar vid Sokli och Loitsana (1) gör att man lättare kan separera lokala faktorer från det regionala klimatet, vilket ökar noggrannheten i rekonstruktionerna av den regionala vegetationen och klimatet. Kombinationen av klassisk pollenanalys (som kan ha genomgått transport över långa avstånd) med stomata från barrträd och växtmakrofossiler (som härstammar från sjön/flodens omgivning), tillsammans med jämförelse av responsen från terrestra och vattenlevande taxa, ger en solid grund för tolkningarna av den regionala vegetationen och klimatet. Klimatparametrar kvantifieras med hjälp av överföringsfunktioner med avseende på pollen- och chironomidsammansättningar, samt från makrofossiler/pollen från klimatindikatorväxtarter, genom att använda både klassisk multivariabel regression och nya tillvägagångssätt baserat maskininlärningsmetoder som används inom paleoklimatologi under det senaste decenniet.

Resultat från studierna vid Sokli och Loitsana har publicerats i 33 vetenskapliga artiklar i internationella tidskrifter, fyra doktorsavhandlingar och tre expertgranskade tekniska rapporter hos SKB. I denna rapport sammanställs dessa data på ett kortfattat och konsekvent sätt tillsammans med nya data. Multiproxydatat var tidigare utspridda i ett stort antal diagram, men är här kombinerade och presenterade på ett kortfattat och sammanhängande sätt. Klimatrekonstruktioner baserade på pollen och indikatorväxtarter har körts om med de senaste protokollen. Dessutom presenteras nya detaljerade vegetations- och klimatrekonstruktioner för hela den sena kvartären vid Sokli och Loitsana. Vegetationsrekonstruktionerna placeras på en ungefärlig tidsskala som bestäms bland annat av nyligen publicerade stalagmitdata från en grotta i norra Sverige (Korallgrottan). Denna rapport presenterar den första detaljerade jämförelsen av vegetations- och klimatutvecklingen mellan de isfria perioderna i Sokli under sena kvartär. Vidare presenteras sedimentloggar från alla borrhål i Sokli och Loitsana och alla dateringsresultat diskuteras och utvärderas. Det senare gäller även för de kvantitativt härledda klimatrekonstruktionerna.

Multiproxyanalyserna från Sokli och Loitsana-sedimenten har resulterat i en mängd unika miljödata för sena kvartär i Fennoskandia, vilka bidrar till att väsentligt revidera tidigare uppfattningar om glaciation, vegetation och klimat i Fennoskandia under de senaste 130 000 åren. Sokli-sekvensen avslöjar att den fennoskandiska inlandsisen var mer dynamisk än tidigare rekonstruktioner samt att det troligen var betydligt mindre is över Fennoskandia än vad man tidigare trott. Nya data för

Tulppio-interstadialen visar att, även under glaciala förhållanden (Marine Isotope Stage (MIS) 4-2 mellan c. 70 000–15 000 år sedan), var Sokli isfritt vid två tillfällen i mitten av MIS 3 för ca 40 000 år sedan (motsvarar Grönland interstadialer (GIS) 11/12 och 8). Tillväxt av is nära Sokli har registrerats under den äldsta av de två isfria perioderna under MIS 3 (Tulppio 1-interstadialen), och nedisningen (här definierad som Saariselkä-glaciationen) mellan Tulppio 1 och 2-interstadialerna, hade troligen sitt ursprung i Saariselkäs fjällskedja ca. 100 km norr om Sokli. Isuppbyggnaden som inträffade under MIS 6 (mer än 130 000 år sedan), MIS 5b (ca 85 000 år sedan), MIS 4-tidigare MIS 3 (ca 70 000–50 000 år sedan) och sena MIS 3–2 (ca 35 000–15 000 år sedan) tros däremot ha vuxit till från de skandinaviska bergen. Isfria förhållanden under delar av MIS 3, ca. 50 000–35 000 år sedan, rapporteras nu ha varit förekommande på olika platser i Fennoskandia såväl som i de centrala delarna av Laurentide och Cordilleran-isarnas utbredningsområde i Nordamerika. I motsats till den klassiska bilden av en glaciation, som beskriver hårda och kala miljöförhållanden, uppvisar Sokli och Loitsana-rekonstruktionerna flera perioder av varma somrar och en rik biota. Detta är i linje med resultat från tidigare studier i Kanada. Soklibäckenet var inte nedisad under det kalla MIS 5d-stadiet (ca 110 000 år sedan). Istället indikerar förekomsten av stäpp-tundravegetation, ett flätat flodmönster och relativt höga sommartemperaturer att ett kontinentalt klimat rådde vid Sokli under denna tid, potentiellt tillsammans med en djup kontinuerlig permafrost.

Resultaten från Sokli visar också att varma interglaciala förhållanden rådde under alla tre varma stadier av MIS 5. MIS 5 definieras som det sista interglaciala komplexet vid Sokli, i överensstämmelse med data från stora delar av det europeiska fastlandet. Nuorttis varma stadium i Soklibäckenet motsvarar MIS 5e (ca 125 000 år sedan) eller interglacialen Eem i den nordväst-europeiska fastlandets stratigrafi; Sokli I motsvarar MIS 5c (ca 95 000 år sedan; Brørup-interstadialen); och Sokli II motsvarar MIS 5a (ca 80 000 år sedan; Odderade-interstadialen). Utvecklingen av vegetation under MIS 5e, 5c och 5a var anmärkningsvärt lik motsvarande utveckling av nuvarande interglacial holocen, även om viktiga och intressanta skillnader också finns. Under alla varma perioder (MIS 5e, 5c, 5a och holocen) var medeltemperaturen i juli, åtminstone tillfälligt, flera grader högre än motsvarande temperatur under sena holocen. Nuorttis varma stadium (MIS 5e) utmärker sig genom den lokala förekomsten av tempererad hassel (Corylus), vintertemperaturer som troligen var högre än idag och betydande klimatvariationer på tidskalan tusentals år. Under det tidiga MIS 5e Tunturi-eventet för ca 127 000–126 000 år sedan blev klimatet betydligt kallare och torrare; denna förändring visar att även ett varmt klimat kan vara högst instabilt. En liknande tidig MIS 5e-avkylning har också rekonstruerats vid platser med hög sedimentackumulation i norra Nordatlanten, i den berömda högupplösta speleothemsekvensen från Corchia, Italien, samt i den nyligen publicerade speleothemsekvensen från Korallgrottan i norra Sverige. Marina data tyder på att nedkylningen av klimatet under denna tid uppkom i samband med en minskning av bildandet av djupvatten i Nordatlanten. Slutligen utesluter miljö-/klimatrekonstruktionerna för MIS 5c vid Sokli att någon betydande ismassa kvarstod i Fennoskandia under denna period. Detta resultat stämmer överens med relativa havsnivåuppskattningar från tektoniskt stabila platser runt om i världen. Utöver en mycket dynamisk inlandsis under sen-kvartär (tidigt och mitten av Weichselglaciationen) uppvisar Soklisekvensen också en mycket högre klimatvariation under denna tidsperiod än vad som tidigare rekonstruerats. Tidigare miljö-/klimatrekonstruktioner för sena kvartär i Fennoscandia baserades mestadels på långdistanskorrelationer av mycket fragmenterade och ofta dåligt daterade lito- och bio(pollen)-stratigrafiska data. Enligt dessa rekonstruktioner var Sokli nedisad i nästan 100 000 år, från början av MIS 5d till starten av holocen. MIS 5c och möjligen MIS 5a var de enda perioderna, inom detta tidsintervall, som beaktades kunde ha haft isfria förhållanden och arktisk tundravegetation.

Slutligen kan noteras att rekonstruktionerna av de holocena vegetation- och klimatförhållanden från Loitsanasjön, vilka uppvisar liknande detaljeringsgrad som äldre sekvenser från Soklibäckenet, är mycket lika det som framställts för andra platser i norra Fennoscandia, inklusive det nyligen studerade Kuutsjärvi ca 10 km öster om Sokli vid Värriö Tunturits kristallina lågfjäll. Detta visar på ett försumbart inflytande av den icke-typiska berggrundsgeokemin i Sokli på rekonstruktionerna av klimatet och den regionala vegetationen.

Contents

1 Introduction

1.1 Background

The classic geological reconstructions of environmental conditions including glaciations, vegetation and climate in Fennoscandia for the late Quaternary (last c. 130 kyr) were largely based on long-distance correlation of often poorly dated and highly-fragmented bio(/pollen)- and litho(/till fabric)-stratigraphic evidence (Andersen and Mangerud 1989, Mangerud 1991, Lundqvist 1992, Donner 1995). Long pollen records (i.e. spanning a long time sequence) from the NW European mainland were used as templates against which local and regional biostratigraphic schemes were correlated. As clearly outlined by Donner (1996), these correlations are fraught with uncertainties, caused by the correlation over long distances, i.e. over an area with a large climate gradient, and truncations of geological beds resulting in incomplete interstadial or interglacial sequences. Additionally, correlations build on the assumption that Late Pleistocene climate and vegetation gradients over central Europe-Fennoscandia were similar as today or steeper, influenced by the presence of the Fennoscandian Ice Sheet, and that climate conditions were similar or warmer than today only during the Eemian Interglacial (Marine Isotope Stage (MIS) 5e between c. 130–115 kyr ago; Figure 1-1). Furthermore, the late Quaternary glacial history of Fennoscandia is mostly based on correlations with the marine oxygen-isotope stratigraphy. Although it is widely acknowledged that the latter record carries a composite signal of e.g. ice volume, ocean water temperature and salinity, the marine oxygen-isotope record is widely used as a proxy for global ice volume changes during the Quaternary (last c. 2.5 million years) (e.g. Kleman et al. 1997).

Long sediment records are rare in Fennoscandia due to repeated glacial erosion by the Fennoscandian Ice Sheet. A unique 30 m-thick sediment sequence of late Quaternary age has survived multiple glaciations in the Sokli basin in northern Finland (Figure 1-2). The thick fossil-bearing lacustrine and fluvial deposits, which are found interlayered with glacial till beds, occur in a sheltered position in a steep depression formed in deeply weathered rocks of a magma intrusion (the Sokli Carbonatite Massif (SCM)) in the Fennoscandian Precambrian Shield. Sokli was positioned under the ice-divide zone during the Last Glacial Maximum (LGM, c. 20 kyr BP in MIS 2), where low basal ice-flow velocities and/or frozen-bed conditions have resulted in limited glacial erosion (Kleman et al. 1997, 1999, Boulton et al. 2001). Moreover, the maintenance of divergent ice flow, from the northern parts of the Scandinavian mountains (Scandes) into the Inari basin to the north and the Baltic basin to the south (Figure 1-2), dictated by the pre-glacial relief, is mentioned as a possible factor for the glacial preservation of pre-LGM sediments and landforms in both central Finnish and Swedish Lapland (Ebert et al. 2015). Although central Finnish Lapland holds a concentration of sediments pre-dating the LGM, the till-covered organic beds are generally only a few decimeters thick and often occur in a secondary position, i.e. the sediments are not found in-situ but have been truncated and transported by the ice sheet (Hirvas 1991). Therefore, the unique sediment preservation in the Sokli basin is probably mainly due to the non-typical bedrock conditions. It is the combination of a steep hollow in the soft, deeply weathered carbonatite rocks of the SCM, combined with the presence of surrounding hills formed in hard fenite rocks, which have provided shelter against glacial erosion (Figure 1-3). Another site with preservation of a thick sediment sequence is Rautuvaara in western Finnish Lapland. Here, a series of individual till beds, interbedded with sorted glacio-lacustrine sediment, but not including any organic-rich unit, can be followed over up to some 400 m on the eastern flank of the Alainen Rautuvaara hill. The sediments form part of an up to 40-m-thick valley-infill consisting of glacial and fluvial deposits. The Rautuvaara Section has earlier been considered as the stratotype for the northern Fennoscandian late Middle and Late Pleistocene (Hirvas 1991). Recent dating using the luminescence dating method indicates that the whole sediment succession was deposited during the Weichselian (Figure 1-1; Lunkka et al. 2014, Howett et al. 2015).

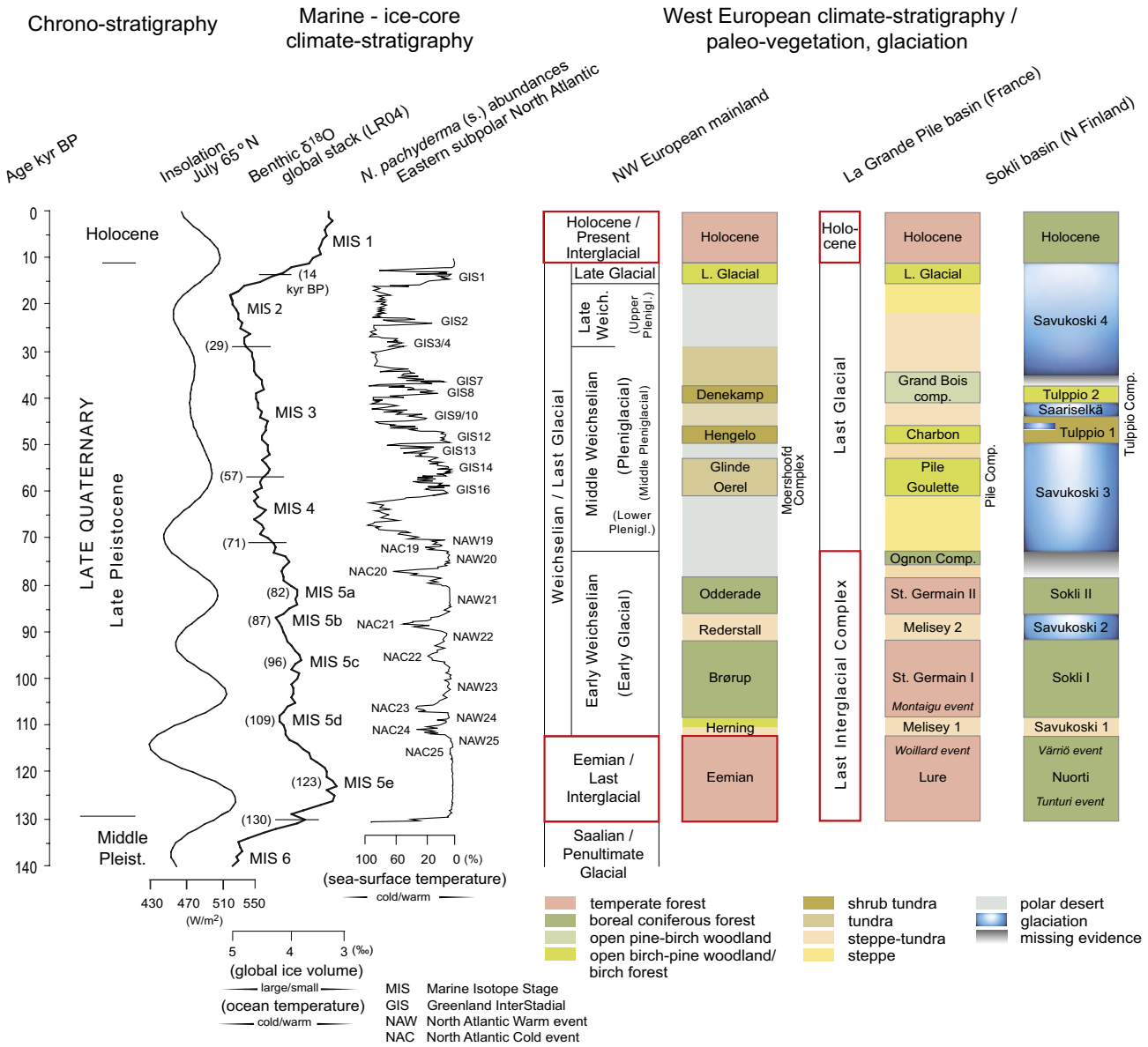

Figure 1-1. *Late Quaternary climate-stratigraphies in marine sediments (globally, after Lisiecki and Raymo 2005; eastern subpolar North Atlantic, after McManus et al. 1994, Bond et al. 1993) and European terrestrial sediments. Shown are the NW European mainland stratigraphy (with important sites such as Twente in the Netherlands (van der Hammen and Wijmstra 1971, van Geel et al. 1989) and Oeral in northern Germany (Behre 1989) and the stratigraphies in the La Grande Pile basin in France (Woillard 1978, Turon 1984) and Sokli basin in northern Finland (Helmens 2014, Helmens et al. 2015, Salonen et al. 2018, this study) (Figure 1-2). Note that the Weichselian (or Last Glacial) in northwest Europe is defined as covering MIS 5d-2, whereas in the La Grande Pile and Sokli basins the Last Glacial corresponds to MIS 4-2. Greenland Interstadials are according to Johnsen et al. (1992) and Dansgaard et al. (1993). Variations in summer insolation at high northern latitudes (Berger and Loutre 1991) are indicated at the left side of the figure. Adapted from Helmens (2014).*

With sediments preserved in their original stratigraphic position, an absolute timeframe obtained through radiocarbon and luminescence dating, and an unusual thickness and fossil-richness of lacustrine and fluvial deposits, the long sediment sequence in the Sokli basin provides a unique possibility for studying late Quaternary environmental and climate change in Fennoscandia. As mentioned at the start of this section, most pre-LGM sedimentary sequences in Fennoscandia that have been studied are highly fragmented, representing parts of an interstadial or interglacial sequence, and many sediment sections are poorly dated; the most common proxies that have been applied in environmental reconstructions are pollen and diatoms (Donner 1995). Long records such as preserved at Sokli have not yet been located at other sites in Fennoscandia. Long environmental/climate records that span the last 130 kyr BP are available, however, from sites directly outside the LGM extent of the Fennoscandian Ice Sheet, on the northern European mainland, where sediments have accumulated, like at Sokli, in glacial depressions formed during the Penultimate Glacial (MIS 6; Helmens 2014). As such, Sokli provides the opportunity for the late Quaternary environmental and climate record to be extended to high European latitudes. It is also important to note that, because of the northern location of the Sokli site and its position under the central part of the LGM ice sheet, ice-free intervals at Sokli most likely meant ice-free conditions over large parts of Fennoscandia. This is supported by an increase in detailed studies during the last two decades on geological sections dated to MIS 3, providing evidence for widespread deglaciation in Fennoscandia, including at Sokli, following sub-continental-scale glaciation in MIS 4 (e.g. Helmens and Engels 2010 and references therein, Wohlfarth 2010 and references therein, Helmens 2014 and references therein, Kleman et al. 2020, Mangerud et al. 2023).

Following reconnaissance studies (Ilvonen 1973a, 1973b, Forsström 1990, Johansson and Räsänen 1994, Helmens et al. 2000, 2007a, Alexanderson et al. 2008), the Sokli sediment sequence has been subjected to detailed studies starting in 2006, mostly funded by SKB, with additional funding from POSIVA (Finland), the Academy of Finland, and the Bolin Center of Climate Change Studies at Stockholm University (Sweden). A complementary study was carried out on the Holocene deposit in Loitsana Lake to obtain a reference section for the interpretation of the results from the older lake deposit in the adjacent Sokli basin. The sediments were studied using a multi-proxy approach in which a large variety of fossil remains, and sediment characteristics, were analyzed and results were integrated. Climate parameters were quantified using an ensemble of proxy-climate calibration methods. Studies have been conducted by an international team of researchers specialized in e.g. the identification of pollen, macrofossils, chironomids (aquatic insects) and diatoms, the analysis of biogeochemical data, as well as different climate reconstruction methods.

The multi-proxy analyses on the Sokli and Loitsana sediments have provided an unprecedented wealth of environmental data for the late Quaternary of Fennoscandia. Most importantly, it has resulted in an environmental/climate record that significantly revises earlier concepts of glaciation, vegetation, and climate in Fennoscandia over the last 130 kyr. According to the earlier views (e.g. Mangerud 1991, Lundqvist 1992, Donner 1995), Sokli was glaciated for nearly 100 kyr from the start of MIS 5d at c. 115 kyr BP to the start of the Holocene at c. 10 kyr BP (Figure 1-1). MIS 5c (centered at c. 96 kyr BP; Brørup Interstadial in the NW European mainland stratigraphy) and possibly MIS 5a (c. 82 kyr BP; Odderade Interstadial) are the only periods that were traditionally considered, within this time interval (Last Glacial), to be ice-free with cold tundra conditions. Warm interglacial conditions prevailed during the preceding interglacial (MIS 5e around c. 125 kyr BP; Last Interglacial or Eemian Interglacial) and the Holocene (Present Interglacial).

In sharp contrast to the earlier views, the Sokli record reveals a highly dynamic Fennoscandian Ice Sheet and significantly less ice-cover over Fennoscandia in both time and space. Furthermore, it does not only infer ice-free conditions for both MIS 5c and 5a but reveals interglacial vegetation successions with summer temperatures exceeding Late Holocene interglacial values by several degrees during these periods (Sokli I and Sokli II warm stages; Figure 1-1). Full glacial conditions during MIS 4-2 (c. 70–10 kyr BP) were interrupted at least twice by deglaciation of the Sokli basin (Tulppio Interstadial Complex around c. 40 kyr BP in mid-MIS 3). Ice-free conditions over large parts of Fennoscandia during MIS 3, in the period between c. 50–35 kyr BP, are now reported from various key sites, recently studied or re-studied (see above), in Fennoscandia. The proxy data from Sokli and Loitsana show that the response of biota to newly deglaciated terrain was fast and warm insolation-forced summers are recorded for the various late Quaternary deglacial phases. The Sokli basin was not glaciated during the cold MIS 5d stage (around at c. 110 kyr BP). Instead, steppe-tundra

vegetation, a braided river pattern and relatively high summer temperatures indicate a strong continental climate regime with the possibility of deep continuous permafrost. Steppe-tundra was widespread on mainland Europe during the cold stages of the late Quaternary (e.g. Granoszewski 2003). A high-resolution analysis of the lake deposit of MIS 5e age in the Sokli basin (Nuortti warm stage) further reveals a distinct millennial-scale climate variability superimposed on the long-term orbitally forced interglacial climate evolution and provides evidence for substantial climate instability under warmer-than-today baseline conditions. In the marine record, a concurrent cooling to the early MIS 5e Tunturi event at Sokli occurs associated with reductions in North Atlantic Deepwater Formation, suggesting a weakening of the Atlantic Meridional Overturning Circulation (AMOC; Irvali et al. 2012, Galaasen et al. 2014). Overall, MIS 5e was the mildest period at Sokli of the last 130 kyr when also winter temperatures seem to have exceeded Late Holocene values. Finally, the prevalence of interglacial conditions during all three warm stages of MIS 5, which has led to the definition of entire MIS 5 at Sokli as the Last Interglacial Complex, restricts the Last Glacial to MIS 4-2 with a total duration of c. 50 kyr (Figure 1-1). In a review paper in which Sokli is compared with long proxy records from Europe and marine data, Helmens (2014) proposes a subdivision of the last climate cycle into an early, overall mild interglacial half (MIS 5) and a late, overall cold glacial half (MIS 4-2), each with duration of c. 50 kyr. The warm interglacial conditions at Sokli during MIS 5c and 5a preclude the persistence of any significant ice mass in Fennoscandiaduring these periods, which is agrees with relative sea-level estimates from tectonically stable locations around the world for MIS 5a (Dorale et al. 2010).

Results from the Sokli and Loitsana studies are published in 33 peer-reviewed scientific papers in international journals, four PhD theses, and three peer-reviewed SKB technical reports (Table 1-1). The present report provides the following improvements and updates:

1) Multi-proxy data that was earlier spread over many diagrams and publications are here combined and presented in a concise and coherent way.
2) Climate reconstructions based on pollen and indicator plant species are re-run using most-recent protocols. A new pollen sum is introduced.
3) New detailed vegetation and climate records for the entire late Quaternary at Sokli are presented.
4) Vegetation developments and climate evolutions that are reconstructed for the various ice-free timeperiods at Sokli are compared in detail for the first time.
5) Sediment logs from all boreholes in the Sokli basin, and the adjacent Loitsana basin, are provided and all dating results are discussed and evaluated.
6) Quantitatively inferred climate estimates are evaluated in detail.
7) A large part of the multi-proxy data for the MIS 5e Sokli lake deposit; the study on the lake sediments of MIS 5a age; and a comparison between the different glacial lake stages; which have been published but not yet reported in a SKB report, are included.
8) Important new data for the Tulppio Interstadial (MIS 3) are presented. Also, a new environmental record based on the Holocene peat deposit, and underlying lacustrine sediment, in the Sokli basin is provided.

The publications for each of the time-slices studied at Sokli and Loitsana, which lie at the basis of the report, including main topic/reconstruction and applied proxies, are summarized in Table 1-2.

Following chapter 1, which provides an introduction to the report and describe the present-day environmental setting of the study site, chapter 2 gives important information/data that lie at the basis of the environmental/climate reconstructions presented in chapters 3-5. Chapter 2 describes sediment recovery and borehole locations; provides a discussion on dating methods and presents all dating results as well as a thorough evaluation of these results; discusses the late Quaternary stratigraphy in the Sokli basin; and provides a discussion on multi-proxy comparisons, and a description of methods used for climate reconstruction. The implications of the Sokli results and comparison with other studies are integrated in all chapters including the summary.

The relevance of the research conducted in the Sokli and Loitsana basins for the description of the historical climate evolution at Forsmark and the definition of climate scenarios in assessments of post-closure safety is summarized in SKB (2020), Section 4.3.5.

Table 1-1. Publications on the Sokli and Loitsana records and related studies.

Alexanderson et al. (2008)	Bos et al. (2009)	Dalton et al. (2022)
Engels (2008)	Engels et al. (2007)	Engels et al. (2010)
Engels et al. (2014)	Felde et al. (2020)	Finné et al. (2019)
Helmens (2009)	Helmens (2013)	Helmens (2014)
Helmens (2019)	Helmens and Engels (2010)	Helmens et al. (2000)
Helmens et al. (2007a)	Helmens et al. (2007b)	Helmens et al. (2009)
Helmens et al. (2012)	Helmens et al. (2015)	Helmens et al. (2018)
Helmens et al. (2021)	Katrantsiotis et al. (2021)	Kylander et al. (2018)
Plikk (2018)	Plikk et al. (2016)	Plikk et al. (2019)
Plikk et al. (2021)	Salonen (2012)	Salonen et al. (2013)
Salonen et al. (2018)	Salonen et al. (2021)	Sánchez Goñi et al. (2017)
Shala (2014)	Shala et al. (2014a)	Shala et al. (2014b)
Shala et al. (2017)	van Meerbeeck et al. (2011)	Väliranta et al. (2009)
Väliranta et al. (2015)		

Table 1-2. Summary of studies at Sokli and Loitsana used in the environmental and climate reconstructions presented in this report.

Time-slice	Main proxy	Topic/reconstruction	Reference
Early Holocene	Lithology, geochemistry, diatoms	Evolution Sokli Ice Lake	Shala et al. (2014a)
Holocene	LOI, C/N, macrofossils, diatoms, chironomids	Lake development	Shala et al. (2014b)
Holocene	Pollen	Vegetation development	Salonen et al. (2013)
Holocene	Pollen, diatoms, chironomids, macrofossils	Comparison of climate records	Shala et al. (2017)
Holocene	Multiple proxies	Environmental and climate records	Shala (2014)
MIS 3	Lithology, diatoms	Evolution Sokli Ice Lake, climate	Helmens et al. (2009)
MIS 3	Chironomids	Climate	Engels et al. (2007)
MIS 3	Pollen, NPP's, macrofossils	Terrestrial and lake ecosystems, climate	Bos et al. (2009)
MIS 5d-c	Macrofossils	Climate	Väliranta et al. (2009)
MIS 5d-c	Lithology, LOI, chironomids, Macrofossils	Fluvial depositional environments, climate	Engels et al. (2010)
MIS 5d-c	Lithology, LOI, pollen, NPP's, macrofossils	Terrestrial and azonal ecosystems, climate	Helmens et al. (2012)
MIS 5a	Pollen, NPP's, macrofossils, diatoms, chironomids	Terrestrial and aquatic/wetland ecosystems, climate	Helmens et al. (2021)
Early MIS 5e	Multiple proxies	Environmental conditions and climate Tunturi event	Helmens et al. (2015)
MIS 5e	Biogeochemistry, diatoms, pollen, NPP's, macrofossils	Lake development	Plikk et al. (2016)
MIS 5e	Geochemistry, diatoms	Lake development	Kylander et al. (2018)
MIS 5e	Pollen	Vegetation and climate (summer and winter temperatures)	Salonen et al. (2018)
MIS 5e	Chironomids	Climate	Plikk et al. (2019)
MIS 5e	Biomarker-isotopes	Trends in summer and winter temperatures	Katrantsiotis et al. (2021)
MIS 5e	Resting spores of diatom *Aulacoseira*	Morphology	Plikk et al. (2021)

Time-slice	Main proxy	Topic/reconstruction	Reference
MIS 5e	Multiple proxies	Environmental and climate records	Plikk (2018)
Holocene, MIS 5d-c	Pollen	Comparison of climate reconstructions	Salonen et al. (2013)
Holocene, MIS 3, 5d-c	Chironomids	Comparison of climate reconstructions	Engels et al. (2014)
Early MIS 5a, MIS 3, Early Holocene	Litholoy, diatoms, chironomids, pollen, NPP's, macrofossils	Comparison of glacial lake stages	Helmens et al. (2018)
Entire record	Lithology, pollen	Reconnaissance study	Helmens et al. (2000)
Entire record	Lithology	Geochronology	Alexanderson et al. (2008)
Entire record	Lithology, pollen	Stratigraphy	Helmens et al. (2007a)
Entire record	Lithology, pollen, macrofossils	Climate-stratigraphy	(Helmens 2014)

1.2 Environmental setting

Sokli is in the northernmost part of the boreal forest biome in northwestern Europe (Figure 1-2). The main tree taxa in the region are birch (*Betula pubescens* and *B. pendula*), pine (*Pinus sylvestris*) and spruce (*Picea abies*). The northern limit of spruce is situated some 100 km north of Sokli. North of the spruce limit, pine forest predominates, succeeded northwards and upwards by birch-pine forest and then sub-arctic birch forest composed of the polycormic mountain birch *B. pubescens* subsp. *tortuosa*. The vegetation of the tundra region beyond the forest limit is mainly a dwarf-shrub tundra dominated by dwarf birch (*B. nana*) and Ericales. Lowland tundra is restricted to a narrow strip of land along the Barents Sea coast in northern Norway but becomes more widespread in the Russian arctic in northeastern Europe. Larch (*Larix sibirica*) starts its present-day range ca. 500 km east of Sokli, where with increasing continentality larch becomes an important component of the Russian northern taiga and the vegetation near the arctic forest limit. South of Sokli, several deciduous trees that are common in the temperate forest of central Europe (e.g. hazel (*Corylus avellana*), elm (*Ulmus glabra*), oak (*Quercus robur*)) reach their northern distribution limits in the boreal forest and transition to the hemi-boreal forest. The northern limit of *Alnus glutinosa* (alder), which thrives in wet habitats, is situated at some 400 km south of Sokli. *A. incana* is present throughout Fennoscandia, growing also in the open vegetation types of the northernmost regions. Mixed deciduous-coniferous forest with a variety of thermophilous trees (but mostly *Quercus*) is present south of c. 60° N.

Figure 1-2 further shows the present-day isotherms of mean July and mean January air temperatures over northern and central Europe (Hijmans et al. 2005). Except for the major mountain ranges, July temperatures increase with decreasing latitude, with the steepest temperature gradient in the east. January temperatures follow a perpendicular pattern to the July temperatures, with winter temperatures decreasing eastwards. The increase in July and decline in January temperatures along latitudinal transects eastward from the North Atlantic Ocean together constitute a gradient in climatic continentality, defined as the temperature amplitude of the warmest minus coldest month divided by the sine of latitude.

Sokli is a deserted mining hamlet located in northeastern Finland close to the border with Russia (lat. 67°48' N, long. 29°18' E, elevation c. 230 meters above sea level (m a.s.l.); Figure 1-3). The geology of the area comprises the Sokli Carbonatite Massif (SCM), which is a round massif about 7 km in diameter within its core Paleozoic carbonate-rich rocks of magmatic derivations/descent (Vartiainen 1980). The carbonatite rocks are surrounded by a fenite halo that developed by metasomatism of the crystalline rocks that surround the magma intrusions (Vartiainen 1980). The top of the carbonatite is almost wholly weathered, leaving a regolith rich in apatite and francolite. The carbonatite rocks of the SCM have relatively high concentrations of calcium (Ca), sulphur (S), iron (Fe), and manganese (Mn) and contain the rare element niobium (Nb; Vartiainen 1980). Dispersed residual phosphorous deposits occur across the carbonatite bedrock (Talvitie et al. 1981). The SCM is the westernmost extension of deposits that form the Russian Kola alkaline rock province. The Precambrian rocks of the Fennoscandian Shield that surround the massif include metavolcanics, metasediments and granitoids (Mikkola 1937), rocks which form the bedrock in major parts of Finnish Lapland.

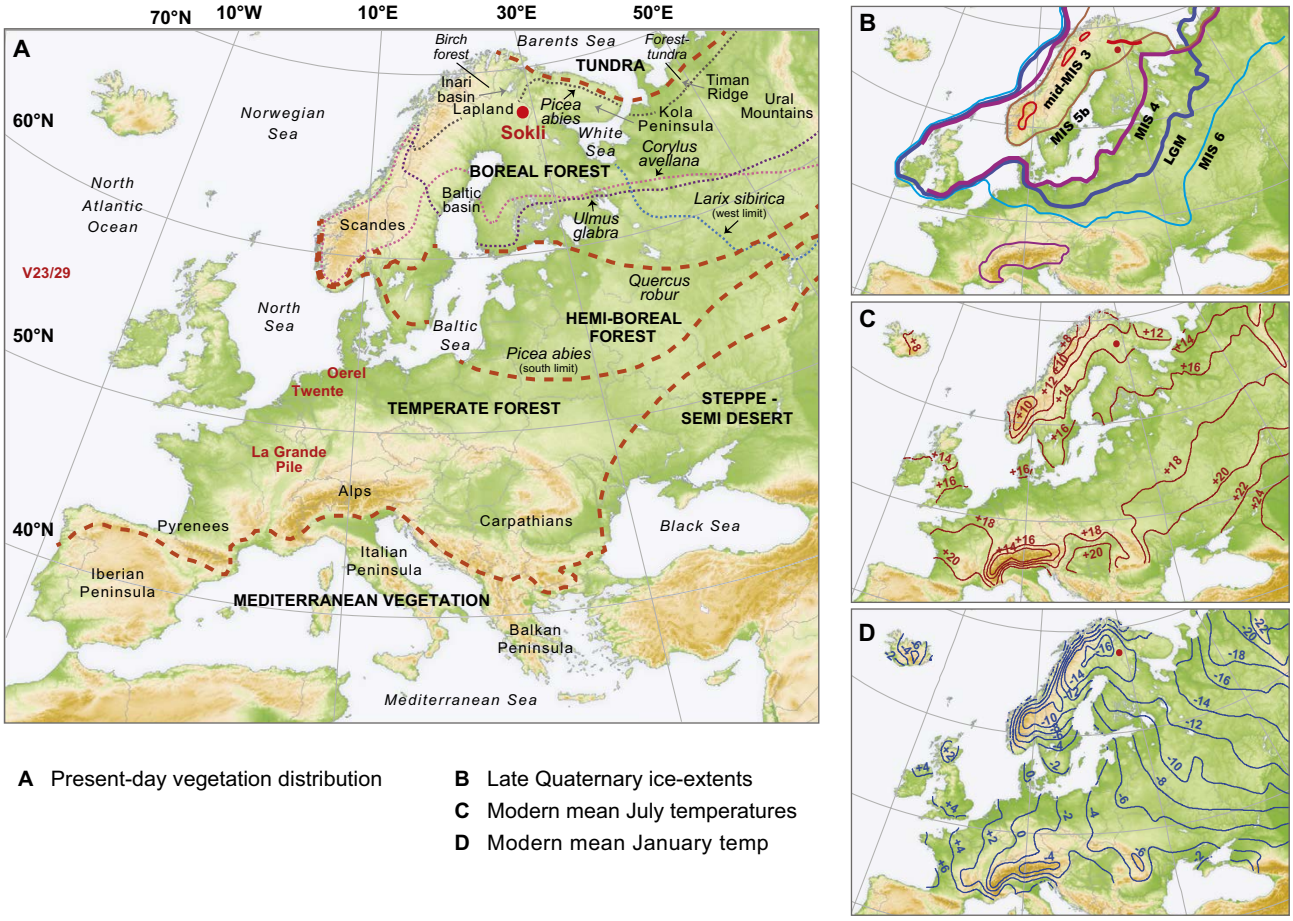

A Present-day vegetation distribution

B Late Quaternary ice-extents

C Modern mean July temperatures

D Modern mean January temp

Figure 1-2. *Map of Europe (A) with present-day distribution of latitudinal vegetation belts and northern (or otherwise indicated) distribution limits of selected tree taxa (based on Donner 1995). The Sokli site and other stratigraphically important sites (see Figure 1-1) are highlighted in red. (B) shows the extent of the south-western portion of the North Eurasian Ice Sheet (including the Fennoscandian and British Ice Sheets) during cold stages of the last c. 160 kyr (based on Svendsen et al. 2004, Carr et al. 2006, Mangerud 2011). The ice extent in mid-MIS 3 follows Arnold et al. (2002) and this study. Also shown is the maximum limit of Pleistocene glaciation of the Alps (Ehlers and Gibbard 2004). Maps C and D provide present-day isotherms of mean July and January temperatures, respectively, over central and northern Europe, according to Hijmans et al. (2005). Adapted from Helmens (2014).*

The deeply weathered carbonatite rocks manifest themselves in the landscape as a circular depression bordered by a hilly ring of fenites (Figure 1-3). The surface of the Sokli mire (Sokliaapa) in the center of the massif lies at an elevation of c. 220 m a.s.l. and the highest fenite hill (Mäskaselkä) reaches 314 m a.s.l. The Sokliaapa is drained by a rivulet called the Soklioja that flows southwestwards into the Yli-Nuortti. The latter is a tributary of the Nuortti River that, in its turn, drains towards the Barents Sea. The highest peaks in the Nuortti drainage basin are the Värriö Tunturit (Värriö fells) at c. 15 km to the southeast of Sokli. This low-mountain ridge exceeds 500 m a.s.l. in elevation and is covered with dwarf-shrub tundra. Mires of the aapa-type (a patterned fen) are extensively present in the region. The Sokliaapa consists of a *Carex-Salix* rich fen directly along the Soklioja, surrounded by a *Carex-Betula nana* moderate-rich fen. The outer, drier parts of the mire consist of an Ericaceae-*Spaghnum* poor fen containing ombotrophic hummocks with *Rubus chamaemorus*. Loitsana Lake is the only place within the Sokli massif where open-water conditions persist today. It has a current water depth between c. 1–2 m.

Sokli has a cool boreal climate. Temperatures in the region are currently increasing with the largest increases occurring after 2000. Since the modern climate calibration data used in our climate reconstructions span the period 1961–2000 (Section 2.3), a mean January and mean July air temperature of c.−14 °C and 13 °C, respectively, which are average values over 1971–2000 (Hijmans 2005), are used as present-day values in the report and figures. Mean annual precipitation amounts to c. 500–550 mm (Drebs et al. 2002).

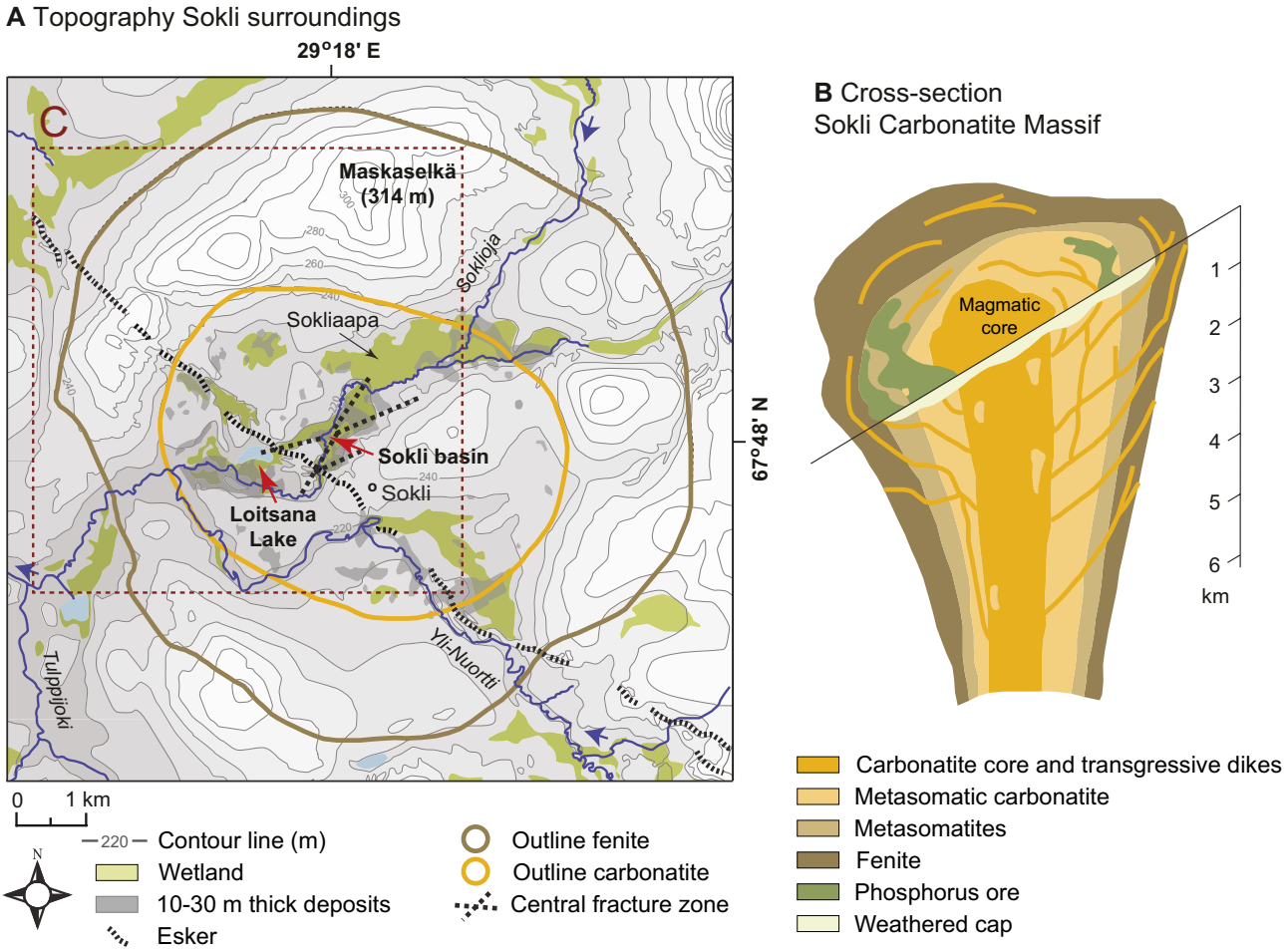

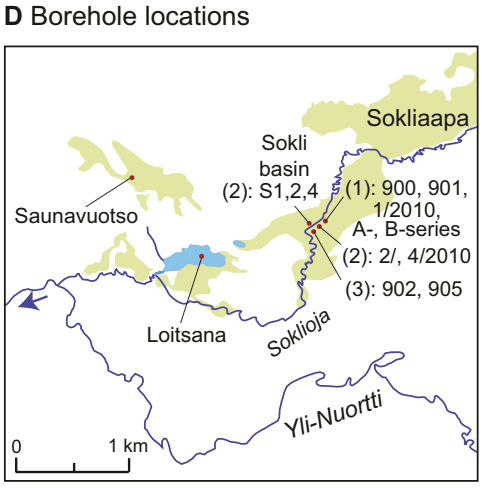

Figure 1-3. *(A) Topographic map of the Sokli basin and direct surroundings with aerial outline of the Sokli Carbonatite Massif (SCM). A cross-section of the SCM is provided in B (after Vartiainen 1998). (C) is a raw hill-shade map created from high-resolution (2 m) digital elevation data (Geological Survey of Finland CC BY 4.0 license; downloaded 2019/10), depicting a distinct meltwater corridor with eskers of sub-glacial origin (ice flow from NW) and fenite hills of the SCM (see B). (D) Locations of boreholes (for explanation see text). Adapted from Helmens et al. (2021).*

2 Methodology and geochronology

2.1 Coring, dating and stratigraphy

Drillings carried out in connection with carbonatite prospecting reveal a string of hollows, with sedimentary infillings up to 10–30 m thick, which follows a NE-SW trending fracture zone through the Sokli Massif (Ilvonen 1973a, 1973b, Talvitie et al. 1981). A 30-m-thick sediment sequence that includes a series of organic-bearing units of late Quaternary age occurs in the center of the massif where two fracture zones cross (Ilvonen 1973a, 1973b, Johansson and Räsänen 1994, Helmens et al. 2000, 2007a). The latter depression is referred as the Sokli basin (Helmens et al. 2000; Figure 1-3).

Heavy percussion drillings were performed in the Sokli basin at three different locations along a 200-m-long transect and, at each location, several boreholes were taken within a few meters distance from each other (Figures 1-3, 2-1). The first sediment cores that were retrieved suffered from major gaps in sediment recovery. Among these are boreholes 900–902 and 905 cored in 1996 (Helmens et al. 2000). Following this, a near continuous sediment record, which reaches down into a diatom-rich gyttja deposit near the base of the basin infill, was collected in 2002 with improved techniques (boreholes A- and B-series; Helmens et al. 2007a). Subsequently, boreholes 1/, 2/ and 4/2010 were drilled, resulting in a complete recovery of the lower diatom gytta deposit and underlying glacio-lacustrine sediment (Plikk et al. 2016). Additionally, coring 2/2010 retrieved a thick gyttja deposit on top of the lower glacial till bed in the upper part of the Sokli sequence (Helmens et al. 2021), as well as a sorted sediment intercalation in the uppermost till bed and a complete sedimentary record for the Holocene, both studied here.

Drillings were carried out in winter from the frozen surface of the Sokli wetland by the Geological Survey of Finland. Use was made of a hydraulic piston corer with a flow-through coring device. Cores were taken into a PVC tube, 2 m long and c. 4 cm in diameter, which was driven by vibration into the sediment while inserted in a steel tube. Coarse and compact diamict deposits of glacial origin (till) obstructed the coring operations on several occasions. Furthermore, sand and gravel that had entered the sampling tubes from above contaminated the diatom gyttja sampling, as the latter low-density sediment was unable to (entirely) push out the coarse sediment. This resulted in compaction of the diatom gyttja cores to various degrees. The contact between the diatom gyttja and the contamination, however, was usually sharp, and the latter was easily removed in the laboratory. The rather homogeneous diatom gyttja was then ‘stretched back’ to its original depths (Plikk et al. 2016). As a last note, the coring at some intervals resulted in an up-ward curving of particularly clayey-silty sediment layers. This distortion was also clearly visible in the laboratory and taken into consideration during sub-sampling. The cores that were retrieved from the Sokli basin by percussion drilling, to depths of 30 m below the surface, in general allowed the lithology/sedimentology of the basin sediment to be studied in detail. The cores and sub-samples were stored at c. −20 °C, which prevented the sediments from drying out while maintaining sample quality.

In addition to the boreholes from the Sokli basin, a 9-m-thick Holocene sediment sequence was retrieved from the nearby Loitsana Lake in 2008 (Figures 1-3, 2-1). Use was made of a Russian peat corer and coring was performed in early spring from the frozen lake surface (Shala et al. 2014b). Cores S1, 2 and 4 (Sokli basin) were collected in early spring using a motorized hand-coring device (deepest layers) and in autumn with a Russian peat corer. The Holocene sediment/sub-samples, which have relatively high water content, were stored above 0 °C.

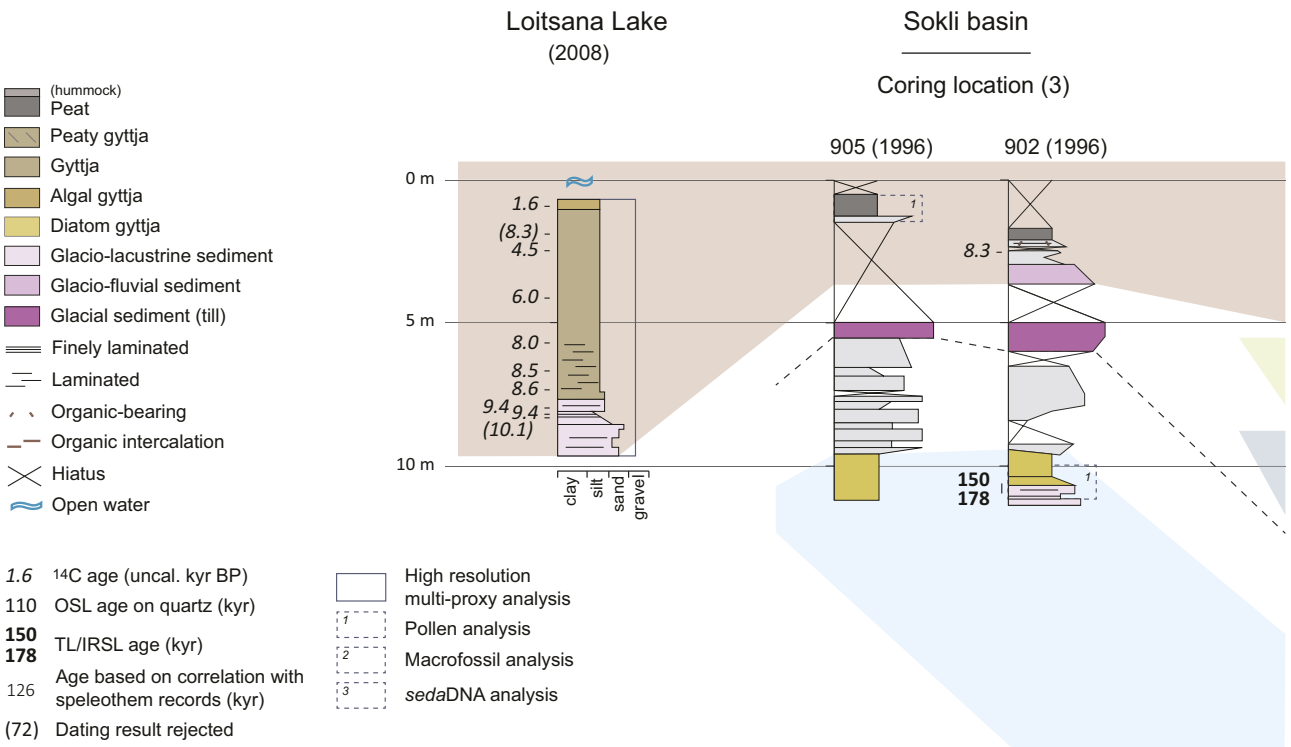

Figure 2-1. *Borehole lithologies and chronologies in the Sokli and Loitsana basins, local climate-stratigraphy, and types of analyses applied to the Sokli and Loitsana sediments. For location of boreholes see Figure 1-3. Adapted from Helmens et al. (2021). (A) percussion drilling in the Sokli basin, with a slice of diatom gyttja of MIS 5e age recovered from a depth of c. 20 m below the surface of the frozen Sokliaapa. (B and C) coring of Holocene sediments in Loitsana Lake using a Russian peat corer (B) and Lymnos device (C).*

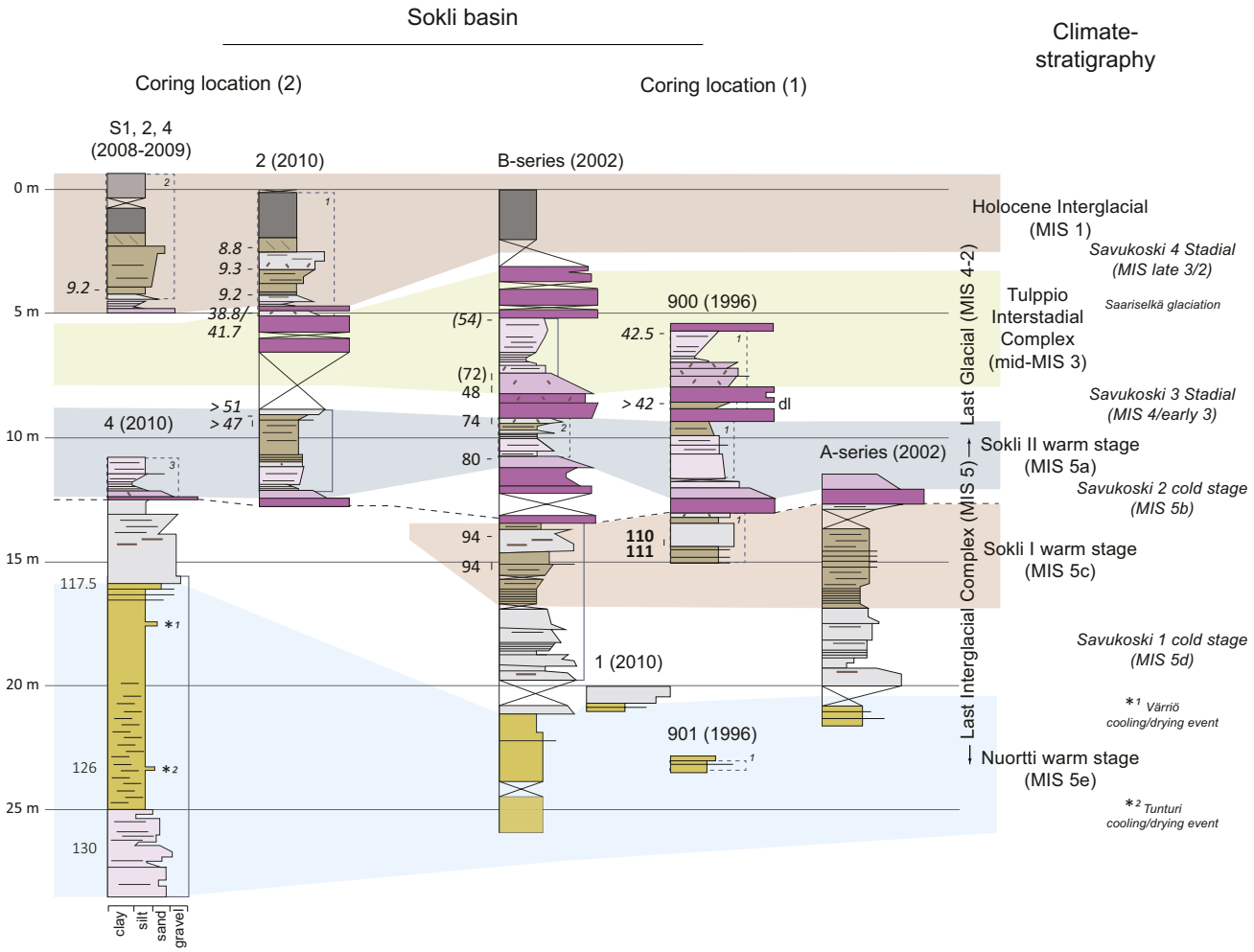

B

C

Figure 2-1. *Cont.*

Dating of the late Quaternary record is not without problems. Many of the ^{14}C dates for sub-till organic beds in northern Finland are around 40 kyr BP (e.g. Mäkinen 2005), i.e. close to the methodological limit of radiocarbon dating. Meaningful dates in this age range can only be obtained if in situ contamination of the ^{14}C sample was reduced to very low levels, and contamination added during handling and processing in the laboratory, and laboratory background radiation, have been minimized (Hogg et al. 2006, Wohlfarth 2009). Despite these uncertainties, consistent series of ^{14}C dates to ages as old as c. 60 uncal. kyr BP have been obtained for long pollen records on the European mainland, providing a chronological framework for vegetation and climate dynamics during MIS 3 that is in general agreement with the Greenland ice core and North Atlantic marine records (e.g. Woillard and Mook 1982, Behre and van der Plicht 1992, Müller et al. 2011). Compared with radiocarbon dating, luminescence dating has the advantages of a greater age range (covers the entire late Quaternary) and the ability to date minerogenic sediment. The experiences with OSL dating in Fennoscandia, however, show that the interpretation of the results is not always straightforward (e.g. Alexanderson and Murray 2007, 2012, Alexanderson et al. 2009). Inconsistent results (including both over- and underestimates of true ages) maybe due to site factors (e.g. the difficulty to assess the water content) as well as the luminescence properties of a sample (incomplete bleaching, fading of the OSL signal, weak signals). Similarly, OSL dating of long pollen records in northwestern Russia has provided a solid chronology for MIS 5 at Lake Ladoga (Andreev et al. 2019), whereas a large scatter in OSL dates for the lower part of a sediment sequence in Lake Yamozero has led to two conflicting MIS 5 age models (Henriksen et al. 2008). Importantly, the classical MIS 5 pollen/climate records from central Europe, e.g. La Grande Pile (Woillard 1978, de Beaulieu and Reille 1992) and Oerel (Behre and Lade 1986, Behre 1989), remain without absolute chronologies and rely on land-sea correlation.

The late Quaternary sediment sequences in the Soki and Loitsana basins are dated by means of a combination of radiocarbon and luminescence dating. The absolute chronology is indicated along the sediment logs in Figure 2-1 and, in more detail, along the lithological columns in the multi-proxy diagrams (Figures 3-1 to 3-6, Figures 3-8 to 3-10). Unpublished dating results are shown in the latter diagrams with their respective laboratory numbers.

The Holocene record from Loitsana Lake is dated by eight AMS ^{14}C datings on macrofossil remains of terrestrial plants (Shala et al. 2014b). Two outliers (shown in brackets in Figure 2-1) are from samples that contained unidentified leaf and epidermal remains, possibly of aquatic origin. Since Loitsana is a hard water lake with carbonates in circulation, the latter samples are suspected to be contaminated by old carbon. The age-depth model presented in Shala et al. (2014b) used IntCal09 (Ramsey 2009, Reimer et al. 2009) and the CLAM package of Blaauw (2010) for R (R Core Team, 2022). For the purposes of the present compilation study, age-depth modelling was done with the Bayesian algorithm Bacon (Blaauw and Christen 2011), using the RBACON library (Blaauw et al. 2022) for R (Figure 3-5). Since the glacial lake stage at the start of the Loitsana record only lasted in the order of c. 25 yr (see Section 3.6), the two ^{14}C ages of c. 9.4 kyr obtained for the glacio-lacustrine sediment were placed at the top of this sediment before applying the Bacon model. For the remaining part of the Loitsana record, the new age-depth model is rather similar to the one in Shala et al. (2014b). Additionally, three AMS ^{14}C datings on bulk sediment (borehole 2/2010) and one using terrestrial plant macrofossils (borehole S1) date the lowermost part a new Holocene pollen and plant macrofossil record from the Sokli mire (Figure 3-6). The age of the minerogenic sediment sample (c. 9.3 ^{14}C kyr), which is of fluvial origin, is slightly older than that of the underlying gyttja and peat (c. 9.2 ^{14}C kyr). This can be explained by the fact that the former bulk sample likely incorporates older soil carbon from the catchment. The chronology is in line with that of the Loitsana Lake record (see also Section 3.5).

Several absolute dates are available for the Tulppio Interstadial Complex of MIS 3 age (Figure 3-4). Wood encountered in the uppermost part of the glacio-lacustrine sediment in borehole 900 was dated at c. 42.5 ^{14}C kyr. Similar as wood from a thin organic-bearing sediment bed found interlayered in the till deposit that underlies this deglacial sediment (dated at > c. 42 ^{14}C kyr; Figure 2-1), and from the Holocene sequence in borehole 905 (c. 8.3 ^{14}C kyr), a thorough chemical pre-treatment was applied to remove possible contaminants. Therefore, the date of c. 42.5 ^{14}C kyr is accepted as a finite age even though it is close to the limit of the radiocarbon dating method (Helmens et al. 2000). Most recent coring (borehole 2/2010) has revealed a c. 30 cm-thick sorted silty to gravelly deposit intercalated near the top of the till bed that overlies the deglacial sediment of the Tulppio 1 Interstadial. A c. 10 cm-thick sorted sandy to gravely bed occurs as well, in the same stratigraphic position, in borehole B-series. One sample from sandy silt in the 2/2010 core was newly AMS ^{14}C-dated at

c. 41.7 kyr (bulk sample) and c. 38.8 kyr (plant macrofossil remains). The bulk sample underwent a thorough chemical pre-treatment to avoid contamination with old carbon from the SCM. The bulk date of the sandy silt, which accumulated in a small floodplain pond (see Section 3.4; Tulppio 2 Interstadial), however, probably slightly over-estimates the true age by incorporating older soil carbon from the catchment (see above). Originally, the time-interval represented by the deglacial sediment sequence was defined as the Tulppio Interstadial (Helmens et al. 2007a). Here, we extent the MIS 3 age interval represented in the Sokli sequence to include the newly dated fluvial deposit and the till that is interbedded in-between this deposit and the underlying glacio-lacustrine sediment and define this as the Tulppio Interstadial Complex (for further discussion see Section 3.4). The glacio-fluvial sediment at the base of the Tulppio Complex is OSL-dated at c. 48 kyr (see below), which is in line with the radiocarbon chronology. An additional OSL age of c. 72 kyr for the deglacial sediment sequence comes from sediment that displays signs of increased glacio-lacustrine influence, which may explain reduced sunlight exposure and incomplete bleaching. Also, the OSL characteristics of the latter sample are very poor. Therefore, the dating result is considered less reliable (Alexanderson et al. 2008) and an outlier in the chronology (Helmens et al. 2007b; Figure 2-1). Finally, an AMS ^{14}C date of 54 ± 7/4 kyr (>48 kyr with 2-sigma) for a very small sample of unidentified seeds from the upper part of the glacio-lacustrine sediment in borehole B-series (unpublished data; UtC 14712) is here considered an outlier as well (Figure 2-1).

The first luminescence datings on the Sokli sediments were performed on boreholes 900 and 902 using thermoluminescence (TL) and infrared stimulated luminescence (IRSL) techniques, in parallel, on feldspar (Figures 2-1, 3-1 and 3-2). The results are regarded reliable based on the TL plateau, laboratory bleaching properties and the agreement between TL and IRSL dates (Helmens et al. 2000). The Sokli sedimentary sequence was subjected to a more detailed optically stimulated luminescence (OSL) dating program with the availability of the long B-series borehole (Alexanderson et al. 2008). A SAR-dose protocol (i.e. measurements on single aliquots) was applied to address sample contamination (e.g. incomplete bleaching; Fuchs et al. 2005, Lian and Roberts 2006). Focus was on quartz although feldspar also was dated in the program. Quartz is quicker and easier zeroed compared to feldspar and fading is usually not a problem in quartz. The OSL dates on quartz obtained from the B-series core have large standard errors that are mainly due to small sample sizes, relatively poor luminescence characteristics, and uncertainties in dose-rate determinations. Nevertheless, OSL ages obtained for glacio-fluvial and fluvial sediment are in sequence and group according to stratigraphic units (Figure 2-1). Furthermore, this absolute chronology agrees with earlier land-sea comparisons (Helmens et al. 2000, 2007a, Alexanderson et al. 2008). In contrast to the OSL dating results on quartz, the IRSL feldspar ages obtained for the B-series borehole are similar, in the order of 120–130 kyr, throughout the depth interval 8–20 m. The feldspar dates most probably over-estimate the true age due to incomplete bleaching (Alexanderson et al. 2008).

The time interval during which the deglacial sediment and overlying sandy gyttja found at depths of c. 9–12.5 m below the surface of the Sokli wetland were deposited is defined as the Sokli II warm stage of the Last Interglacial Complex (MIS 5) (Helmens 2014; Figure 2-1) and this ice-free interval has earlier been correlated to MIS 5a centered at c. 82 kyr BP (Lisiecki and Raymo 2005; Figure 1-1). This is in line with the OSL dates of c. 74 kyr and c. 80 kyr for the Sokli II sediment sequence (Figure 3-3). Additionally, wood from the gyttja deposit has recently been AMS ^{14}C dated at >47 and >51 kyr (Helmens et al. 2021). Furthermore, two OSL dates of c. 94 kyr support the correlation of the gyttja deposit that is found at depths of c. 13–17 m (Sokli I warm stage) with MIS 5c around c. 96 kyr BP (Figure 3-2). The thick diatom gyttja deposit that stretches as a marker horizon near the base of the Sokli basin infill (Nuortti warm stage) is dated as older than c. 94 kyr BP (OSL) and c. 110–111 kyr BP (TL/IRSL), and younger than c. 150–178 kyr BP (TL/IRSL). This agrees with a correlation to MIS 5e dated between c. 115–130 kyr BP (Figure 3-1).

The vegetation and climate records obtained from the MIS 5e, 5c and 5a deposits at Sokli have a distinct interglacial character, being like that for the present interglacial (the Holocene) (Chapter 4), and entire MIS 5 (c. 130–71 kyr BP) is defined as the Last Interglacial Complex in the Sokli basin (Helmens 2014). This definition does not take into consideration possible differences in winter temperatures, since these are hard to reconstruct based on north European plant data, even for the Holocene. MIS 5 is also defined the Last Interglacial Complex at the famous La Grande Pile site in France (Figure 1-1). In contrast, MIS 5c and 5a are defined in the NW European mainland stratigraphy as the Brørup and Odderade Interstadials, respectively, of the Last Glacial (Figure 1-1). During

these interstadials, boreal forest developed, in contrast to the preceding Eemian Interglacial (MIS 5e) and the Holocene when temperate forest established. Helmens (2014) suggests that the absence of temperate forest in northwest-central Europe during MIS 5c and 5a is due to factors related to increased continentality, including low winter temperatures. The prevalence of interglacial conditions during the warm stages of MIS 5 as reconstructed at Sokli and La Grande Pile agrees with data from northeast-central Europe (Bolikhovskaya and Molodkov 2014). The latter results further agree with pollen records from loess-palaeosol sequences on the East European Plain, and a mollusc-based ESR (electron spin resonance) chronostratigraphy for the continental margin of northern Eurasia, indicating that during most of MIS 5 the vegetation cover in eastern Europe has evidently been of interglacial character (Molodkov and Bolikhovskaya 2009, 2010). The overall warm conditions during all three sub-stages of MIS 5 (5e, 5c, 5a) can be ascribed to higher-than-present summer insolation (Figure 1-1), with possible feedback mechanisms causing a strong decrease in winter temperature in northwest-central Europe during MIS 5c and 5a (Šeirienė et al. 2014).

The Sokli basin was glaciated during MIS 5b (Savukoski 2 cold stage of the Last Interglacial Complex), MIS 4 – early MIS 3 (Savukoski 3 Stadial) and late MIS 3 – MIS 2 (Savukoski 4 Stadial). The glacial advance that interrupts the Tulppio Interstadial Complex in mid-MIS 3 is here defined as the Saariselkä glaciation. Sokli was not glaciated during cold MIS 5d (Savukoski 1 cold stage) when strong continental conditions prevailed. Finally, two distinct cooling/drying events that interrupt the long-term climate evolution of the Nuortti warm stage (MIS 5e) have been defined the Tunturi (Helmens et al. 2015) and Värriö events (Salonen et al. 2018). The events are dated to c. 127–126 kyr BP (Tunturi event) and c. 120 kyr BP (Värriö event) based on an event-stratigraphic correlation with U/Th-dated speleothem records from Europe, including a new high-resolution stalagmite isotope record from Korallgrottan in northern Sweden (Salonen et al. 2018, Finné et al. 2019; see Chapter 4).

2.2 Multi-proxy comparisons

For the purposes of a reconnaissance study, boreholes 900–902 and 905 were subjected to a low-resolution palynological analysis and the lithology was described in detail (Helmens et al. 2000; Figure 3-1). The Sokli and Loitsana sediments were studied in detail using a multitude of biotic and abiotic environmental and climate proxies since the availability of long sediment records in 2002 (Figure 2-1).

A multi-proxy approach has many benefits over the analysis of single proxies. The analysis of multiple proxies reduces the uncertainties and limitations of single proxies. Also, it allows the reconstruction of a suite of past environmental conditions, both on the local (catchment) and regional scale. It thereby facilitates the discrimination between local versus regional signals in the proxy data. A multi-proxy analysis also serves as an important validation tool for the quantitative climate reconstruction through comparison of climate records inferred from different proxies. Comparisons between proxies further allow e.g. differences in response time between aquatic and terrestrial proxies to be assessed. Finally, in the study of the Holocene sediment sequence from Loitsana Lake, Shala (2014) notes that the response to changes in environmental conditions can be highly individualist, further promoting the use of multi-proxy studies. Despite the many advantages, the interpretation of large datasets generated by the analysis of multiple proxies is not always straightforward. Aquatic and biogeochemical proxies are influenced by a complex and often interrelated suite of environmental/climate parameters that complicates the identification of individual or main driving factors/processes. Although increasing used in Holocene and Late-Glacial reconstructions (e.g. Rosén et al. 2001, Bigler et al. 2002, Stančikaitė et al. 2015, Gałka et al. 2015, Bos et al. 2017), multi-proxy studies on pre-LGM deposits further remain rare, providing few studies for comparison. The chironomid analysis on the deposits of MIS 5e (Plikk et al. 2019), MIS 5d-c (Engels et al. 2010), MIS 5a (Helmens et al. 2021) and MIS 3 age (Engels et al. 2007) at Sokli are one of the first studies where chironomids are used for environmental and climate reconstructions on these timescales. The lakes that occupied the Sokli and Loitsana basins during the late Quaternary were relatively small and shallow and, as a result, the lake sediments are rich in a large variety of plant/animal fossil remains. In combination with biogeochemical data and detailed lithological descriptions of sediments, this has aided in the interpretation of multi-proxy data.

A similar suite of proxies was analyzed for most of the time-slices with ice-free conditions at Sokli. The proxies that are analyzed in the deposits of MIS 5e, 5d-c, 5a, mid-MIS 3 (Tulppio 1 Interstadial) and Holocene age (Loitsana Lake record) include pollen/spores, NPP's (non-pollen palynomorphs) and stomata (i.e. the palynological analysis); macrofossils, diatoms and other siliceous microfossils (e.g. phytoliths); aquatic insects (chironomids); and LOI (loss-on-ignition) and lithology. Note that stomata were not analyzed in the sediments of MIS 5d-c and mid-MIS 3 age. The MIS 5e lake sequence was additionally analyzed for C/N (carbon/nitrogen rations), FTIRS (Fourier-transform infrared spectroscopy)-inferred BSi (biogenic silica), XRF (X-ray fluorescence)-based elementary data and biomarker isotopes. C/N was also measured on the Holocene sediment sequence from Loitsana Lake, and XRF-based elementary data is available for the Early-Holocene glacial lake sediment. The new Holocene record from the Sokli mire is based on palynology, macrofossils, LOI and lithology, whereas the Tulppio 2 Interstadial sediment (mid-MIS 3) was only subjected to a combined palynological and LOI/lithology analysis.

The analysis of pollen and spores (palynology) in lake sediments has provided invaluable information on changes in vegetation and climate around the globe at different time-resolutions and for different parts of the Quaternary. There are, however, challenges in the interpretation of pollen/spore assemblages that accumulated in tundra and boreal environments. The first challenge concerns the influence of long-distance transported tree pollen in the tundra. Modern vegetation-pollen relationships studied in lake sediment (e.g. Aario 1940, Prentice 1978) show that the pollen spectra from the boreal forest are generally dominated by the forest's three main tree elements *Pinus*, *Betula* and *Picea*. Pollen percentages of *Pinus* fall gradually from pine to birch forest, to increase again at the expense of *Betula* in the tundra. The increase in representation of *Pinus* relative to *Betula* occurs as the forest thins out, and *Pinus* pollen with their greater dispersal capability are blown in from the south. Long-distance transported pollen may dominate the pollen record in the tundra, where pollen production is low, and might lead to erroneous interpretations of forested conditions. A second challenge relates to the presence of boreal wetlands. Modern pollen traps in mires (Hicks 1994) reveal the same tendency in vegetation-pollen relationship as the modern lake samples, however, traps in mires show relatively high and variable pollen percentage values of taxa such as *Salix*, *B. nana*, Ericales, Cyperaceae and Poaceae. The latter taxa are typically found in the tundra. As pollen from local wetland are often over-represented in the pollen record, this swamping has the potential of an erroneous reconstruction of tundra vegetation while the area was vegetated with boreal forest. These limitations/uncertainties of the pollen/spore analysis can be reduced by combining the analysis with macrofossils and stomata. Plant macrofossils such as seeds, leaves, bark and needles originate from the lake's immediate surroundings and provide evidence for the local presence of wetland and trees (e.g. Birks 2001). Conifer stomata, which are part of the epidermis of conifer needles, are used as evidence for local presence of individual conifer taxa as well (Sweeney 2004). Plant macrofossils can be identified to genera or species level, compared to pollen/spores that are often identified to family or genera level. However, macrofossil abundances are strongly influenced by taphonomic factors, where a long distance to the littoral/shore or to inflow of running water sharply reduces the amount of macrofossil remains in lake sediments (e.g. Hannon and Gaillard 1997, Väliranta 2006a). Therefore, the absence of a taxon in the macrofossil sample cannot be taken as proof for the absence of this taxon in the contemporary vegetation. Palynological samples further contain microfossils of various origin. Among these are spores of fungi and green algae and vegetative remains of aquatic plants. These non-pollen palynomorphs (NPP's) increase the number of paleo-environmental indicators in the palynological analysis (van Geel 2001). Among the NPP's, there are fossils that are not properly identified, but some of them nevertheless provide environmental information, where the ecological information is inferred from the co-occurrence with identified taxa and environmental parameters.

The analysis of diatoms, which are unicellular algae with shells made of amorphous biogenic silica, has a long track record in reconstructing past environmental conditions and provides information on e.g. pH, nutrients, water transparency/turbidity, turbulence, water depth/littoral conditions, water-column mixing and lake ice cover duration (e.g. Battarbee et al. 2003, Kilham et al. 1996, Weckström et al. 2014). Chironomids are aquatic insects that are identified by the head capsules of their larvae preserved in lake sediments. Like diatoms, chironomids are a long used environmental proxy (e.g. Thienemann 1954). Most recently, chironomids have evolved as a strong climate proxy (Brooks 2006, Walker and Cwynar 2006, Heiri et al. 2014, Brooks and Langdon 2014).

Among the biogeochemical proxies, C/N ratios, measured in elemental analysis, are used among others to discriminate between different sources of sedimentary organic matter. In general, high C/N ratios (> 10) indicate input of organic matter from higher plants (littoral/wetland/terrestrial), and low ratios (< 10) reflect input from phytoplankton (Wetzel 2001). Organic content measured by LOI is often used as an indicator for in-lake and catchment productivity, whereas BSi content in lake sediments is a proxy for diatom abundance and primary production (Conley and Schelske 2001). BSi was measured in the Sokli studies using Fourier-transform infrared spectroscopy (FTIRS), a method that recently has arisen as a fast and cost-effective approach to reconstruct past environmental conditions using sediments (Vogel et al. 2008, Rosén et al. 2010). However, the organic content of lake sediments is also influenced by changes in depositional environment such as influx of minerogenic sediment due to encroachment of running water or slope processes. These processes are usually traceable in core lithology and elemental composition data such as inferred through X-ray fluorescence (XRF) core scanning. Recent advancements in the XRF technique enable non-destructive, in-situ measurements at sub-millimeter scales (Croudace et al. 2006). The elementary record is influenced by factors such as source rock composition, weathering and depositional/post-depositional processes and can be used to infer changes in e.g. minerogenic input, redox processes and lake levels (Kylander et al. 2011). Finally, the isotope composition of macrophyte- and terrestrial plant-derived *n*-alkanes (lipid biomarkers) is increasing used in paleo-environmental and -climate studies (Sachs et al. 2009).

Composite diagrams with a selection of multi-proxy data are provided in Figures 3-1 (MIS 5e), 3-2 (MIS 5d-c), 3-3 (MIS 5a), 3-4 (MIS 3), 3-5 (Holocene; Loitsana Lake) and 3-6 (Holocene; Sokli wetland). Multi-proxy data obtained on the glacial lake sediments at the base of the MIS 5a and Holocene lake deposits, and the glacial lake sediment of mid-MIS 3 age, are summarized separately in Figures 3-8 to 3-10. For each of the diagrams presented in Figures 3-1 to 3-6, a common local zonation is applied to the fossil records of aquatic and telmatic plant/animal taxa. The local zonation also takes into consideration lithology and changes in biogeochemical data. The regional zonation, which is applied to the fossil record of terrestrial plant taxa, is provided with a prefix corresponding to the climate/chrono-stratigraphic unit in question. The zonations applied here largely follows those of the original papers (Table 1-2). Notably, macrofossils of plants such as *Carex*, *Juncus*, *Poaceae*, *Salix*, *Betula nana* and Ericales, for which a local wetland source can be assumed, are given in part B of the diagrams that summarizes aquatic and telmatic plant/animal taxa. In addition, the pollen/spore records of Cyperaceae, *Salix* and ferns, which mostly seem to have originated from local wetland/moist shore habitats as well (see Chapter 3), are shown here. The latter are listed in the original publications among the terrestrial plant taxa. The pollen sum on which all pollen/spore percentages are calculated, however, remain the same as in the original papers. The pollen sum is discussed in more detail, and a new pollen sum is introduced, in Chapter 4. To be noted, sample-resolution may vary between proxies and within the time-slice that was studied. Minerogenic sediment was often analyzed with a relatively low sample resolution considering the relatively short time duration represented by this sediment. In contrast, as an example, the sediment intervals that represent the millennial-duration Tunturi and Värriö climate events (MIS 5e) are analyzed at high resolution.

2.3 Climate reconstruction methods

Two methods are used to quantitatively infer climate from the Sokli fossil datasets. These are the climate indicator plant species method and the transfer function approach. The first method follows Iversen (1954) and Kolstrup (1980) and makes use of individual plant species, which present-day northern distribution limits show a strong correlation to mean July air temperature. The latter value is used as a minimum mean July temperature (min. T_{jul}) required by the plant in order to flower and reproduce. The plant species are mostly identified by their macrofossils, although some were identified by pollen or NPPs.

The transfer function approach is applied to fossil assemblages (Birks 2003, Birks et al. 2010). It uses a calibration set linked to current meteorological data. The calibration set consists of modern assemblages analyzed in surface sediment from a series of lakes situated along a gradient that covers changes in the parameter of interest, in this study mostly mean air July temperature (T_{jul}). The established relationship between the modern assemblages and current climate is used in combination with the fossil

data to model past changes in T_{jul}. At Sokli, the transfer function approach has been applied to fossil pollen and chironomid assemblages and occasionally diatom assemblages. The focus here is on the pollen-inferred T_{jul}, whereas references are made to the chironomid-based reconstructions. Similar as plants, chironomids show a close relationship with mean July air temperatures (e.g Walker et al. 1991a, 1991b, Brooks et al. 2007) and have been used to develop chironomid-T_{jul} transfer functions for different parts of northern Europe (e.g. Olander et al. 1999, Larocque et al. 2001, Luoto 2009).

2.3.1 Climate indicator plant species

Minimum mean July air temperatures (min. T_{jul}) presented here follow the approach introduced in Väliranta et al. (2015). In this protocol, current plant species distribution data in Finland are linked to measured meteorological data over a T_{jul} gradient from c. 7.5 to 17 °C. This gradient spans over several bioclimatic zones from hemiboreal, via boreal to subarctic and many plant species reach their northern distribution limit within this gradient. Only in the northernmost part of the country, the plant distributions are constrained by altitude-related (orohemiarctic) factors. A unique modern spatial species-specific plant distribution dataset (http://www.luomus.fi/kasviatlas) covers the whole Finland and is subject to continuous botanical surveys. Long-term meteorological climate normal data are readily available. Thus, the plant distribution database can be used to correlate modern species distributions with climate. These factors provide an excellent setting to exploit observed modern plant species-temperature relationships for paleo-temperature reconstructions.

A total of 15 climate indicator plant species with a current clear northern distribution limit strongly related to T_{jul} were identified in the Sokli fossil datasets (Table 5-1). For each taxon, current T_{jul} is interpolated over a 10×10 km grid cell and several grid cells are analyzed containing the taxon occurrence along its northern distribution boundary. A median T_{jul} and T_{jul} range, i.e. the lowest and highest value along the species-specific distribution boundary in the grid cells, are calculated. The mean value integrates all July temperature values, i.e. also for those occurrences that may be located in unusually favourable microhabitats and exceptionaly ideal microclimates. The climate normal period of the meteorological data is 1970–2000 (Venäläinen et al. 2005) and the botanical survey data used is limited to this period as well (Lampinen and Lahti 2012).

It should be stressed that the T_{jul} values inferred from the indicator plant species are minimum values only, which implies that the true paleo-July temperatures may have been (considerably) higher. In addition, since most indicator species are identified by means of macrofossils, which occurrences are sporadic (see Section 2.2), the paleo-climate record is discontinuous.

2.3.2 Pollen-based climate reconstructions

Pollen-based T_{jul} reconstructions were earlier performed using a combined pollen-climate calibration dataset from Finland, Norway and northern Sweden (deposit of MIS 3 age; Seppä and Birks 2001), and two different ones, i.e. one from Finland and direct surroundings and another from a more continental region in northwestern Russia (Holocene, MIS 5d-c; Salonen et al. 2012, 2013). Transfer functions were developed by means of weighted averaging-partial least squares regression (WA-PLS; ter Braak and Juggins 1993).

In this report, all reconstructions follow the approach of Salonen et al. (2018, 2019). These studies present a new pollen-climate calibration dataset, synthesized based on the European Modern Pollen Database (EMPD; Davis et al. 2013), and uses an ensemble of pollen-climate calibration models including classical and machine-learning approaches. The dataset extends the calibration lakes of Seppä and Birks (2001) and Salonen et al. (2012, 2013) with modern lake samples from the European mainland and the British Isles. Lakes are excluded from semi-arid and dry-summer climates to focus the pollen-climate modelling on plant taxa that are likely components in the northern European vegetation during the late Quaternary. The final dataset includes 807 lakes and modern climate data are extracted for each lake using the CRU CL v. 2.0 modern climate dataset for 1961–1990 (New et al. 2002). Salonen et al. (2018, 2019) use six different methods to create pollen-climate models. These are WA-PLS (ter Braak and Juggins 1993) and weighted averaging regression (WA; Birks et al. 1990); maximum likelihood response curves (MLRC; Birks et al. 1990); the modern analogue technique (MAT; Overpeck et al. 1985); and two machine-learning approaches based on regression tree ensembles, i.e. the random forest (RF; Breiman 2001) and the boosted regression tree (BRT; De'ath 2007).

The climate reconstruction is summarized as a median of all six reconstructions. To estimate the likelihood of non-analogue errors, the compositional distance (squared chord distance) between each fossil pollen sample and the best matching modern pollen calibration sample is calculated (Overpeck et al. 1985, Birks 1998).

In addition to the reconstructions of T_{jul}, mean January temperatures (T_{jan}) are estimated based on the MIS 5e pollen record. These climate parameters (T_{jul}, T_{jan}) are chosen due to their ecological influence on vegetation and their low correlation (r = 0.27) in the calibration data (Salonen et al. 2018), facilitating the modelling of the independent effects of each variable (cf. Juggins 2013). Nevertheless, analyses of northern European surface pollen data show summer temperature to be the dominant ecological driver. In significance testing using a redundancy analysis permutation test (Telford and Birks 2011), the T_{jul} reconstruction is significant (p = 0.001), while for the T_{jan} reconstruction a significant result (p = 0.011) is yielded for part of the MIS 5e record, covering a long and stable T_{jan} increase across the upper c. 60 % of the MIS 5e sequence. Reconstruction errors, estimated by 10-fold cross validations, are in the range of 1.12–2.05 °C for the T_{jul} reconstructions, and 1.79–3.44 °C for the MIS 5e T_{jan} estimates, depending on the calibration model. Pollen-based T_{jan} reconstructions are not performed for the other time-intervals represented in the Sokli sequence. The pollen records for these periods are derived from smaller and shallower lakes than the lake of MIS 5e age, resulting in noise caused by pollen contributions from local wetland habitats.

The pollen-based climate reconstructions are evaluated in the light of local (azonal) changes and site-specific conditions, as reconstructed in detail in Chapter 3, since these factors have the potential of significantly influencing the fossil pollen assemblages and thereby biasing/corrupting the climate estimates. Notably, the chironomid-based climate reconstructions have also been extensively validated against the lake histories (Engels et al. 2007, 2010, Shala et al. 2017, Plikk et al. 2019, Helmens et al. 2021). As a final validation, the climate estimates inferred from different proxies are compared.

3 Reconstructions of environmental changes within the Sokli and Loitsana basins

This chapter provides a detailed summary of changes in late Quaternary depositional environments within the Sokli and Loitsana basins, and associated developments in local aquatic and telmatic (i.e. the transitional habitat zone from aquatic to terrestrial) ecosystems, which have been inferred from the sedimentary sequences and their fossil records. These environmental reconstructions were made in first instance to separate local drivers (acting at the lake/catchment level) from regional climate, thereby increasing the accuracy of the regional vegetation (Chapter 4) and climate reconstructions (Chapter 5). The reconstructions presented in this chapter, by themselves, have resulted in exceptionally detailed accounts on the environmental histories of a variety of lake types of different ages, and different fluvial regimes, as well as of contemporary compositions/successions in aquatic and telmatic plant/animal communities. The environmental reconstructions also provide qualitative information on climate, in particularly changes in degree of continentality, which complement the quantitative climate reconstructions of Chapter 5.

Four organic-bearing lake deposits are represented in the late Quaternary sedimentary infills of the Sokli and Loitsana basins, dated to MIS 5e (Nuortti warm stage), 5c (Sokli I warm stage), 5a (Sokli II warm stage) and the Holocene (Figures 1-1 and 2-1). The oxbow lake of MIS 5c age forms part of a fluvial regime that prevailed in the Sokli basin during MIS 5d-c. In addition, thick minerogenic sediment beds of glacio-lacustrine origin, deposited in the Sokli Ice Lake during deglaciation, occur at the base of the MIS 5e, 5a and Holocene lake sediment sequences as well as interbedded in the till sequence of MIS 4-2 age (Tulppio 1 Interstadial of mid-MIS 3 age). All these lacustrine and fluvial deposits have been subjected to detailed multi-proxy analyses. In addition, the Holocene peat deposit in the Sokliaapa (mire) in the Sokli basin is studied here. Glacial lakes occupied large areas along the retreating margins of the Northern Hemisphere ice sheets; however, fossils in glacial lake sediments have been rarely analyzed in detail. The generally low fossil content and often broken/corroded nature of the fossil remains made these analyses particularly time-consuming. Note that developments in the Sokli Ice Lake during the MIS 5a, 3 and Holocene deglaciations are dealt with separatedly at the end of this chapter (Section 3.6).

The fossil remains of aquatic and telmatic plant and animal taxa are shown together in the parts B of the multi-proxy diagrams in Figures 3-1 to 3-6 and in the diagrams of Figures 3-8 to 3-10. A common zonation is applied to each diagram that also takes into consideration changes in lithology and biogeochemical data. This integration of proxy data allows concise and consistent descriptions of communal changes, and changes in sedimentation, through time and facilitate the identification of driving mechanisms. Various proxies are also combined in the original publications to describe/interpret the environmental records (Table 1-2) and the local zonations applied here largely follow those of the original papers. Furthermore, the interpretations presented in this chapter largely follow the original papers.

The four lake deposits/fossil records represented in the Sokli and Loitsana sedimentary sequences have one driving mechanism in common, i.e. lake infilling. The different origins of the lakes, however, also resulted in a set of drivers that are quite unique to each lake. These include changes in mixing (Nuortti lake) and flooding regimes (Sokli I oxbow lake and associated fluvial sediments of MIS 5d-c age), wetland expansion and encroachment of running water (Sokli II lake), and input of flowing water from various sources (river versus groundwater from esker; Holocene Loitsana Lake). Not all mechanisms that drive the environmental records are solely related to local dynamics, but climate played a role as well. Identifying the climate signal has contributed to the climate reconstructions presented in Chapter 5. At the same time, the identification of marginal wetland zones has facilitated the reconstruction of regional vegetation development (Chapter 4) and contributed to the evaluation of the pollen-based climate reconstructions. Equally important, the detailed local environmental records have allowed an evaluation of the chironomid-inferred climate estimates. Finally, the littoral/wetland habitats described here hosted a number of plant species that are used as climate indicators (Chapter 5).

The unique character and chronology of each lake record provide strong evidence that the late Quaternary deposits at Sokli occur in-situ and that fossil remains are not re-deposited as suggested in Forsström (1990). Furthermore, there is no evidence for a domino-like stacking of glacio-tectonically upthrusted sediment wedges as suggested by P.L. Gibbard in Otvos (2015).

3.1 The Nuortti warm stage (MIS 5e) lake

A steep depression was carved out in the deeply weathered and fragtured rocks of the Sokli Carbonatite Massif (SCM) during the Penultimate Glaciation (MIS 6). The ice-divide zone of the Fennoscandian Ice Sheet was situated at this time over the northernmost part of Finland. This ice-sheet configuration would have allowed for more glacial erosion at Sokli than during the Last Glacial Maximum (LGM; MIS 2) when the divide was located over Sokli/central Finnish Lapland (Johansson 1995). At least 9 m of diatom gyttja accumulated in the Sokli basin during the Nuortti warm stage (MIS 5e) of the Last Interglacial Complex (MIS 5) (Figure 3-1). The original thickness of this lacustrine deposit, however, might have significantly exceeded the 9 m recorded in borehole 2/2010 (Figure 2-1). It is likely that the sediments were compressed by the weight of the ice-sheet during younger phases of glaciation (see also Section 3.3).

High percentage values of planktonic diatoms and the representation of the diatom genus *Cyclotella* in the fossil record (Figure 3-1B) indicate that the Nuortti lake was initially deep and stratified. The presence of an early, stratified lake with regularly anoxic bottom conditions is supported by the preservation of laminations in the lower part of the sediment record (indicating low levels of bioturbation). The sediment and fossil records for the upper part of the diatom gyttja deposit reveal an increasingly shallowing lake. Light yellowish spots marking the deposit's uppermost part have been interpreted as a sign of desiccation caused by subaerial exposure or bottom freezing (Björck et al. 2000). The diatom gyttja becomes interlayered with sand near the top of the sequence and then turns to fluvial sands and gravels. The latter transition is conformable (i.e. non-erosive) in the B-series borehole and it is at this coring location (location 1) that the final birch forest phase of the Nuortti warm stage (zone Nu-VII; Figure 3-1A) is recorded (borehole 901). The early birch phase (zone Nu-I) occurred when over 3 m of silty-sandy glacio-lacustrine sediment was deposited in the earliest part of the stage. The latter sediment shows multiple upward-fining sequences of sand grading into silt or clay, probably representing a series of glacier meltwater pulses. A massive silt layer, deposited upon a more distal position of the ice-margin, occurs at the top of the glacial lake sequence.

The Nuortti diatom gyttja deposit is characterized by a rich algal record consisting of diatoms and green algae. The percentage of biogenic silica (BSi) in the sediment is high, on average some 40 %. Diatom fossils are well-preserved and species of Fragilariaceae are found in their colonial form, as chains. Characteristically, planktonic diatoms are nearly equally abundant to, or dominate over, benthic diatoms throughout the main part of the lake sequence. *Pediastrum* and *Tetraëdron minimum* dominate the green algal record. *T. minimum* re-occurs with peak values in the order of 2 000–11 000 % (calculated based on the Pollen Sum). *Pediastrum* is represented by six species of which *P. boryanum* v. *pseudo-glabrum* reaches 1 400 % in the uppermost part of the sequence; total *Pediastrum* concentrations amount here to over 16 000 colonies/cm^3 sediment. In contrast, the chironomid assemblage is dominated by only two species. These are *Corynocera ambigua*, an oligo-mesotrophic taxon associated with clear, alkaline waters with a dense cover of submerged macrophytes, and *Cladotanytarsus mancus*-T, a mesotrophic warm-indicating taxon (Olander et al. 1999, Brodersen and Lindegaard 1999). Chironomid concentrations range from close to zero to 300 headcapsules/gram sediment. Plant macrofossils are near absent from the fossil record. The scarcity of macrofossil remains of plants, and the generally low representation of wetland plants in the microfossil record, suggest that the lake maintained a large open-water body throughout a major part of its infilling history. It also shows that the lake-bathometry was probably steep, due to pre-glacial, differential weathering of the carbonatite bedrock. The organic content of the diatom gyttja deposit, measured by loss-on-ignition (LOI), averages at about 20 %. Carbon/nitrogen (C/N) ratios, mostly at 15–20, suggest an equally large input of aquatic and terrestrial organic matter.

The fossil record of the Nuortti lake deposit, e.g. with a distinct representation of the nutrient-demanding diatom genus *Stephanodiscus*, indicate a relatively large influence of the SCM on the aquatic ecosystem and a warm climate. Similarly, changes in nutrient conditions were an important factor driving compositional changes in aquatic assemblages through time. The nutrient levels seem to, for an important part, relate to changes in mixing regime resulting from long- and short-term changes in climate and lake infilling.

A Nuortti warm stage (MIS 5e) (Last Interglacial Complex)
Terrestrial plant taxa

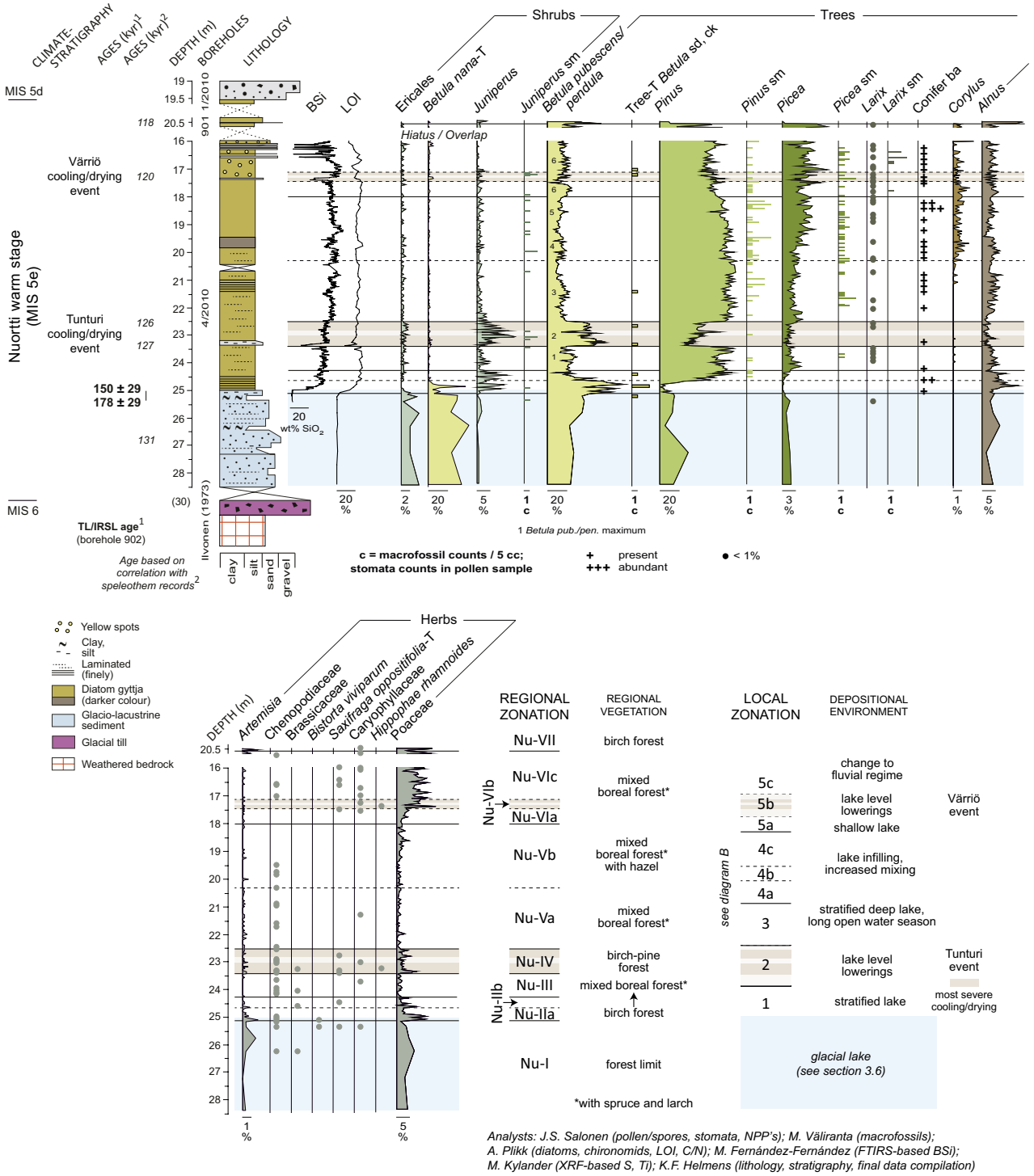

Figure 3-1. *Selection of environmental and climate proxies for the Nuortti warm stage (MIS 5e) lake deposit in the Sokli basin based on Plikk et al. (2016, 2019, 2021), Salonen et al. (2018) and Kylander et al. (2018). Fossil remains of terrestrial plant taxa are summarized above (part A) and of aquatic and telmatic taxa below (B). Core lithology and biogeochemistry are given in both A and B. Part A further shows the climate/chrono-stratigraphy and absolute chronology. Developments in regional vegetation and the regional zonation, and in depositional environment and local zonation, are summarized together in the lower part of A. Abbreviations used for fossil remains: as=astrosclereid; ba=bark; bd=bud scale; car=caryopses; ck:=catkin scale; ct=conductive tissue; ed=epidermis; ep=ephippia; f=fruit; fc=frontoclypeus; hb=hair base cell; hc=head capsule; l=leave; ls=leave spike; lv=leavy stem; ms=megaspore; nl=needle; nt=nutlet; oo=oogonia; os=oospore; pr=perigynia; red=rooth epidermis; rs=resting spore; sb=statoblast; sc=scale; sd=seed; sg=sporangia; sl=spindle; sm=stomata; sp=spore; sr=sterigmata; st=stem; t=tissue; tr=tooth remain; tw=twig; vr= vegetative remain; wi=wing.*

B Nuortti warm stage (MIS 5e) (Last Interglacial Complex)
Aquatic and telmatic taxa

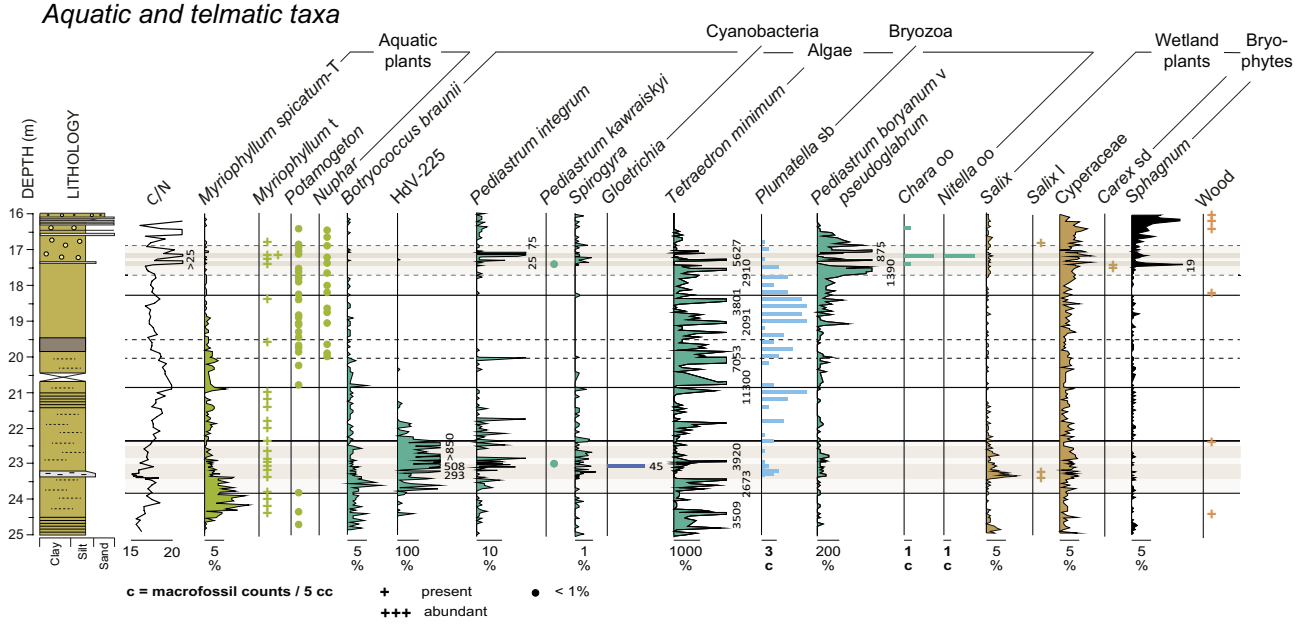

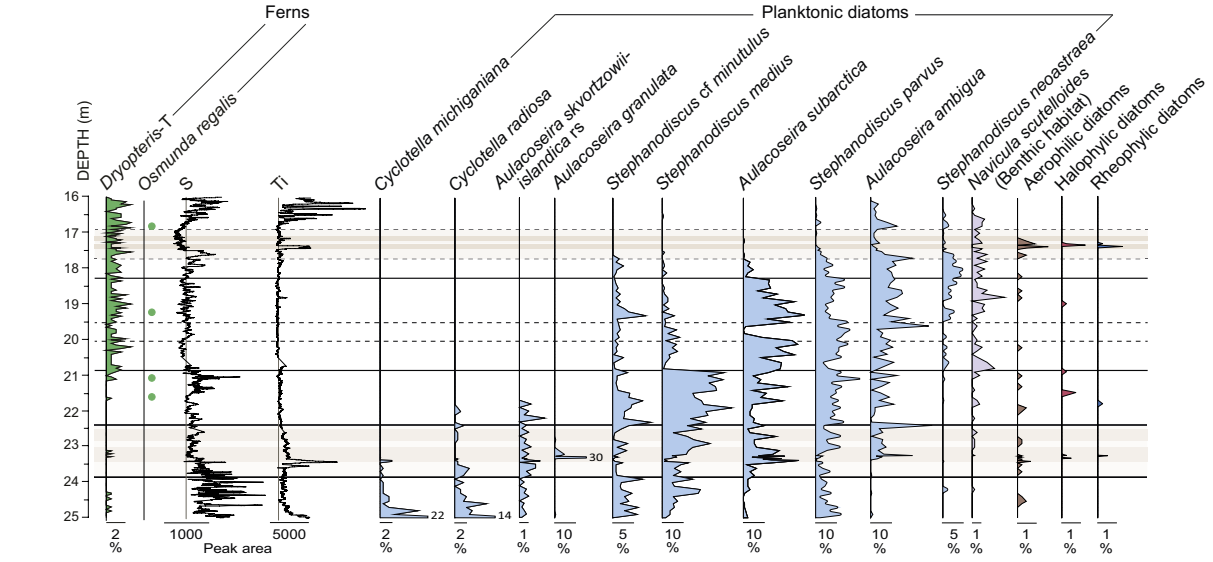

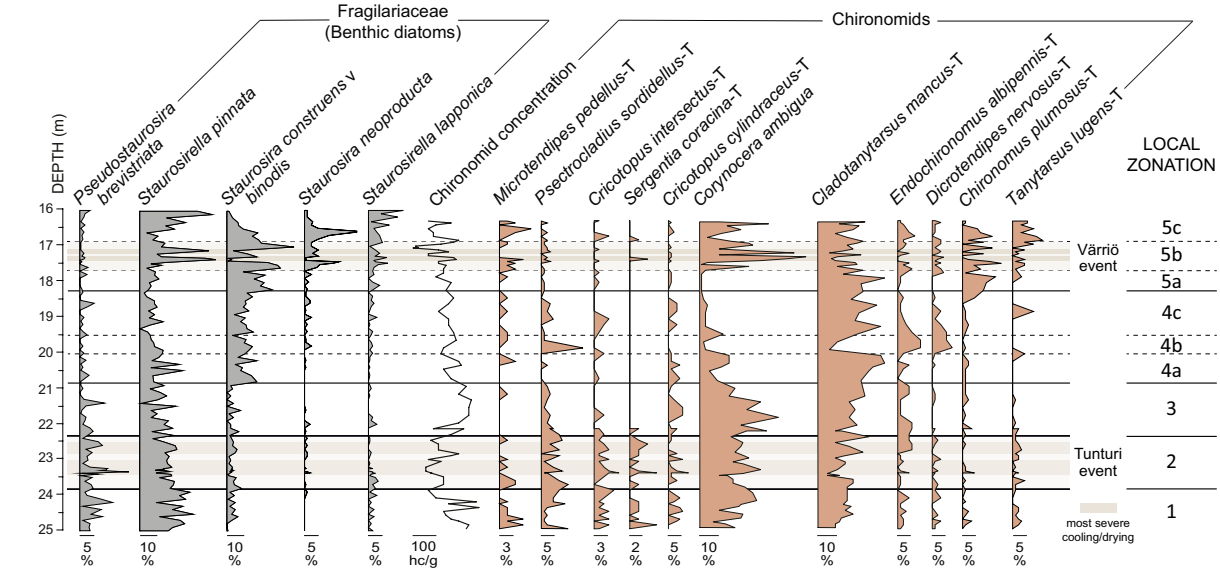

Figure 3-1. *Cont.*

3.1.1 Long-term changes in mixing regime and lake infilling

The laminations in the lower half of the Nuortti lake sequence are interpreted by Plikk et al. (2016) as possibly consisting of iron hydroxide and iron sulfide precipitates as described in Renberg (1981). These laminations can form and be preserved in high latitude lakes that are dimictic and sufficiently productive for anoxia to develop in the hypolimnion (i.e. the cold bottom waters) during the stagnation periods. Plikk et al. (2016) make this interpretation based on a high correlation of sulfur (S) and iron (Fe) in the XRF data, and their enhanced values in the lower laminated portion of the diatom gyttja sequence. Kylander et al. (2018) give an alternative interpretation of the geochemical data and propose that the increases in S and Fe, as well as manganese (Mn) and calcium (Ca), describe greater inputs of non-carbonaceous detrital material from SCM rock types typically rich in mainly S and Fe, but also Ca and Mn. However, the latter study comes to the same conclusion as Plikk et al. (2016) in that periods preserving laminations most likely had conditions that were more anoxic.

The fossil record in the laminated sediments shows a distinct increase in nutrient availability upwards in the sequence. It starts in local zone 1, continues on average during the Tunturi event (local zone 2), and culminates during the upper part of local zone 3. The pioneering green alga *Botryococcus braunii* is well-represented during local zone 1. In the lower part of the zone, it is accompanied by high percentage values of the oligo-mesotrophic diatoms *Cyclotella michiganiana* and *C. radiosa*, and *Tetraëdron minimum*. *T. minimum* is commonly reported from open waters of eutrophic lakes since the Holocene thermal maximum (Jankovská and Komárek 2000), though it is also found in oligotrophic lakes in northern Finland (Forsström et al. 2005, Weckström et al. 2010). In the upper part of local zone 1, nutrient-demanding (phosphate (P)) *Stephanodiscus* (*S.* cf *minutulus, S. medius*) increase and high pollen percentage values are recorded for *Myriophyllum spicatum*-type (including *M. verticillatum* and *M. sibiricum*). The latter are submerged aquatic plants that presently occur in sheltered waters of eutrophic lakes or in Ca-rich waters. This early rise in nutrient conditions coincides with a major change in regional vegetation, i.e. from open birch forest to a mixed boreal forest with spruce and larch (zones Nu-II and -III). It probably, at least partly (see below), results from soil development, causing external nutrient load to the lake due to enhanced weathering (Fritz and Anderson 2013). Strontium (Sr) on average increases in the elemental data throughout major part of the diatom gyttja deposit, suggesting increasing chemical weathering (Cohen 2003, Zeng et al. 2013). The increase in LOI during local zone 1, and decrease in titanium (Ti; proxy for minerogenic input), can be ascribed to the stabilization of the catchment through closure of the soil cover.

S. medius dominates the planktonic diatom assemblage during local zone 3 and, together with enhanced representations of *S.* cf *minutulus* and *S. parvus,* and high BSi values, reflect a now highly productive, nutrient-rich lake (Bradbury 1988, Kilham et al. 1996). Peak values of *Corynocera ambigua* suggest clear and/or alkaline waters and chironomid concentrations are high. The overall low values of *T. minimum* during local zone 3, and in the upper part of local zone 1, possibly reflect a lower competitive ability of this species under nutrient-rich (high P) conditions.

The overall increase in nutrient levels during local zones 1-3 might be the result of a climate-induced change in mixing regime. The absence of autumn-blooming diatoms such as *A. ambigua*, and the dominance of benthic Fragilariaceae over planktonic diatoms, suggest that the mixing periods were short during local zone 1 (Lotter and Bigler 2000). This possibly results from a pronounced seasonality with long cold winters and short warm summers. Warm summers during local zone 1 are supported by *C. michiganiana* and *C. radiosa*, i.e. diatoms favoured by deep, warm waters and stable summer stratification (Stoermer 1993, Wolin 1996, Whitlock et al. 2012). In contrast, the increase in the planktonic/benthic diatom ratio in local zone 3 may reflect an increase in the length of the growing season (Lotter and Bigler 2000). This can possibly be associated with shorter winters leading to an early ice-out, conditions favourable to *S. medius* and *S. minutulus.* These diatom taxa bloom during early spring when P is regenerated from the hypolimnion (Bradbury 1988, Bradbury and Dieterich-Rurup 1993, Interlandi et al. 1999, Bracht et al. 2008. When also taking into consideration the presence of the autumn-blooming *A. ambigua* in local zone 3, the increased trophic state during this zone might be attributed to strong internal P loading, resulting from prolonged mixing in combination with pronounced summer stratification related to warm summers. The pollen assemblages during local zone 3 (zone NU-Va) reconstruct mean July temperatures that surpass the present-day value by several degrees and an increase in winter temperatures (Salonen et al. 2018). Interestingly, resting spores of *A. skvortzowii-islandica* disappear from the fossil record during local zone 3. Originally thought to be endemic of Lake Baikal in eastern Russia (Edlund et al. 1996), the presence of *A. skvortzowii-islandica* in the early Nuortti lake might reflect the continental climate regime of eastern Russia.

A marked change in the aquatic ecosystem occurs at the transition from local zone 3 to 4. *S. medius* is replaced by the Si-demanding *Aulacoseira subarctica* as the dominant planktonic diatom taxon while *A. ambigua* increases its representation. *T. minimum* re-occurs with high values and *Cladotanytarsus mancus*-T becomes the dominant chironomid taxon. The sediment record shows a transition to non-laminated sediment. The change in the algal community suggests less effective internal loading of P related to increased mixing and decreased bottom-water anoxia. This in turn could be caused by a change towards a cooler climate and/or a reduction in water depth, i.e. factors reducing the summer thermocline stability. A transition to shallower water at the base of local zone 4 is suggested by an increase of periphyton (i.e. diatoms attached to plants) such as *Navicula scutelloides* and *Staurosira construens* v. *binodis*. In addition, pollen of the aquatic plants *Potamogeton* and *Nuphar*, spores of ferns, and stomata of conifers (*Pinus, Picea*) become (near) continuously recorded from the lower part of local zone 4 onwards, suggesting a shallowing of the lake, a closer proximity to the littoral, and an increased influence of the lake's surroundings. The apparent reduction in water depth is most probably related to progressive lake infilling. The strongly reduced representation of the chironomid taxon *C. ambigua* might indicate a change to more turbid (less transparent) water conditions. The lake, however, remained productive, and P likely continued to be recycled from the lake sediment, as indicated by high BSi values, decreasing C/N values, a distinct representation of the bryozoan *Plumatella*, and high percentage values of eutrophic *S. parvus*.

S. construens v. *binodis* shows another rise in percentage values at the base of local zone 5 and, together with an increase in planktonic diatoms common in shallow lakes and near-shore areas of deeper lakes (e.g. *S. neoastraea*), indicate a further decrease in lake water depth. At the top of the lake sequence (local zone 5c), the littoral diatom taxon *Staurosirella pinnata* and chironomid taxon *Microtendipes pedellus*-T increase, pollen values of sedges (Cyperaceae) are enhanced, and stomata of *Larix* become well-represented in the fossil record, reflecting a now very shallow, overgrowing lake. It is likely that also the high grass (Poaceae) pollen percentage values (Figure 3-1A) originate from a local wetland zone. *Chironomus plumosus*-T is well-represented during local zones 5a and 5c, as well as during the milder phases of the Värriö climate event (local zone 5b). It suggests shallow eutrophic lake water conditions with low oxygen levels (Brooks et al. 2007). *S. pinnata* is known to tolerate rapidly changing environments and often dominates shallow waters with sandy substrates (Haworth 1976, Jones and Birks 2004). Although *Tanytarsus lugens* is a classical cold indicator taxon (Brooks 2006, Self et al. 2011), the enhanced representation of this chironomid taxon in the upper sandy sediment probably reflects it pioneer character in coarse substrates as well (Axford et al. 2009, Luoto and Sarmaja-Korjonen 2011).

3.1.2 Millennial-scale events

The long-term lake development described above is interrupted by two millennial-scale climate perturbations, i.e. the early Nuortti Tunturi and late Nuortti Värriö events. Both climate events left a profound imprint on the multi-proxy record.

The most prominent change in regional vegetation is recorded during the Tunturi event. The mixed boreal forest that developed early in the Nuortti warm stage was replaced by open, subarctic birch-dominated forest (zone Nu-IV). The change in vegetation was abrupt, had a step-wise recovery, and indicates a summer cooling in the order of 2 °C (see Chapter 5). A brief recovery phase with sharply increasing *Pinus* pollen values intersects the two main cooling phases. In contrast to the regional vegetation, the aquatic proxies show an earlier response to the climate perturbation, and a slightly longer duration of the Tunturi event, defined here as local zone 2.

Local zone 2 is defined by high percentage values of type HdV-225. This unidentified algal spore type is recorded in Late-Glacial and Early Holocene lake sediments from Europe and Canada where it is associated with dynamic conditions (e.g. shallow/fluctuating water levels; van Geel et al. 1989, Boyd et al. 2003). At Sokli, it occurs in the lake sediments of early MIS 5a age (Helmens et al. 2021) and in minerogenic sediment of fluvial (Helmens et al. 2012) and glacio-lacustrine origin (Bos et al. 2009, Shala et al. 2014b, Helmens et al. 2018; this study). In the Nuortti lake sequence, minerogenic input ((Ti) is enhanced throughout local zone 2 and, together with the recording of plant taxa that tolerate an unstable soil cover (*Juniperus, Hippophaë rhamnoides*), is ascribed to increased soil erosion. *Psectrocladius sordidellus*-T is well-represented during the milder phases of local zone 2. This chironomid taxon is associated with submerged macrophytes (Tarkowska-Kukuryk 2014, Salgado et al. 2018). Chironomid concentrations are typically low. Furthermore, at the base of local zone 2,

B. braunni shows peak values, *T. minimum* returns in the fossil record, and *Pediastrum integrum* increases. The latter green alga is associated with cold, oligotrophic waters of lakes and swamps (Komárek and Jankovská 2001, Sarmaja-Korjonen et al. 2006, Weckström et al. 2010). Collectively, the aquatic community change at the base of zone 2 suggests a decrease in trophic status, a decline in lake-water temperature, increased influence of shallow water environments and, overall, a more dynamic local environment.

The most pronounced impact of the Tunturi event on the aquatic ecosystem is recorded during the two coldest phases with birch forest, particularly during the earliest one. All three dominant *Stephanodiscus* species (*S.* cf *minutulus*, *S. medius*, *S. parvus*) (nearly) disappear from the fossil record and are replaced by *A. subarctica* and *A. ambigua*, suggesting a breakdown of the thermal summer stratification. Minor increases in Fragilariaceae (e.g. *Pseudostaurosira brevistriata*) may indicate lake level lowering, but also prolonged period of ice cover (Lotter and Bigler 2000). At the same time, hyper-eutrophic *A. granulata* and the cyanobacteria *Gloeotrichia* show peak values. The peaks directly follow a distinct increase in minerogenic input. As such, the imbalance in P/N ratio reflected by these two taxa is probably the result of increased nutrient loading connected with soil erosion. Similar increases in high nutrient species (e.g. *A. granulata* and *Gloeotrichia*) and minerogenic input are recorded during the Younger Dryas and the Little Ice Age in Europe (Björck et al. 2000, Rioual et al. 2007, Cvetkoska et al. 2014, Pędziszewska et al. 2015, Zawiska et al. 2015).

Several more features in the fossil record suggest drops in lake level during the birch phases. These include peaks in the shallow-water green alga *Spirogyra*; occurences of aerophilic and halophilic diatoms; and increased pollen percentage values of telmatic *Salix* (also macrofossils present) and Cyperaceae. Notably, although *Juniperus* is well-represented in the pollen record during the Tunturi event, pollen values are lower during the coldest phases compared to the intermediate milder phase. The shrub *Juniperus* is known to be frost-susceptible and prefers a winter snow-cover (Iversen 1954, Lauber and Wagner 1998). Its decreased values during the cooling peaks may therefore indicate relatively dry climatic conditions.

The late Nuortti Värrio event shows a similar structure as the Tunturi event, including two phases with severe conditions being preceded, intersected and followed by milder intervals (zone Nu-VIb; local zone 5b). However, whereas the Tunturi event shows the most pronounced, cooling-induced changes in regional vegetation, the Värriö event provides the most distinct evidence for drying-induced lake level drops. This might be due to a relatively close location of the Sokli site to a major ecotone (forest limit; see Chapter 4) at the start of the Tunturi event, whereas the Värriö event took place in an already shallow lake. In other words, both events might have experienced cooling and drying in a similar way, but the Tunturi proxy record might be more sensitive in revealing changes in regional vegetation and the Värriö event in lake level changes. Alternatively, the Tunturi event was mainly summer cold and the Värriö event mostly winter cold and dry (Section 4.6).

Planktonic diatoms mostly disappear from the fossil record at the base of local zone 5b, to return again, although in much lower values, at the base of local zone 5c. The periphyton *S. construens* v. *binodis* further increases and *Pediastrum boryanum* v. *pseudoglabrum* shows a sharp increase. Both taxa are associated with shallow, macrophyte-rich, eutrophic environments (Bradbury and Winter 1976, Cronberg 1982). Evidence for even shallower waters during the two most severe phases of the Värriö event include peak values for littoral *S. pinnata*; minor peaks in *Spirogyra*; occurences of aerophilic, halophilic and rheophylic diatoms; and increased pollen percentage values of Cyperaceae (*Carex* macrofossils present) and Poaceae. The two most severe phases further show high percentage values of *C. ambigua*, reaching almost 60 %, and peak values for *Sphagnum*. The strong representations of *C. ambigua* might reflect alkaline water conditions in the now strongly reduced lake water volumes (see also Section 3.6). The spores of the bryophyte *Sphagnum*, with peak values mirroring the Ti record, probably originated from the catchment. *Sphagnum* spore percentages also strongly increase in the upper sandy sediment of local zone 5c, and concur here with wood remains and high C/N ratios, reflecting a shallow lake and increased influence of the lake's surroundings/catchment.

In addition to reductions in water depths during the Tunturi and Värriö events, a sudden drop in lake level is recorded during local zone 4b. The local zone is characterized by sudden increases in *P. sordidellus*-T, *Endochironomus albipennis*-T and *Dicrotendipes nervosus*-T. This chironomid assemblage, together with the enhanced representation of *S. parvus*, suggests shallow, eutrophic and macrophyte-rich waters.

3.2 Fluvial dynamics during the Savukoski 1 cold stage (MIS 5d) and Sokli I warm stage (MIS 5c)

Following the infilling of the Nuortti lake, a fluvial regime prevailed in the Sokli basin during the Savukoski 1 cold stage (MIS 5d) and Sokli I warm stage (MIS 5c) of the Last Interglacial Complex (MIS 5). Presently, the Sokli wetland is drained by a small rivulet called the Soklioja. The location of Sokli on the main water divide, separating the drainage basins of the Baltic Sea in the southwest and the Arctic Ocean to the northeast, however, makes it prone to changes in the local drainage pattern due to differential post-glacial rebound. It is possible that the Yli-Nourtti earlier flowed through the Sokli basin in a northeastern direction. This river drains the low mountains of the Värriö Tunturit and has a broader floodplain (Figures 1-3 and 3-7).

The c. 7.5 m-thick fluvial sequence dated to the Savukoski 1 cold stage and Sokli I warm stage was studied at coring location 1, where the multi-proxy analyses were carried on the B-series borehole (Figures 1-3 and 2-1). The lowermost c. 2 m of fluvial sediment has the most coarse-grained lithology and, apart from a few samples of silty sediment, was not included in the fossil analysis. It consists of two fining-upward sequences in which a diamicton of sand and sub-angular rock fragments, reaching cobble size, grades into sand (Figure 3-2). The sediment is also most coarse-grained at the base of the fluvial sequence in borehole 4/2010, but overall fines-up from gravelly to sandy sediment, lacking the diamict intercalations. The upper c. 2 m of minerogenic sediment deposited during Savukoski 1 consists of sorted sands and silts and has a relatively rich fossil content. The sediment and fossil record depict a dynamic depositional environment, with frequent changes in the position of watercourses, suggesting a braided river pattern. The latter is supported by the presence of steppe-tundra vegetation as inferred from the regional pollen record (zone Sa1-I; Figure 3-2A). This vegetation type implies a continental climate regime with low precipitation values and, probably, a relatively large sediment supply due to an incomplete soil cover, i.e. conditions leading to a braided fluvial pattern.

The uppermost c. 3.5 m of fluvial sediment was deposited during the Sokli I warm stage. It predominantly consists of organic-rich sediment with LOI values reaching 20–30 %. The sandy gyttja accumulated in an oxbow lake, after which stream channel deposition prevailed. The regional pollen record shows an interglacial vegetation development to mixed boreal forest with spruce and larch (zones SoI-I to –III). The change from a dynamic, braided fluvial pattern during the Savukoski 1 cold stage to a meandering river pattern with prolonged sedimentation in an oxbow lake during the Sokli I warm stage was probably caused by an increase in atmospheric humidity as the climate changed from a continental to a more oceanic regime. The fluvial sequence is abruptly overlain by glacial till and is most probably truncated at the top.

The fluvial sequence, especially the upper organic-bearing portion, has an exceptionally rich and abundant macrofossil content. Characteristically, it includes the fossil remains of a variety of (aquatic) insects living in running water (stream-inhabiting chironomids, Ephemeroptera, Simuliidae, Sciaridae) and (semi-) terrestrial habitats (*Metriocnemus eurynotus, Limnophyes*) (Figure 3-2B). Notably, sediments deposited in low energy environments have relatively large abundances of stream-inhabiting taxa. In contrast, those sediments interpreted as being deposited under running water conditions are almost devoid of these fossils. The latter deposits are rich in (semi-) terrestrial taxa that mostly probably were washed-in from the floodplain, or transported from the catchment, by running water. Klink (1989) notes that black flies (Simuliidae), although inhabitants of streams and rivers, are rarely represented in the fossil record from fluvial sediments. It is only when stream flow diminishes (for instance upon entering a lake) that remains of black flies preserve. This situation is exemplified in the fluvial sediment studied here. The macrofossil record further represents a large variety of aquatic and telmatic plants/animals. The taxa richness can be ascribed to the many habitats associated with a fluvial depositional environment, warm summers, and the nutrient-rich bedrock. Compositional changes in fossil assemblages seem for an important part be driven by shifts in flooding regime.

A Savukoski 1 cold stage (MIS 5d) - Sokli I warm stage (MIS 5c)
(Last Interglacial Complex)
Terrestrial plant taxa

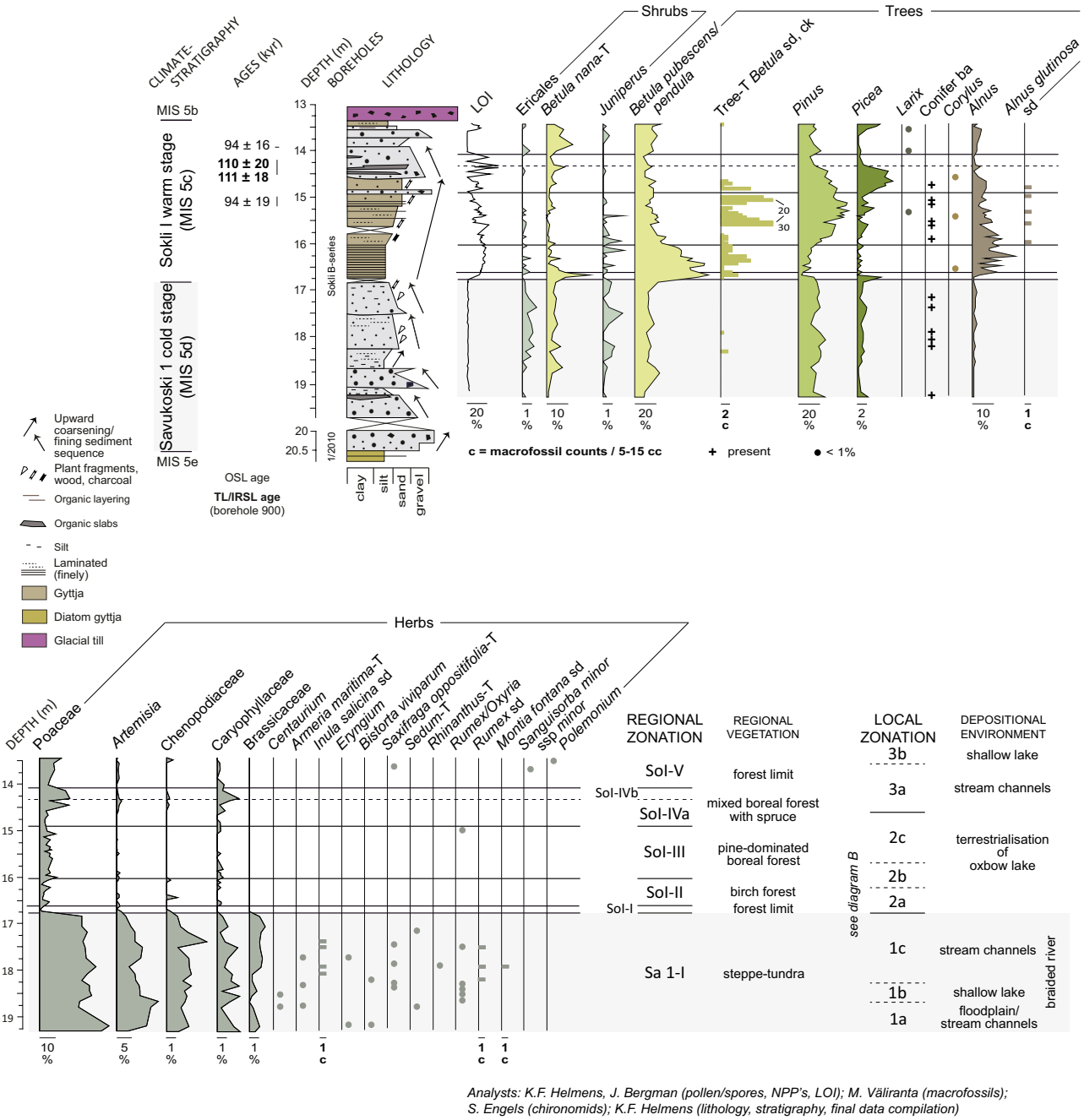

Figure 3-2. *Selection of environmental and climate proxies for the Savukoski 1 cold stage (MIS 5d) and Sokli I warm stage (MIS 5c) fluvial sequences in the Sokli basin based on Väliranta et al. (2009), Engels et al. (2010) and Helmens et al. (2012). For explanation of the diagrams see caption of Figure 3-1.*

B Savukoski 1 cold stage (MIS 5d) - Sokli I warm stage (MIS 5c) (Last Interglacial Complex)
Aquatic and telmatic taxa

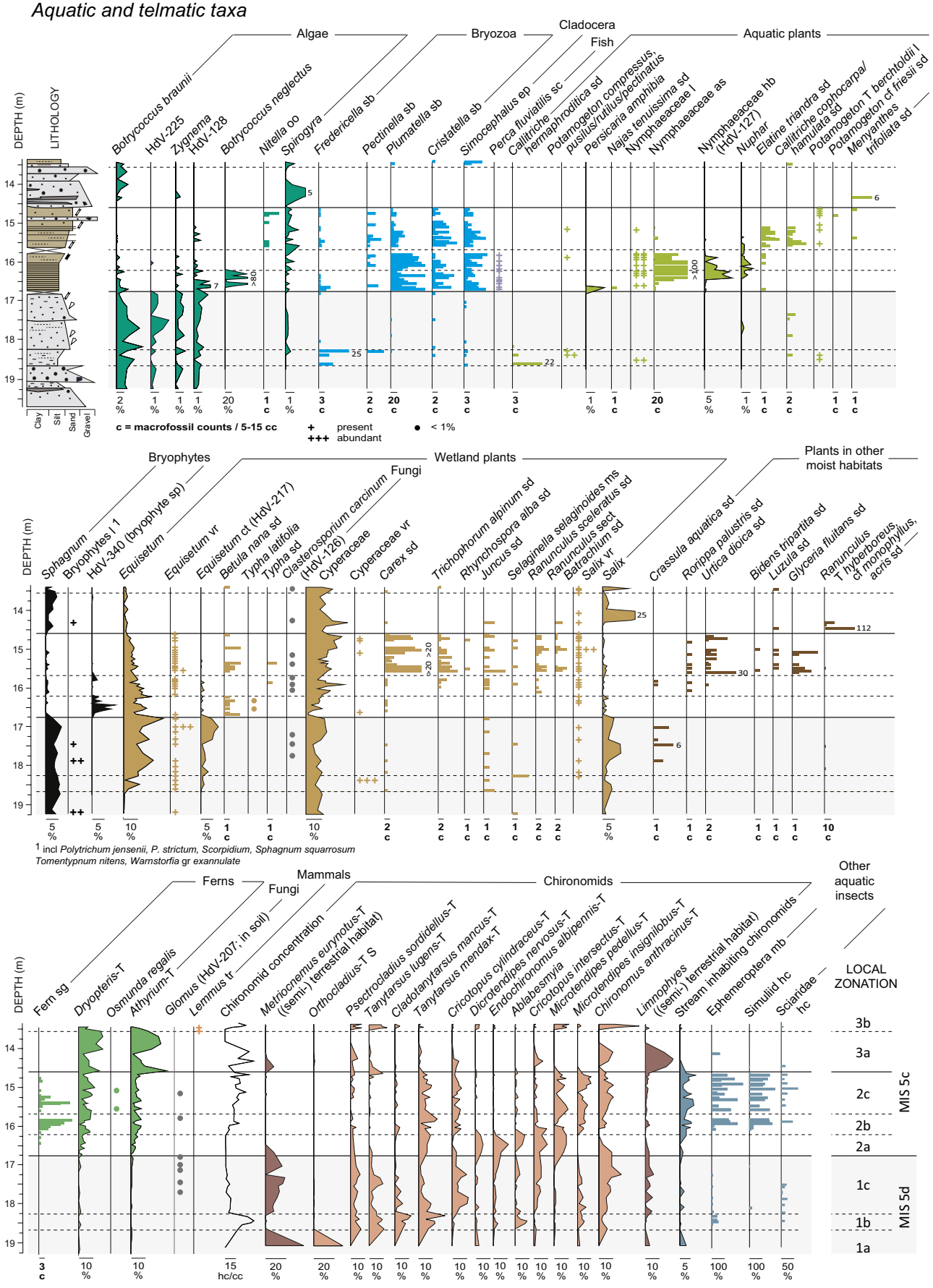

Figure 3-2. *Cont.*

3.2.1 A braided river pattern (Savukoski 1 cold stage)

The Savukoski 1 minerogenic sediment/fossil sequence (local zone 1; Figure 3-2B) reveals a series of depositional environments, i.e. a floodplain environment, a distinct lake stage, and several phases with stream channel deposition.

The lowermost coarse-grained stream channel deposit is intercalated near its top with slabs of silty sediment rich in exceptionally well-preserved bryophyte remains (local zone 1a). The bryophyte assemblage consists of *Aulacomnium turgidum*, *Polytrichum jensenii*, *P. strictum*, *Warnstorfia exannulata* group and *Scorpidium* spp. and indicates a nearby minerotrophic fen and an environment with wet depressions influenced by (seasonal) flooding (Ulvinen et al. 2002). The chironomid assemblage reflects the shallow water to (semi-) terrestrial conditions on a floodplain as well. It is dominated by *Metriocnemus eurynotus* and *Orthocladius*-T S. *Metriocnemus* is indicative of (semi-) terrestrial or very shallow water habitats (Cranston et al. 1983).

The second coarse-grained stream channel deposit is abruptly overlain by a c. 0.5 m-thick silt layer (local zone 1b). A pebble lag occurs at the base of the silt layer, whereas the upper part is finely laminated with sand and organic matter. The silty sediment most probably accumulated in a lake that occupied an abandoned stream channel. Despite the low LOI (2–4 %), a relatively rich fossil assemblage is recorded. The aquatic plant family Nymphaeaceae is well-represented near the base of the layer. Upwards, with the transition to a more sandy lithology, a variety of aquatic plants (*Potamogeton* T *berghtoldii, P. compressus*, *Callitriche cophocarpa/hamulata*) and chironomid taxa (*Cladotanytarsus mancus*-T, *Tanytarsus mendax*-T) appear that indicate a moderate to high-nutrient availability. Also, wetland expanses (macrofossils of e.g. Cyperaceae, *Juncus*, *Selaginella selaginoides*) and mandibles of mayflies (Ephemeroptera) are found. Mayflies, which are aquatic insects, primarily live in streams; their fossil remains become preserved in the sediment here probably due to a decrease in water flow in the partly overgrown lake. The chironomid taxa *Psectrocladius sordidellus*-T and *Ablabesmyia* are also well-represented in the silt layer and are both associated with macrophyte abundances. Notably, the chironomid concentration reaches its highest values of the entire MIS 5d-c fluvial sequence (35 headcapsules/cc). This is, however, considerably lower than the up to 300 head-capsules/g recorded in the Nuortti lake sequence (Fig 3-1B). The lake sediment further reveals a variety of bryozoa, in particular *Fredericella*, as well as the aquatic plant *Callitriche hermaphoditica*. The latter occurs in clear, brackish coastal waters, lakes and rivers. As will be shown below, the successional development recorded in the silt layer, which reflects the infilling of the lake, is remarkably similar as depicted in the oxbow lake deposit of local zone 2. The silts of local zone 1b, however, generally lack the large abundances of macrofossil remains, the high organic content, and the bio-diversity of the oxbow lake sediment. These differences can be ascribed to the different climate regimes, and fluvial dynamics, under which the sediments of local zones 1 (Savukoski 1 cold stage) and 2 (Sokli I warm stage) were deposited.

Two relatively fine-grained stream channel deposits occur in the upper part of local zone 1 (local zone 1c). Conditions within the channels were less energetic than during deposition of the gravely sediment in the lower part of the fluvial sequence and likely included prolonged phases of standing water. This is particularly so for the lower deposit which contains fossil remains of a variety of stream-inhabiting taxa including the insect black fungus gnats (Sciaridae). Characteristically, the fossil record of the stream channel deposits include taxa originating from the floodplain or catchment. These are the (semi-) terrestrial chironomids *M. eurynotus* and *Limnophyes*; the herb *Crassula aquatic*; and the soil fungus *Glomus* (HdV-207; van Geel et al. 1989). *C. aquatic* presently occurs on open, nutrient-rich, moist sediment that is seasonally flooded. In addition, the bryophyte assemblage with *P. jensenii*, *Sphagnum squarrosum*, *W.* group *exannulata*, *Tomentypnum nitens* and *A. turgidum* reflects an environment influenced by surface water flow and flooding (Ulvinen et al. 2002). The lower stream channel deposit further shows relatively high percentages values of the pioneer green algal *Botryococcus braunii* and algal type HdV-225. The latter is associated with open water and ephemeral pools (van Geel et al. 1989). In contrast, the upper stream channel deposit shows high abundances of spores, conductive tissue (HdV-217; van Geel et al. 1989) and vegetative remains (stem fragments) of *Equisetum*, as well as high percentage values of Cyperaceae pollen, indicating locally abundant stands of wetland vegetation.

Starting at the base of the silt deposit of local zone 1b, many of the abundant chironomid taxa indicate intermediate to warm summer conditions (e.g. *C. mancus*-T, *Ablabesmyia*, *C. cylindraceus*-T, *C. intersectus*-T) (Engels et al. 2010). Similarly, several plant taxa (e.g. *P. compressus*, *Nyphar*, *C. aquatica*) indicate July temperatures at least in the order of today's values (Väliranta et al. 2009). The warm summers comply with a continental climate regime with long cold winters and short warm summers.

Conditions were possibly colder during the deposition of the gravelly sediment at the base of the MIS 5d fluvial sequence (Figure 3-2A). Relatively high pollen percentages of Poaceae and *Artemisia*, and the near absence of pollen of shrubs, suggest a sparse vegetation cover and a vegetation type resembling a polar desert. The chironomid *Orthocladius*-T S is currently common on Svalbard and is frequently recorded in lake sediments dated to the Younger Dryas Stadial in Norway (Brooks et al. 2007). *M. eurynotus*-T is also able to tolerate cold climate conditions. A more severe climate during the early part of MIS 5d, compared with the later part, is also recorded on the European mainland (Helmens 2014, and references therein).

3.2.2 The Sokli I warm stage oxbow lake

The infilling of an oxbow lake, which remained flooded throughout the infilling process, is recorded in great detail in the c. 2.5 m-thick, highly compacted sandy gyttja deposit of local zone 2. The gyttja is interbedded with thin silt lamina in its lowermost part, and becomes increasingly interlayered with sand and wood upwards in the deposit. The subsequent return to coarse-grained stream channel deposition (local zone 3a), and the infilling of a pond (local zone 3b), conclude the Sokli I sediment/ fossil record (Figure 3-2B).

The aquatic plants *Persicaria amphibia* and *Najas tenuissima* are recorded at the very base of the gyttja deposit. *N. tenuissima* thrives on soft mud in water less than 1.5 m deep. It presently has scarce occurrences in southern Finland. *P. amphibia* is found along the major watercourses in Fennoscandia. In oxbow lakes, *P. amphibia* can tolerate the relatively high level of disturbance associated with flooding during the early phases of infilling of the lakes (Westhoff et al. 1981). Subsequently, Nymphaeaceae are abundantly represented by a variety of fossil remains (local zones 2a and 2b, lower part). These include leave fragments, astrosclereids (recorded as macrofossils and HdV-129 (Pals et al. 1980), base cells of hairs (HdV-127; Pals et al. 1980) and pollen of *Nuphar*. HdV-127 is considered a better indicator of the local presence of *Nuphar/Nymphaea* than pollen of the entomophilous (i.e. insect-pollinated) taxa of Nymphaeaceae (Ralska-Jasiewiczowa et al. 1992). In contrast to *P. amphibia*, the water lily *Nymphaea alba* favors more moderate levels of disturbance, e.g. when sediment infill in an oxbow lake decreases the strength of water flow during flooding (Westhoff et al. 1981). A further reduction in water flow is recorded with the transition to a sandier lithology halfway local zone 2b. From here onwards, fossil remains of various aquatic insects typical of lotic (flowing water) conditions start to be continuously preserved in large abundances, among which the stream-inhabiting chironomids *Eukiefferiella* and *Tvetenia*. In contrast, chironomid and diatom concentrations (Helmens et al. 2012) are very low in the lower portion of the gyttja deposit. It is likely that these fossil remains were washed away during flooding.

Confined to local zone 2a are high percentage values of *Botryococcus* cf *neglectus*, HdV-128 and bryophyte spores (HdV-340; van Geel et al. 1989). The green alga *B. neglectus* is presently found in relatively small, oligotrophic and mesotrophic water bodies (Jankovská and Komárek 2000), whereas the optimal environment of algal type HdV-128 is slowly moving water (van Geel et al. 1983). Despite in low concentrations, the chironomid assemblage in local zone 2a is divers. It includes various littoral taxa and taxa associated with macrophyte abundances (*Dicrotendipes nervosus*-T, *Endochironomus albipennis*-T, *Cricotopus intersectus*-T, *Microtendipes pedellus*-T) and suggests moderate nutrient levels. Subsequently, rising nutrient levels (to meso-/eutrophic conditions in local zone 2c) are revealed by increasing percentage values of *Tanytarsus mendax*-T and *Cricotopus cylindraceus*-T, and appearances of the aquatic plants *Elatine triandra*, *Callitriche cophocarpa/ hamulata, Potamogeton* T *berchtoldii* and *P.* cf *friesii*. The chironomid *Chironomus anthracinus*-T shows a high occurrence in the upper sandy part of the gyttja deposit (local zone 2c), and in the minerogenic sediment of local zones 1 (MIS 5d) and 3, possibly reflecting an affinity for coarse substrate.

Several wetland plants initiate their macrofossil records with the transition to a sandier lithology halfway local zone 2b, and a rich wetland assemblage is depicted in local zone 2c. Most characteristically are the high pollen percentage values of Cyperaceae and high macrofossil abundances of the sedges *Carex* spp., *Trichophorum alpinum* and *Rhynchospora alba*. *Clasterosporium carcinum* (HdV-126; Pals et al. 1980) is a fungus that is parasitic on *Carex* spp. (van Geel et al. 1983). Other wetland taxa that are represented by macrofossils include Poaceae, *Juncus*, *S. selaginoides*, *Ranunculus sceleratus*, *R.* sect. *Batrachium*, *Typha*, *Equisetum, Salix* and *Betula nana.* Open water, however, persisted throughout infilling of the oxbow lake as indicated by high fossil occurrences of the bryozoa *Plumatella*, *Cristatella, Pectinatella* and *Fredericella*. Scattered occurrences of *Pectinatella* are presently only reported from southern locations on the European mainland (Wood and Okamura 2005). The cladocera *Simocephalus* is also well-represented in the fossil record from the gyttja deposit and suggests open, shallow water, eutrophic conditions and dense stands of vegetation (van Geel et al. 1983). Fossil scales of the fish *Perca fluviatilis* (perch) are found in the lower part of the gyttja where Nymphaeaceae dominate.

The fossil record in the gyttja deposit further depicts the local presence of an *Alnus* carr (marshy forest) with *Alnus glutinosa* and abundant ferns in the undergrowth. *A. glutinosa* reaches its current northern distribution limit some 400 km south of Sokli, whereas the thermophilous fern *Osmunda regalis*, of which spores are found, has nowadays a rare occurrence on shaded, moist soil along lakes and rivers in southernmost Fennoscandia. Furthermore, the herbs *Rorippa palustris*, *Urtica dioica*, *Bidens tripartita, Luzula* and *Glyceria fluitans* are recorded by macrofossils and these plants were probably present in moist shore habitats as well. *B. tripartita* favors nitrogen-rich moist habitats, which occur where fresh organic material accumulates and decomposes (Jansen et al. 2000), and the presence of nitrogen-rich habitats is indicated by *R. sceleratus* as well.

The coring site became part of the active river system again during local zone 3a. The sandy to gravely stream channel deposit contains in its lower part slabs of organic-bearing sediment (LOI to 30 %), showing peak occurrences for a variety of taxa. These include various species of *Ranunculus* (*R*. T *hyperboreus*, *R*. T *auricomus* cf *monophyllum*, *R*. T *acris*), *Salix*, Cyperaceae, *Menyanthes trifoliata*, the green alga *Spirogyra*, ferns (*Athyrium*-T) and (semi-) terrestrial *Limnophyes*. The fossil assemblage indicates that the organic-rich intercalations represent shore/wetland vegetation that most probably was locally eroded and re-deposited together with the coarse-grained stream channel sediment. The sands and gravels themselves contain few fossil remains apart from high percentages of fern spores.

A thin sandy gyttja bed, with a pebble lag at its base, is found on top of the stream channel deposit (local zone 3b). The gyttja seems to have been deposited in a shallow pond. Interestingly, it contains fossil teeth of *Lemmus*.

A large number of plant taxa that are represented in the fossil record of the Sokli I warm stage deposit reach their present-day northern distribution limit south of Sokli. In addition, several chironomid taxa (e.g. *E. albipennis*-T, *Ablabesmyia*, *D. nervosus*-T) suggest warm summers. Both proxies clearly indicate past July temperatures that were significantly higher than the present July temperature at Sokli (Väliranta et al. 2009, Engels et al. 2010).

3.3 The Sokli II warm stage (MIS 5a) lake

The Sokli basin was glaciated during the Savukoski 2 cold stage (MIS 5b) and then deglaciated during the the Sokli II warm stage (MIS 5a) of the Last Interglacial Complex (MIS 5). The south-eastern margin of the Fennoscandian Ice Sheet might have been situated at the so-called Pudasjärvi End Moraine during the MIS 5b ice advance (Johansson et al. 2011). The moraine, which is situated some 300 km south of Sokli, represents a pronounced complex of till-covered ice-marginal landforms (Sutinen 1992). In the Sokli basin, the glaciation is recorded by a diamiction that reaches a total thickness of c. 2 m in the B-series borehole (coring location 1; Figures 1-3 and 2-1). The diamicton here is clast supported in its lower part, whereas a sandy matrix dominates in the weakly stratified upper part, and is interpreted as basal till possibly overlain by ablation till (Helmens et al. 2007a). The basal till is also encountered at coring location 2, at a similar depth as at location 1, i.e. at c. 12.5 m below the surface of the Sokli wetland. Its thickness is only c. 0.1 m in borehole 4/2010.

However, the till in the latter borehole occurs at the base of a core segment and difficulties penetrating the compact, coarse diamicton might have let to slight deviations in core depths.

On top of the diamicton, the sediment becomes more sorted and fines-upward to sand. This glacio-fluvial sediment, in its turn, is abruptly overlain by a laminated silt-clay deposit of glacio-lacustrine origin (Helmens et al. 2018). Both the c. 1 m-thick glacial lake deposit and overlying c. 2 m of gyttja of the Sokli II warm stage (MIS 5c) in borehole 2/2010 (coring location 2) have been the subject of multi-proxy analysis. It is likely that the waterlogged depression in which the gyttja deposit accumulated formed due to compression of the older basin sediments during the preceding glaciation. The regional pollen record in the lake sequence depicts a vegetation development towards pine-dominated boreal forest. An early shrub tundra phase is additionally recorded at coring location 1. The lake at this site, however, was very shallow (Cyperaceae pollen up to 40 % and dominance of *Carex* seeds; Helmens et al. 2000, 2007a, 2021) and became infilled with sediment early in MIS 5a. The Sokli II gyttja deposit in borehole 2/2010 becomes near the top increasingly interlayered with sand before turning to sand interbedded with thin organic laminae and then gravel. A c. 2 m long hiatus separates the lake deposit from till. The organic content of the gyttja is low, < 13 % (Figure 3-3A), indicating a relatively large input of minerogenic sediment into the lake throughout its infilling process.

Macrofossils and NPP's are not found in large abundances in the Sokli II lake sequence, but their records are diverse. Combined with the pollen/spore, diatom, chironomid and sediment records, they trace in detail the development of the Sokli Ice Lake in the earliest part of the warm stage (see Section 3.6), and the subsequent infilling of a relatively small and shallow lake confined to the Sokli basin. Characteristic for the gyttja deposit are the fossil occurrences of the shallow aquatic plant *Ceratophyllum* (Figure 3-3B). This plant presently tolerates highly polluted waters where human-induced eutrophication has led to an impoverishment of the flora (Westhoff et al. 1981). The diatom record with c. 90 % of Fragilariaceae, and representations of *Staurosira construens* var. *subsalina*, *Staurosirella leptostauron* and *Cocconeis placentula*, indicate alkaline waters. Similarly, the dominance of *Corynocera ambigua* in the chironomid record might be due to alkaline water conditions, although macrophyte abundances might have (additionally) played a role. High nutrient levels in the lake are further revealed by the recording of the cyanobacteria *Gloeotrichia* and the diatom taxa *Epithemia sorex* and *E. adnata*, which are all capable of atmospheric nitrogen fixation in case of an imbalance in the P/N ratio. It is possible that the relatively small water volume of the Sokli II lake enhanced the influence of the local bedrock on the lake's geochemistry, thereby resulting in eutrophic/alkaline lake water conditions. Notably, the MIS 5b glaciation followed a long time-interval with ice-free conditions at Sokli. The availability of deeply weathered rocks might additionally have influenced the nutrient status of the lake. The fossil record in the glacial lake sediment also reflects remarkably high nutrient levels (Section 3.6).

Open-water conditions during the early phase of gyttja deposition (local zone 1a in Figure 3-3B) are indicated by the fossil occurrences of the bryozoa *Plumatella* and *Cristatella mucedo*. The diatom and chironomid records reveal littoral conditions, whereas the fossil records of *Salix*, Cyperaceae (e.g. *Carex*) and *Equisetum* show the additional presence of a wetland zone. Many of the prevailing chironomid taxa are associated with shallow/littoral habitats and/or macrophyte abundances. These include *Polypedilum nubeculosum*-T, *Endochironomus albipennis*-T, *Tanytarsus pallidicornis*-T, *Psectrocladius sordidellus*-T, *Cricotopus intersectus*-T, *C. cylindraceus*-T, *Dicrotendipes nervosus*-T and *Microtendipes pedellus*-T. The diatom record is dominated by the littoral taxon *Staurosirella pinnata*, while the relatively high representations of *Staurosira construens* var. *venter* and *S. construens* var. *binodis* probably reflect their littoral and/or periphytic (growing on plants) habitat preferences as well. The aquatic plant assemblage of local zone 1a consists of a variety of *Callitriche* species (*C.* cf *cophocarpa, C. hermaphroditica, C. hamulatae*), narrow-leaved *Potamogeton* (*P. pusilus/pectinatus/rutilus*, *P. berchtoldii*, *P. compressus*), *Ceratophyllum* and *Myriophyllum spicatum*-T (including *M. verticillatum* and *M. sibiricum*). *P. pusilus* and *P. pectinatus* are presently recorded in meso-haline waters.

A Sokli II warm stage (MIS 5a) (Last Interglacial Complex)
Terrestrial plant taxa

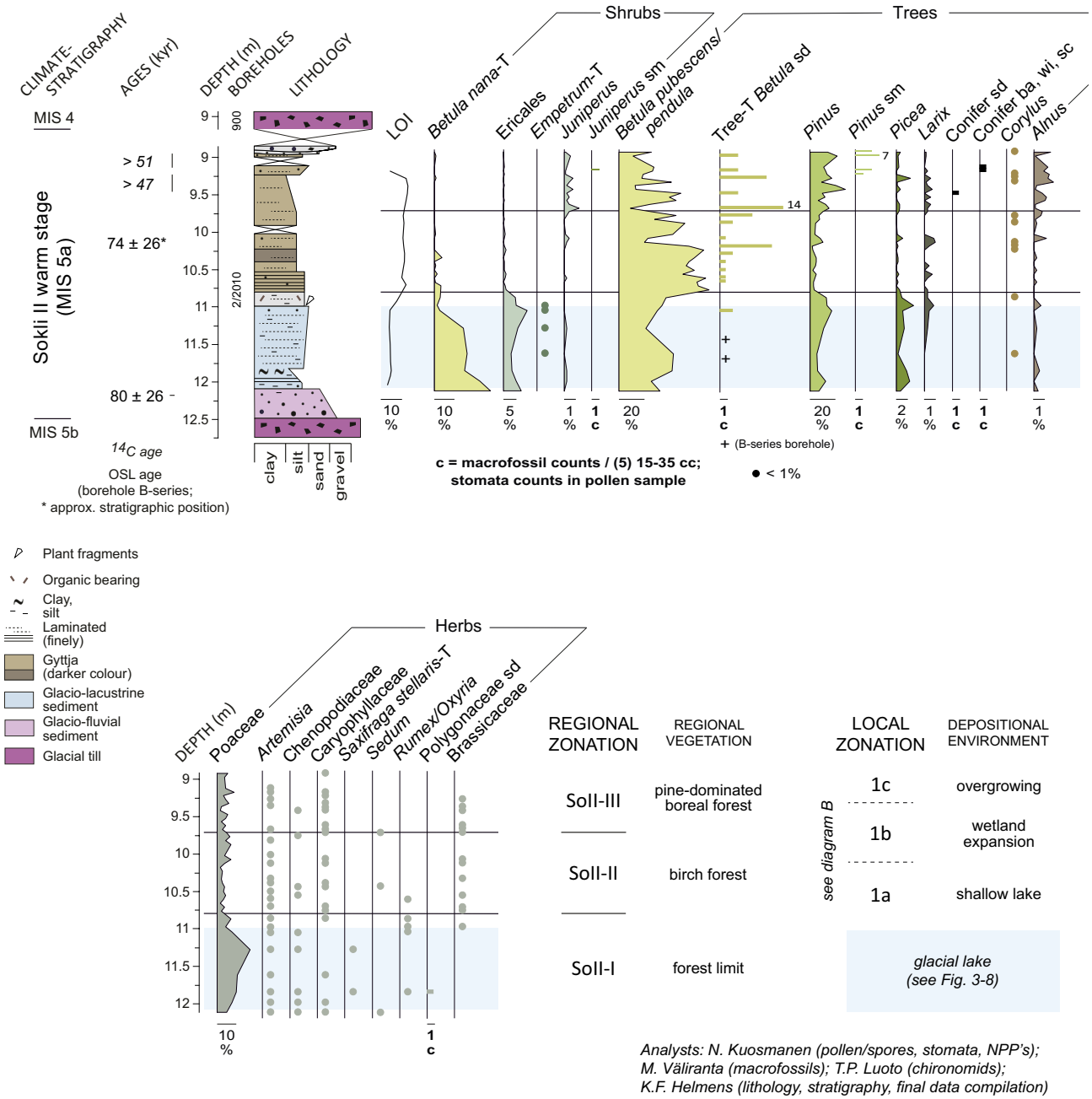

Figure 3-3. *Selection of environmental and climate proxies for the Sokli II Interglacial (MIS 5a) lake deposit in the Sokli basin based on Helmens et al. (2021). For explanation of the diagrams see caption of Figure 3-1. Note that multi-proxy data obtained on the glacial lake sediment at the base of the MIS 5a lake sequence are summarized separately in Figure 3-8.*

B Sokli II warm stage (MIS 5a) (Last Interglacial Complex)
Aquatic and telmatic taxa

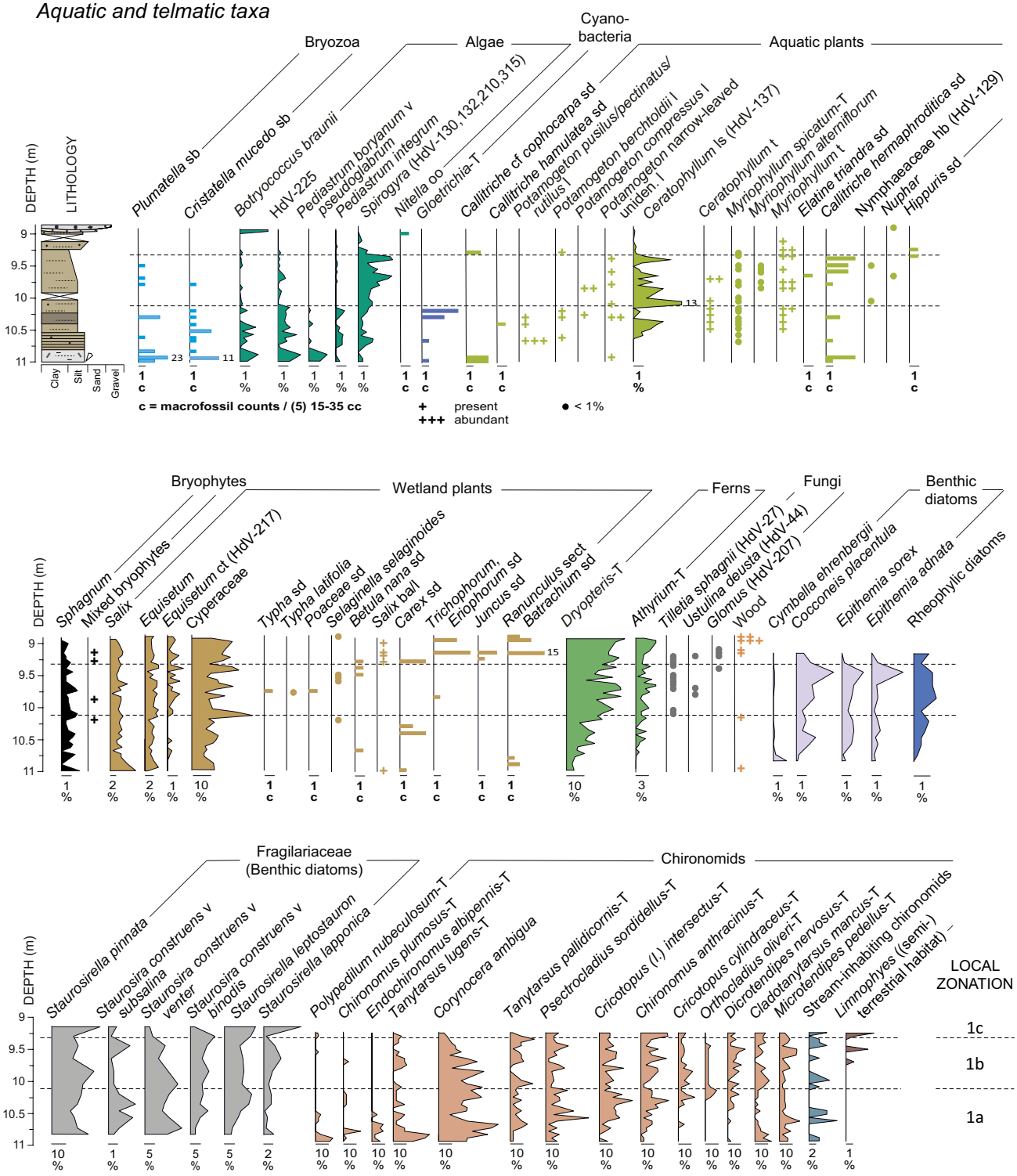

Figure 3-3. *Cont.*

A further shallowing of the lake, accompanied by an extension in the wetland zone, is depicted in local zone 1b. The zone is characterized by enhanced representations of *Ceratophyllum* and *Spirogyra*. *Ceratophyllum* is found as leaf spikes (HdV-137; van Geel et al. 1989) and plant tissue. It is identified as *C. demersum* in a *Seda*DNA analysis on the glacial lake sediment (Peter Heinztman, personal communication, 2021). Two species of the aquatic plant *Ceratophyllum* presently occur in Finland, i.e. *C. demersum* and *C. submersum*. The latter has only few localities along the southern coastline that have established during the last two decades. *C. demersum* occurs in shallow, eutrophic, oligo- to mesosaprobic water bodies (i.e. exclusively oxidizing to partly reducing decomposition; Westhoff and den Held 1975). The green alga *Spirogyra* (Zygnemataceae) is represented by four NPP types (HdV-130, -132, -210, -315; Pals et al. 1980, van Geel et al. 1983, 1989, van der Wiel 1983) and is characteristic of stagnant, shallow, meso-eutrophic freshwaters (van Geel and Grenfell 1996). The chironomid taxon *Orthocladius oliveri*-T, also recorded in local zone 1b, is related to shallow, eutrophic waters as well. Whereas narrow-leaved *Potamogeton* was abundantly represented during local zone 1a, *Myriophyllum* (including *M. alterniflorum*) becomes more abundant in local zone 1b. The aquatic plant assemblage is further enriched with *Elatine triandra*, *Nuphar* and *Hippuris*. Finally, an increase in pollen percentages of Cyperaceae and the presence of spores and conductive tissue of *Equisetum* (HdV-217; van Geel et al. 1989) indicate an extending wetland zone during local zone 1b. Other wetland taxa that are recorded by macrofossils are *Poaceae*, *Typha*, *S. selaginoides* and *Betula nana*. van Geel (1978) found the fungus *Tilletia sphagnii* (HdV-27) to be almost completely restricted in its occurrence to peat containing *Sphagnum* remains.

The sandy lithology and fossil record in the uppermost part of the gyttja deposit (local zone 1c) depict the final stage of infilling and overgrowing of the Sokli II lake. Aquatic taxa (bryozoa, green algae, aquatic plants) mostly disappear from the fossil record. In contrast, wetland plants are well-represented in the macrofossil record (*Carex, Eriophorum, Trichophorum*, *Juncus*, *Salix*, *Ranunculus* sect *Batrachium*). Pollen percentages of *Alnus* increase, while the continuing increase in fern spores suggests that ferns, like alder, were probably growing in the wetland or in a moist shore habitat as well. Concurrent with the expanding wetland zone, the encroachment of running water becomes visible in the fossil record, transporting with it material from the catchment. Stream-inhabiting chironomids and rheophylic diatoms (e.g. *Meridion circulare*, *Diatoma mesodon*) occur throughout the gyttja deposit, but the (semi-) terrestrial chironomid taxon *Limnophyes* increases its representation upwards in the deposit, the soil fungus *Glomus* is recorded, and large abundances of wood fragments are found. The fungal *Ustulina deusta* (HdV-44; van Geel 1978) grows on wood substrate.

The aquatic/wetland assemblages with *C. cophocarpa*, *P. compressus*, *C. demersum*, *E. triandra* and *Typha*, and the predominance of intermediate- to warm-water chironomid taxa, indicate that mean July temperatures during the Sokli II warm stage exceeded present-day values by several degrees (Helmens et al. 2021).

3.4 The Tulppio Interstadial Complex (mid-MIS 3)

The Sokli basin was glaciation once more during the Savukoski 3 Stadial (MIS 4), and then deglaciated twice during the Tulppio Interstadial Complex (TIC) in mid-MIS 3. The Fennoscandian Ice Sheet probably advanced into southern Finland and beyond during the MIS 4 glaciation (Svendsen et al. 2004). Originally, it was believed that the ice-sheet maintained a sub-continental size during MIS 3, before its maximal expansion in the LGM (e.g. Donner 1995). However, many key geological data published in the past c. 20 years are indicating ice-free conditions in the central areas of Eurasian, Laurentide and Cordilleran glaciation during part(s) of MIS 3 (e.g. Ukkonen et al. 1999, Helmens et al. 2000, 2007, Olsen et al. 2001a, 2001b, Wohlfarth 2010 and references therein; Helmens 2014 and references therein, Sarala et al. 2016, Dalton et al. 2016, 2022, McMartin et al. 2019, Mangerud et al. 2023).

There are several lines of evidence at Sokli that point to an active ice-sheet that was probably warm-based in MIS 4/early 3 (Helmens et al. 2018). The MIS 3 glacio-fluvial sands and pebbles that overly the MIS 4 till deposit, and part of the till, contain interstratified and chucks of organic debris reworked from the MIS 5e diatom gyttja deposit in the Sokli basin (Helmens et al. 2000). The persistence of distinct clayey laminae throughout the overlying glacio-lacustrine sequence further suggests a continuing influence of the ice-sheet on sediment deposition, even in the case of a distal position. Finally, the

fossil record from the glacio-lacustrine sediment registers a glacier re-advance phase in which an earlier opened spillway was blocked by ice, resulting in the re-occurrence of a large, deep-water glacial lake stage (Section 3.6). Added to this, new data presented here shows that the Fennoscandian Ice Sheet subsequently overrode the Sokli basin, and then retreated once more in mid-MIS 3, during which fluvial sediment was deposited in the basin.

The up to c. 2-m thick minerogenic, fining-upward and then coarsening-upward, laminated silt-clay sequence of glacio-lacustrine origin, that overlies the MIS 4 till at coring location 1 at depths of c. 5–7 m below the surface of the Sokli wetland, was studied using multiple proxies on the B-series borehole (Figures 1-3 and 2-1). The fossil remains of aquatic and telmatic taxa encountered in the glacial lake sediment are presented in Figure 3-9 and discussed in Section 3.6 focussing on the ice-marginal environment. Terrestrial plant taxa, lithology and chronology are shown in Figure 3-4.

The glacio-lacustrine sediment is overlain by c. 2 m of till. Helmens et al. (2000, 2007a) describes the sediment contact as gradual and notes the occurrence of a dropstone in the laminated sediment just below the contact. The till deposit has earlier been interpreted as representing the last glaciation of the Sokli basin, starting during the late part of MIS 3 and lasting into the earliest portion of the Holocene (Helmens et al. 2000, 2007a). However, new ^{14}C dating on a sorted sediment bed found intercalated in the uppermost part of the till, in the more recently obtained 2/2010 borehole (Figures 2-1 and 3-4), shows that this sediment dates to MIS 3 as well. The c. 30 cm-thick sediment intercalation consists of fine gravel grading into sandy silt and interbedded with coarse sand. A palynological analysis of the sandy silts records a dominance of wetland/shore plants (Cyperaceae*, Salix, Sphagnum,* ferns) and green algae (*Pediastrum, Botryococcus braunii, Zygnema*, HdV-128) (Figure 3-4B). Together with findings of macroscopic remains of e.g. twigs, plant tissue and bryophytes, it is likely that the silts accumulated in a small floodplain pond. A similar sorted c. 10 cm-thick sandy to gravely bed is found in the same stratigraphic position in borehole B-series (Figure 2-1). The deglacial sediment below the till has earlier been defined as the Tulppio Interstadial (Helmens et al. 2007b). Here, based on the new evidence, the entire sediment sequence from the glacio-fluvial sediment on top of the MIS 4 till bed to the fluvial sediment intercalation is defined as the Tulppio Interstadial Complex (TIC). The ice-free intervals represented by the glacio-fluvial and -lacustrine sequence is named the Tulppio 1 Interstadial and by the fluvial sediment the Tulppio 2 Interstadial, and the intervening glaciation is named the Saariselkä glaciation/Stadial. This new interpretation means that the late MIS 3-2 glaciation (Savukoski 4 Stadial) is represented by only c. 15 cm of till (Figure 2-1). The Fennoscandian Ice Sheet during the last glaciation, however, was cold-based in central Finnish Lapland, lasting well into the deglaciation phase, which not only resulted in limited glacial erosion, but also in limited glacial deposition (Johansson 1995).

Wood encountered in the uppermost part of the glacio-lacustrine sequence (Tulppio 1 Interstadial) has been ^{14}C-dated at c. 42.5 kyr, and an OSL age of c. 48 kyr was obtained on the underlying glacio-fluvial deposit. ^{14}C ages of c. 38.8 kyr (plant macrofossil remains) and c. 41.7 kyr (bulk sample) are newly obtained on the fluvial sediment bed (Tulppio 2 Interstadial), in which the latter date probably over-estimates the true age by incorporating older soil carbon from the catchment (see Section 2.1). The TIC records two ice-free intervals, one before c. 45 and the second one at about 42 cal. kyr (Reimer et al. 2009), separated by a phase with renewed glaciation of the Sokli site. The pollen record for the Tulppio 1 Interstadial shows shrub tundra vegetation, whereas birch forest is recorded for the Tulppio 2 Interstadial (Chapter 4). The TIC seems to record the millennial-scale climate variability of the middle part of MIS 3 around c. 40 kyr BP and is here correlated to GIS 12-8 in the Greenland record (Figure 1-1). The dynamic, warm-based ice-sheet conditions at the end of the MIS 4 glaciation (see above), and the possible persistence of glacier ice in the Saariselka low-mountain range some c. 100 km to the north of Sokli, may explain the rapid, millennial-scale response of the Fennoscandian Ice Sheet during the TIC. An early MIS 3 ice-marginal retreat pattern towards the north has been reconstructed based on N-S trending, till-covered eskers in the Sokli region OSL-dated to 65 ± 13 kyr BP (Johansson 2007a).

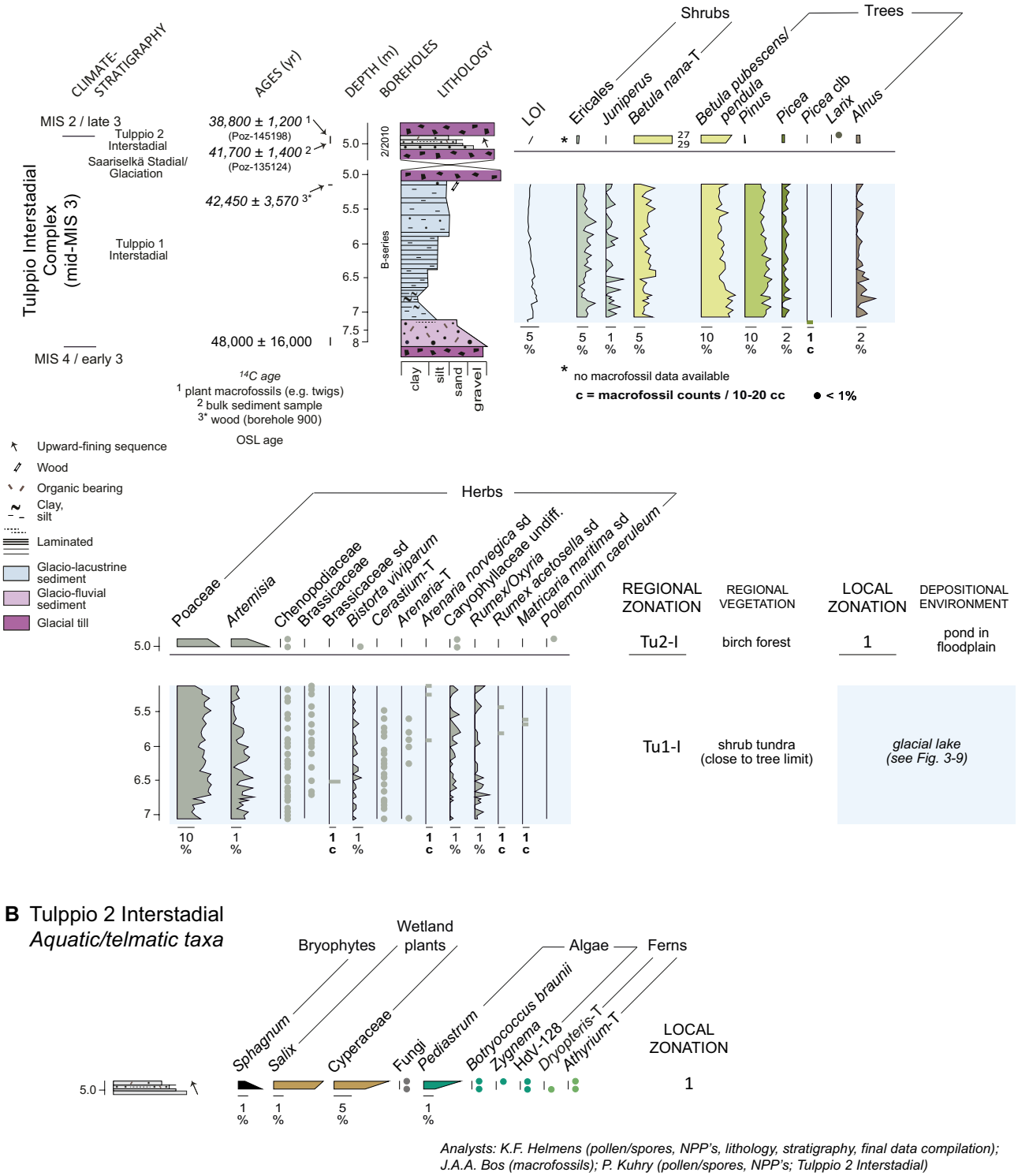

Figure 3-4. *Selection of environmental and climate proxies for the Tulppio Interstadial Complex (mid-MIS 3) in the Sokli basin based on Bos et al. (2009) and this study. For explanation of the diagram see caption of Figure 3-1. Note that multi-proxy data obtained on the glacial lake sediment of the Tulppio 1 Interstadial are summarized separately in Figure 3-9.*

Well-dated environmental records for parts of MIS 3 have recently been published for two other sites in northern Finland, i.e. Petäjäselkä to the west of Sokli (Sarala and Eskola 2011, Väliranta et al. 2012) and Kaarreoja northwest of the Saariselka mountain range (Sarala et al. 2016). The stratified sediment sequences at both sites contain organic-bearing sediment that is ^{14}C-dated at 35.3 ± 0.6 (Petäjäselkä) and 30.2 ± 0.3 kyr (Kaarreoja), and is bracketed by OSL dates as younger than c. 73–58 kyr and older than c. 32 kyr (Petäjäselkä), and younger than c. 52 kyr (Kaarreoja). Fluvial disturbance might explain the infinite ^{14}C age (>45 kyr BP) on wood from the Kaarreoja site (Sarala et al. 2016). Although the OSL dates have relatively large error margins, importantly, OSL and ^{14}C ages occur in sequence. The ice-free interval at Petäjäselkä, for which a vegetation at or very close to the birch tree line is recorded (Väliranta et al. 2012), might correspond to the ice-free interval at Sokli in the later part of the TIC (Tulppio Interstadial 2; GIS 8). The birch forest phase with pine, recorded near the end of the Kaarreoja vegetation succession (Sarala et al. 2016), occurred later, at c. 35 cal. kyr BP (GIS 7). The peat in the upper part of the Kaarreoja organic-bearing sediment sequence is covered by glacio-fluvial sands, in is turn overlain by the youngest till bed correlated to MIS 2 (Sarala et al. 2016). Furthermore, till interbedded in-between two fluvial sediment sequences at the Hannukainen mine, west of Sokli, has been OSL-dated as younger than c. 35–56 kyr and older than c. 39 kyr BP and might represent a mid-MIS 3 glaciation (Salonen et al. 2014) corresponding to the Saariselkä glaciation at Sokli around c. 40 cal. kyr BP. Similarly, OSL dating of the detailed stratigraphy at the Rautuvaara mine, consisting of glacio-lacustrine sediment sequences interbedded with till, suggests that western Finnish Lapland was ice-free during two separate time intervals in MIS 3 (Lunkka et al. 2014). The latter is supported by the study of Howett et al. (2015) that dates the ice-free periods at Rautuvaara, using OSL, to c. 47–55 kyr and c. 33–36 kyr BP. Based on the ^{14}C ages obtained for the pre-LGM interstadial deposits in central Swedish Lapland, Wohlfarth (2010) suggests ice-free conditions around and prior to 40 cal. kyr BP and ice-cover thereafter. In-line with this interpretation, Hättestrand and Robertsson (2010) tentatively consider the two phases with birch vegetation during the Tärendo II Interstadial of MIS 3 age. The severe cold phase that is recorded between the periods of warmer climate probably caused a glacier re-advance out of the mountains but not reaching the Riipiharju study site (Hättestrand 2008). Well-dated stratigraphic records from Norway show a similar picture for MIS 3 as is emerging from Sweden and Finland. The Ålesund Interstadial represents a 4000-yr-long mild period (GIS 8-7; Mangerud et al. 2003) during which the coast, as well as large inland areas (Olsen et al. 2001a, 2001b), were ice-free. An ice advance beyond the coastline, dated to around c. 40 cal. kyr BP (Skjonghelleren Stadial; GST 9-10; Mangerud et al. 2003), separates the Ålesund Interstadial from warm interstadial conditions in early MIS 3 (Bo/Austnes Interstadial; Mangerud 2004).

Based on the detailed stratigraphic data from northern Finland, northern Sweden and Norway, it is likely to conclude that central Finnish Lapland was ice-free at least twice during MIS 3, around c. 47 kyr BP (GIS 12-11) and in the period at c. 42–35 kyr BP (GIS 8-7), separated by a period of glaciation around c. 40 kyr BP (GS 11-9). The TIC deviates considerably from the earlier sequence of events inferred from the Sokli sequence. The latter tentatively correlated the Tulppio Interstadial to GIS 14 around c. 53 kyr BP and considered the interstadial as the only phase during which Sokli was ice-free in MIS 3 (Helmens et al. 2007b, 2009).

3.5 The Holocene

Following the last deglaciation of the Sokli region in the earliest part of the Holocene at c. 10.7 cal. kyr BP, at least 2 m of glacio-lacustrine silty sediment (see Section 3.6) and 7 m of gyttja was deposited in Loitsana Lake. The lake is situated in a subglacial meltwater corridor that crosses the Sokli wetland (Sokliaapa) in a NW-SE direction, directly west of the Sokli basin. The corridor consists of sediment accumulations (eskers) and erosional features such as the deep Loitsana basin (Figure 1-3).

The Loitsana lake sequence was subjected to a multi-proxy analysis in order to obtain a modern reference section for the older lake deposits in the Sokli basin. It allows a direct comparison between the present-day environmental setting of the lake and the fossil remains and biogeochemical data stored in the lake sediment. Also, changes in e.g. the drainage pattern that might have occurred in the course of the Holocene may still be traceable in the landscape. Importantly, Holocene environmental and climate records are readily available from Fennoscandia for comparison, in contrast to the older records in the Sokli sequence that are unique. The latter is particularly relevant considering the non-typical bedrock geochemistry at Sokli.

For the purpose of the present compilation study, the Holocene sediments that underlie the Sokliaapa (wetland) in the Sokli basin are additionally studied. The Holocene sediment in borehole 2/2010 was subjected to pollen/spore and NPP analysis, and several ^{14}C datings were carried out. This record is further complemented with unpublished macrofossil and ^{14}C data from the nearby S1 and S2 cores. Cores S1-2 are located on the opposite side of the Soklioja rivulet from borehole 2/2010 but show a remarkably similar lithology (Figures 1-3 and 2-1). This new Holocene record represents a depositional environment that had not been earlier studied in any detail at Sokli, i.e. peatland, and it traces in detail the Holocene peatland development at the site. Furthermore, the Early Holocene sandy sediment at the base of the peat deposit provides a possibility to further explore the influence of a floodplain environment on the fossil record. Note that the pollen sum used in this study excludes the pollen of Cyperaceae since these are greatly over-represented in the pollen record from the peat.

At first glance, the Loitsana fossil record reveals a seemingly unusual sequence of events. In contrast to the MIS 5 interglacial lake records that show aquatic conditions gradually being replaced by wetland in the course of lake infilling, Loitsana depicts an early phase of peatland development following by open water. However, the fossil remains of wetland plants in the early part of the Loitsana sequence occur in sediment that is characterized by high sedimentation rates and large abundances of stream-inhabiting chironomids. Therefore, the early phase of peatland development is interpreted to represent the initial terrestrialisation of the southern portion of the lake, being situated closest to the Soklioja rivulet, with fragments of wetland vegetation being transported to the northern part of the lake by running water. Following the redirection of the Soklioja away from Loitsana Lake c. 6.8 cal. kyr BP, Loitsana became an isolated esker lake. The change in drainage pattern might have been caused by the expanding peatland in combination with a sudden lowering in the water table. Alternatively, a thick delta deposit that is linked to the meltwater corridor might initially have obstructed the river, diverting water flow to the south through a now abandoned stream channel, and northwards into Loitsana Lake (Figure 1-3). Once the delta was eroded, the Soklioja attained its current course.

3.5.1 Loitsana Lake

Similar to the diatom records from the MIS 5c (Helmens et al. 2012) and MIS 5a lake deposits (Section 3.3), the diatom assemblages in the Loitsana gyttja predominately consist of alkaliphilous Fragilariaceae (Figure 3-5B). The local alkaline bedrock probably caused this mass-occurrence, although disturbances through fluvial/minerogenic influx and groundwater inflow from the esker might additionally have contributed to the mass-occurrence in the Loitsana record. Fragilariaceae are a group of taxa that are generally considered opportunistic and pioneering due to their wide range of ecological preferences and often dominate lakes that have some sort of disturbance (Lotter et al. 1999, Anderson 2000, Bigler et al. 2003). Although recorded in low percentage values, the successional development in which planktonic taxa (*Stephanodiscus parvus*, *Cyclotella ocellata, C. radiosa*) are being replaced by tychoplanktonic (*Melosira varians*) and then benthic taxa (*Epithemia adnata, Cymbella ehrenbergii, Amphora libyca*) depicts the gradually shallowing of Loitsana Lake as it is filled-in with sediment. The *Cyclotella* species occur in finely laminated sediment and suggest that the lake was stratified with anoxic bottom water conditions (Saros et al. 2014) in the period c. 9.4–8.6 cal. kyr BP. This local zone (1b) is further characterized by high abundances of the bryozoan *Plumatella repens* and low C/N values (c. 10), suggesting a high in-lake productivity. *Cladotanytarsus mancus*-T, which attains peak percentage values, is one of the dominant chironomid taxa in the Nuortti warm stage lake sequence and is a mesotrophic warm-indicating taxon (Olander et al. 1999, Brodersen and Lindegaard 1999). The aquatic plant and chironomid assemblages in the Loitsana lake sequence support warm summers in the early part of the Holocene (Shala et al. 2017).

In contrast to the diatom record, the chironomid record shows a large turnover in species that seems to be largely driven by changes in nutrient availability (Luoto 2011). The chironomid taxa *Endochironomus albipennis*-T and *Cricotopus cylindraceus*-T, and the diatom species *S. parvus*, indicate nutrient-rich conditions at the start of the record. The enhanced trophic state in the earliest part of the Holocene might be the result of morphometric eutrophication (Hofmann 1998), i.e. a condition created by a reduction in lake volume, which at Loitsana happened following the drainage of the Sokli Ice Lake (see Section 3.6). The trophic state shifts to mesotrophic in local zone 1b (*Cladotanytarsus mancus*-T) and to oligo-mesotrophic in local zone 1c (*Microtendipes pedellus*-T, *Sergentia coracina*-T, *Corynocera oliveri*-T). Following the diversion of the Soklioja rivulet c. 6.8 cal. kyr BP, nutrient levels increase

again (*C. ambigua, Dicrotendipes pulsus*-T, *Tanytarsus pallicornis*-T, *Paratanytarsus penicillatus*-T), to return to meso-eutrophic levels in the uppermost shallow waters of local zone 3 (*Cladotanytarsus mancus*-T, *C. plumosus*-T, *Tanytarsus mendax*-T). *Chironomus anthracinus*-T and the diatom species *Martyana martyi* closely follow the records of stream-inhabiting chironomids and rheophylic diatoms (e.g. *Meridion circulare* var. *circulare*, *Amphora pediculus*) and probably relate to minerogenic sediment load.

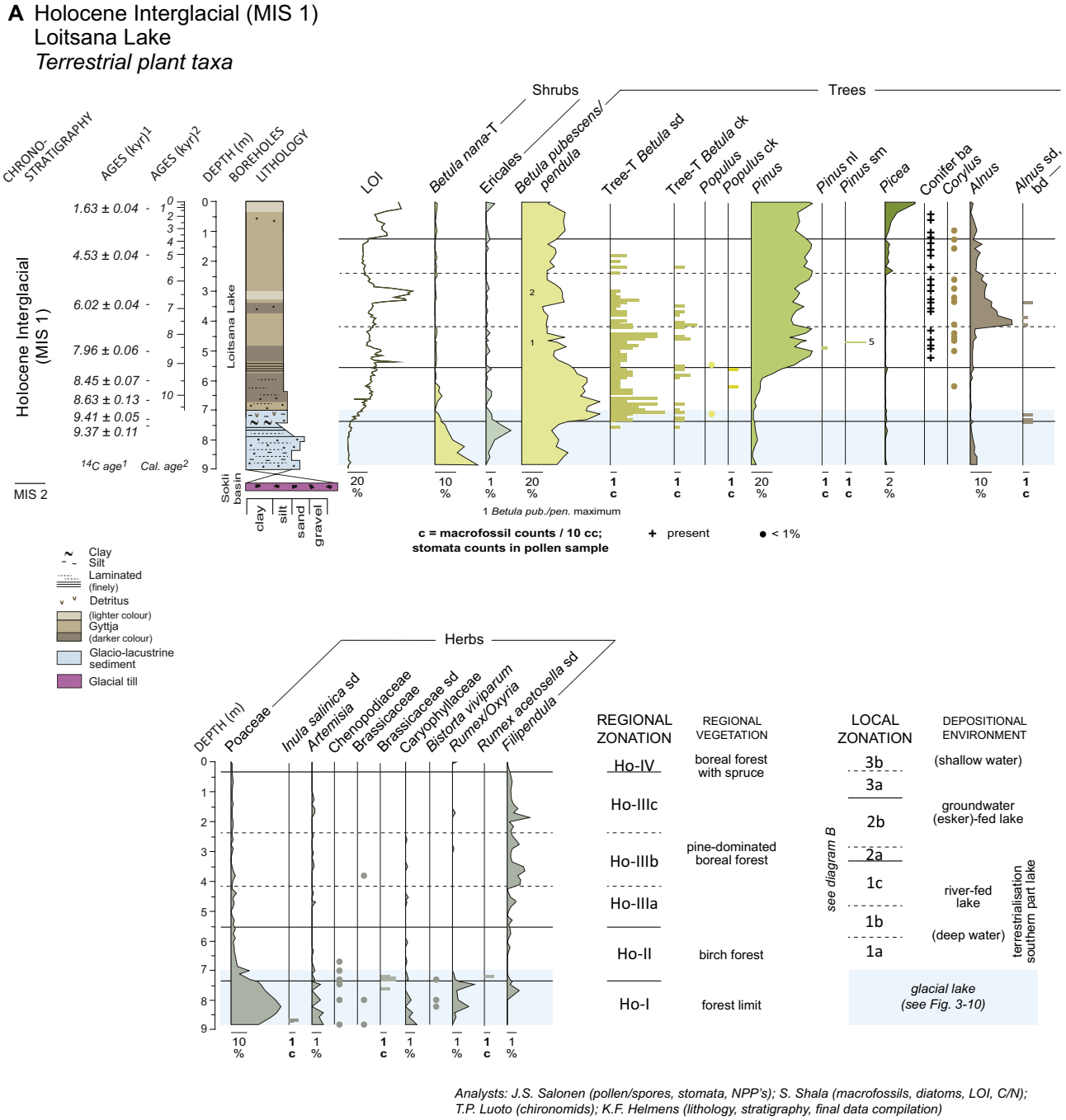

Analysts: J.S. Salonen (pollen/spores, stomata, NPP's); S. Shala (macrofossils, diatoms, LOI, C/N); T.P. Luoto (chironomids); K.F. Helmens (lithology, stratigraphy, final data compilation)

Figure 3-5. *Selection of environmental and climate proxies for the Holocene lake deposit in Loitsana Lake based on Shala et al. (2014b) and Salonen et al. (2013). For explanation of the diagrams see caption of Figure 3-1. Note that multi-proxy data obtained on the glacial lake sediment at the base of the Holocene lake sediment sequence are summarized separately in Figure 3-10.*

B Holocene Interglacial (MIS 1)
Loitsana Lake
Aquatic and telmatic taxa

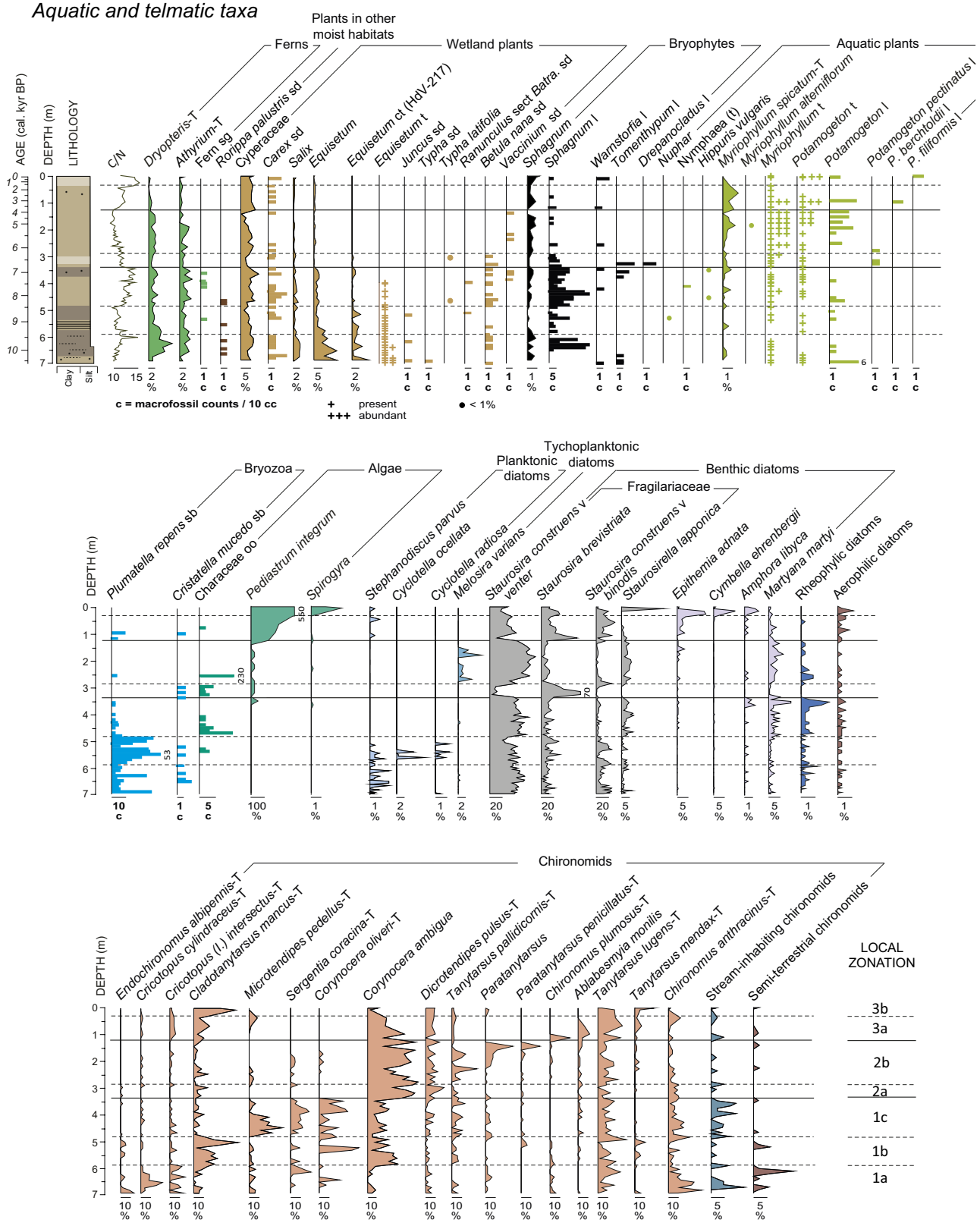

Figure 3-5. *Cont.*

Fossil remains of aquatic plants are encountered in the lower part of the Loitsana sequence, however, their abundances significantly increase under shallower water conditions in the sequence's upper part. *Myriophyllum* is here represented by tissue and pollen of *M. spicatum*-T and *M. alterniflorum*, and *Potamogeton* is recorded by tissue and leave fragments including those of *P. pectinatus*, *P. berchtoldii* and *P. filiformis*. The species assemblage depicts the relatively high nutrient availability during local zones 2 and 3. *Staurosira construens* var. *venter* peaks during local zone 2b, probably reflecting its periphytic (growing on plants) habitat preference. Also, *Corynocera ambigua* attains peak values during local zone 2. This chironomid taxon has a complex ecology (Brodersen and Lindegaard 1999), but has been found to prefer habitats with abundant vegetation (Mothes 1968). Its dominance in the Loitsana chironomid record, similarly as in the MIS 5e and 5a lake sequences, however, is probably due to alkaline water conditions.

The upper c. 1 m of gyttja represents the last c. 3.5 cal. kyr. The humid conditions of the Late Holocene might have increased water flow through the esker, resulting in a lake water body with low DOC content that favoured the green algaa *Pediastrum integrum* (Weckström et al. 2010; local zone 3). It might also have increased water flow in Loitsana Lake, from the esker in the east to the lake's outlet in the west (Figure 1-3), thereby reducing sediment accumulation rates. Varies proxies show a further shallowing of the lake and increased influence from the wetland and catchment during local zone 3. These include rising LOI (to c. 50 %) and C/N values, an increase in the shallow-water green alga *Spirogyra*, and the continuous recording of *Carex* seeds. Furthermore, periphyton (*S. construens* var. *binodis*), shallow-water (*Staurosirella lapponica*, *S. brevistriata*) and aerophylic diatoms (*Achnanthes exigua*) are all well-represented. *E. adnata, C. ehrenbergii* and *A. libyca* all show peak values in the uppermost local zone 3b, indicating elevated conductivity/pH values in the now greatly reduced lake water volume. Interestingly, a phase with high LOI (c. 70 %) and high percentage values of *S. brevistriata* (70 %) is also picked-up shortly after c. 6.8 cal. kyr BP in local zone 2a, possibly recording a sudden, temporal lowering in lake level. This water level lowering might be related to the diversion of the Soklioja away from Loitsana Lake (see above), or might have contributed to the redirection in the rivulet. Abrupt lake level drops are also recorded in the Nuortti warm stage lake sequence and ascribed to millennial-scale climate events, superimposed on the long-term interglacial climate development (Section 3.1.2).

As mentioned earlier, the fossil remains of wetland plants and shore taxa (*Rorippa palustris*, ferns, semi-terrestrial chironomids) in the lower deep-water part of the Loitsana lake sequence most probably were transported to the coring-site from nearby areas by running water. The wetland assemblages shows that in the period between c. 10.5 to c. 9.4 cal. kyr BP (local zone 1a), semi-aquatic conditions with Cyperaceae, *Salix*, *Equisetum*, *Juncus* and *Typha* developed into a meso-oligotrophic wet fen with Cyperaceae, *Betula nana* and *Sphagnum*. Fluvial inflow into the lake, and inwash of plant fragments, diminished during the mild phase between c. 9.4–8.6 cal. kyr BP (local zone 1b). A rich fen, with e.g. *Sphagnum* and brown mosses (*Warnstorfia, Tomenthypnum, Drepanocladus*), however, continues to be recorded after this period until c. 6.8 cal. kyr BP (local zone 1c). At this point, the Soklioja diverted its course away from Loitsana Lake and macrofossil remains of wetland plants mostly disappear from the fossil record.

3.5.2 The Sokliaapa

The c. 4 m-thick Holocene sediment sequence in the Sokliaapa in the Sokli basin, at c. 1 km to the east of Loitsana Lake, shows a highly variable lithology (Figure 3-6). On top of the laminated silt-clay sequence of glacio-lacustrine origin, which here has a thickness of only c. 15–30 cm, sand gradually fines-up to silt, followed by c. 10 cm of peat. The thin peat bed (local zone 2b) has a LOI of almost 60 % and a microfossil assemblage that predominantly consists of Cyperaceae pollen and fungal spores (Figure 3-6B). The latter represent HdV-126 (*Clasterosporium carcinum*; Pals et al. 1980), which is parasitic on *Carex* spp. (van Geel et al. 1983), HdV-200, HdV-201 and HdV-55A. HdV-200 and -201 have a similar ecology and suggest the presence of relatively dry microhabitats on the standing culms of wetland plants or on plant remains in temporary desiccating pools (van Geel et al. 1989, Kuhry 1997). HdV-55A is probably produced by a representative of Sordariaceae, i.e. saprotrophic fungi that obtain their nutrients from non-living organic material (e.g. decaying plant remains; van Geel 1978, 1983). The fossil assemblage, which further includes seeds of *Carex* and *Betula*, reflects the conditions of a marsh.

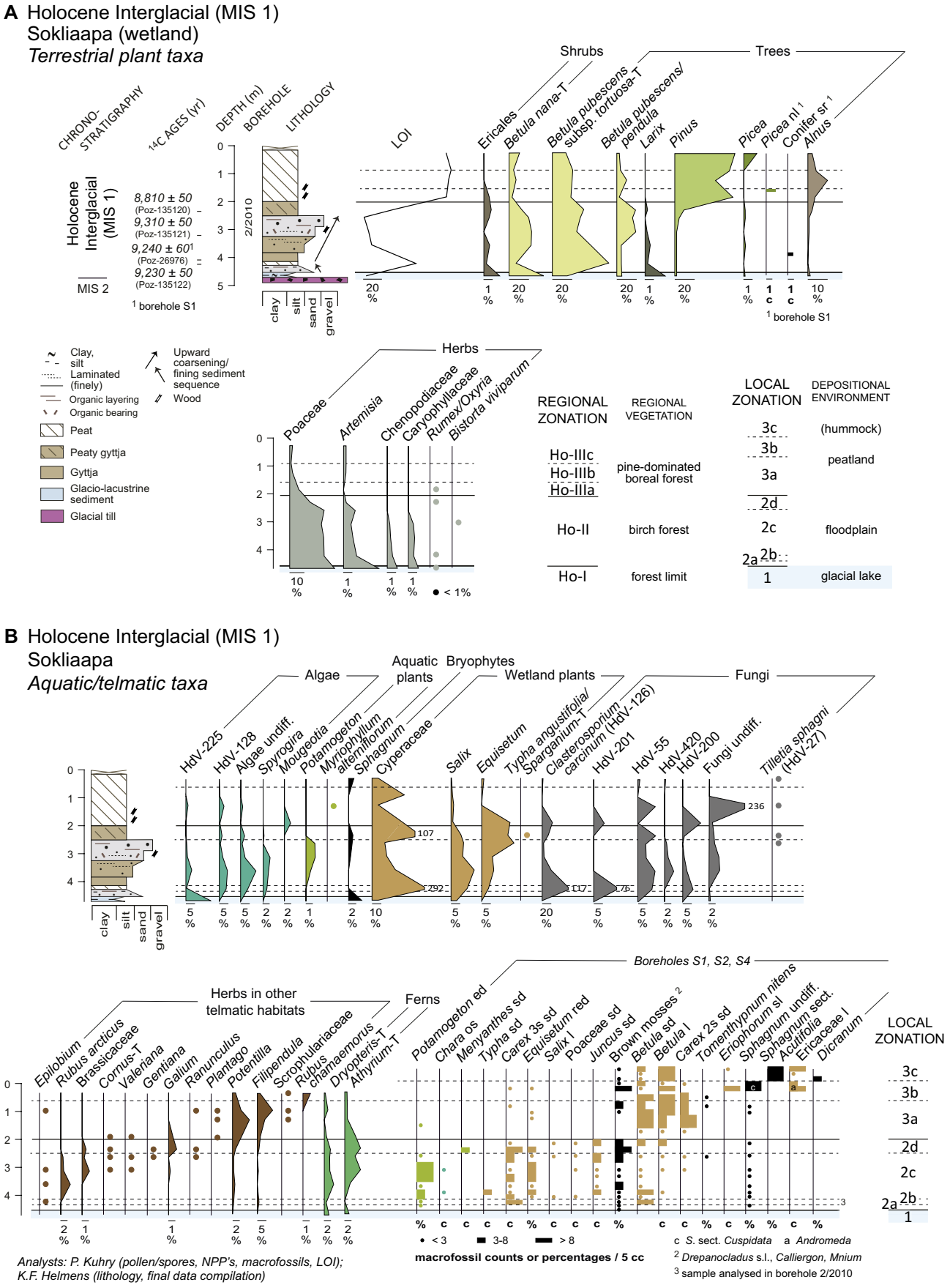

Figure 3-6. *Selection of environmental and climate proxies for the Holocene deposit in the Sokli basin based on this study. For explanation of the diagram see caption of Figure 3-1.*

The c. 1.75 m thick deposit on top of the peat bed consists of gyttja that becomes increasingly interlayered with sand and wood. The sediment then courses-up to fine, unsorted gravel interbedded with thin sandy gyttja laminae (local zone 2c). The fossil record is characterized by wetland elements (e.g. Cyperaceae, *Carex*, *Salix*, *Equisetum*, *Juncus*, *Typha*), algae (e.g. HdV-128, *Spyrogira, Chara*) and the aquatic plant *Potamogeton*. Fungal type HdV-420 is probably a Sordariaceae (Kuhry 1997). The lithology and fossil assemblage shows shallow, nutrient-rich waters with dense stands of vegetation, increasingly influenced by fluvial inputs, and suggests deposition in a floodplain environment. The wetland assemblage resembles the assemblage encountered in the lower part of local zone 1a of the Loitsana record and has a similar age (c. 10 cal. kyr BP). The sandy lithology at the base of the Loitsana sequence further suggests that both assemblages record an early phase of dynamic floodplain conditions.

The sandy/gravelly gyttja deposit is abruptly overlain by a c. 0.5 m-thick gyttja layer rich-in large plant fragments (local zone 2d), which in its turn is overlain by c. 2 m of peat (local zone 3). The fossil assemblage in the gyttja layer, with *Menyanthes*, Cyperaceae, *Carex*, *Equisetum*, *Juncus*, *Betula* and brown mosses, represents a transitional phase from the semi-aquatic conditions recorded in the floodplain sediment of local zone 2c to fen conditions of the overlying peat deposit. The peat deposit, which contains large wood fragments in its lower part, has an LOI approaching 100 %. It depicts a fen assemblage first characterized by *Carex*, *Betula*, abundant fungal remains, *Potentilla* and *Filipendula* (local zone 3a), followed by one dominated by *Eriophorum, Betula*, Ericaceae (incl. *Andromeda*), brown mosses, *Sphagnum* (incl. *S.* sect. *Cuspidata*) and *Rubus chamaemorus* (local zone 3b). Finally, a succession towards more ombrotrophic conditions with *Sphagnum* sect. *Acutifolia* and *Dicranum* is recorded in localized hummocks (local zone 3c). The base of the peat deposit coincides with the establishment of pine-dominated boreal forest at Sokli, which is dated at Loitsana Lake (and supported by the new ^{14}C chronology for the Sokliaapa) to c. 9.2 cal. kyr BP.

The change from the dynamic floodplain conditions in the earliest part of the Holocene to the accumulation of 2 m of peat over the Holocene is intriguing. It recalls the abrupt transition from the dynamic floodplain environment in MIS 5d (Savukoski 1 cold stage) to the accumulation of a thick gyttja deposit in an oxbow lake during MIS 5c (Sokli I warm stage) (Section 3.2). It is possible that both transitions represent an enhancement in atmospheric humidity as the climate changed from dry continental conditions to a moister oceanic regime. Reconstructions of continentality index based on chironomids, both for Loitsana Lake (Engels et al. 2014) and Kharinei Lake in northeast European Russia (Jones et al. 2011), suggest that the climate was at its most continental before c. 8.5 cal. yr BP. The continental conditions in the Early Holocene are supported by the increased seasonality of the solar insolation at 60 °N at this time (summer c. 10 % higher, winter c. 20 % lower) (Berger and Loutre 1991).

3.6 The Sokli Ice Lake (early MIS 5a, mid-MIS 3, Early Holocene)

Glacier meltwater trapped between the retreating ice-margin of the Fennoscandian Ice Sheet and higher unglaciated terrain gave rise to the formation of the Sokli Ice Lake at the start of the Nuortti (MIS 5e), Sokli II (MIS 5a) and Holocene (MIS 1) warm periods and the Tulppio Interstadial Complex (mid-MIS 3). Glacial lakes formed extensively along the retreating margins of the Fennoscandian and Laurentide Ice Sheets around the peak of high-latitude summer insolation at ca. 10 kyr cal. BP (e.g. Dyke 2004, Stroeven et al. 2016, Helmens et al. 2018). The formation of the glacial lakes was facilitated by a land-surface that was inclined towards the retreating ice-fronts, due to isostatic depression, and the production of large amounts of meltwater in the warming climate.

The evolution of the Sokli Ice Lake following the deglaciations of the Sokli site has been reconstructed using geomorphological evidence (meltwater channels, eskers), topographic data and a high-resolution digital elevation model (Johansson 1995, Helmens et al. 2009, Shala et al. 2014a). The reconstruction for the Early Holocene is presented in Figure 3-7 (Shala et al. 2014a) and is representative for all deglaciation phases (Helmens et al. 2018). It shows that the Sokli Ice Lake varied in surface area and water depth depending on the position of the ice-front and the location of spillways/overflow sites. During Lake Stages 1 (deglaciation) and 2, the level of the glacial lake was controlled by the col at the head of the Törmäoja canyon that has a present elevation of 240 m a.s.l.. The glacial lake reached its maximum spatial extension during Lake Stage 2. Opening of the Nuortti canyon resulted in partial (Lake Stage 3; col at 220 m a.s.l.) and final drainage of the Sokli Ice Lake.

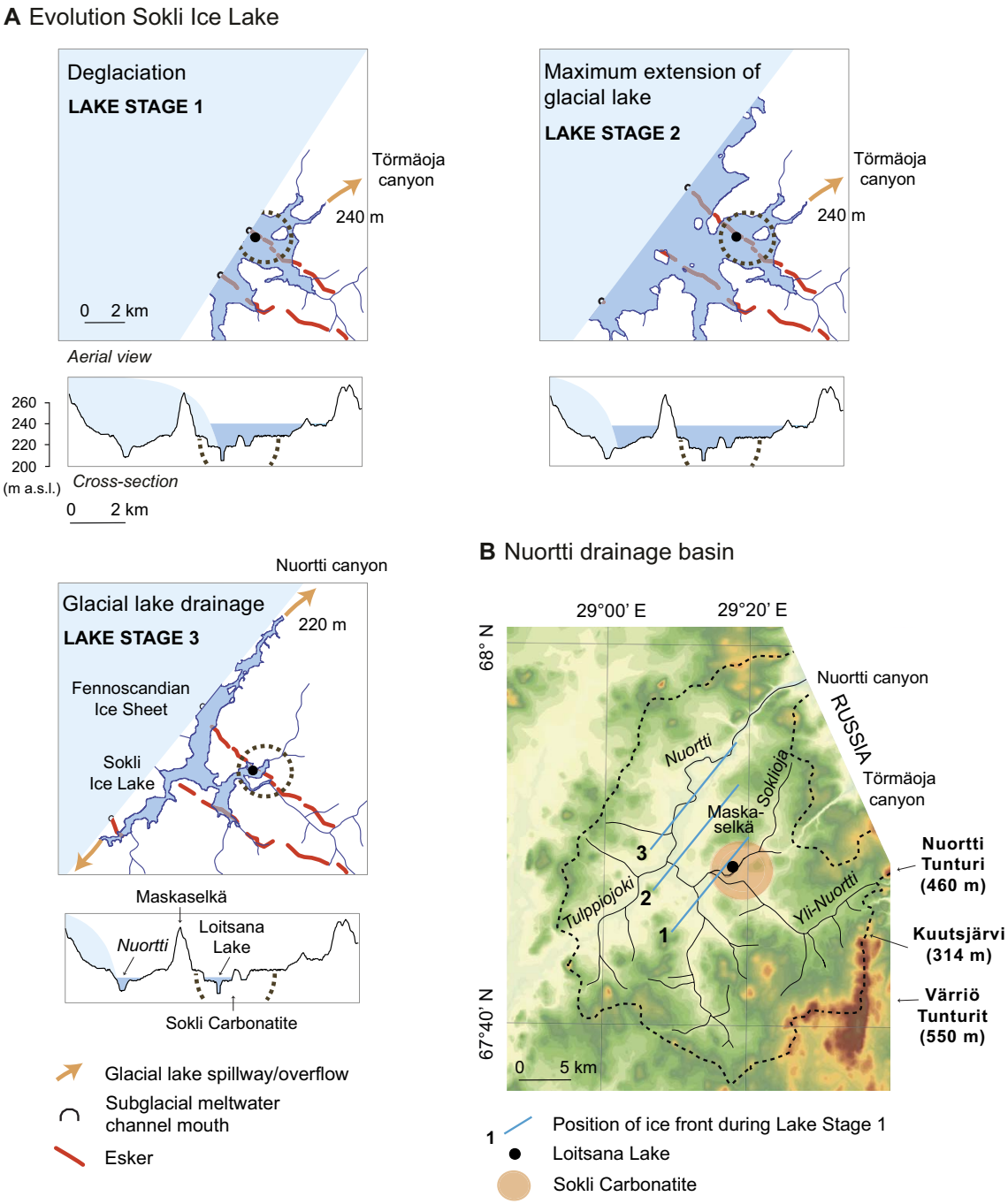

Figure 3-7. *(A) Evolution of the later stages of the Sokli Ice Lake in the Early Holocene; cross-sections show maximum water depths in Loitsana Lake. Note that elevations are modern values. Adapted from Shala et al. (2014a). A similar glacial lake evolution occurred during the early MIS 5a and mid-MIS 3 deglaciation episodes (Helmens et al. 2018). Lake Stage 1: deglaciation of the study site. Lake Stage 2: maximum spatial extent of the glacial lake. Lake Stage 3: partial drainage resulting in a smaller and shallower glacial lake. (B) Position of the ice front during the different deglaciation stages.*

The evolution of the Sokli Ice Lake is clearly recorded by the sediments in the Sokli and Loitsana basins. The ice-marginal retreat, and occurrence of deep-water conditions, during Lake Stages 1 and 2 are depicted as upward-fining sequences of sandy and silty sediments grading into rhythmically laminated silts and clays. Following the sudden decrease in lake level and size associated with the opening of the Nuortti River canyon (Lake Stage 3), silts and sands were deposited (Figures 3-8 to 3-10). The ice lake evolution is also traceable in the XRF-based geochemical record that is available for the Early Holocene glacial lake sequence. With the ice-margin close to the coring-site (Lake Stage 1), erosion of the Sokli Carbonatite Massif (SCM) is reflected in enhanced representations of elements typical for the local bedrock (Ca, S, Nb). A decrease in sediment input enriched in these elements is recorded during Lake Stage 2, i.e. when the SCM became entirely submerged in the expanding ice lake (Figure 3-7), to increase again during the shallow waters of Lake Stage 3 (Shala et al. 2014a; Figure 3-10).

The fossil records from the glacial lake sediments also trace the Sokli Ice Lake evolution in detail (Figures 3-8 to 3-10). They reveal marked compositional shifts in biotic assemblages in concordance with the changes in size and depth of the Sokli Ice Lake. Furthermore, fossil assemblages and successive developments appear to be influenced by actual water depth. Overall deepest lake conditions are reconstructed for early MIS 5a, and shallowest waters in the Early Holocene. This can be expected due to infilling of the Sokli basin and progressive lowering of the glacial lake outlet channels resulting from erosion. The overall coarse-grained glacio-lacustrine sediment of early MIS 5e age contains few fossil remains and is not included in the environmental reconstructions presented below.

Glacial lake sediments have rarely been included in proxy-based paleo-environmental and -climate studies, with the consequence environmental and climate conditions during deglaciation of the large N-Hemisphere ice-sheets remain largely unknown. The fossil records from the Sokli Ice Lake sediments provide overwhelming evidence for warm, insolation-forced summers during the different deglaciation phases in the late Quaternary (early MIS 5a, mid-MIS 3, Early Holocene and Helmens et al. 2018 and references therein). Furthermore, rich biota is recorded in the glacial lake and along its shore, reflecting boreal conditions (e.g. *Typha*, *Potamogeton friesii*, *Nymphaea*, *Cristatella mucedo, Psectrocladius sordidellus*-T), and open sub-arctic woodland on recently deglaciated land.

Although glacial lakes covered large parts of northern Europe and North America, contemporaneous glacial lakes generally were relatively small, confined to the deeper parts in the landscape. The glacial lakes went through complex evolutions as the topography changed and spillways opened up along the retreating ice-margins (e.g. Dyke 2004, Boyd 2007, Johansson 2007b, Carrivick and Tweed 2013). This is exemplified by the study of Jansson (2003) that mapped a total of 26 glacial lakes (65 sub-stages) in Labrador/Ungava, eastern Canada, during the Early Holocene retreat of the Laurentide Ice Sheet. Within the glacial lakes, protected bays were common features and, in combination with inflow of rivers draining unglaciated terrain, allowed aquatic and telmatic biota to flourish in the lakes and along their shores. This is shown in the studies by Boyd et al. (2003) and Boyd (2007) on Glacial Lake Hind and our studies on the Sokli Ice Lake (Johansson 1995, Bos et al. 2009, Engels et al. 2007, Helmens et al. 2009, 2018, 2021, Shala et al. 2014a). Glacial Lake Hind is one of several interconnected proglacial lakes that formed across the Canadian prairies in front of the retreating margin of the Laurentide Ice Sheet. Rich biota was further promoted by enhanced nutrient levels in the recently deglaciated terrain combined with insolation-forced warm summers (Helmens et al. 2018).

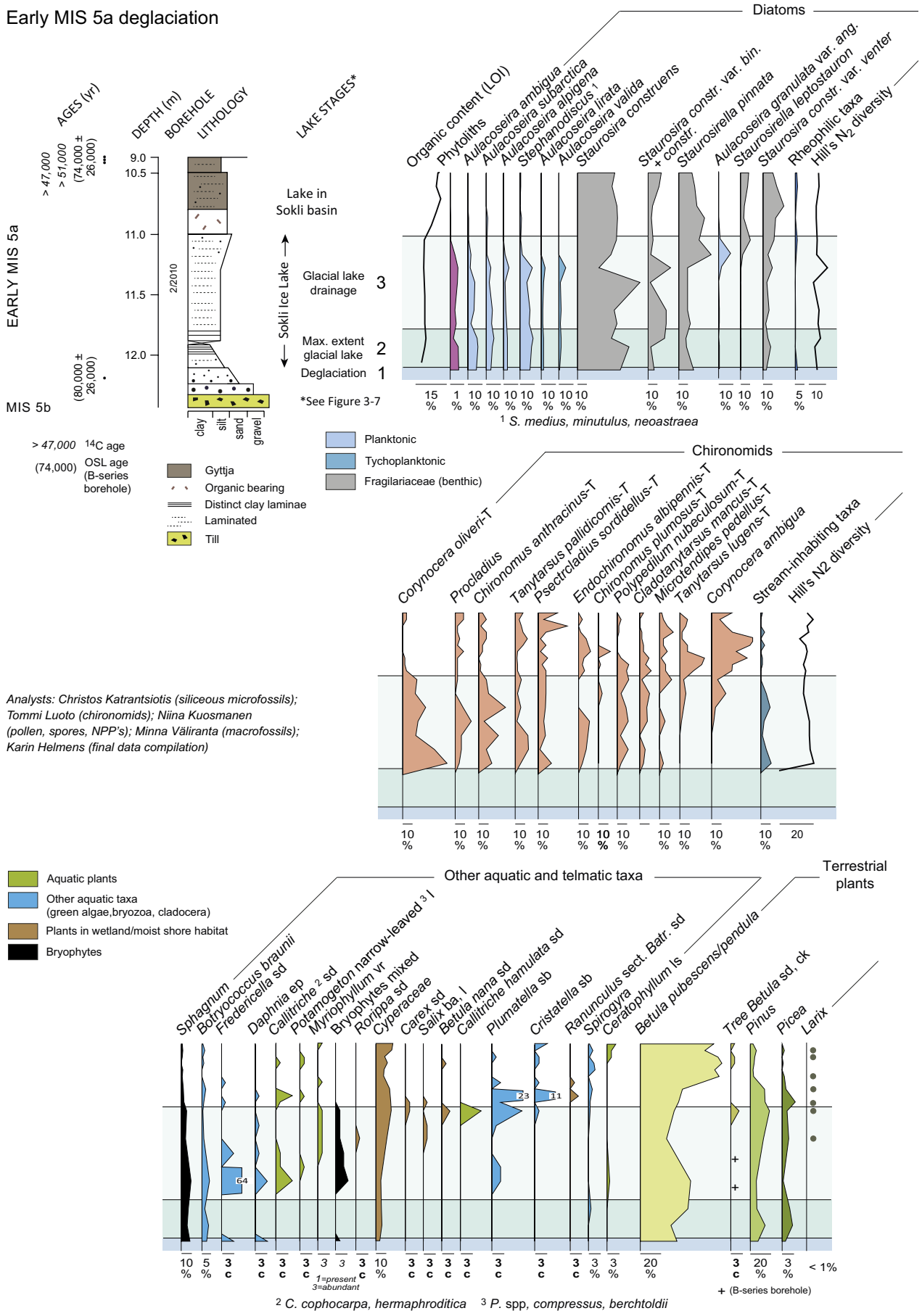

Figure 3-8. *Selection of proxy data for deglacial sediment in the Sokli basin dated to early MIS 5a based on Helmens et al. (2021). Adapted from Helmens et al. (2018).*

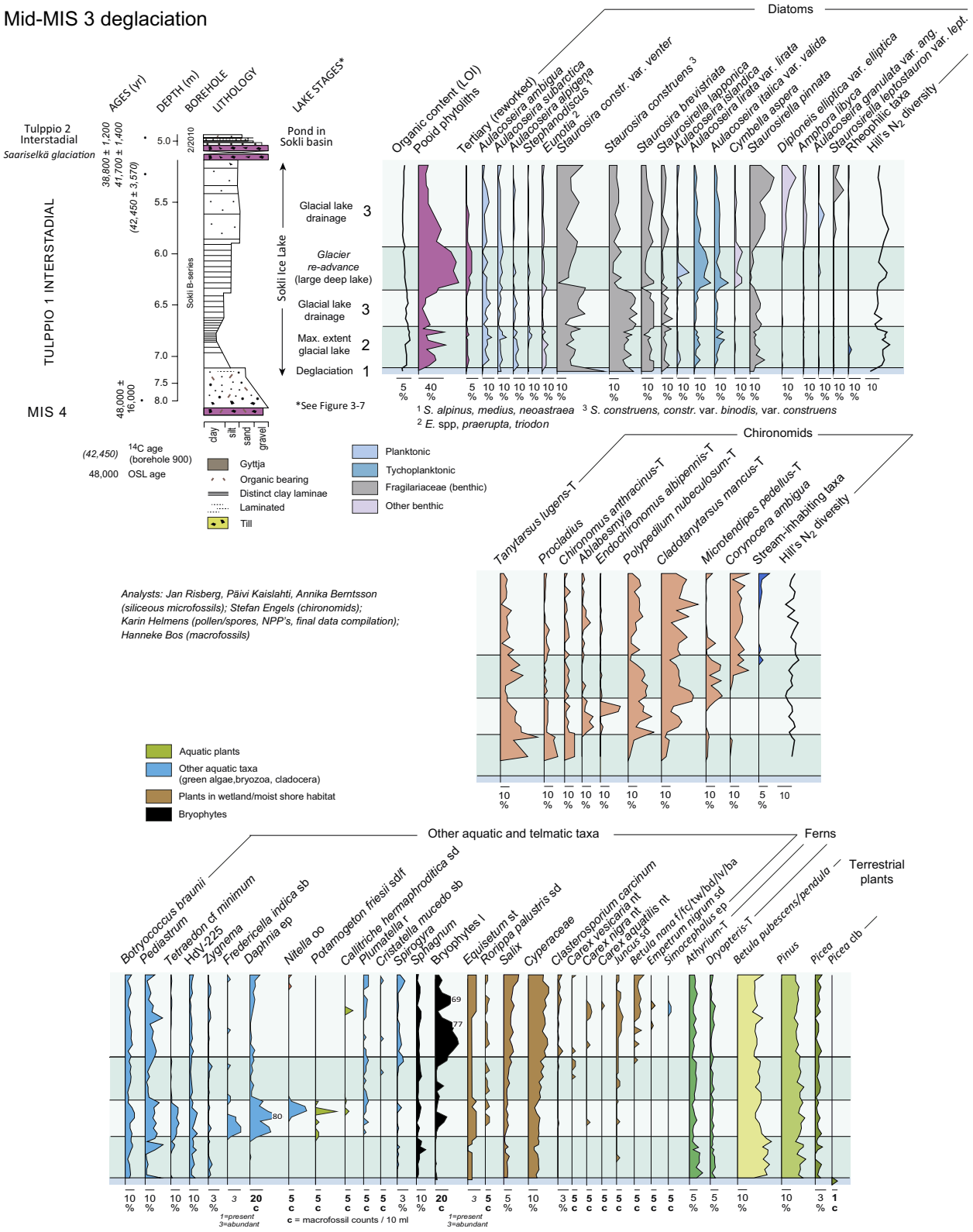

Figure 3-9. *Selection of proxy data for deglacial sediment in the Sokli basin dated to mid-MIS 3 based on Engels et al. (2007), Bos et al. (2009) and Helmens et al. (2009). Adapted from Helmens et al. (2018).*

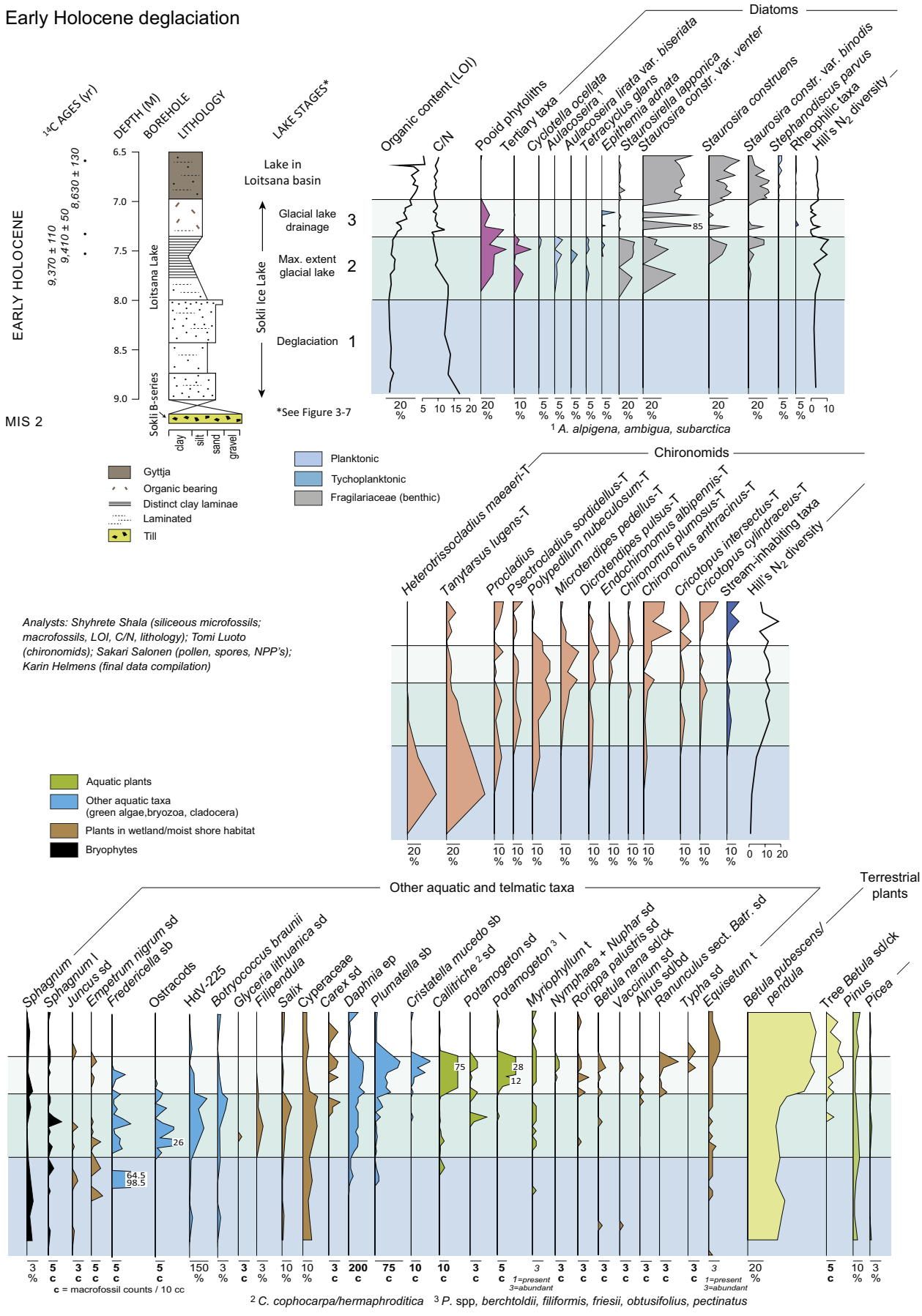

Figure 3-10. *Selection of proxy data for Early Holocene deglacial sediment in Loitsana Lake based on Shala et al. (2014a, 2014b, 2017). Adapted from Helmens et al. (2018).*

3.6.1 Deglaciation and ice-marginal retreat

The fossil content and diversity of fossil remains in the glacial lake sediment sequences of early MIS 5a, mid-MIS 3 and Early Holocene age in general increase with increasing distance of the ice-margin from the coring-site (Lake Stages 1-2; Figures 3-8 to 3-10). The diversity of diatoms and chironomids in the diagrams is expressed by Hill's N_2 values (effective number of occurrences; Hill 1973). C/N values, available for the Early Holocene deglacial sediment, show a gradual decline during Lake Stages 1 and 2 suggesting a rise in in-lake productivity. Turbulent waters and turbid water conditions occur close to ice-margins and significantly decrease primary productivity (Henley et al. 2000). Also, the fossil record in the coarse-grained ice-marginal sediment at the base of the studied sequences (Lake Stage 1) can be expected to be diluted due to high sedimentation rates (Risberg et al. 1999) and plant/animal remains to be more easily destroyed in this high-energy environment.

Chironomids that are recorded among the first colonizers of the Sokli Ice Lake are the deep-water taxa *Heterotrissocladius maeaeri*-T, *Tanytarsus lugens*-T and *Procladius*. *H. maeaeri*-T is also reported to have dominated the deep waters of the Late-Glacial Baltic Ice Lake in southern Finland (Luoto et al. 2010). The diatom record predominately consists of Fragilariaceae and *Aulacoseira*. Fragilariaceae is a group of taxa that is characterized as pioneering and opportunistic, since they colonize quickly, have high reproduction rates and are more adaptive to a changing environment (Risberg et al. 1996, Lotter et al. 1999). They often occur in lakes that have some sort of disturbance as, in this case, recently deglaciated lakes (Bigler et al. 2003). The encountered planktonic *Aulacoseira* species (*A. ambigua*, *A. subarctica*, *A. alpigena*) are all heavily silicified and most probably reflect a large influx of Si into the glacial lake and enhanced levels of turbulence. A high Si-level is further suggested by findings of *Tetracyclus glans* (Michel et al. 2006). Statoblasts of the bryozoan *Fredericella indica* (Økland and Økland 2001) and high abundances of pooid phytoliths and Tertiary diatoms in the sediment indicate wave action and significant shore erosion. Tertiary diatoms are exemplified by species like *Pliocaenicus costatus*, a relict freshwater taxon from the Pliocene, and *Paralia sulcata* of marine-origin, their robust structure allowing for multiple phases of re-working (Helmens et al. 2009, and references therein). The cladoceran *Daphnia* (water flea) is additionally well-represented among the first lake colonizers.

Striking for the deglacial phase of MIS 3 age (Figure 3-9) is the co-occurrence of peak abundances of *Procladius* with a large variety of algae (*B. braunii*, *Pediastrum*, *Tetraedon* cf. *minimum*, *Zygnema*, *Spirogyra*, HdV-225; high diatom-inferred Hill's N_2) in the finely laminated clayey sediment at the end of the deep-water Lake Stage 2. This might reflect density stratification, a process typical for glacial lakes in which cold sediment-loaded meltwater extends below warmer and more transparent river-fed water (Carrivick and Tweed 2013, and references therein). The latter probably favoured a diverse algal community. *Procladius* is a ubiquitous chironomid taxon with a wide environmental tolerance, including turbid water inflows (Greffard et al. 2012), and is found in lakes with a large variability in limnological conditions, such as hypolimnetic oxygen availability and water temperature (Brodersen et al. 2004).

The fossil record from the overall relative shallow water deglacial sediment of Early Holocene age shows the presence of the dwarf shrub *Empetrum nigrum*, the tall herbs *Rorippa palustris* and *Filipendula*, the grass *Glyceria lithuanica*, as well as *Carex*, *Juncus Equisetum* and *Sphagnum*, in what probably was local shore or wetland habitats along the glacial lake shoreline (Figure 3-10). The occurrences of the diatom taxa *Epithemia adnata* and *Rhopalodia gibba* in the upper part of the Lake Stage 2 sediment of Early Holocene age suggest pH values exclusively above 7 (van Dam et al. 1994). High abundances of ostracod remains indicate enhanced Ca-concentrations. This lake water chemistry mostly probably resulted from rapid leaching of carbonates and other soluble minerals from surface soils shortly after deglaciation (Engström et al. 2000). An enhanced level of nutrients in the glacial lake during the latter part of Lake Stage 2 in MIS 3, and particularly during early MIS 5a, is further suggested by relatively high percentage values of *Stephanodiscus* species (*S. medius*, *S. minutulus*, *S. neoastraea*, *S. alpinus*).

3.6.2 Glacial lake drainage

The local establishment of diverse aquatic and telmatic communities is recorded in the silty/sandy glacial lake sediments during Lake Stage 3. This stage followed the opening of a spillway that resulted in a drastic decrease in water depth and size of the Sokli Ice Lake (Figure 3-7). The margin of the Fennoscandian Ice Sheet during Stage 3 was situated at a distance of less than 10 km from the coring-site (i.e. before deglaciation of the Nuortti canyon).

Remarkably rich fossil assemblages are encountered in the Early Holocene sediment (Figure 3-10). The fossil remains reflect a shallow lake and even further shallowing, accompanied by an extension in the wetland zone (macrofossils of *Carex*, *Ranunculus* sect. *Batrachium, B. nana*, *Vaccinium*, *Typha, Alnus*), higher up in the Stage 3 silts. Characteristic are the high representations of the bryozoa *Plumatella repens* and *Cristatella mucedo* and the shallow-water plant *Callitriche cophocarpa*/*hermaphroditica*; the occurrences of *Nymphaea* and *Nuphar*; and the large variety of *Potamogeton* species (*P. berchtoldii, P. filiformis, P. friesii, P. obtusifolius, P. pectinatus*). The pioneering, narrow-leaved *Potamogeton* species thrive in shallow (0.1–1.5 m) water depths. *C. mucedo* indicates more coloured water with less wave action than *F. indica* (Økland and Økland 2005). Nutrient levels were relatively high as indicated by e.g. *P. friesii*, *P. berchtoldii* and *P. pectinatus, Typha*, and the chironomid taxon *Endochironomus albipennis*-T (Moller Pillot 2009). The chironomid record further shows various littoral taxa (*Polypedilum nubeculosum*-T, *Microtendipes pedellus*-T, *Dicrotendipes nervosus*-T). In contrast to these rich biotic communities, diatom assemblages are largely dominated by *Staurosira construens* var. *venter*, showing peak values reaching >85 %. This might reflect the littoral and periphytic (growing on plants) habitat preferences of this diatom species and/or tolerance to poor light conditions (Bigler et al. 2003). LOI values are remarkably high, rising to 20 %. The silty sediment occurs interbedded with thin organic laminae at a site close to the former glacial lake shore (Saunavuotsoin Figure 1-3). This shows that postglacial carbon storage started within the glacial lake sediment, i.e. prior to the accumulation of peat that was initiated over large parts of northern Europe (e.g. Oksanen et al. 2001), and central and eastern Canada (Dredge and Cowan 1989), due to the presence of the relatively impermeable glacial lake silts and clays.

The silty/sandy Lake Stage 3 sediment of MIS 3 age also records in detail shallowing waters, however, this trend is interrupted by the re-occurrence of a large, deep-water lake stage caused by a glacier re-advance phase (Figure 3-9). Initially, *F. indica* (Økland and Økland 2005) and the chironomid taxon *Ablabesmyia* (Vallenduuk and Moller Pillot 2007) suggest moderate nutrient availability. Subsequently, nutrient levels increase as indicated by high percentage values for *E. albipennis*-T combined with occurrences of *P. friessi* and the macro-alga *Nitella*. The appearance of the cladoceran *Simocephalus* in the upper sandy part of the deposit suggests shallow, open water, eutrophic conditions and dense stands of vegetation (van Geel et al. 1983). Strongly reduced water depths here are further indicated by enhanced values for the shallow-water alga *Spirogyra* and the littoral diatom taxon *Staurosirella pinnata*. High abundances of bryophyte leaves, seeds of *Carex*, *Juncus*, *B. nana* and *E. nigrum*, increased percentage values of Cyperaceae and *Salix* pollen, and a near continuous registration of hyphopodia of *Clasterosporium caricinum* (HdV-126), i.e. a fungus that parasitizes on *Carex* (van Geel et al. 1983), record a distinct expansion of the wetland zone. The glacier re-advance phase that interrupted the shallow-lake Stage 3 resulted in the temporal re-occurrence of deep water (increases in tycho-planktonic diatom taxa and deep-water *T. lugens*-T), a large lake-size (*Aulacoseira islandica* and Serieyssol et al. 2009), oligotrophic lake water conditions (*Cymbella aspera* and Krammer and Lange-Bertalot 1986) and significant shore erosion (>50 % of phytoliths).

Finally, the silty Glacial Lake Stage 3 deposit of early MIS 5a age contains macro-remains of *Plumatella*, *Callitriche* (*C. cophocarpa*, *C. hermaphroditica, C. hamulata*), narrow-leaved *Potamogeton* (e.g. *P. compressus*) and the shallow-water plant *Ceratophyllum* (Figure 3-8). Characteristic is the combined appearance of *Tanytarsus pallidicornis*-T and *Psectrocladius sordidellus*-T, i.e. chironomid taxa presently common in the sublittoral and littoral zones of boreal lakes mostly found living among *Phragmites* stands (Luoto 2010). Nutrient availability was overall high as indicated by occurrences of *E. albipennis*-T and *Chironomus plumosus*-T (Brooks et al. 2001), and a high representation of *Stephanodiscus* among the diatoms. The enhanced nutrient level, and high chironomid species diversity (high Hill's N_2 values), might be related to inflow of running water close to the coring-site.

The latter is indicated by relatively high abundances of stream-inhabiting chironomid taxa (e.g. *Eukiefferiella*, *Rheocricotopus*) as well as the type of lamination of the silty deposit, i.e. laminae of varying grain-sizes (clay to fine sand) and thicknesses. A strong reduction in water depth during deposition of the uppermost sandy part of the deposit is indicated by littoral *M. pedellus*-T and *S. pinnata*, and macrofossils of *Carex*, *Salix* and *B. nana*. Interestingly, the diatom *Aulacoseira granulata* var. *angustissima* appears with peak values in the upper sandy sediment of Lake Stage 3 both during early MIS 5a and MIS 3 and, together with increased representations of the diatom taxa *Staurosirella leptostauron*, *Diploneis elliptica* and *Amphora libyca*, reflect alkaline waters with high Ca-concentrations (Gómez et al. 1995, Jones and Birks 2004). This lake water chemistry was recorded in the Early Holocene glacial lake sequence already during the relatively shallow-water Lake Stage 2. It is possible that the glacial lake volume during MIS 3 and early MIS 5a became only reduced enough during Lake Stage 3 in order for alkaline water conditions to be established.

4 Reconstruction of regional vegetation development

This chapter gives a detailed account of the developments in regional vegetation at Sokli over the last 130 kyr. It is a unique opportunity to reconstruct changes in vegetation over such a long period in Fennoscandia, a part of Europe where few sediment/fossil records have escaped the widespread erosion by the Fennoscandian Ice Sheet. As an introduction to this chapter, it is important to highlight that the results obtained on the late Quaternary glacial history of Sokli and on changes in regional vegetation during ice-free periods have been unexpected in many ways. Based on the long-distance correlation of litho-(till fabric) and bio-stratigraphic (pollen) fragmentary evidence, the warm stages MIS 5c (centered at c. 96 kyr BP; Figure 1-1) and possibly MIS 5a (c. 82 kyr BP) were the only time-intervals of the Last Glacial Period (c. 120–10 kyr BP) considered to be ice-free at Sokli (Hirvas 1991). The vegetation during these periods was inferred as tundra or an open vegetation close to the forest-limit. Sub-arctic birch forest was reconstructed for areas presently covered by mixed boreal forest south of Sokli, and the location of the conifer (pine) tree-limit was thought to be situated in the present temperate central-southern boreal zone in south Fennoscandia (Donner 1995 and references therein). In sharp contrast, the long Sokli record not only shows ice-free conditions both for MIS 5c and 5a, the combined pollen, stomate and macrofossil data for these time-intervals reconstruct inter-glacial vegetation developments towards boreal forest and summer temperatures exceeding present-day values by several degrees, similar as during the Holocene Interglacial. Sokli was not glaciated during cold MIS 5d (c. 109 kyr BP), when steppe-tundra prevailed, and the region was deglaciated twice in mid-MIS 3 (c. 40 kyr BP) with developments of a treeline vegetation and birch forest. These highly dynamic environmental conditions inferred from the Sokli data were not restricted to what was earlier defined as the Last Glacial Period. A high-resolution analysis on the unique 9 m-thick lake deposit of MIS 5e age (c. 125 kyr BP) shows two millennial-scale cooling events intersecting interglacial warmth, with mixed boreal forest being replaced by birch forest during the early MIS 5e Tunturi event. Numerous studies on deposits of MIS 5e (Eemian Interglacial) age in central Europe suggest that the interglacial was characterized by a rather stable climate evolution with only minor short-term climate variability (Cheddadi et al. 1998, Rioual et al. 2001, 2007, Kühl et al. 2007) and MIS 5e was earlier thought to have a stable climate evolution in northern Fennoscandia as well (Saarnisto et al. 1999).

This is the first time that the vegetation that developed in the Sokli region during the different ice-free intervals of the late Quaternary is compared in detail. A figure is introduced (Figure 4-1A) that schematically shows the developments in regional vegetation on an absolute timescale for which the details are provided below. Summer temperatures that are independently inferred from aquatic/wetland taxa, as reconstructed/discussed in Chapter 5, are summarized to the right of the vegetation record (Figure 4-1B). Stratigraphy and solar insolation are provided at the left side of the figure. This chapter will focus on the main vegetation types that established at Sokli as part of the long-term MIS 5e, 5c, 5a and Holocene interglacial vegetation developments, and the MIS 5d and mid-MIS 3 vegetation, to explore their relationship to climate and/or other environmental conditions. This can be considered an important step, in addition to the characterization of the local environment in the Sokli and Loitsana basins (Chapter 3), towards the evaluation of the quantitative climate reconstructions presented in Chapter 5. Furthermore, references are made in the text to a new high-resolution Holocene vegetation and climate record from Kuutsjärvi in the nearby Värriö Tunturit (Salonen et al. 2024; for location see Figure 3-7). This lake is situated in Precambrian crystalline rocks, allowing an evaluation of a possible influence of the local carbonatite bedrock at Sokli on its vegetation and climate records.

Figure 4-1 reveals remarkably similar developments in regional vegetation during the Holocene and the three warm stages of MIS 5 age, although some important and interesting differences occur. The interglacial vegetation successions are characterized by the replacement of an open woodland vegetation by birch forest and then (mixed) boreal forest with pine (MIS 5a), spruce (MIS 5c, Holocene) and temperate hazel (MIS 5e). The local presence of larch is inferred for all 4 warm periods as well as for the mid-MIS 3 Tulppio 2 Interstadial defined here. The interpretations in terms of regional vegetation presented in this chapter largely follow those of the original publications (Table 1-2). The reconstructions make use of studies on modern pollen-vegetation relationships (Aario 1940, Prentice

1978, Hicks 1994) and modern pollen spectra encountered in pollen-climate calibration lakes (Seppä et al. 2004).

The fossil records of terrestrial plant taxa are presented in part A of the multi-proxy diagrams in Figures 3-1 to 3-6 and are summarized in Figure 5-1A. Note that the palynological data in Figure 5-1A, as well as the pollen-based climate reconstructions in Figures 5-1B and 5-2, are based on a pollen sum that deviates from the one used in the original studies (and diagrams in Figures 3-1 to 3-6). The pollen sum is a selection of pollen/spore taxa on which all percentage values of plant taxa and NPP's are calculated. The original studies use a pollen sum that is similar as applied in the modern pollen-climate calibration samples. An exception are the spores of *Equisetum* and *Sphagnum* that have been excluded from the sum, except for the MIS 5e study where *Sphagnum* spores are part of the pollen sum (Salonen et al. 2018). Enhanced spore percentages of *Equisetum* are accompanied in the multi-proxy datasets by macrofossils and/or NPP's pointing to a local wetland source. Spores from the bryophyte *Sphagnum* is included in the pollen sum of the modern calibration dataset as representing boreal/sub-arctic conditions. Since the latter conditions are the frame in which most of the Sokli past vegetation changes operate, the spores of *Sphagnum* relate to the presence of wetland as well. It has further become apparent during the Sokli studies, and the present final compilation of data, that spores of ferns as well as pollen of sedges (Cyperaceae) and *Salix* mostly originated from local (azonal) habitats (see Chapter 3). The new pollen sum used in Figures 5-1 and 5-2 excludes all spore taxa. A pollen sum without spores is widely applied in long pollen records from central Europe. Nevertheless, Cyperaceae and *Salix* are not excluded from the new sum since these plant taxa are important elements in the present-day arctic tundra vegetation. However, the pollen records of the latter plants, together with their macrofossil/NPP records, are presented in part B of the multi-proxy diagrams in Figures 3-1 to 3-6. Furthermore, the over-representation of Cyperaceae and *Salix* in pollen assemblages during phases with extensive wetland is taken into consideration in the reconstruction of the regional vegetation (this Chapter) and the evaluation of the pollen-based climate reconstructions (Chapter 5). Also, phases with wetland expansion, and sudden lake levels drops, are highlighted along the lithological column in Figure 5-1.

The timescale for the vegetation record of the Nuortti warm stage (MIS 5e) at the base of the Sokli sequence in Figure 4-1A is based on an event-stratigraphic correlation to U/Th-dated speleothem records from Europe (adapted from Salonen et al. 2018). It includes a novel, well-dated and high-resolution early MIS 5e stalagmite-based carbon/oxygen isotope record from Korallgrottan (Coral Cave) in northern Sweden (Finné et al. 2019). The Coral Cave record dates the deglaciation phase to the MIS 6/5e transition at c. 131 kyr BP. This is the first absolute age determination derived from land-based evidence for the timing of deglaciation in northern Fennoscandia following the Penultimate Glacial (MIS 6). The Coral Cave record depicts an increase in growth rate paired with isotopic indications of a warmer climate at c. 127 kyr BP, comparing well with indications of wetter and warmer conditions in other parts of Europe at this time (Finné et al. 2019 and references therein). It also agrees with decreasing continentality (see Section 3.1.1) and establishment of warm interglacial conditions early in the Nuortti Interglacial (this chapter and Chapter 5). Remarkably, the following cooling/drying of the Tunturi event is clearly depicted at Coral Cave as a millennial-scale cooling between c. 126.8 and 125.7 kyr BP, occurring nearly concomitantly with drier conditions recorded in speleothems from France and Italy (Finné et al. 2019 and references therein). Among the latter, the stacked, extensively dated, and high-resolution oxygen isotope record from Corchia Cave (central Italy) dates the early MIS 5e dry interval to 127–126 ± 0.7 kyr BP (Tzedakis et al. 2018) and these ages are used in Figure 4-1A for the Tunturi event. Growth of the Coral Cave stalagmite ceased at c. 124.5 kyr BP. Correlation to speleothem records from Belgium and the northern Alps, and further supported by Greenland ice-core and Norwegian Sea data, suggest that the MIS 5e interglacial ended at c. 117.5 kyr (Salonen et al. 2018 and references therein). Using these anchor points, and assuming constant sedimentation rates, the Värriö cooling/drying event at Sokli dates to just younger than 120 kyr BP, comparing well to a late MIS 5e aridity event at Corchia Cave dated to 119 kyr BP (Tzedakis et al. 2018). The Corchia Cave record depicts another distinct event at c. 122 kyr BP that might correlate to the sudden lake level drop of local zone 4b in Figure 3-1B, occurring at the base of zone Nu-VII (Figure 5-1), with an age of c. 123 kyr BP in Figure 4-1.

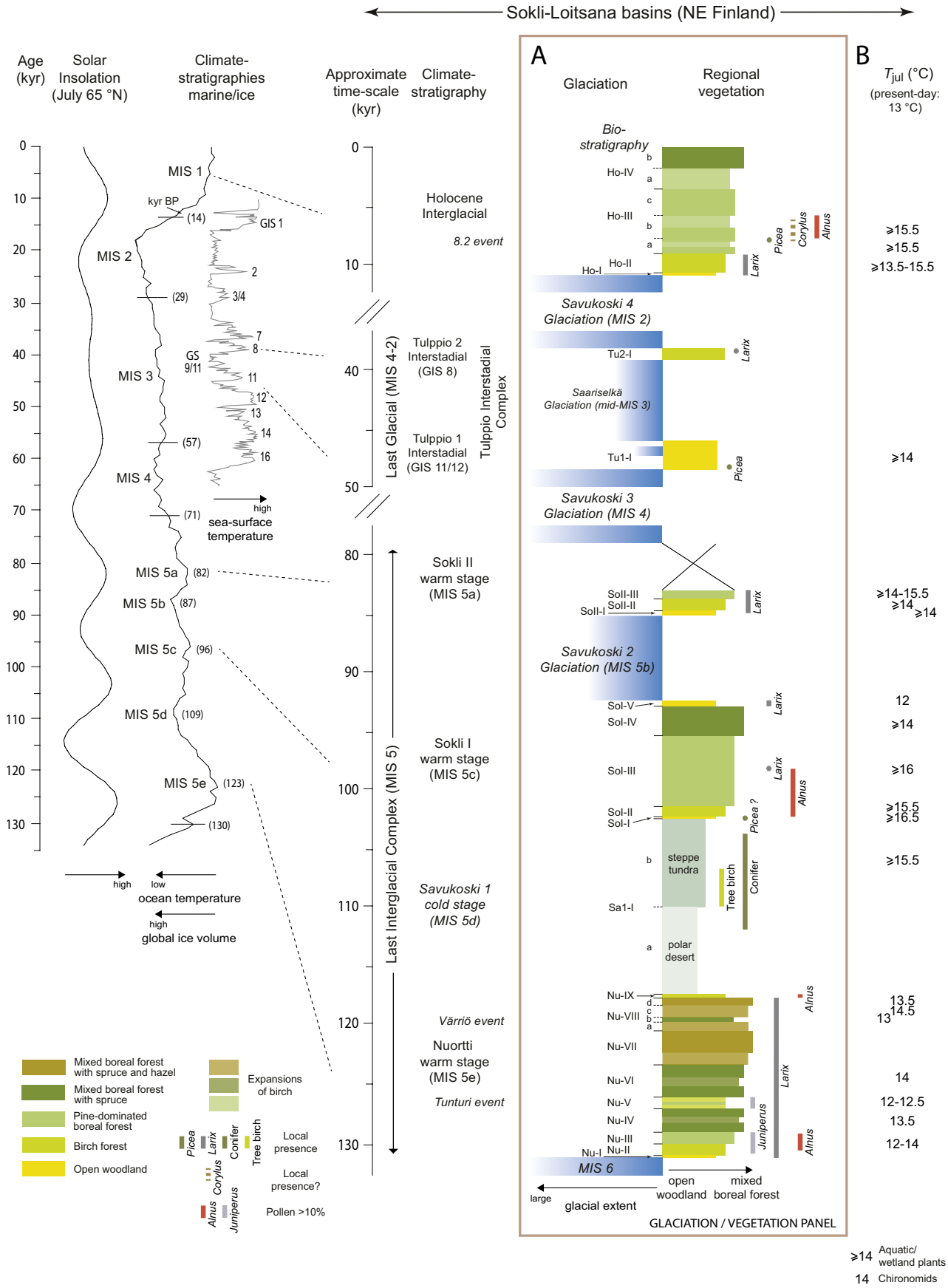

Figure 4-1. *(A) Reconstruction of developments in regional vegetation at Sokli during the ice-free intervals of the late Quaternary on an approximate timescale; periods with glaciation are indicated to the left. (B) Mean July air temperatures (T_{jul}) independently inferred from aquatic/wetland plant taxa and chironomids. Climate-stratigraphies and solar insolation are shown at the left side of the figure (see also Figure 1-1).*

According to the speleothem-based correlation described above, the Nuortti warm stage lasted in the order of c. 13 kyr. This corresponds well with the duration of no more than 13 kyr for the Eemian interglacial forest phase in Germany, central Europe, as inferred from annually laminated diatomite sections (Turner 2002). Although climate records derived from a variety of natural archives are available for the warm stages MIS 5c and 5a, these do not provide a consistent chronology for these periods. This is due to incomplete records, differences in time-resolutions, differences in response times between proxies, and different dating methods and tuning approaches (Wohlfarth 2013, Helmens 2014). The duration of the Brørup (MIS 5c) and Odderade Interstadials (MIS 5a) on mainland Europe are estimated at 5–10 kyr based on annually laminated diatomites and peat accumulation rates (Behre and van der Plicht 1992 and references therein). These estimates, together with the insolation-forced chronology of the marine oxygen-isotope stack, are used for the approximate timing/duration of the Sokli I (MIS 5c) and Sokli II warm stages (MIS 5a) in Figure 4-1. The Tulppio Interstadial Complex (MIS 3) is dated to c. 48–40 kyr BP and correlated to GIS 12-8 in the Greenland ice-core stratigraphy (see Section 3.4). Finally, the timescale for the Holocene record in Figure 4-1 is based on Bayesian age-depth modelling using radiocarbon dates from the Loitsana lake sequence (see Section 2.1). Precise age determinations are lacking to estimate the duration of the deglacial phases at the start of the Nuortti (MIS 5e), Sokli II (MIS 5a) and Holocene warm periods. According to the deglaciation history of northern Finland (Johansson 2007b, Stroeven et al. 2016), the duration of the Sokli Ice Lake following the last deglaciation of the Sokli site lasted c. <100 yr and possibly <25 yr. This time estimate is also used for the glacial lake phases early in MIS 5e and 5a.

4.1 Steppe-tundra

Steppe-tundra vegetation was widespread on mainland Europe during the cold stages of the late Quaternary (e.g. Granoszewski 2003). Steppe-tundra associations are recorded at Sokli during the Savukoski 1 cold stage (MIS 5d; Figure 4-1A). Areas that presently maintain steppe-tundra have a strong continental climate regime with deep continuous permafrost.

The fossil pollen spectra encountered in the fluvial sediment of the Savukoski 1 cold stage are characterized by high percentages of non-arboreal pollen taxa (NAP to c. 60 %; Figures 3-2A and 5-1) representing a combination of steppe and tundra elements. Relatively high pollen percentage values for *Artemisia* (c. 10–15 %) and Chenopodiaceae, together with a high representation of grasses (Poaceae to c. 50 %), suggest the presence of dry, steppe-like vegetation. Presently, the herbs *Artemisia* and Chenopodiaceae are common elements in the steppe and steppe-like vegetation of central and northeastern Eurasia (Shahgedanova 2008). Poaceae are a main constituent of the northern Eurasian tundra, but high pollen percentage values are primarily reported from modern pollen samples in the steppes (Tarasov et al. 1998).

The shrub *Betula nana* (dwarf birch) is represented in the Savukoski 1 pollen assemblages as well, and like other recorded plants such as sedges (Cyperaceae), is a typical element of the present-day northwestern and north-central Eurasian low-arctic shrub tundra (Shahgedanova and Kuznetsov 2008). NAP further includes a variety of heliophilous (light-demanding) herbs (Brassicaceae, Caryophyllaceae, *Centaurium, Armeria maritima*-T*, Eryngium, Bistorta viviparum*, *Sedum*-T), the arctic-alpine herb species *Saxifraga oppositifolia*-T (including *S. aizoides*; Seppä 1996), and the (dwarf) shrubs *Juniperus*, *Salix* and Ericales. Lycopodiaceae (lycopods; not shown in the multi-proxy records) and Polypodiaceae (ferns) are represented by low spore percentages only, mostly those of *Huperzia selago*.

The macrofossil record indicates that the steppe-tundra was not tree-less. Well-preserved bark tissue of conifer trees, either pine (*Pinus*) or spruce (*Picea*), as well as seeds of tree-type birch are found in the sediment. These trees were probably present as scattered occurrences in favorable spots. Larch (*Larix*) may also have been present. This tree is generally very poorly represented in the fossil record (see Sections 4.2 and 4.4). The regional vegetation seems to have been rather similar throughout zone Sa1-I (Figure 3-2A). Relatively high pollen percentage values for Poaceae and *Artemisia* and the near absence of pollen of shrubs in the lower gravelly sediment, however, suggest a sparser vegetation cover, possibly comparable to a polar desert (zone Sa1-Ia; Figure 4-1A).

At present, steppe-tundra associations are rare. The co-occurrence of steppe and arctic-alpine species are described for the Chukotka Peninsula in northeastern Siberia (Yurtsev 1981) in Zlotin (2008) and the Kangerlussuaq area in west-central Greenland close to the Greenland Ice Sheet (Böcher 1954 in Pennington 1980). Steppe-like vegetation in arid north-eastern Eurasia ('cold steppes') is not confined to the Siberian Arctic. For instance, south of the steppe-tundra in east Siberia, open larch forest with steppe communities and thickets of birch and pine occurs, where larch has a high resistance to extremely low temperatures and effects of permafrost changes (Tishkov 2008). Steppe communities are also described for the basins of the great Siberian rivers such as the Lena (Tishkov 2008). Notably, xerophilous plant species, plants adapted to a very dry climate or habitat, are absent from the northern European – west Siberian provinces (Shahgedanova and Kuznetsov 2008). In west-central Greenland, steppe communities dominated by Poaceae, *Artemisia* and Cyperaceae occur on dry, south-facing slopes; on wind-exposed slopes and ridges characterized by a discontinuous plant cover with much destabilized mineral soil; and on sand and loess. Their presence contrasts markedly with the low shrub tundra background dominated by *B. nana* and the Ericaceae *Ledum palustre* (Böcher 1954).

At present, precipitation values are low in eastern Siberia and west-central Greenland. A thin snow cover combined with low winter temperatures has formed a permafrost layer of several hundred meters thickness (Tumel 2008, Claesson Liljedahl et al. 2016). The low precipitation values and thin active layer in summer result in dry habitats, particularly on south-facing slopes. The steppe communities form in response to local controls, especially moisture availability, with steppe plants occupying dry local habitats; disturbances and sandy substrates furthermore support their presence (e.g. Kienast et al. 2008).

In the mosaic of steppe and tundra in the Kangerlussuaq area (west-central Greenland), *Artemisia* pollen percentages ranging from 1 to 40 % are recorded (Pennington 1980). The highest values occur in terrestrial moss polsters from the steppe vegetation itself and relatively low percentage values (2–7 %) in surface lake samples in which pollen of dwarf birch is over-represented with values of up to 70 %. Pollen values of over 50 % for *Artemisia*, Chenopodiaceae and Poaceae are depicted in surface pollen data along the Lena River (Tarasov et al. 1998). In contrast, *Artemisia* is represented by a few percentages only in surface lake samples from the northern European Russian tundra (Paus 2000, Salonen et al. 2011).

It is possible that the local sandy floodplain within the Sokli basin during the Savukoski 1 cold stage provided suitable habitats, in addition to the surrounding slopes, for some of the herbs that are recorded in the pollen and macrofossil data from the fluvial sediment. Chenopodiaceae and Brassicaceae, for instance, flourish well on freshly deposited mineral-rich river sediment (Hoek 1997). Moreover, the pollen spectra from the fluvial sands at the base of the Holocene peat deposit in the Sokli basin shows Poaceae pollen values up to c. 20–25 % compared to < c. 5–10 % in the lacustrine sediment from Loitsana Lake during the Early Holocene (Figures 3-5 and 3-6), indicating local presence. Interestingly, the herbaceous taxa *A. maritima* and *Centaurium* are halophytes (salt-tolerant) and presently occur in Fennoscandia in mostly southern, coastal areas. Their presence in the fossil record of zone Sa1-I may indicate soils with high salt concentrations as nowadays found in continental Eurasia (Tishkov 2008). The herb *Inula salicina* occurs today in the so-called alvar vegetation on limestone islands in the southern Baltic Sea. The flora of the open alvar landscape is adapted to tolerate dryness, strong wind, thin snow cover, frost and flooding, conditions that can also be expected to have occurred in the steppe-tundra environment during the Savukoski 1 cold stage. Several of the herbs of the alvar are considered glacial relicts (Berglund et al. 1996).

A continental climate regime with (short) warm summers at Sokli during MIS 5d, warm enough for the presence of tree taxa, is supported by the aquatic proxies (plant/insects) that show mean July air temperatures at least in the order of present-day values (13 °C) to as high as c. 15.5 °C or more (Figures 4-1B, 5-1C; Engels et al. 2010). The present mean January temperature at Sokli is −14 °C and mean annual precipitation 500–550 mm. The chironomid taxon *Orthocladius*-T S (Figure 3-2B) is currently common on Svalbard (Brooks et al. 2007), suggesting colder summers during deposition of the lower gravelly sediment. Svalbard is underlain by continuous permafrost as well. According to the marine oxygen-isotope record, MIS 5d may have lasted in the order of c. 15 kyr (Figure 4-1).

4.2 Vegetation in the ice-margin environment

The ice-margin of the Fennoscandian Ice Sheet receded from the Sokli site a number of times over the last c. 130 kyr (Figure 4-1A). These multiple deglacial phases, and the thick fossil-bearing glacial lake deposits that were left behind in the Sokli and Loitsana basins, provide a unique opportunity to reconstruct the earliest vegetation at the moment of deglaciation.

The Sokli area was deglaciated, and glacial lake sediment was deposited, in the early parts of the Nuortti (MIS 5e), Sokli II (MIS 5a) and Holocene warm stages and during the Tulppio 1 Interstadial in mid-MIS 3. The paleo-botanical data for each of the deglacial phases (zones Nu/SoII/Tu1/Ho-I in Figures 3-1A, 3-3A to 3-5A; Figure 5-1A) depict a vegetation in close vicinity to the sub-arctic birch forest-line, consisting of low-arctic shrub tundra with scattered tree birches, or a so-called birch tree-line ecotone vegetation (indicated as open woodland in Figure 4A). *Betula pubescens/pendula* in general dominates the tree pollen spectra with percentage values up to c. 45 %, seeds of tree *Betula* are found, and NAP is relatively abundant. *B. nana* is particularly well-represented in the early MIS 5e and 5a pollen records. Dwarf birch is an important component of the present-day birch tree-line ecotone. NAP further consists of Ericales, Poaceae, Cyperaceae and lycopods. Rich herb floras are represented in the pollen and macrofossil records and include heliophilous (light-demanding) taxa (*Artemisia*, Chenopodiaceae, Brassicaceae, Caryophyllaceae (including *Cerastium*- and *Arenaria*-T), *I. salinica*, *Matricaria maritima, Rumex/Oxyria*) and the arctic-alpine plant species *Bistorta viviparum, Arenaria norvegica* and *Saxifraga stellaris*-T. *S. oppositifolia, S. nivalis, S. cespitosa* and *Dryas octopetala* are additionally recorded by *Seda*DNA data (Peter Heinztman, personal communication, 2021). The pollen of *Pinus* in this type of assemblages, which reach values to around c. 20 %, can be considered as long-distance transport (Prentice 1978).

Seeds of tree *Betula* were not encountered in the glacial lake sediment of MIS 3 age, but pollen values for *B. pubescens/pendula* at >30 % suggest a distributional limit not far away from Sokli. It is possible that birch trees were present in the ice-marginal environment during MIS 3 in environmentally favorable areas. Birch is not the only tree that is recorded near the ice-margin. Pollen of *Larix* is found (early-MIS 5a and -Holocene) as well as macrofossil remains of *Picea* (MIS 3) and *Alnus* (Early Holocene). Larch is generally poorly represented in the fossil record and even low percentage values can be taken as evidence for its local presence (see Section 4.4). Spruce might have been present in the ice-marginal environment during early-MIS 5e and -5a as well (*Picea* pollen values to c. 2–3 %). The pollen production of spruce is relatively poor and even low percentage values can represent local presence of small populations (von Post 1930). Abundant needles of *Picea* are found in the sediment of Glacial Lake Hind in Canada (Boyd et al. 2003; Section 3.6). Furthermore, in addition to an abundance of seeds of tree birch, a bud scale of *Pinus* has been retrieved from glacio-fluvial sediment at the base of the Holocene lake sediment sequence in Kuutsjärvi (Bogren 2019).

The establishment of birch forest at Sokli is recorded during the latest stage of sedimentation in the Sokli Ice Lake, both in early-MIS 5e and -Holocene. At this stage (Lake Stage 3; Figure 3-7), the ice-margin of the Fennoscandian Ice Sheet was situated at some 4 km from the Sokli site and Sokli had been deglaciated some 25–100 years. Birch forest established itself at Sokli in early MIS 5a sometime after the final drainage of the Sokli Ice Lake. The fact that forested conditions were achieved already in the ice-marginal environment during early-MIS 5e and -Holocene might be related to the slow melting of the large MIS 6 and LGM icesheets, allowing birch to migrate in congruent pace with the retreating ice-margin. As earlier suggested by Saarnisto et al. (1999), any periglacial vegetation zone at the front of the withdrawing ice-margin must have been narrow.

As discussed in Section 3.6, the rich aquatic/wetland biota that are recorded in the glacial lake sediments reflect boreal conditions and reconstruct mean July temperatures at least as warm as today (Figures 4-1B and 5-1C). The warm summers during the various deglaciation phases are in accordance with high Milankovitch-forced summer insolation at high latitudes at the start of the MIS 5 warm stages and the Holocene, and higher-than-present day values in mid-MIS 3 (Figure 4-1). Apparently, aquatic/wetland taxa reacted quickly to the warm summer conditions, as they do not depend on e.g. soil formation, and small tree populations rapidly occupied newly deglaciated terrain as well. However, the open woodland vegetation on land, overall, was sub-arctic in origin. This suggests a large disequilibrium between regional vegetation and climate at the start of the warm periods. The rapid response of tree taxa (birch, spruce, larch, pine, alder) lends support for a northerly survival of trees north of the central European mountain chains, under glacial conditions (Willis and Andel 2004, Heikkilä et al. 2009, Väliranta et al. 2011).

4.3 Pioneer birch forest

Despite warm summers, the terrestrial vegetation remained in disequilibrium with climate for another millennium. This birch forest phase is distinctly represented near the base of all four warm stages recorded in the Sokli sequence, not only during Nuortti (MIS 5e), Sokli II (MIS 5a) and the Holocene Interglacial, which were preceded by glaciation, but also in the early part of the Sokli I warm stage (MIS 5c) that followed cold conditions with steppe-tundra (Figure 4-1A). Biostratigraphically, the birch forest phase corresponds to zones Nu/SoI/SoII/Ho-II as well as Tu2-I (Figures 3-1A to 3-5A; Figure 5-1A).

The birch forest phase at the start of the vegetation successions is characterized by exceptionally high pollen percentages of *B. pubescens/pendula* reaching values up to c. 80 %. Pollen of Cyperaceae and *Alnus* from local (azonal) habitats slightly depress these values in early MIS 5c. In modern pollen spectra from the present-day sub-arctic birch forest in northern Fennoscandia, pollen of *Betula* reach c. 35–50 %, the percentage *Pinus* pollen is c. 30 %, and NAP is relatively abundant and diverse (Prentice 1978). The fossil percentage values also greatly exceed means of c. 30–35 % for *Betula* in the modern pollen-climate calibration data from Finland and Russia (Salonen et al. 2012). Furthermore, *B. pubescens/pendula* pollen accumulation rate (PAR) values calculated for the Early Holocene at both Loitsana and Kuutsjärvi greatly exceed *Betula* PAR values from the present-day birch forest in northern Europe (unpublished data). Similarly, *Betula* pollen percentages are high, and always exceed the threshold PAR value for open birch forest (Seppä and Hicks 2006), in Early Holocene records from NE European Russia (Väliranta et al. 2011). A pronounced birch phase at the start of the MIS 5e, 5c and 5a warm stages is not limited to northern Europe. These birch phases are also distinctly recorded in long pollen sequences from central Europe (Helmens 2014), including La Grande Pile in France (de Beaulieu and Reille 1992), Oerel in Germany (Behre 1989) and Horoszki Duże in Poland (Granoszewski 2003). The percentage of *Betula* pollen here reach values of c. 50 to 80 %. The shortest period with birch forest is depicted in early MIS 5a.

Betula spp. are fast immigrants due to the advantage of an abundant production of wind-dispersed fruits, rapid reproductive rates, fast growth rates and a young reproductive-maturity age (Birks 1986). This strong pioneer character of *Betula*, combined with time needed for slow soil forming processes, might have been important factors in the delayed establishment of boreal forest at the start of the interglacials at Sokli (Helmens et al. 2018, 2021). Similarly, Paus (2013) and Amon et al. (2014) mention seed dispersal, soil development and competition as factors influencing Late Glacial and Early Holocene forest development in Norway and the Baltic region. Väliranta et al. (2011) mention competition of niches (Giesecke and Bennett 2004) as a possible factor explaining the considerable time-lag of up to 1 500 yr between the first macrobotanical and/or stomata findings of *Picea* and the establishment of closed (mixed) spruce forest in northeastern Europe.

The early birch forest phase at Sokli lasted c. 1 500 yr in the Early Holocene and c. 1 000 yr in early MIS 5e (Figure 4-1A). If the fine laminations in the lower part of the lake deposit of MIS 5c age have an annual origin (likely related to spring melt), a duration of c. 800 years is estimated for the early MIS 5c birch phase (Engels et al. 2010). Periods with *Betula* pollen values reaching c. 60–80 % in Early Holocene pollen records from southern Finland and Sweden lasted c. 500–1 000 yr (Heikkilä and Seppä 2003, Antonsson and Seppä 2007). The relatively short duration with pioneer birch forest at Sokli in MIS 5e and 5c, compared to the Holocene, might be related to differences in summer insolation (Figure 4-1), with higher insolation values in early MIS 5e and 5c possibly increasing the compatibility of conifer trees and/or enhancing weathering/soil formation. The fact that the shortest period with birch forest is recorded during MIS 5c is probably because this warm stage was not preceded by glaciation and weathering/soil formation had long been started. The new Holocene pollen record from the Sokliaapa shows that the polycormic mountain birch (*B. pubescens* subsp. *tortuosa*) initially predominated during the pioneer birch phase, followed by the spread of *B. pubescens/ pendula* (Figure 3-6A). The pollen of *B. pubescens* subsp. *tortuosa* was not separated from those of *B. pubescens* in the older deposits at Sokli. The pollen of the different species (e.g. *B. nana*)/ sub-species of birch are distinguished using a combination of size and morphological characteristics as in Terasmaë (1951) and Mäkelä (1996).

Birch forest is additionally registered during the Tulppio 2 Interstadial (mid-MIS 3). The pollen spectra in the fluvial sediment is dominated by pollen of *B. pubescens* and *B. nana* (Figures 3-4A and 5-1A). The relatively high percentage values Poaceae pollen are probably related to the floodplain environment (see also Section 4.1).

4.4 Developments in boreal forest

The pioneer birch forest phase is succeeded by pine-dominated boreal forest during all four warm stages (zones Nu/ SoI/ SoII/Ho-III in Figures 3-1A to 3-3A, 3-5A, 3-6A; Figure 5-1A). During the Holocene, pine forest established in the Early Holocene at c. 9.2 kyr BP, lasted some 7 000 yr, and was replaced by mixed boreal forest with spruce (zone Ho-IVb) in the Late Holocene at c. 2 kyr BP (Figure 4-1A). The same succession is depicted in the Kuutsjärvi pollen record (Salonen et al. 2024). *Picea* needles occur in the Sokliaapa record prior to the *Alnus* expansion (Figure 3-6) dated at Loitsana to c. 8 kyr BP (Figure 3-5). In addition, pollen percentages of *Picea* at c. 1–2 % from about 5.5 kyr BP onwards, accompanied by *Picea abies Seda.* DNA at Kuutsjärvi (Salonen et al. 2024), show that local populations of spruce were present before the final expansion in the Late Holocene. Numerous paleo-ecological studies show that *Picea abies* expanded in Fennoscandia during the Holocene thousands of years after all other boreal species had established (Giesecke and Bennett 2004, Latałowa and van der Knaap 2006). In contrast, *Picea* expands in vegetation model simulations prior to the period when the species becomes abundant in the pollen records and climate forcing parameters used in the model cannot explain the absence or insignificant abundance of *Picea abies* in Fennoscandia during the Early and mid-Holocene (Miller et al. 2007). *Picea abies* is a strong competitor in northern Europe and driving or limiting factors for Holocene changes in its abundance are still not completely understood (Miller et al. 2007).

Pine-dominated forest also lasted into the late part of MIS 5c before being replaced by boreal forest with spruce (SoI-IV). This takes into consideration that the gravelly fluvial deposit interlayered in the uppermost part of the MIS 5c gyttja most probably represents a relatively brief time window with high sedimentation rates (Figure 3-2A). A vegetation close to the forest limit seems to be recorded in the uppermost part of the MIS 5c pollen sequence (SoI-V), depicting cooling at the end of the warm stage. *Picea* pollen values of 5 % suggest the continuous presence of spruce in the open vegetation. Rising *Pinus* pollen percentage values accompanied by *Pinus* stomata (and diverse conifer macrofossil remains) show the establishment of pine forest in MIS 5a as well. Note that tree pollen percentages following the early birch forest phase in MIS 5c and 5a are depressed due to pollen/spores from local (azonal) habitats. Due to a hiatus in core recovery, the later half of the MIS 5a vegetation record is missing.

In contrast to the warm MIS 5c, 5a and Holocene stages, the pine-dominated forest in MIS 5e is followed by mixed boreal forest with spruce early in the warm stage (Nu-IV). The boreal forest is temporarily replaced by birch forest during the Tunturi cold event (Nu-V), after which *Picea* pollen percentages continue to rise, to values of c. 10 % in the later part of the warm stage (zone Nu-VII). The latter zone is further characterized by the local presence of temperate *Corylus*, being near continuously recorded with relative pollen abundances (c. 1 %) only seen in Finnish surface-lake sediments samples within the modern occurrence limits of hazel (Salonen et al. 2012). The mixed boreal forest is replaced by birch forest at the end of the warm stage (Nu-IX). The fact that mixed boreal forest with spruce and larch (see below) established at Sokli early in MIS 5e, and that larch persisted throughout major part of the warm stage, is intriguing. Both trees are cold tolerant and can grow on permafrost. A likely explanation for their occurrences in MIS 5e lies in the distinctly continental climate conditions of early MIS 5e (see Section 3.1.1 and Chapter 5), which might have enabled these conifers to occupy vital niches.

Larix is recorded by pollen during all three warm stages of MIS 5 age (and additionally stomata in MIS 5e), the mid-MIS 3 Tulppio 2 Interstadial, and in the early part of the Holocene both at Sokli and Kuutsjärvi (Salonen et al. 2024). Pollen of *Larix* is only sparsely reported from till-covered sediments (Forsström 1990 and references therein) and *Larix* is rare in Holocene pollen records from Fennoscandia. *Larix* pollen is dated to c. 10 kyr BP in a high-elevation lake record in Norway (Paus 2010) and cones and wood of *Larix sibirica*, also dated to the Early Holocene, are reported from the Swedish Scandes (Kullman 1998). *Larix* pollen has a short-distance dispersal and poor preservation (Gunin et al. 1999, MacDonald et al. 2000) and, as an example, only single *Larix* pollen grains are encountered in modern lake samples from the boreal forest and forest tundra in northwestern Russia where larch is an important component in the zonal vegetation (Salonen 2012). Also, the pollen of larch has rather in-distinct morphological characters, making it relatively easy to miss and difficult to identify during the palynological analysis. Identifications of *Larix* pollen at Sokli and Kuutsjärvi have been crosschecked and compared with modern reference material. In conclusion, it is likely that larch is under-represented in the palynological record in Fennoscandia.

4.5 On the azonal occurrences of *Alnus*

In contrast to the successional developments in vegetation types and occurrences of tree taxa discussed in sections 4.1 to 4.5, the pattern of *Alnus* pollen is erratic. Phases with *Alnus* pollen values over 10 % are indicated to the right in Figure 4-1A.

High *Alnus* pollen percentages (up to c. 20 %) are recorded during the pioneer birch forest and early pine forest phases in MIS 5c, to persist with values around c. 5 % into the mixed boreal forest with spruce. Seeds of alder are encountered where several wetland taxa (e.g. *Carex* spp., *Rhynchospora alba*, *Typha*) and taxa in other moist habitats (e.g. *Rorippa palustris*, *Urtica dioica*) start their macrofossils records and are identified as *Alnus glutinosa*. *A. glutinosa* may have been present in an *Alnus* carr (marshy forest) with abundant ferns in the undergrowth (Section 3.2). *Alnus* pollen percentages up to c. 20 % are also detected in the mid-Holocene. The co-occurrence with taxa such as *Filipendula* and *Typha latifolia* (Figure 3-5), and the high pollen percentage values (see below), suggest the presence of *A. glutinosa* as well. Alder is further recorded throughout major part of MIS 5e, with values just over 10 % during the early pioneer birch forest phase. The three periods with high *Alnus* pollen percentages in MIS 5e, 5c and the Holocene show a remarkable similar pattern in which alder rapidly expands, probably in response to local (azonal) habitat availability, followed by a gradual retreat. A similar pattern, and percentage values of *Alnus* pollen as in the mid-Holocene, are dated at Kuutsjärvi to c. 6–4 kyr BP (Salonen et al. 2024), in contrast to Loitsana where this is dated to c. 8–6 kyr BP. This supports the idea that the occurrences of alder are strongly regulated by local habitat availability.

The northern limit of *A. glutinosa* is currently situated at some 400 km south of Sokli. *A. incana* is present throughout Fennoscandia, growing also in the open vegetation types of the northernmost regions. *Alnus* reaches values of c. 5–20 % in modern pollen assemblages from central and southern Finland; values abruptly fall to < 5 % north of the distribution area of *A. glutinosa* where also *A. incana* is scarce (Prentice 1978, Salonen et al. 2012). Today, *A. incana* sparsely grows in moist wetland habitats along small streams and lakes in the Värriö nature reserve just east of Sokli. In northwest Europe, groves of *A. glutinosa* often occur at the swampy margins of nutrient-rich lakes. The tree is particularly well adapted to this habitat because it can tolerate anoxic conditions in the waterlogged soils (Hannon and Gaillard 1997). A wetland habitat explains why *A. glutinosa* was present at Sokli in the early parts of the interglacials when the dominant vegetation on land was pioneering birch forest.

In conclusion, *Alnus* pollen is included in the pollen sum in northern Europe and at Sokli, however, the data presented here shows that it behaved as a wetland taxon and because of this probably is strongly over-represented in the pollen sum. Occurrences of *Alnus* pollen are also used as biostratigraphic markers, however, the relation to azonal habitat availability makes *Alnus* unsuitable to be included in biostratigraphic zonation.

4.6 Millennial-scale vegetation changes

The most distinct response of vegetation to a change in climate of millennial duration is recorded during the early MIS 5e Tunturi cold event (zone Nu-V; Figure 3-1, 4-1A, 5-1A). The mixed boreal forest with spruce and larch that developed early in the MIS 5e warm stage is suddenly replaced by sub-arctic, open birch-dominated forest with abundant juniper in the under-growth. The recovery was stepwise and included a brief phase with sharply increasing *Pinus* pollen values intersecting the two main cooling phases. *Alnus* shows a distinct decrease in pollen percentages during the event probably due to the lowering in water levels as reconstructed by the aquatic proxies (Section 3.1.2).

The late MIS 5e Värriö cold event shows a same structure as the Tunturi event including two phases with severe conditions interrupted by a brief recovery phase. Whereas the aquatic proxies sensitively record dry climatic conditions that led to lowered lake levels, the response of the regional vegetation to the Värriö event is more complex (zone Nu-VIIIb). The representation of birch in the regional vegetation diminishes during the event, and those of *Picea* and *Pinus* increase. *Picea* shows the highest pollen percentage values right at the start and end of the event, and during the recovery phase. In addition, *Corylus* pollen values overall fall. In contrast to the summer cooling during the Tunturi event, it is likely that the change in climate during the Värriö event was mostly a winter/continentality phenomena. Salonen et al. (2012) show that winter temperatures presently have a relatively large

influence on deciduous *Corylus*. According to Seppä et al. (2004), growing season length and frost sensitivity are major factors determining the current northern distribution limits of most temperate trees in northern Europe. Winter cooling might have favoured the recorded expansions in conifers.

Interestingly, the Värriö event occurs superimposed on an interval with enhanced pollen values for *B. pubescens/pendula* (zones Nu-VIIIa, c), suggesting a relatively long time-interval with climate instability as the MIS 5e warm stage approached its end. The vegetation, and lake levels (Section 3.1.1), temporarily recovered during zone Nu-VIIId, to conditions close to those recorded preceding the birch interval, before final cooling led to the replacement of boreal forest by birch forest (zone Nu-VII). Notably, the early MIS 5e Tunturi event is also preceded by a minor climate perturbation with enhanced *B. pubescens/pendula* values. Additionally, three more phases with relatively high birch values are recognized in MIS 5e pollen record, and two in the Holocene sequence, and these are highlighted in Figure 4-1 as possible millennial-scale climate perturbations as well. The oldest Holocene event is dated around 8.2 kyr BP and is probably related to the 8.2 event. Both during the youngest Holocene event (around c. 6.5 kyr BP) and one of the MIS 5e events, lake level lowering is recorded (Chapter 3). It should be noted though that the Holocene pollen record lacks the high temporal resolution of the MIS 5e record, whereas significant contributions of pollen from local (azonal) habitats, combined with a relatively low-resolution analysis, hamper the detection of short-term events in the MIS 5c and 5a proxy records.

5 Climate reconstruction

Mean July air temperatures (T_{jul}) are reconstructed from the fossil records in the Sokli and Loitsana basins by a combination of two methods, the transfer function approach applied to pollen and chironomid assemblages and by using individual climate indicator plant species mostly identified by macrofossils. The former method is widely used on Late-Glacial – Holocene timescales. The climate indicator plant species method is traditionally applied to pre-LGM deposits in central Europe to explore summer and winter temperatures during the Eemian Interglacial and the Weichselian (Kolstrup 1979, Zagwijn 1996, Aalbersberg and Litt 1998).

The paleo-climate data presented here focus on the pollen- and plant macrofossil-inferred reconstructions and follow the approaches introduced in Salonen et al. (2018, 2019) and Väliranta et al. (2015), respectively (see also Section 2.3). Salonen et al. (2018, 2019) provide a new pollen-climate calibration dataset that extends calibration lake samples from Fennoscandia, Svalbard and northwestern Russia with modern lake samples from the European mainland and British Isles. Modern climate data is extracted for each lake (see Section 2.3.2). An ensemble of methods that includes classical and machine-learning approaches is used to create pollen-climate models. Data evaluation is facilitated by the calculation of analogue distance, i.e. the compositional distance between each fossil pollen spectra and the best matching modern calibration pollen assemblage (Overpeck et al. 1985, Birks 1998), and by geographical plots of best matching calibration samples. In Väliranta et al. (2015), current plant distribution data from Finland, spanning over several bioclimatic zones from hemiboreal, via boreal to subarctic, are linked to measured meteorological data over a T_{jul} gradient from c. 7.5 to 17 °C. The protocol makes use of a unique modern spatial species-specific plant distribution dataset (http://www.luomus.fi/kasviatlas) that covers entire Finland and is subject to continuous botanical surveys. Climate indicator plant species identified in the Sokli and Loitsana fossil records and their minimum July air requirements (min. T_{jul}), i.e. the median of the July mean at the species northern distribution limit, are listed in Table 5-1; the table also shows the T_{jul} range, i.e. the lowest and highest value along the species-specific distribution boundary. Reconstruction errors for the pollen-based T_{jul} estimates are in the range of 1.12–2.05 °C.

Table 5-1. Climate indicator plant species used in the present study with median of mean July air temperature and mean July temperature range determining the species' current northernmost distribution limit in Finland.

Taxon	Median of July mean (°C)	July mean range (°C)
Urtica dioica	12	10.1–13.1
Callitriche cophocarpa	13.7	13.5–13.9
Potamogeton friesii	13.8	13.6–14.5
Ceratophyllum demersum	13.9	12.9–14.1
Potamogeton compressus	13.9	13.1–14.3
Ranunculus sceleratus	14.2	14–15.9
Rhynchospora alba	14.7	14.5–15.1
Alnus glutinosa	14.8	14.3–15.2
Elatine triandra	15.2	14.5–15.9
Glyceria fluitans	15.4	15–16
Typha latifolia/angustifolia	15.5	14.5–16
Glyceria lithuanica	15.7	15.4–16.1
Crassula aquatica	15.8	14.3–16.1
Bidens tripartita	16.1	15.5–16.8
Najas tenuissima	16.6	16.1–16.7

The paleo-climate data are presented in the climate panel of Figure 5-1. The pollen-based T_{jul} inferences (B in Figure 5-1) are summarized in a thick black line that is the smoothed median result of the six different pollen-climate calibration models. Analogue distance, where a short distance means a good fit, is indicated to the left; the red dashed vertical line represents the mean distance to best modern analogue in the Late Holocene samples. For the pollen records of MIS 5c and 5a age, an additional T_{jul} reconstruction is shown where the median value is compared with the median result by applying a pollen sum that excludes sedges (Cyperaceae). Note that pollen-climate calibration data for steppe-tundra (MIS 5d at Sokli; Figure 4-1) is not included in the calibration set of Salonen et al. (2018, 2019). Part C in the climate panel provides the min. T_{jul} values inferred from individual climate indicator plant species, where the black dashed curve summarizes the results. These aquatic/wetland plant species are mostly identified by means of their macrofossil remains. It is important to note that the macrofossil record is sporadic, with occurrence being strongly related to distance to the littoral/shore or inflow of running water and representation of an aquatic/wetland taxon depends on local (azonal) habitat availability (e.g. Koff and Vandel 2008). Therefore, the climate record in C is discontinuous.

Figure 5-1A is a summary of pollen data (and biostratigraphic zonation), as well as macrofossil/stomata-inferred presence of tree taxa, where the pollen sum is adjusted from the one used in the multi-proxy diagrams (Figures 3-1 to 3-6 and 3-8 to 3-10) by excluding all spore plants (see Chapter 4). Furthermore, periods with glaciation, glacial lake conditions, wetland expansion or sudden lake level lowering are highlighted in and along the lithological column at the left side of the figure. Finally, the geographic locations of modern pollen analogues are plotted on the maps of Figure 5-2, with samples grouped according to biostratigraphic zones.

Figure 5-3 provides an additional reconstruction of mean January air temperatures (T_{jan}) inferred from the MIS 5e pollen record. Reconstruction errors are in the range of 1.79–3.44 °C depending on the calibration model.

The results from the quantitative climate reconstructions are validated, and results between methods are compared, in Section 5.1 below, before a synthesis of paleo-climate data is presented in Section 5.2.

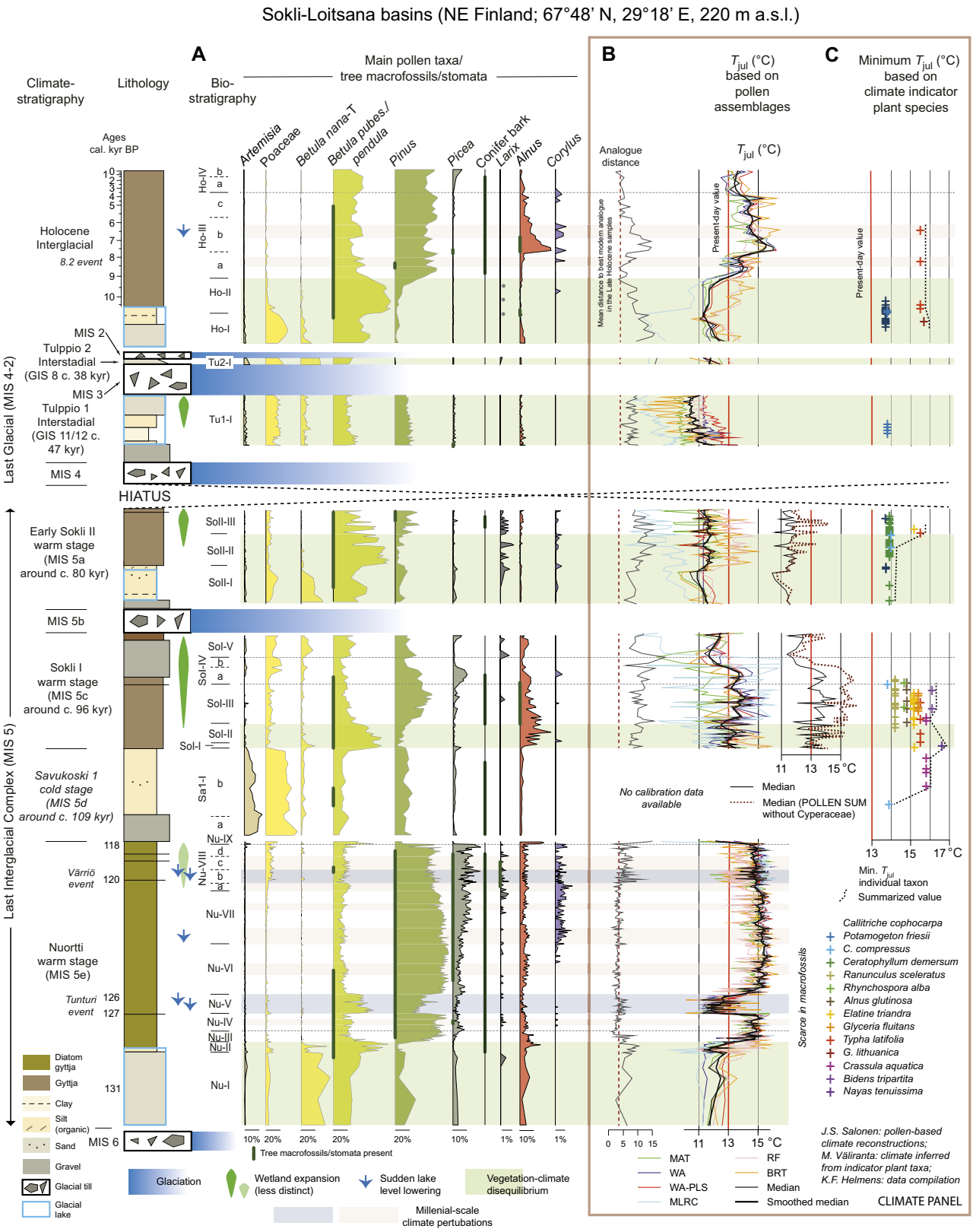

Figure 5-1. *(B, C) Quantitative climate reconstructions inferred from the late Quaternary Sokli and Loitsana fossil records. (B) shows the pollen-based mean July air temperature (T_{jul}) inferences. Values are summarized in a thick black line that is the smoothed median result of six different pollen-climate calibration models. Analogue distances are indicated to the left. For the pollen records of MIS 5c and 5a age, an additional T_{jul} reconstruction is shown as well as the median result by applying a pollen sum without Cyperaceae. (C) Minimum T_{jul} inferences based on climate indicator plant species (Table 5-1). The red vertical line in both (B) and (C) is the present-day (1971–2000 mean) T_{jul} at Sokli (c. 13 °C). (A) provides a summary of pollen data, macrofossil/stomata-inferred local presence of tree taxa and biostratigraphy. Distinct intervals with vegetation-climate disequilibrium are shown as green shading. Periods with glaciation, glacial lake condition, wetland expansion or sudden lake level lowering are also highlighted.*

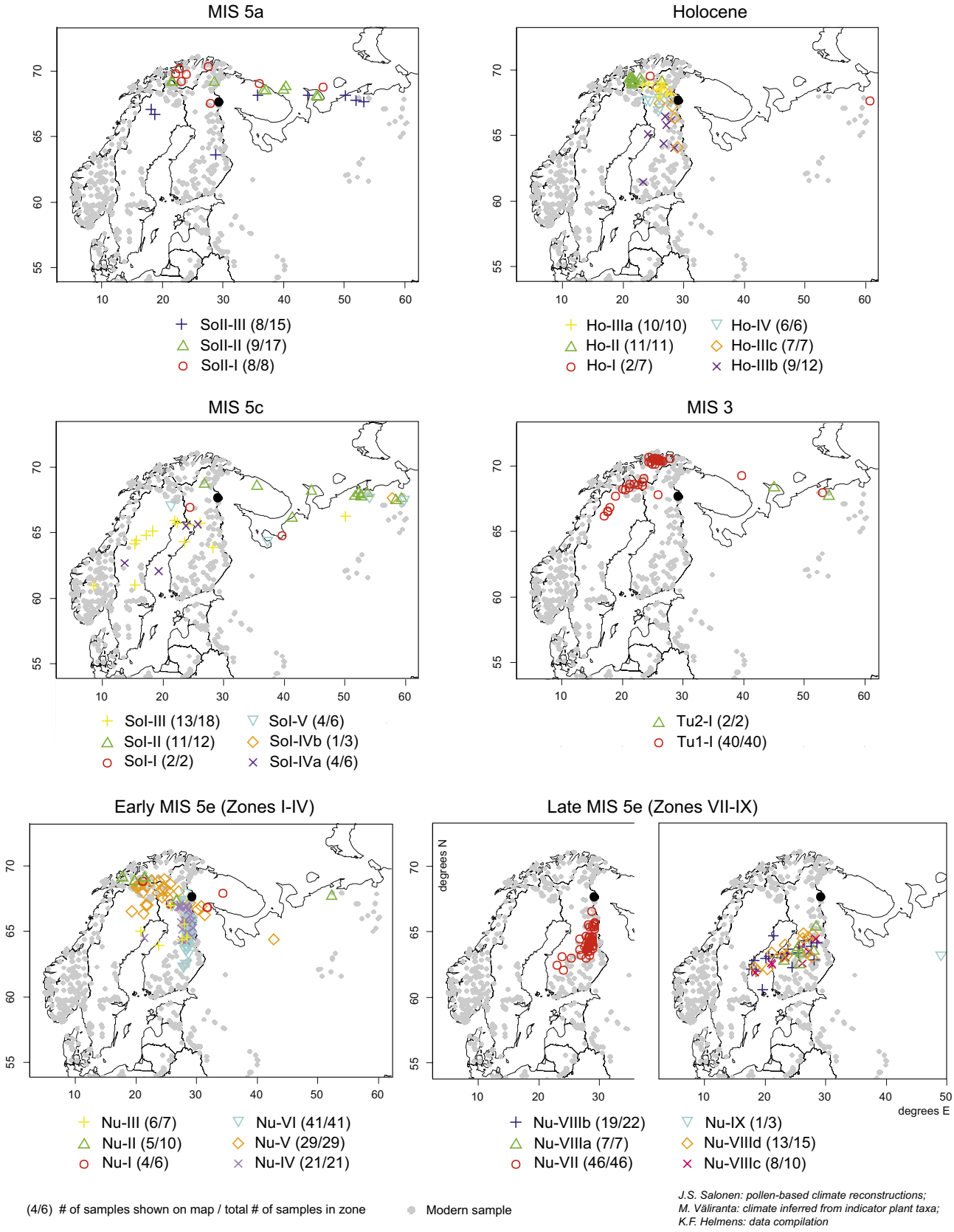

Figure 5-2. *Geographic location of modern pollen analogues plotted at the mean latitude and longitude of the five most compositionally similar modern pollen samples, with samples grouped according to biostratigraphic zones. Samples with a relatively poor fit are left out; threshold for inclusion is two times (MIS 5e) or three times (MIS 5c, 5a, Holocene) the mean Late Holocene analogue distance.*

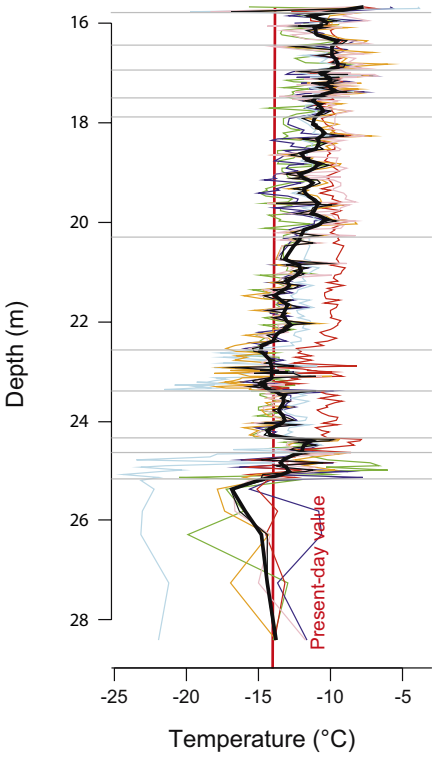

Figure 5-3. *Reconstruction of mean January air temperature (T_{jan}) inferred from the MIS 5e pollen record. Values are summarized in a thick black line that is the smoothed median result of six different pollen-climate calibration models (coloured lines). Reconstruction errors are in the range of 1.79–3.44 °C depending on the calibration model. The red vertical line is the present-day (1971–2000 mean) T_{jan} at Sokli (c. −14 °C). See also Figure 5-1.*

5.1 Evaluation of the quantitative climate inferences

5.1.1 Early phase with vegetation-climate disequilibrium

The climate records for the earliest parts of the Nuortti (MIS 5e), Sokli I (MIS 5c) and Sokli II (MIS 5a) warm stages and the Holocene, and the Tulppio 1 Interstadial (mid-MIS 3), are characterized by large differences between T_{jul} values inferred from pollen assemblages and T_{jul} based on climate indicator plant species. The paleo-botanical data reconstructs an open birch tree-line ecotone vegetation in the ice-marginal environments, followed by the development of sub-arctic birch forest (Figure 4-1A; Sections 4.2 and 4.3). These vegetation types presently occur in the northernmost parts of Finland and, accordingly, the pollen-based reconstructions show T_{jul} values mostly at c. 11–12 °C (Figure 5-1B). In sharp contrast, aquatic/wetland plants (and chironomids) record boreal conditions (Section 3.6) and consistently reconstruct T_{jul} values up to several degrees higher than today's value at c. 13 °C (Figure 5-1C). The discrepancy between T_{jul} reconstructed by regional vegetation versus aquatic/wetland proxies points to a phase of vegetation-climate disequilibrium at the start of the warm periods. Likely factors for the delayed response of terrestrial vegetation on land to the insolation-forced warm summers are slow soil forming processes and competition, where *Betula* with its distinct pioneer characteristics was a strong competitor (Sections 4.2 and 4.3).

Macrofossil remains of the aquatic plants *Callitriche cophocarpa* and *Potamogeton friesii*, the wetland taxon *Typha latifolia*, and the grass *Glyceria lithuanica* indicate a min. T_{jul} in the order of c. 13.5–15.5 °C during the Early Holocene. Lake water conditions in the Early Holocene were eutrophic due to leaching of freshly eroded surface soils, sudden decreases in lake volume and overall, relatively small lake volumes (Sections 3.5.1 and 3.6). Shala et al. (2017), however, shows that chironomid-inferred T_{jul} continues to be elevated at c. 14–15 °C when nutrient levels drop, i.e. sometime following the final drainage of the Sokli Ice Lake, indicating that temperature is most probably the main factor that drives the also high chironomid-based T_{jul} values for the Early Holocene. The present-day distribution of aquatic plants is regulated by temperature, not by edaphic factors or water chemistry (Lampinen and Lahti 2016). For aquatic plants, the nutrient status of the water is not crucial as many macrophytes are able to absorb

nutrients from the sediment (Moss 1982, van Donk and van de Bund 2002). Instead, the length of the open-water season (the growing season) controls vascular aquatic plant communities and their reproduction regardless of the lake's nutrient status (Rørslett 1991, Väliranta 2006b).

The MIS 3 glacial lake sediment contains macrofossils of *P. friesii* indicating that T_{jul} was at least c. 14 °C. Similar temperatures are indicated by the aquatic plants *C. cophocarpa, C. compressus* and *Ceratophyllum demersum* in early MIS 5a. The assemblage including the aquatic plant *Elatina triandra* and the wetland taxa *Ranunculus sceleratus* and *T. latifolia* reconstructs min. T_{jul} values in the order of c. 14–15.5 °C for early MIS 5c, with macrofossils of aquatic *Nayas tenuissima* suggesting min. T_{jul} as high as c. 16.5 °C in the earliest phase with more open vegetation. The chironomid assemblage in the lowermost part of the MIS 5c lake deposit, with *Ablabesmyia*, *Endochironomus albipennis*- and *Dicrotendipes nervosus*-T, reconstructs T_{jul} at c. 16 °C as well (Engels et al. 2010). Macrofossil remains are scarce in the lake deposit of MIS 5e age. Chironomid-based T_{jul} inferences for early MIS 5e show values between c. 12–14.5 °C (Plikk et al. 2019) and warm summer are supported by occurrences of the diatom taxa *Cyclotella michiganiana* and *C. radiosa* (Section 3.1). Finally, the deglacial sediments of Early Holocene, mid-MIS 3 and early MIS 5a age further contain several chironomid taxa that have intermediate to warm July air temperature optima in the order of c. 13–15.5 °C in a regionally enhanced modern chironomid-climate calibration dataset from Finland (Luoto et al. 2014a, 2014b). These include *Psectrocladius sordidellus*-, *Microtendipes pedellus*-, *Cladotanytarsus mancus*-, *Polypedilum nubeculosum*-, *Chironomus anthracinus*-, *Cricotopus intersectus*- and *C. cylindraceus*-T (Helmens et al. 2018).

Warm summers in northern Europe during the Early Holocene are inferred from various proxies including aquatic plants, chironomids, diatoms, and megafossils (Kullman 1995, Rosén et al. 2001, Bigler et al. 2003, Allen et al. 2007, Paus 2010, Velle et al. 2010, Jones et al. 2011, Birks et al. 2012, Luoto et al. 2014a, Rantala et al. 2015, Väliranta et al. 2015, Paus and Haugland 2017). Importantly, a rich plant assemblage of wetland plants (e.g. *Cicuta virosa*), ferns (*Thelypteris palustris, Matteuccia struthiopteris*) and aquatics (e.g. *Sparganium*) depicted in *Seda*DNA data from Kuutsjärvi, just east of Sokli, records warm Early Holocene summers as well (Salonen et al. 2024). Furthermore, Early Holocene warm summers are proposed by Ritchie et al. (1983) based on fossils remains of e.g. *Typha* dated to 11.8–6 kyr BP (and clustering at c. 10 kyr BP) at 12 high-latitude sites in northern Canada. *Typha* is one of the first taxa detected in Early Holocene macrofossil records from European Russia as well (Wohlfarth et al. 2004, Väliranta et al. 2015). The plant is a very prolific, wind-dispersing, early successional taxon. It can rapidly colonize new areas, from one seed to 58m^2 cover in 2 years in suitable habitats (Grace and Wetzel 1981). Highest summer temperatures during the Early Holocene are in accordance with high summer insolation in the northern hemisphere at this time (Figure 1-1).

The pollen-based T_{jul} reconstructions for the earliest parts of the warm stages of MIS 5e, 5c and 5a age, and for the Tulppio 1 and 2 Interstadials (mid-MIS 3), are characterized by big differences in T_{jul} values between calibration models, large analogue distances, and wide spreads in geographic location of modern pollen analogues (Figures 5-1B and 5-2). Furthermore, a relatively large number of samples from these assemblages (biostratigraphic zones Nu/SoI/SoII/Hol-I and -II, Tu1/Tu2-I) exceed the threshold for inclusion on the maps of Figure 5-2. These characteristics make the temperature reconstructions unreliable. The occurrence of non-analogue vegetation is an important factor that explains the unreliable T_{jul} reconstructions during the birch forest phases. As discussed in Section 4.3, the fossil assemblages with exceptionally high pollen percentages of *B. pubescens/pendula* up to c. 80 % do not have a modern analogue in northern Europe. *Betula* (including the shrub *B. nana*) reaches values of c. 30–50 % in modern pollen spectra from the sub-arctic birch forest in northern Fennoscandia and northwest Russia (Prentice 1978, Salonen et al. 2012). Furthermore, harmonization between the fossil and calibration data sets probably contributed to the on average relatively high pollen-inferred T_{jul} values, and large differences in reconstructed values between calibration models, at the start of MIS 5e. As part of this process, pollen of *B. nana*, which reach high percentages here, are amalgamated with those of *B. pubescens/pendula*, since dwarf birch is not differentiated from tree birch in the modern pollen samples, despite differences in auto-ecology. The high pollen-inferred T_{jul} values for the birch forest phase of MIS 5c age, and large analogue distances, are driven by an over-representation of *Alnus* pollen from azonal wetland habitats (Section 4.5; see also Section 5.1.2). *Alnus* prefers moist habitats (Mossberg and Stenberg 2003), is a strong pollen producer (Bradshaw 1981), and can be greatly over-represented in the pollen record when locally present (Tinsley and Smith 1974).

5.1.2 The climate records for MIS 5e and the Holocene

After the noisy interval early in MIS 5e and the Holocene, the pollen-based climate reconstructions stabilize with the establishment of pine-dominated boreal forest (zones Nu-III and Hol-IIIa).

Differences in T_{jul} values between calibration models are small and modern analogue distances short throughout the warm boreal forest phases of zones Nu-IV, -VI and -VII in MIS 5e. The analogue distances are similar or lower compared to the mean distance for Late Holocene samples. This suggests robust reconstructions with small errors due to climate-vegetation disequilibrium, non-analogue paleo-vegetation or -climate, or pollen from local (azonal) habitats. T_{jul} inferences reach c. 15 °C during the early MIS 5e boreal phase (zone Nu-IV) and close to c. 16 °C during the long phase with mixed boreal forest that follows the Tunturi event (zones Nu-VI and -VII). An overall slight decrease in T_{jul} is reconstructed from the base of zone Nu-VII, in the middle part of the MIS 5e record, onwards. Reconstructions of winter temperatures show an opposite trend with T_{jan} gradually increasing from c. −13 °C to c. −10 °C, compared to present-day values of c. −14 °C, during zones Nu-VI and -VII (Figure 5-3). Although the T_{jan} reconstruction should be interpreted with caution, due to the comparatively weak signal of winter temperature in north European pollen data, the first-order trend towards warmer winters during MIS 5e, validated by independent diatom (Section 3.1.1) and biomarker-isotope data (Katrantsiotis et al. 2021), is considered the most salient feature (Salonen et al. 2018). The geographic plots in Figure 5-2 demonstrate that best modern analogues for the MIS 5e boreal forest pollen assemblages are in east-central Finland, south of Sokli (zones Nu-IV and -VI). A shift in the analogue locations south- and west-wards is shown during zone Nu-VII, in parallel with the trend towards warmer winters.

Analogue plots show larger geographical spreads, and analogue distances increase, during the Tunturi event (zone Nu-V), around the Värriö event (zone Nu-VIII), and during the subsequent change to sub-arctic birch forest (Nu-IX). The T_{jul} depression during the Tunturi event is estimated to be c. 3–2 °C and less than 1 °C during the Värriö event. As discussed in Section 4.6, cooling during the Värriö event might have been mostly in winter. Minor depressions in T_{jul} are furthermore recorded for several of the other millennial-scale phases with increased *B. pubescens/pendula* pollen percentages. T_{jul} slightly increases after the Värriö event, to values close to those attained during zone Nu-VII (c. 15 °C), before dropping to c. 12 °C during the final birch forest phase. The latter value, however, is probably overestimated due to high pollen percentages of *Alnus*. Both the Tunturi and Värriö climate perturbations are characterized by sudden drops in lake levels and overall shallow water conditions are recorded from about the base of zone Nu-VIII onwards due to lake infilling. It is likely that the minor wetland expansions that accompanied these changes in lake level/water depth (Section 3.1) contributed to the relatively poor analogue fits during these periods.

During the Holocene, short analogue distances are displayed briefly during the period with pine-dominated boreal forest between c. 9.2 and 8.5 cal. kyr BP, and after c. 5.7 cal. kyr BP where pine forest is succeeded by mixed boreal forest with spruce. In-between these two periods, between c. 7.6 to 5.7 cal. kry BP (zone Ho-IIIb), analogue distances and reconstructed T_{jul} values (reaching over 15 °C) closely follow the curve of *Alnus* pollen percentages. Moreover, whereas high *Alnus* pollen percentage values are recorded in the Loitsana sequence in the early part of the mid-Holocene, similar values, and the same trend, and T_{jul} over 15 °C, are dated at nearby Kuutsjärvi to the late part of the mid-Holocene between c. 6–4 kyr BP (Salonen et al. 2024). As discussed in Sections 4.5 and 5.1.1, *Alnus* expands with azonal habitat availability (moist ground such as wetland), occurs over-represented in the pollen records, and as shown here has a significant impact on the pollen-based climate reconstruction. A comparison with the Kuutsjärvi record shows that *Alnus* over-estimates the pollen-inferred T_{jul} values by c. 1.5 °C during the mid-Holocene. Nevertheless, the high *Alnus* pollen percentage values of up to c. 20 %, and the co-occurrence with taxa such as *Filipendula* and *Typha latifolia*, suggest the local presence of *Alnus glutinosa* at Loitsana during the mid-Holocene (Section 4.5). The northern limit of *A. glutinosa* is currently situated at some 400 km south of Sokli. As climate indicator plant taxa, *A. glutinosa* and *T. latifolia* reconstruct a min. T_{jul} at c. 15–15.5 °C (Table 5-1). Except for alder, pollen from azonal wetland habitats is limited in the Loitsana pollen record. However, sedge (Cyperaceae) pollen values at c. 5 % (Figure 3-5B) might explain the relatively low pollen-inferred T_{jul} values (when corrected for the over-estimation in T_{jul} caused by *Alnus* pollen) compared to those reconstructed using the climate indicator plant species method for the mid-Holocene (Section 5.1.3). T_{jul} values drop with the transition to the Late Holocene at c. 4 cal. kyr BP (zone Ho-IV). Additionally, minor dips in T_{jul} are recorded around the 8.2 event and the interval with enhanced birch pollen values and relative low lake levels around c. 6.5 cal. kyr BP.

The early MIS 5e Tunturi event provides evidence for substantial cooling under warmer-than-today conditions (Helmens et al. 2015, Salonen et al. 2018, Plikk et al. 2019, Katrantsiotis et al. 2021). The cooling event is matched by a major decline in sea-surface temperatures, accompanied by reducing North Atlantic Deepwater formation, recorded in marine core MD03-2664 from a high sediment-accumulation rate site on the Eirik Drift in the northeast Atlantic Ocean, just south of Greenland, at this time (Irvali et al. 2012, Galaasen et al. 2014). Moreover, a major cooling event intersecting peak Eemian (MIS 5e) warmth is recorded in detail in a high-resolution core M23323 from the Norwegian Sea (Bauch et al. 2011). The cooling event recorded in the latter marine core has approximately the same temperature decrease, structure, and duration as reconstructed at Sokli. Furthermore, a spike in ice-rafted-debris suggests that widespread expansions of winter sea-ice cover accompanied the surface cooling of the Norwegian Sea (Bauch et al. 2011). The latter might explain the dry climate reconstructed at Sokli during the Tunturi event. The cooling in the Norwegian Sea record, and the start of the Eemian here, have been dated several thousands of years later than at Sokli and at the Eirik Drift (Bauch et al. 2011); it should be noted, however, that uncertainties in marine chronologies can result in age differences of up to 3–5 kyrs between marine records (Govin et al. 2015).

5.1.3 The climate records for MIS 5c and 5a

In contrast to the pollen-inferred T_{jul} records for MIS 5e and the Holocene, which stabilize following the early interval with climate-vegetation disequilibrium, substantial differences in reconstructed T_{jul} between calibration models, large analogue distances, and wide spreads in modern analogue geographic locations continue during MIS 5c and 5a. This behavior reflects the distinctly different nature of the MIS 5e, 5c, 5a and Holocene lakes. The lake of MIS 5e age maintained a large open-water body throughout major part of its infilling history, bordered by a limited wetland zone, whereas during the Holocene, Loitsana Lake remained relatively large in the coring-site due to continuous inflow of groundwater from the adjacent esker. Therefore, the pollen-based climate records from these lakes suffer in general little from noise induced by local wetland habitats.

The lake of MIS 5c age occupied an abandoned stream channel on the floodplain of a small meandering river. Although open water prevailed during the infilling of the oxbow lake, the first signs of terrestrialisation become visible with the transition to pine-dominated boreal forest (zone SoI-III). Rich aquatic and wetland communities and plants found in moist shore habitats (Figure 3-2B) provide a wealth of climate indicator species and show that T_{jul} exceeded the present-day values of c. 13 °C by several degrees. Four plant species indicate T_{jul} higher than c. 14 °C (*Callitriche compressus, Ranunculus sceleratus, Rhynchospora alba*, *A. glutinosa*), another four higher than c. 15 °C (*Elatine triandra, Glyceria fluitans, T. latifolia, Crassula aquatic*), whereas *Bidens tripartita* indicates T_{jul} at least at c. 16 °C. Similarly, aquatic and wetland plants (*C. cophocarpa, Ceratophyllum demersum, E. triandra* and *T. latifolia*) in the relatively small and shallow MIS 5a lake (Figure 3-3B) during the pine-dominated boreal forest phase (zone SoII-III) show that T_{jul} was at least c. 13.5–15 °C. In order words, many plant species that currently have a much more southerly distribution grew in the Sokli region during the warm stages MIS 5c and 5a (Väliranta et al. 2009, Helmens et al. 2021).

In contrast, the pollen-inferred T_{jul} for the boreal phases in MIS 5c (zones SoI-III and -IVa) and 5a run at (much) lower values of c. 14 °C (MIS 5c) and c. 12 °C (MIS 5a). The wetland expansions have a distinct impact on the pollen records, with pollen of sedges reaching c. 20 % (MIS 5c) and over 30 % (MIS 5a). Cyperaceae are common taxa in modern calibration samples from the tundra and have some of the lowest T_{jul} optima in the pollen-climate calibration dataset from Fennoscandia (Salonen et al. 2012, 2013). In order to evaluate the influence of the high Cyperaceae pollen percentages on the pollen-based climate reconstructions for MIS 5c and 5a, the median of their T_{jul} records is compared with median T_{jul} values recalculated using a re-fined pollen sum that excludes Cyperaceae (red dashed curves in Figure 5-1B). The exclusion of sedge pollen leads to c. 1.5–2 °C higher T_{jul} values in MIS 5c, raising T_{jul} to higher than 15 °C, and warmer summers, higher than c. 13 °C, in MIS 5a. Importantly, the range in T_{jul} estimated by the different calibration models in MIS 5c (not indicated in Figure 5-1B) is lowered to values similar or even lower than during the boreal forest phases in the Holocene suggesting a relatively reliable pollen-based climate reconstruction. In addition to Cyperaceae, however, the shrub *Salix* and herbs like Ranunculaceae, Rosaceae, Apiaceae and Poaceae, which are also represented in the pollen records, probably all occurred in local (azonal) habitats as well and, as a result, T_{jul} values may still be under-estimated. This is the case for the period with fluvial sand/gravel deposition in the late part of MIS 5c where the analogue distance is the highest of all intervals in Figure 5-1B.

5.1.4 The MIS 5d cold stage

Climate in areas with steppe-tundra vegetation today, i.e. a vegetation type that is reconstructed at Sokli during MIS 5d (Section 3.2.1), is strong continental with large differences between summer and winter temperatures and low precipitation values. In east Siberia, mean January temperatures and annual precipitation values are as low as c. −40 °C and 200 mm, respectively (Shahgedanova 2008), and in the Kangerlussuaq area in west-central Greenland −26 °C and 150 mm, respectively (Eisner et al. 1995). A continental climate regime with (short) warm summers during MIS 5d, warm enough for the presence of tree taxa (Figure 5-1A), is supported by the aquatic proxies that suggest T_{jul} in the order of c. 11–13 °C (chironomids; Engels et al. 2010) and at least c. 14–16 °C (*C. compressus*, *Crassula aquatica*).

5.2 Uncertainties and climate synthesis

There are several assumptions, shortcomings, and possibilities for errors in proxy-based climate reconstructions, which are relevant to the studies at Sokli and are discussed below.

The basic assumption throughout the climate reconstruction methods is methodological uniformitarianism (Birks and Birks 1980, Birks 2003, Birks and Seppä 2004), namely that modern-day observations and relationships can be used as an analogue or model for past conditions and, more specifically, that fossil taxa-climate relationships have not changed with time, at least in the late Quaternary. The Quaternary is a geological period characterized by highly variable environmental and climate conditions that involved large latitudinal shifts in vegetation belts as well as longitudinal displacements in vegetation (expansions of steppes). This opens the possibility for non-analogue paleoclimates and -vegetation types that may yield biased reconstructions (e.g. Salonen et al. 2013). Reconstructing climate from changes in regional vegetation further assumes that the post-glacial vegetation development in northern Europe took place in approximate dynamic equilibrium with climate. The fact that open sub-arctic birch vegetation is recorded at Sokli in the ice-marginal environment, both in early MIS 5e, 5a and the Holocene, and during deglaciation in mid-MIS 3, while the aquatic ecosystem had a boreal character, points to a phase of distinct climate-vegetation disequilibrium at the start of the warm periods. This phase was prolonged for c. 1 000–1 500 yrs due to the persistence of a non-analogue vegetation type. Slow soil forming processes on land and competition are likely factors that led to the pioneer birch forest vegetation that has no close modern analogue in northern Europe. The birch forest phase was followed by pine-dominated boreal forest, however, despite warm summers, mixed boreal forest with spruce only established late in the Holocene and MIS 5c. *Picea* is cold tolerant and can grow on permafrost and the reason for the delayed development of mixed boreal forest with spruce in Fennoscandia is still poorly understood. Boreal forest with spruce and larch established at Sokli early in MIS 5e, to persist throughout major part of the warm stage. A likely explanation lies in the distinctly continental climate conditions of early MIS 5e, which might have enabled conifers to occupy vital niches. All these three developments, i.e. climate-vegetation disequilibrium during deglaciation, the persistence of pioneer birch forest vegetation, and the delayed response of spruce have their influence on the pollen-based climate reconstructions. Added to this, there are strong indications that alder behaved like a wetland plant, rapidly expanding upon habitat availability followed by gradual decline. As a result, alder should not be included in the pollen sum and the pollen-based climate reconstruction.

Also evident from the Sokli and Loitsana studies is the large influence of wetland vegetation on the pollen-inferred climate estimates. Modern lakes used in the Fennoscandian pollen-climate calibration datasets are carefully selected avoiding lakes that, for instance, have large marginal wetlands (Salonen et al. 2013). The modern pollen assemblages from these lakes are considered to capture the atmospherically mixed pollen of regional vegetation that is related to climate, with little non-climatic noise from local (azonal) habitats. For older lake deposits, however, such a selection often cannot be made. These deposits are scarce, particularly in formerly glaciated northern Europe; they may no longer have a relationship with the present-day landscape/drainage system; and the character of the paleo-lake usually only becomes apparent upon proxy analysis. However, even in Holocene studies, the possible effect of azonal habitats on the climate reconstructions should be taken into consideration. For instance, lake level lowering due to a change in climate or catchment hydrology may have led to temporal extensions in wetland habitats that is not apparent in the present-day lake setting. Boreal wetlands

are rich in plant taxa that commonly occur in the open tundra and wetland plants occur often over-represented in the pollen record. Therefore, the presence of wetland has the potential of significantly underestimating true paleo-temperatures.

The climate indicator plant species that are used in the Sokli and Loitsana studies currently display clear northern distribution limits in Finland that strongly relate to mean July air temperature. However, outlies do occur beyond these boundaries. Occurrences in unusually favourable microhabitats or exceptionally ideal microclimates are few in comparison with species frequency south of the northern limit of main occurrence and outlie occurrences are integrated in the T_{jul} values presented in Table 5-1. It is important to highlight that none of the aquatic/wetland climate indicator plants species identified in the Sokli and Loitsana fossil records, indicating warmer-than-present day summers, occur at Sokli or Loitsana today, even though suitable habitats such as moist, nutrient-rich soils are extensively available. Furthermore, T_{jul} values inferred from climate indicator plant species are minimum values, i.e. the current mean July temperature at the taxon's northern distribution limit. Therefore, the true T_{jul} values may have been (significantly) higher. Additionally, because of the nature of the macrofossil record, plants that occurred in a wetland habitat are not necessarily all represented in the fossil record. Also, here there is a potential for underestimation of true T_{jul} values.

Although a strong climate proxy (e.g Brooks 2006, Walker and Cwynar 2006), chironomids are influenced by a variety of environmental conditions, such as water depth, nutrient availability, and macrophyte abundance, which have the potential to override the climate signal (e.g. Velle et al. 2005, Luoto and Ojala 2016). Therefore, similar as with the pollen inferred climate reconstruction, the climate inferences from chironomid assemblages extracted from the Sokli and Loitsana sediments are evaluated against the environmental history of the paleo-lakes (Engels et al. 2007, 2010, Shala et al. 2017, Plikk et al. 2019, Helmens et al. 2021). Another important aspect to be mentioned in respect to the Sokli/Loitsana studies is the length or the temperature range of the modern calibration transect. The calibration transects used in the chironomid-based climate reconstructions are shorter, particularly at the warm end, than the one used in the pollen-based reconstructions. The paleo-temperature that is reconstructed is limited by the highest/lowest current T_{jul} of the transect and, because of the so-called 'edge effect', is even under-estimated at the warm and over-estimated at the cold end. The effect of transect length on reconstructed paleo-temperatures may explain, at least part of, the overall slightly lower T_{jul} values reconstructed for the boreal phases at Sokli using chironomid assemblages compared to pollen assemblages or climate indicator plant species.

The numerical methods used to model the past temperature values in the transfer function approach can additionally bias the quantitative reconstructions. In the approach presented in Salonen et al. (2018, 2019), an ensemble of calibration models, including classical and machine-learning ones, are used in the pollen-based temperature reconstructions. Some recent studies using simulated non-analogue fossil data (Goring et al. 2015, Juggins et al. 2015) have suggested that regression-tree ensemble models may be more robust in non-analogue conditions compared to classical methods such as WA (Birks et al. 1990), WA-PLS (ter Braak and Juggins 1993) and MAT (Overpeck et al. 1985). However, due to remaining challenges in the evaluation of model performances regarding fossil samples that lack good modern analogues in the calibration data, all six methods are used here as they all show acceptable performance in cross-validations, as well as generally similar and realistic reconstructed paleo-climate patterns (Salonen et al. 2018). Reconstruction errors, estimated by 10-fold cross validations, are in the range of 1.12–2.05 °C for the pollen-inferred T_{jul} reconstructions, and 1.79–3.44 °C for the MIS 5e T_{jan} estimates, depending on the calibration model (Salonen et al. 2018).

Important to be mentioned is also the influence of location of modern calibration data in respect to degree of continentality on reconstructed T_{jul} values. The detailed information available on plant species distribution in Finland shows that T_{jul} requirements of climate indicator plants species are generally slightly higher in continental eastern Finland compared to the Baltic Sea coast in the west. This trend towards higher July temperatures in the east is also visible on a larger European scale. Isarin and Bohncke (1999) note that the current northerly extension of *Typha latifolia* approximates the 13 °C July isotherm on the British Isles; coincides with the 15 °C July isotherm in Sweden; whereas even further east in central Russia this species appears limited by the 17 °C July isotherm. Higher T_{jul} optima in the east are also estimated for chironomid taxa (Self et al. 2011, Engels et al. 2014). Furthermore, Salonen et al. (2013) find that reconstructed pollen-based T_{jul} values using

calibration data from Finland run at lower values throughout by c. 1.5–2.5 °C than those modelled using a training set from a more continental region in northwestern Russia. Similarly, Norwegian calibration datasets reconstruct approximately 1.0–2.7 °C colder than Russian models when applied to fossil chironomid assemblages from a lake in Siberia (Self et al. 2011). It is likely that the taxa require higher T_{jul} values in the east to compensate for the shorter growing season. Winters are long and cold in northeastern Eurasia, and summers (particularly the month July) warm but short, while spring and autumn are indistinct and very short lasting. The higher T_{jul} requirements with increasing continentality pose a problem for the paleo-temperature reconstructions. The applicability of modern calibration sets in T_{jul} reconstructions may be limited to relatively narrow continentality regimes, as the inferred/modelled T_{jul} responses are also a function of the specific distribution of seasonal temperatures in the region (Self et al. 2011, Salonen et al. 2013). The application of modern trainings sets to fossil records that have similar climate (continentality) regimes, however, implies that the degree of continentality can be independently inferred from the fossil data. Additionally, the distribution of seasonal temperatures may have changed over time, further complicating this issue. When not adjusted for, T_{jul} values may be under-estimated for continental regimes and over-estimated in oceanic settings.

It becomes clear from the above that quantitative climate inferences from geological proxy records should be treated with caution. As a very important step, climate parameters inferred from fossil assemblages using the transfer function approach should be validated against the lake's environmental history and climate reconstructions from various proxies should preferably be compared (Birks and Birks 2006, Birks et al. 2010, Juggins and Birks 2012, Juggins 2013). This approach is applied in the Sokli studies. It is 1) the detailed reconstructions of lake histories and fluvial dynamics; 2) validation of quantitative climate records against the local (azonal) records; 3) combination of classic pollen data (which may suffer from e.g. long-distance transport) with conifer stomata and plant macrofossils; 4) comparing response-time between terrestrial plant taxa (influenced by e.g. soil formation) and aquatic plants/insects; and, finally, 5) the comparison of the quantitative climate estimates reconstructed using different proxies and methods, which have provided a solid basis for the climate reconstructions at Sokli. Figure 5-4 lists the most likely paleo-T_{jul} or -minimum T_{jul} values for the various time intervals when Sokli was ice-free during the last 130 kyr, based on the evaluations presented in this chapter. In addition, T_{jan} values for MIS 5e and qualitative inferences on winter conditions are summarized. Nevertheless, because of the limitations/uncertainties discussed in this section, and considering the error limits in the pollen- and chironomid-based climate reconstructions and minimum July mean ranges of the individual climate indicator plant taxa, the climate inferences presented in Figure 5-4 should be considered as the best possible estimations of these paleo-climate parameters.

As a final note, comparisons between the Holocene vegetation/climate records from Loitsana Lake at Sokli and Kuutsjärvi in the nearby crystalline mountains of the Värriö Tunturit (Salonen et al. 2024) show no apparent influence of the carbonatite bedrock at Sokli on the paleo-records of regional vegetation and climate.

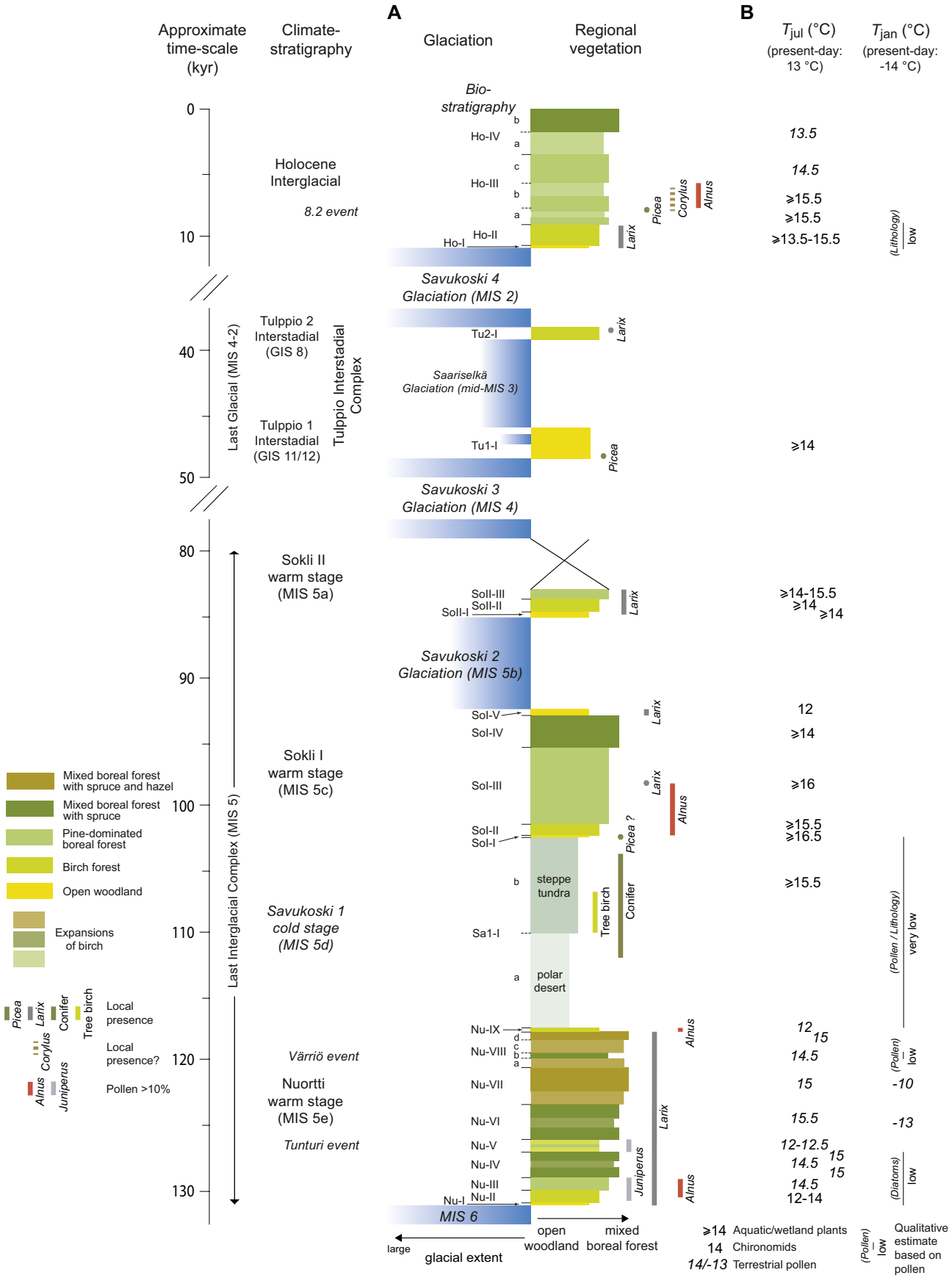

Figure 5-4. *(B) Summary of paleo-climate data inferred from pollen and chironomid assemblages and aquatic/wetland climate indicator plant species, based on a detailed evaluation of the quantitatively inferred climate estimates, shown along side the late Quaternary vegetation/glaciation record at Sokli (A). Qualitative estimates of winter temperatures based on various proxies are provided in addition to pollen-based T_{jan} inferrences for MIS 5e.*

6 Conclusions

This report summarizes in a concise, consistent, and coherent way interpretations of late Quaternary environmental- and climate-proxy data from the Sokli site in northern Finland, published in a total of 36 peer-reviewed scientific papers and SKB technical reports over the last 15 years. Additionally, the report presents some new data on the Tulppio Interstadial of mid-MIS 3 age and the Holocene peat deposit in the Sokli basin.

Sediment logs of all boreholes in the Sokli and Loitsana basins are presented; all dating results are provided and evaluated; climate reconstructions are re-run using the most recent protocols, introduced in Salonen et al. (2018, 2019) and Väliranta et al. (2015), and results are evaluated/validated; vegetation developments and climate evolutions reconstructed for each of the ice-free periods over the last 130 kyr at Sokli are for the first time compared in detail. Sokli was ice-free during the Nuortti (MIS 5e centered at c. 125 kyr BP), Sokli I (MIS 5c, c. 95 kyr BP) and Sokli II (MIS 5a, c. 80 kyr BP) warm stages of the Last Interglacial Compex (MIS 5); the Tulppio 1 and 2 Interstadials in mid-MIS 3 (around c. 40 kyr BP; GIS 11/12, 8); and the Savukoski 1 cold stage in MIS 5d (c. 110 kyr BP). The MIS 5e, 5c and 5a warm periods correspond to the Eemian Interglacial (MIS 5e) and Brørup and Odderade Interstadials (MIS 5c and 5a, respectively) in the NW European mainland stratigraphy.

The Sokli and Loitsana sediments are dated by means of a combination of radiocarbon and luminescence dating techniques. OSL dates have large standard errors mainly due to small sample sizes, relatively poor luminescence characteristics, and uncertainties in dose-rate determination. However, the OSL ages on glaciofluvial and fluvial sediment are in sequence and group according to stratigraphic units; the youngest age determination agrees with AMS ^{14}C dates; and the oldest ages are in line with TL/IRSL dates. Moreover, the absolute chronology agrees with earlier land-sea comparisons.

The conclusions are outlined in the following.

- Four organic-bearing lake deposits of different ages are represented in the late Quaternary sedimentary infills of the Sokli and Loitsana basins. Each lake deposit displays concurrent shifts in biotic and abiotic proxies including lithology; reconstructs in detail the lake infilling history and associated successional developments in aquatic and telmatic plant/animal communities; and provides detailed information on regional vegetation developments and climate. Each lake record is unique in terms of sediment characteristics and fossil assemblages. Additionally, they have fossil taxa in common. However, aquatic/wetland taxa peak in different parts of the records, reflecting the different origin and environmental histories of the lakes.
- The lacustrine and fluvial deposits in the Sokli and Loitsana basins, and their fossil records, reconstruct a consistent sequence of events. The oldest lake (MIS 5e age) was relatively large and deep and occupied a steep depression carved out in the Sokli Carbonatite Massif by the Fennoscandian Ice Sheet during MIS 6 glaciation. Following the infilling of the lake, a fluvial regime, with an oxbow lake, prevailed during MIS 5d-c. Glaciation in MIS 5b resulted in compression of the older sediments, under the weight of the ice sheet, and the return of a waterlogged topographic depression. The MIS 5a lake, however, was small and shallow and was infilled with sediment during the early half of the warm stage. Full glacial conditions ruled during MIS 4-2, except for two periods in mid-MIS 3 when Sokli was deglaciated; a glacial lake is recorded in the early ice-free interval (dated to before c. 45 cal. kyr BP; GIS 12-11) and fluvial conditions during the latter one (c. 42 cal. kyr BP; GIS 8). Thick glacio-lacustrine sediment beds were laid down in the Sokli Ice Lake also in the earliest parts of MIS 5e, 5a and the Holocene. Although sharing many characteristics, each glacial lake deposit in the Sokli and Loitsana sequences is unique. Finally, following the latest deglaciation, lacustrine conditions continued in Loitsana Lake throughout the Holocene, in a topographic depression of glacio-fluvial origin, whereas peat accumulation prevailed in the Sokli basin. Loitsana initially received water and sediment from the Soklioja rivulet, before becoming groundwater-fed from the adjacent esker.
- The chronology, unique character of each lake record as well as the consistent sequence of events described above provide strong evidence that the late Quaternary deposits at Sokli occur *in-situ* and that fossil remains are not re-deposited.

- A rich algal record consisting of diatoms and green algae characterizes the 9 m-thick diatom gyttja deposit of MIS 5e age. The green alga *Tetraëdron minimum* re-occurs with peak values and six species of *Pediastrum* are identified. In contrast, plant macrofossils are nearly absent from the fossil record. The c. 2.5 m-thick, highly compacted oxbow lake deposit of MIS 5c age has an exceptionally rich and abundant macrofossil content. Characteristically, it includes the fossil remains of a variety of (aquatic) insects living in running water (stream-inhabiting chironomids, Ephemeroptera, Simuliidae, Sciaridae) and (semi-) terrestrial habitats, the latter transported from the floodplain/catchment by running water as well. Macrofossils and NPP's (non-pollen palynomorphs) are not found in large abundances in the c. 2 m-thick MIS 5a lake deposit, but their records of aquatic and wetland taxa are diverse. The lake filled-in with sediment early in the MIS 5a warm stage and the latter part of MIS 5a is missing from our records. The fossil/sediment record of the 7 m-thick Holocene lake deposit from Loitsana reconstructs an early phase of peatland development, represented by e.g. abundant leave fragments of the bryophyte *Sphagnum*, followed by open water with a rich aquatic plant community and high representations of the green alga *P. integrum*. It depicts the terrestrialisation of the southern portion of the lake when still fed by the Soklioja rivulet, whereafter Loitsana became an isolated esker lake. The new record of the c. 2 m-thick Holocene peat deposit in the Sokliaapa (wetland) in the Sokli basin contains rich NPP and plant macrofossil assemblages and shows changes in fen vegetation before the final succession to ombrotrophic conditions. Finally, diverse NPP and plant macrofossil assemblages encountered in the c. 2 m-thick fluvial deposits of MIS 5d and Early Holocene age, the latter underlying the peat deposit in the Sokli basin, reflect a dynamic floodplain environment. The former deposit contains an exceptionally well-preserved, c. 110 kyr old bryophyte assemblage that reflects the shallow water to (semi-) terrestrial conditions, influenced by (seasonal) flooding, on a floodplain.
- The reconstructions of late Quaternary depositional environments within the Sokli and Loitsana basins, and associated developments in local (azonal) aquatic and telmatic ecosystems, which have been inferred from the sedimentary sequences and their fossil records, have resulted in an exceptional wealth of environmental data for the late Quaternary in Fennoscandia. The environmental records obtained from the four lake deposits have one driving mechanism in common, i.e. lake infilling. In addition, each lake record has a unique set of drivers. These include changes in mixing regimes (MIS 5e); flooding regimes (MIS 5c); wetland expansion and encroachment of running water (MIS 5a); and changes in source of running water (river versus esker-fed groundwater; Holocene). Not all mechanisms that drive the environmental records are solely related to local dynamics, but climate played a role as well.
- The thick minerogenic glacio-lacustrine deposits of early-MIS 5a, Early-Holocene and mid-MIS 3 age have relatively rich fossil records and sensitively reconstruct the evolution of the Sokli Ice Lake following the deglaciations. The fossil aquatic/wetland communities have a boreal character, driven by high insolation-forced summers, in contrast to the paleo-vegetation on land that was sub-arctic. High nutrient levels in the lake are the result of enhanced nutrient levels in the recently deglaciated terrain.
- The mid-MIS 3 deglacial sediment/fossil record stands out. The glacio-fluvial sediment and underlying MIS 4 till bed contain reworked organic debris. A glacier re-advance phase is recorded in which an earlier opened spillway was blocked by ice, resulting in the re-occurrence of a large, deep-water glacial lake stage. In addition, new data shows that the Fennoscandian Ice Sheet subsequently overrode the Sokli basin, and then retreated once more shorthly after. The evidence points to an active ice sheet that was probably warm-based.
- The Sokli and Loitsana proxy records reveal four interglacial vegetation successions dated to MIS 5e, 5c and 5a and the Holocene. The vegetation successions are remarkably similar, although important and interesting differences occur. They are characterized by the replacement of an open woodland vegetation by birch forest and then (mixed) boreal forest with pine (MIS 5a), spruce (MIS 5c, Holocene) and temperate hazel (MIS 5e). The local presence of larch is inferred for all four warm stages as well as for the mid-MIS 3 Tulppio 2 Interstadial.

- An open woodland vegetation followed by the establishment of sub-arctic birch forest is recorded in the ice-marginal environment. Any periglacial vegetation zone at the front of the withdrawing ice-margin must have been narrow. The rapid response of tree taxa (birch, spruce, larch) to newly deglaciated terrain lends support for a northerly survival of trees under glacial conditions as suggested by other studies. Pioneer birch forest, which does not have a close modern analogue, persisted c. 1 kyr despite overwhelming evidence from aquatic/wetland taxa for warm insolation-forced summers. The shortest duration with birch forest (c. 800 yr) is recorded in early MIS 5c, i.e. the only warm stage that was not preceded by glaciation and soil formation had long been started. The longest birch-phase (c. 1 500 yr) occurred in the Early Holocene under relatively low summer insolation. Local stands of spruce occurred in the following pine-dominated boreal forest, when aquatic/wetland taxa point to warm summers, but mixed boreal forest with spruce only developed late in MIS 5c and the Holocene. *Picea abies* is a strong competitor in northern Europe and driving or limiting factors for Holocene changes in its abundance are still not completely understood. In contrast, mixed boreal forest with spruce and larch established at Sokli early in MIS 5e and persisted throughout major part of the warm stage. A likely explanation for the latter lies in the distinctly continental climate conditions of early MIS 5e, which might have enabled conifers to occupy vital niches. Alder shows an erratic pattern. Within a certain climate-envelop, it behaves like a wetland taxon, rapidly expanding upon habitat availability followed by gradual decline. Finally, steppe-tundra, with scattered birch trees and conifers, prevailed during the cold MIS 5d stage in response to a strong continental climate regime.
- Climate indicator plant species reconstruct minimum mean July air temperatures (min. T_{jul}) in the order of c. 14–15.5 °C for the Early Holocene; c. 14 °C in early MIS 5a and the Tulppio 1 Interstadial (mid-MIS 3); and c. 14–15.5 °C for early MIS 5c, with macrofossils of aquatic *Nayas tenuissima* suggesting min. T_{jul} as high as c. 16.5 °C in the earliest phase with more open vegetation. Chironomid-based T_{jul} inferences for early MIS 5e show T_{jul} values in the order of c. 12–14.5 °C and warm summer are supported by occurrences of the diatom taxa *Cyclotella michiganiana* and *C. radiosa.* Today's T_{jul} value at Sokli is c. 13 °C, which is the average mean value over 1971–2000 and the baseline T_{jul} value used in the climate reconstructions The higher-than-present summer temperatures reconstructed for the Early Holocene at Sokli are in-line with various proxy data from nearby Kuutsjärvi and different sites in Fennoscandia, north European Russia and Canada.
- Pollen-based T_{jul} inferences reach c. 15 °C during the early MIS 5e boreal phase and close to c. 16 °C during the long phase with mixed boreal forest that follows the Tunturi event. An overall slight decrease in T_{jul} is reconstructed from the middle part of the MIS 5e record onwards. Reconstructions of winter temperatures show an opposite trend with T_{jan} gradually increasing from c. −13 °C to c. −10 °C, compared to present-day values of c. −14 °C. T_{jul} depression during the early MIS 5e Tunturi event (c. 126–127 kyr BP ago) is estimated at c. 3-2 °C and less than 1 °C during the late MIS 5e Värriö event (c. 120 kyr BP ago). Cooling during the Värriö event might have been mostly in winter. Sudden drops in lake levels, and probably relatively dry climatic conditions, further characterize both the Tunturi and Värriö millennial-scale climate perturbations. The Tunturi cooling is matched by a major decline in sea-surface temperatures accompanied by reducing North Atlantic Deepwater formation recorded in high-resolution marine data from the northwest Atlantic Ocean. The mixed boreal forest that developed at Sokli early in MIS 5e was abruptly replaced by open birch forest with an unstable soil cover during the Tunturi event. T_{jul} slightly increases after the Värriö event, to values close to those attained before the climate perturbation, before dropping to c. 12 °C during the final birch forest phase of the MIS 5e warm stage.
- An exceptionally rich climate indicator species assemblage shows that T_{jul} exceeded the present-day values at Sokli by at least several degrees during the pine-dominated boreal forest phase in MIS 5c. The combined aquatic/wetland plant assemblage that includes *Callitriche compressus, Ranunculus sceleratus, Rhynchospora alba*, *Alnus glutinosa*, *Elatine triandra, Glyceria fluitans, Typha latifolia, Crassula aquatic* and *Bidens tripartita* indicates T_{jul} at least at c. 16 °C. T_{jul} during the following mixed boreal forest phase with spruce was at least c. 15 °C. Similarly, min. T_{jul} at c. 15 °C is inferred for the pine-dominated boreal forest phase in MIS 5a and the mid-Holocene. In order words, many plant species that currently have a much more southerly distribution grew in the Sokli region during the warm stages MIS 5c and 5a. The prevalence of warm interglacial conditions during all three warm stages of MIS 5 (5e, 5c, 5a) as reconstructed at Sokli agrees with data for large parts of mainland Europe.

- Climate in the present-day areas with steppe-tundra vegetation is strongly continental with large differences between summer and winter temperatures, low precipitation values and occurrence of deep continuous permafrost. A continental climate regime with (short) warm summers at Sokli during MIS 5d, warm enough for the presence of tree taxa, is supported by the aquatic proxies that suggest T_{jul} in the order of c. 11–13 °C (chironomids) and at least c. 14–16 °C (climate indicator plant species).
- Comparisons between the Holocene vegetation/climate records from Loitsana Lake at Sokli and Kuutsjärvi in the nearby crystalline mountains of the Värriö Tunturit (Salonen et al. 2024) show no apparent influence of the carbonatite bedrock at Sokli on the vegetation and pollen- and plant species-based climate reconstructions.
- The results obtained at Sokli have resulted in an environmental and climate record that significantly revises earlier concepts of glaciation, vegetation and climate in Fennoscandia over the last 130 kyr. Previous environmental/climate reconstructions for the late Quaternary in Fennsocandia were mostly based on the long-distance correlation of highly fragmented and often poorly dated litho- and bio(pollen)-stratigraphic data, and comparison with the global ice volume record inferred from the marine oxygen-isotope stratigraphy. According to these early reconstructions, Sokli was mostly glaciated for nearly 100 kyr, from the start of MIS 5d to the start of the Holocene. MIS 5c and possibly MIS 5a are the only periods considered, within this time interval (Last Glacial), with ice-free conditions and arctic tundra vegetation.

7 Acknowledgements

The first author sincerely thanks Jens-Ove Näslund (SKB) for his interest, knowledge, good collaboration and continuous support throughout the execution of the Sokli projects. Johan Liakka (SKB) is thanked for his collaboration during the final phase of the current compilation project. I am grateful to Peter Kuhry (Stockholm University) for the palynological and plant macrofossil analysis of the Tulppio 2 Interstadial and Sokliaapa Holocene deposits; students of the MSc-level course 'Polar and Alpine environments' are acknowledged for their contribution to the macrofossil analysis of the Sokliaapa sediment. The Bolin Centre for Climate Research at Stockholm University is acknowledged for funding to the Sokli studies (KFH). JSS acknowledges funding from the Academy of Finland (projects 278692, 310649, 331426). We further thank Christian Bigler (Umeå University) and Anne Bjune (Bergen University) for their extensive reviews of the report.

References

SKB's (Svensk Kärnbränslehantering AB) publications can be found at www.skb.com/publications.

Aalbersberg G, Litt T, 1998. Multiproxy climate reconstructions for the Eemian and early Weichselian. Journal of Quaternary Science 13, 367–190.

Aario L, 1940. Waldgrenzen und subrezenten Pollenspektren in Petsamo Lappland. Annales Academiae Scientiarum Fennicae A. LIV. 8. (In German.)

Alexanderson H, Murray A S, 2007. Was southern Sweden ice free at 19–25 ka, or were the post LGM glaciofluvial sediments incompletely bleached? Quaternary Geochronology 2, 229–236.

Alexanderson H, Murray A S, 2012. Problems and potential of OSL dating Weichselian and Holocene sediments in Sweden. Quaternary Science Reviews 44, 37–50.

Alexanderson H, Eskola K O, Helmens K F, 2008. Optical dating of a Late Quaternary sediment sequence from northern Finland. Geochronometria 32, 51–59.

Alexanderson H, Johnsen T, Murray A S, 2009. Re-dating the Pilgrimstad interstadial with OSL: a warmer climate and a smaller ice sheet during the Swedish Middle Weichselian (MIS 3)? Boreas 39, 367–376.

Allen J R M, Long A J, Ottley C J, Pearson D G, Huntley B, 2007. Holocene climate variability in northernmost Europé. Quaternary Science Reviews 26, 1432–1453.

Amon L, Veski S, Vassiljev J, 2014. Tree taxa immigration to the eastern Baltic region, southeastern sector of Scandinavian glaciation during the Late-glacial period (14,500–11,700 cal. B.P.). Vegetation History and Archaeobotany 23, 207–216.

Andersen B G, Mangerud J, 1989. The last interglacial-glacial cycle in Fennoscandia. Quaternary International 3–4, 21–29.

Anderson N J, 2000. Diatoms, temperature and climatic change. European Journal of Phycology 35, 307–314.

Andreev A A, Shumilovskikh L S, Savelieva L A, Gromig R, Fedorov G B, Ludikova A, Wagner B, Wennrich V, Brill D, Melles M, 2019. Environmental conditions in northwestern Russia during MIS 5 inferred from the pollen stratigraphy in a sediment core from Lake Ladoga. Boreas 48, 377–386.

Antonsson K, Seppä H, 2007. Holocene temperatures in Bohuslän, southwest Sweden: a quantitative reconstruction from fossil pollen data. Boreas 36, 400–410.

Arnold N S, van Andel T H, Valen V, 2002. Extent and dynamics of the Scandinavian Ice Sheet during Oxygen Isotope Stage 3 (65,000–25,000 yr B.P.). Quaternary Research 57, 38–48.

Axford Y, Briner J P, Miller G H, Francis D R, 2009. Paleoecological evidence for abrupt cold reversals during peak Holocene warmth on Baffin Island, Arctic Canada. Quaternary Research 71, 142–149.

Battarbee R W, Jones V J, Flower R J, Cameron N G, Bennion H, Carvalho L, Juggins S, 2003. Diatoms. In Smol J P, Birks H J B, Last W M (eds). Tracking environmental change using lake sediments volume 3: terrestrial, algal and siliceous indicators. Dordrecht: Kluwer Academic Publishers, 155–202.

Bauch H A, Kandiano E S, Helmke J, Andersen J, Rosell-Mele A, Erlenkeuser H, 2011. Climatic biSection of the last interglacial warm period in the Polar North Atlantic. Quaternary Science Reviews 30, 1813–1818.

Behre, K-E, 1989. Biostratigraphy of the Last Glacial Period in Europe. Quaternary Science Reviews 8, 24–44.

Behre, K-E, Lade U, 1986. Eine Folge von Eem und 4 Weichsel-Interstadialen in Oerel/Niedersachsen und ihr Vegetationsablauf. Eiszeitalter und Gegenwart 36, 11–36. (In German.)

Behre K-E, van der Plicht J, 1992. Towards an absolute chronology for the last glacial period in Europe: radiocarbon dates from Oerel, northern Germany. Vegetation History and Archaeobotany 1, 111–117.

Berger A, Loutre M F, 1991. Insolation values for the climate of the last 10 million years. Quaternary Science Reviews 10, 297–317.

Berglund B E, Björse G, Liljegren R, 1996. From the Ice Age to the Present Day. In Gustafsson L, Ahlén I (eds). Geography of plants and animals (National Atlas of Sweden), London: Coronet Books Inc, 14–24.

Bigler C, Larocque I, Peglar S M, Birks H J B, Hall R I, 2002. Quantitative multiproxy assessment of long-term patterns of Holocene environmental change from a small lake near Abisko, northern Sweden. The Holocene 12, 481–496.

Bigler C, Grahn E, Larocque I, Jeziorski A, Hall R, 2003. Holocene environmental change at Lake Njulla (999 m a.s.l.), northern Sweden: a comparison with four small nearby lakes along an altitudinal gradient. Journal of Paleolimnology 29, 13–29.

Birks H J B, 1986. Late-Quaternary biotic changes in terrestrial and lacustrine environments, with particular reference to north-western Europe. In Berglund B E (ed). Handbook of Holocene Palaeoecology and Palaeohydrology. New Jersey: John Wiley & Sons, 3–65.

Birks H J B, 1998. Numerical tools in paleolimnology: progress, potentialities and problems. Journal of Paleolimnology 20, 307–332.

Birks H H, 2001. Plant macrofossils. In J. P. Smol, H. J. B. Birks & W. M. Last (eds). Tracking Environmental Change Using Lake Sediments. Volume 3: Terrestrial, Algal, and Siliceous Indicators. Dordrecht: Kluwer Academic Publishers, Pages 49–74.

Birks H J B, 2003. Quantitative paleoenvironmental reconstructions from Holocene biological data. In Mackay A, Battarbee R W, Birks H J B, Oldfield F (eds). Global change in the Holocene. London: Edward Arnold Publishers Ltd, 107–123.

Birks H J B, Birks H H (eds), 1980. Quaternary palaeoecology. London: Edward Arnold Publishers Ltd.

Birks H H, Birks H B J, 2006. Multi-proxy studies in palaeolimnology. Vegetation History and Archaeobotany 15: 235–251.

Birks H J B, Seppä H, 2004. Pollen-based reconstructions of late-Quaternary climate in Europe – progress, problems, and pitfalls. Acta Palaeobotanica 44, 317–334.

Birks H J B, Ter Braak C J F, Line J M, Juggins S, Stevenson A C, Ter Braak C J F, 1990. Diatoms and pH reconstruction. Philosophical Transactions of the Royal Society of London, Series B 327, 263–278.

Birks H J B, Heiri O, Seppä H, Bjune A E, 2010. Strengths and weaknesses of quantitative climate reconstructions based on late-Quaternary biological proxies. Open Ecology Journal 3, 68–110.

Birks H H, Jones V J, Brooks S J, Birks H J B, Telford R J, Juggins S, Peglar S M, 2012. From cold to cool in northernmost Norway: Lateglacial and early Holocene multi-proxy environmental and climate reconstructions from Jansvatnet, Hammerfest. Quaternary Science Reviews 33, 100–120.

Björck S, Noe-Nygaard N, Wolin J, Houmark-Nielsen M, Hansen H, Snowball I, 2000. Eemian Lake development, hydrology and climate: a multi-stratigraphic study of the Hollerup site in Denmark. Quaternary Science Reviews 19, 509–536.

Blaauw M, 2010. Methods and code for 'classical' age-modelling of radiocarbon sequences. Quaternary Geochronology 5, 512–518.

Blaauw M, Christen J A, 2011. Flexible paleoclimate age-depth models using an 928 autoregressive gamma process. Bayesian analysis 6, 457–474.

Blaauw M, Christen J, Aquino Lopez M, 2022. rbacon: Age-Depth Modelling using 931 Bayesian Statistics. R package version 2.5.8. Vienna: Institute for Statistics and Mathematics of WU (Wirtschaftsuniversität Wien).

Bogren F, 2019. Evidence for birch forests and a highly productive environment near the margin of the Fennoscandian ice sheet in the Värriötunturit area, northeastern Finland. Master thesis. Stockholm University, Sweden.

Bolikhovskaya N S, Molodkov A N, 2014. Chronology and climatic peculiarities of the period between c. 94 and 70 ka (MIS 5b–5a) inferred from palynological and IR-OSL analyses of the Voka reference section (south-eastern coast of the Gulf of Finland). In Abstracts, International Conference INQUA-SEQS 2014, Ekaterinburg, Russia, September 10–16 2014. Ekaterinburg: Ural Federal University, 20–22.

Bond G, Broecker W, Johnsen S, Mc Manus J, Labeyrie L, Jouzel J, Bonani G, 1993. Correlations between climate records from North Atlantic sediments and Greenland ice. Nature 365, 143–147.

Bos J A A, Helmens K F, Bohncke S J P, Seppä H, Birks H J B, 2009. Flora, vegetation and climate near Sokli, northern Fennoscandia, during Oxygen Isotope Stage 3. Boreas 38, 335–348.

Bos J A A, De Smedt P, Demiddele H, Hoek W Z, Langohr R, Marcelino V, van Asch N, van Damme D, van der Meeren T, Verniers J, Boeckx P, Boudin M, Court-Picon M, Finke P, Gelorini V, Gobert S, Heiri O, Martens K, Mostaert F, Serbruyns L, van Strydonck M, Cromb P, 2017. Multiple oscillations during the Lateglacial as recorded in a multi-proxy, high-resolution record of the Moervaart palaeolake (NW Belgium). Quaternary Science Reviews 162, 26–41.

Boulton G S, Dongelmans P, Punkari M, Broadgate M, 2001. Palaeoglaciology of an ice sheet through a glacial cycle: the European ice sheet through the Weichselian. Quaternary Science Reviews 20, 591–625.

Boyd M, 2007. Early postglacial history of the southeastern Assiniboine delta, glacial Lake Agassiz basin. Journal of Paleolimnology 37, 313–329.

Boyd M, Running IV G L, Havholm K, 2003. Paleoecology and geochronology of Glacial Lake Hund during the Pleistocene-Holocene transition: a context for Folsom surface finds on the Canadian Prairies. Geoarchaeology: An International Journal 18, 583–607.

Bracht B, Stone J, Fritz S, 2008. A diatom record of late Holocene climate variation in the northern range of Yellowstone National Park, USA. Quaternary International 188, 149–155.

Bradbury J P, 1988. A climatic-limnologic model of diatom succession for paleolimnological interpretation of varved sediments at Elk Lake, Minnesota. Journal of Paleolimnology 1, 115–131.

Bradbury J P, Dieterich-Rurup K V, 1993. Holocene diatom paleolimnology of Elk Lake, Minnesota. In Bradbury, J P, Dean, W E (eds). Elk Lake, Minnesota: evidence for rapid climate change in the north-central United States. Boulder: Geological Society of America Special Paper Colorado, 215–237.

Bradbury J P, Winter T C, 1976. Areal Distribution and Stratigraphy of Diatoms in the Sediments of Lake Sallie, Minnesota. Ecology 57, 1005–1014.

Bradshaw R H W, 1981. Modern pollen-representation factors for woods in south-east England. Journal of Ecology 69, 45–70.

Breiman L, 2001. Random forests. Machine Learning 45, 5–32.

Brodersen K P, Lindegaard C, 1999. Classification, assessment and trophic reconstruction of Danish lakes using chironomids. Freshwater Biology 42, 143–157.

Brodersen K P, Pedersen O, Lindegaard C, Hamburger K, 2004. Chironomids (Diptera) and oxy-regulatory capacity: an experimental approach to paleolimnological interpretation. Limnology and Oceanography 49, 1549–1559.

Brooks S J, 2006. Fossil midges (Diptera: Chironomidae) as palaeoclimatic indicators for the Eurasian region. Quaternary Science Reviews 25, 1894–1910.

Brooks S J, Birks H J B, 2001. Chironomid-inferred air temperatures from Lateglacial and Holocene sites in north-west Europe: progress and problems. Quaternary Science Reviews 20, 1723–1741.

Brooks S J, Langdon P G, 2014. Summer temperature gradients in northwest Europe during the Lateglacial – Holocene transition (15–10 ka BP) inferred from chironomid assemblages. Quaternary International 341, 80–90.

Brooks S J, Bennion H, Birks H J B, 2001. Tracing lake trophic history with a chironomid–total phosphorus inference model. Freshwater Biology 46, 513–533.

Brooks S J, Langdon P G, Heiri O, 2007. The Identification and use of Palaeoarctic Chironomidae Larvae in Palaeoecology. London: Quaternary Research Association.

Böcher T W, 1954. Oceanic and continental vegetation complexes in south-west Greenland. Copenhagen: Hans Reitzels Forlag.

Carr S J, Holmes R, van der Meer J J M, Rose J, 2006. The Last Glacial Maximum in the North Sea Basin: micromorphological evidence of extensive glaciation. Journal of Quaternary Science 21, 131–153.

Carrivick J L, Tweed F S, 2013. Proglacial lakes: character, behaviour and geological importance. Quaternary Science Reviews 78, 34–52.

Cheddadi R, Mamakowa K, Guiot J, de Beaulieu J-L, Reille M, Andrieu V, Granoszewski W, Peyron O, 1998. Was the climate of the Eemian stable? A quantitative climate reconstruction from seven European pollen records. Palaeogeography, Palaeoclimatology, Palaeoecology 143, 73–85.

Claesson Liljedahl L, Kontula A, Harper J, Näslund J-O, Selroos J-O, Pitkänen P, Puigdomenech I, Hobbs M, Follin S, Hirschorn S, Jansson P, Kennell L, Marcos N, Ruskeeniemi T, Tullborg E-L, Vidstrand P, 2016. The Greenland Analogue Project: Final report. SKB TR-14-13, Svensk Kärnbränslehantering AB.

Cohen A S, 2003. Paleolimnology: The History and Evolution of Lake Systems. Oxford: Oxford University Press.

Conley D J, Schelske C L, 2001. Biogenic silica. In Smol J P, Birks H J B, Last W M (eds). Tracking Environmental Change Using Lake Sediments. Volume 3: Terrestrial, Algal, and Siliceous Indicators. Dordrecht: Kluwer Academic Publishers. 281–294.

Cranston P S, Oliver D R, Saether O A, 1983. The larvae of the Orthocladiinae (Diptera: Chironomidae) of the Holarctic region. Keys and Diagnoses. Entomologica Scandinavica Supplement 19, 149–291.

Cronberg G, 1982. Pediastrum and Scenedesmus (Chlorococcales) in sediments from lake Växjösjön, Sweden. Archiv für Hydrobiologie Supplementband Algologcial Studies 29, 500–507.

Croudace I W, Rindby A, Rothwell R G, 2006. ITRAX. Description and evaluation of a new multi-function X-ray core scanner. In Rothwell R G (ed). New Techniques in Sediment Core Analysis. London: Geological Society of London, 51–63.

Cvetkoska A, Levkov Z, Reed J M, Wagner B, 2014. Late Glacial to Holocene climate change and human impact in the Mediterranean: The last ca. 17 ka diatom record of Lake Prespa (Macedonia/Albania/Greece). Palaeogeography, Palaeoclimatology, Palaeoecology 406, 22–32.

Dalton A S, Finkelstein S A, Barnett P J, Forman S L, 2016. Constraining the late Pleistocene history of the Laurentide Ice Sheet by dating the Missinaibi Formation, Hudson Bay Lowlands, Canada. Quat. Sci. Rev. 146, 288–299.

Dalton A S, Pico T, Gowan E J, Clague J J, Forman S L, McMartin I, Sarala P, Helmens K F, 2022. The marine $\delta^{18}O$ record overestimates continental ice volume during Marine Isotope Stage 3. Global and Planetary Change 212, 103814.

Dansgaard W, Johnsen S J, Clausen H B, Dahl-Jensen D, Gundestrup N S, Hammer C U, Hvidberg C S, Steffensen J P, Sveinbjörnsdottir A E, Jouzel J, Bond G, 1993. Evidence for general instability of past climate from a 250-kyr ice-core record. Nature 364, 218–220.

Davis B A S, Zanon M, Collins P, Mauri A, Bakker J, Barboni D, Barthelmes A, Beaudouin C, Birks H J B, Bjune A E, Bozilova E, Bradshaw R H W, Brayshay B A, Brewer S, Brugiapaglia E, Bunting J, Connor S E, de Beaulieu J L, Edwards K J, Ejarque A, Fall P, Florenzano A, Fyfe R, Galop D, Giardini M, Giesecke T, Grant M J, Guiot J, Jahns S, Jankovska V, Juggins S, Kahrmann M, Karpińska-Kołaczek M, Kołaczek P, Kühl N, Kuneš P, Lapteva E G, Leroy S A G, Leydet J, Lopéz Sáez J A, Masi A, Matthias I, Mazier F, Meltsov V, Mercuri A M, Miras Y, Mitchell F J G, Morris J L, Naughton F, Nielsen A B, Novenko E, Odgaard B, Ortu E, Overballe-Petersen M V, Pardoe H S, Peglar S M, Pidek I A, Sadori L, Seppä H, Severova E, Shaw H, Święta-Musznicka J, Theuerkauf M, Tonkov S, Veski S, van der Knaap P W O, van Leeuwen J F N, Woodbridge J, Zimny M, Kaplan J O, 2013. The European Modern Pollen Database (EMPD) project. Vegetation History and Archaeobotany 22, 521–530.

De'ath G, 2007. Boosted trees for ecological modeling and prediction. Ecology 88, 243–251.

de Beaulieu J-L, Reille M, 1992. The last climatic cycle at La Grande Pile (Vosges, France) a new pollen profile. Quaternary Science Reviews 11, 431–438.

Donner J, 1995. The Quaternary history of Scandinavia. World and Regional Geology 7. Cambridge: Cambridge University Press.

Donner J, 1996. The Early and Middle Weichselian interstadials in the central area of the Scandinavian glaciations. Quaternary Science Reviews 15, 471–479.

Dorale J A, Onac B P, Fornós J J, Ginés J, Tuccimei P, Peate D W, 2010. Sea-level highstand 81,000 years ago in Mallorca. Science 327, 860–863.

Drebs A, Nordlund A, Karlsson P, Helminen J, Rissanen P, 2002. Climatological statistics of Finland 1971–2000. Helsinki: Finnish Meterological Institute.

Dredge L A, Cowan W R, 1989. Quaternary geology of the southwestern Canadian Shield. In Fulton R G (eds). Quaternary Geology of Canada and Greenland. Boulder: Geological Society of America, 214–235.

Dyke A S, 2004. An outline of North American deglaciation with emphasis on central and northern Canada. Developments in Quaternary Sciences. 2, 373–424.

Ebert K, Hall AM, Kleman J, Andersson J, 2015. Unequal ice-sheet erosional impacts across low-relief shield terrain in northern Fennoscandia. Geomorphology 233, 64–74.

Ehlers J, Gibbard PL (eds), 2004. Quaternary Glaciations – Extent and Chronology. Amsterdam: Elsevier.

Eisner W R, Törnqvist T E, Koster E A, Bennike O, van Leeuwen J F N, 1995. Paleoecological studies of a Holocene lacustrine record from the Kangerlussuaq (Søndre Strømfjord) region of west Greenland. Quaternary Research 43, 55–66.

Engels S, 2008. Exploring early- and mid-Weichselian climate variability in Europe by applying chironomids as a proxy. PhD thesis. Vrije Universiteit, Netherlands.

Engels S, Bohncke S J P, Bos J A A, Brooks S J, Heiri O, Helmens K F, 2007. Chironomid-based palaeotemperature estimates for northeast Finland during Oxygen Isotope Stage 3. Journal of Paleolimnology 40, 49–61.

Engels S, Helmens K F, Väliranta M, Brooks J, Birks H J B, 2010. Early Weichselian (MIS-5d and 5c) temperatures and environmental changes in northern Fennoscandia as recorded by chironomids and macroremains at Sokli, northeast Finland. Boreas 39, 689–704.

Engels S, Self A E, Luoto T P, Brooks S J, Helmens K F, 2014. A comparison of three Eurasian chironomid–climate calibration datasets on a W–E continentality gradient and the implications for quantitative temperature reconstructions. Journal of Paleolimnology 51, 529–547.

Engström D R, Fritz S C, Almendinger J E, Juggins S, 2000. Chemical and biological trends during lake evolution in recently deglaciated terrain. Nature 408, 161–166.

Edlund M B, Stoermer E F. Taylor C M, 1996. Auclacoseira skvortzowii sp. nov. (Bacillariophyta), a poorly understood diatom from Lake Baikal, Russia. Journal of Phycology 32, 165–175.

Felde V A, Flantua S G A, Jenks C R, Benito B M, de Beaulieu J-L, Kuneš P, Magri D, Nalepka D, Risebrobakken B, ter Braak C J F, Allen J R M, Granoszewski W, Helmens K F, Huntley B, Kondratienė O, Kalniņa L, Kupryjanowicz L, Malkiewicz M, Milner A M, Nita M, Noryśkiewicz B, Pidek I A, Reille M, Salonen J S, Šeirienė V, Winter H, Tzedakis P C, Birks H B J, 2020. Compositional turnover and variation in Eemian pollen sequences in Europe. Vegetation History and Archaeobotany, short communication 29, 101–109.

Finné M, Salonen JS, Frank N, Helmens K F, Schröder-Ritzrau A, Deininger M, Holzkämper S, 2019. Last Interglacial Climate in Northern Sweden-Insights from a Speleothem Record. Quaternary 2, 29.

Forsström L, 1990. Occurrence of larch (*Larix*) in Fennoscandia during the Eemian interglacial and the Brørup interstadial according to pollen analytical data. Boreas 19, 241–248.

Forsström L, Sorvari S, Korhola A, Rautio M, 2005. Seasonality of phytoplankton in subarctic Lake Saanajärvi in NW Finnish Lapland. Polar Biology 28, 846–861.

Fritz S C, Anderson N J, 2013. The relative influences of climate and catchment processes on Holocene lake development in glaciated regions. Journal of Paleolimnology 49, 349–362.

Fuchs M, Straub J and Zöller L, 2005. Residual luminescence signals of recent river flood sediments: A comparison between quartz and feldspar of fine- and coarse-grain sediments. Ancient TL 23, 25–30.

Galaasen E V, Ninnemann U S, Irvali N, Kleiven H K F, Rosenthal Y, Kissel C, Hodell D A, 2014. Rapid reductions in North Atlantic deep water during the peak of the last interglacial period. Science 343, 1129–1132.

Gałka M, Tobolski K, Bubak I, 2015. Late Glacial and Early Holocene lake level fluctuations in NE Poland tracked by macro-fossil, pollen and diatom records. Quaternary International 388, 23–38.

Giesecke T, Bennett K D, 2004. The Holocene spread of Picea abies (L.) Karst. in Fennoscandia and adjacent areas. Journal of Biogeography 31, 1523–1548.

Goring S, Salonen J S, Luoto M, Williams J, 2015. Non-analogues in paleoecological reconstruction: model behaviour and implications. In Dy J G, Emile-Geay J, Lakshmanan V, Liu Y (eds). Proceedings of the Fifth International Workshop on Climate Informatics: CI 2015, Boulder, CO, 24–25 September 2015. Boulder: National Center for Atmospheric Research.

Govin A, Capron E, Tzedakis P C, Verheyden S, Ghaleb B, Hillaire-Marcel C, St-Onge G, Stoner J S, Bassinot F, Bazin L, Blunier T, Combourieu-Nebout N, El Ouahabi A, Genty D, Gersonde R, Jimenez-Amat P, Landais A, Martrat B, Masson-Delmotte V, Parrenin F, Seidenkrantz M-S, Veres D, Waelbroeck C, Zahn R, 2015. Sequence of events from the onset to the demise of the Last Interglacial: Evaluating strengths and limitations of chronologies used in climatic archives. Quaternary Science Review 129, 1–36.

Gómez N, Riera JL, Sabater S, 1995. Ecology and morphological variability of Aulacoseira granulata (Bacillariophyceae) in Spanish reservoirs. Journal of Plankton Research 17, 1–16.

Grace J B, Wetzel R G, 1981. Habitat partitioning and competitive displacement in cattails (*Typha*): experimental field studies. The American Naturalist 118, 463–474.

Granoszewski W, 2003. Late Pleistocene vegetation history and climatic changes at Horoszki Duże, Eastern Poland: a paleobotanical study. Acta Palaeobotanica, Supplement 4, 3–95.

Greffard M H, Saulnier-Talbot É, Gregory-Eaves I, 2012. Sub-fossil chironomids are significant indicators of turbidity in shallow lakes of northeastern USA. Journal of Paleolimnology 47, 561–581.

Gunin P D, Vostokova E A, Dorofeyuk N I, Tarasov P E, Black C C, 1999. Geobotany Vol. 26. Vegetation Dynamics of Mongolia. Dordrecht: Springer Netherlands.

Hannon G, Gaillard M-J, 1997. The plant macrofossil record of past lake-level changes. Journal of Paleolimnology 18, 15–28.

Haworth EY, 1976. Two Late-Glacial (Late Devensian) Diatom Assemblage Profiles from Northern Scotland. New Phytologist 77, 227–256.

Heikkilä M, Seppä H, 2003. A 11,000 yr palaeotemperature reconstruction from the southern boreal zone in Finland. Quaternary Science Reviews 22, 541–554.

Heikkilä M, Fontana S L, Seppä H, 2009. Rapid Lateglacial tree population dynamics and ecosystem changes in the eastern Baltic region. Journal of Quaternary Science 24, 802–815.

Heiri O, Brooks S J, Renssen H, Bedford A, Hazekamp M, Ilyashuk B, Jeffers E S, Lang B, Kirilova E, Kuiper S, Millet L, Samartin S, Thoth M, Verbruggen F, Watson J E, van Asch N, Lammertsma E, Amon L, Birks H H, Birks H J B, Mortensen M F, Hoek W Z, Magyari E, Sobrino C M, Seppä H, Tinner W, Tonkov S, Veski S, Lotter A F, 2014. Validation of climate model-inferred regional temperature change for late-glacial Europe. Nature Communications 15, 4914–4919.

Helmens K F, 2009. Climate, vegetation and lake development at Sokli (northern Finland) during early MIS 3 at ca. 50 kyr: revising earlier concepts on climate, glacial and vegetation dynamics in Fennoscandia during the Weichselian. SKB TR-09-16, Svensk Kärnbränslehantering AB.

Helmens K F, 2013. The Last Interglacial-Glacial cycle (MIS 5-2) re-examined based on long proxy records from central and northern Europe. SKB TR-13-02, Svensk Kärnbränslehantering AB.

Helmens K F, 2014. The Last Interglacial-Glacial cycle (MIS 5-2) re-examined based on long proxy records from central and northern Europe. Quaternary Science Reviews 86, 115–143.

Helmens K F, Engels S, 2010. Ice-free conditions in eastern Fennoscandia during early Marine Isotope Stage 3: lacustrine records. Boreas 39, 399–409.

Helmens K F, 2019. The last 130 000 years in Fennoscandia reconstructed based on a long and fossil-rich sediment sequence preserved at Sokli in northern Finland: New evidence for highly dynamic environmental and climate conditions. SKB TR-18-04, Svensk Kärnbränslehantering AB.

Helmens K F, Räsänen M E, Johansson P, Jungner H, Korjonen K, 2000. The Last Interglacial-Glacial cycle in NE Fennoscandia: a nearly continuous record from Sokli (Finnish Lapland). Quaternary Science Reviews 19, 1605–1623.

Helmens K F, Johansson P W, Räsänen M E, Alexanderson H, Eskola K O, 2007a. Ice-free intervals continuing into Marine Isotope Stage 3 at Sokli in the central area of the Fennoscandian glaciations. Bulletin of the Geological Society of Finland 79, 17–39.

Helmens K F, Bos J A A, Engels S, van Meerbeeck C J, Bohncke S J P, Renssen H, Heiri O, Brooks S J, Seppä H, Birks H B J, Wohlfarth B, 2007b. Present-day temperatures in northern Scandinavian during the Last Glaciation. Geology 35, 987–990.

Helmens K F, Risberg J, Jansson K N, Weckström J, Berntsson A, Kaislahti Tillman P, Johansson P W, Wastegård S, 2009. Early MIS 3 glacial lake evolution, ice-marginal retreat pattern and climate at Sokli (northeastern Fennoscandia). Quaternary Science Reviews 28, 1880–1894.

Helmens K F, Väliranta M, Engels S, Shala S, 2012. Large shifts in vegetation and climate during the Early Weichselian (MIS 5d-c) inferred from multi-proxy evidence at Sokli (northern Finland). Quaternary Science Review 41, 22–38.

Helmens K F, Salonen J S, Plikk A, Engels S, Väliranta M, Kylander M, Brendryen J, Renssen H, 2015. Major cooling intersecting peak Eemian Interglacial warmth in Northern Europe. Quaternary Science Reviews, short communication 122, 293–299.

Helmens K F, Katrantsiotis C, Salonen S J, Shala S, Bos J A A, Engels S, Kuosmanen N, Luoto T P, Väliranta M, Luoto M, Ojala A, Risberg J, Weckström J, 2018. Warm summers and rich biotic communities during N-Hemisphere deglaciation. Global and Planetary Change 167, 61–73.

Helmens K F, Katrantsiotis C, Kuosmanen N, Luoto T P, Salonen S J, Väliranta M, 2021. Prolonged interglacial warmth during the Last Glacial in northern Europe. Boreas 50, 331–350.

Henley W E, Patterson M A, Neves R J, Lemly D A, 2000. Effects of sedimentation and turbidity on lotic food webs: a concise review for natural resource managers. Reviews in Fisheries Science 8, 125–193.

Henriksen M, Mangerud J, Matiouchkov A, Murray AS, Paus A, Svendsen J I, 2008. Intriguing climatic shifts in a 90 kyr old lake record from northern Russia. Boreas 37, 20–37.

Hicks S, 1994. Present and past pollen records of Lapland forests. Review of Palaeobotany and Palynology 82, 17–35.

Hijmans R J, 2014. raster: Geographic data analysis and modeling. R package version 2.2–31. Vienna: Institute for Statistics and Mathematics of WU (Wirtschaftsuniversität Wien).

Hijmans R J, Cameron S E, Parra J L, Jones PG, Jarvis A J, 2005. Very high resolution interpolated climate surfaces for global land areas. International Journal of Climatology 25, 1965–1978.

Hill M O, 1973. Diversity and evenness: a unifying notation and its consequences. Ecology 54, 427–432.

Hirvas H, 1991. Pleistocene stratigraphy of Finnish Lapland. Helsinki: Geological Survey of Finland. (Bulletin Vol 354)

Hoek W Z, 1997. Nederlandse Geografische Studies. Vol 231. Atlas to Palaeogeography of Lateglacial vegetations. Utrecht/Amsterdam: Royal Dutch Geographical Society.

Hofmann W, 1998. Cladocerans and chironomids as indicators of lake level changes in north temperate lakes. Journal of Paleolimnology 19, 55–62.

Hogg A G, Fifield L K, Turney C S M, Palmer J G, Galbraith R, Baille M G K, 2006. Dating ancient wood by high-sensitivity liquid scintillation counting and accelerator mass spectrometry – pushing the boundaries. Quaternary Geochronology 1, 241–248.

Howett P J, Salonen V-P, Hyttinen O, Korkka-Niemi K, Moreau J, 2015. A hydrostratigraphical approach to support environmentally safe siting of a mining waste facility at Rautuvaara, Finland. Bulletin of the Geological Society of Finland 87, 51–66.

Hättestrand M, 2008. Vegetation and climate during Weichselian ice free intervals in northern Sweden: Interpretations from fossil and modern pollen records. PhD thesis. Stockholm University, Sweden.

Hättestrand M, Robertsson A-M, 2010. Weichselian interstadials at Riipiharju, northern Sweden; interpretation of vegetation and climate from fossil and modern pollen records. Boreas 39, 296–311.

Ilvonen E, 1973a. Eem-interglasiaalinen kerrostuma Savukosken Soklilla, Pohjois-Suomessa, orgaanisten kerrostumien ja glasiaaligeologisen tutkimuksen valossa. Licentiate's thesis, University of Turku, 144 pp.

Ilvonen E, 1973b. Eem-Kerrostuma Savukosken Soklilla. Geologi 25, 81–84.

Interlandi S, Kilham S, Theriot E, 1999. Responses of phytoplankton to varied resource availability in large lakes of the Greater Yellowstone Ecosystem. Limnology and Oceanography 44, 668–682.

Irvali N, Ninnemann U S, Galaasen E V, Rosenthal Y, Kroon D, Oppo D W, Kleiven H F, Darling K F, Kissel C, 2012. Rapid switches in subpolar North Atlantic hydrography and climate during the Last Interglacial (MIS 5e). Paleoceanography 27. https://doi.org/10.1029/2011PA002244

Isarin R F B, Bohncke S J P, 1999. Mean July temperatures during the Younger Dryas in northwestern and central Europe as inferred from climate indicator plant species. Quaternary Research 51, 158–173.

Iversen J, 1954. The late-glacial flora of Denmark and its relation to climate and soil. Danmarks Geologiske Undersøgelse II 80, 87–119.

Jankovská V, Komárek J, 2000. Indicative value of Pediastrum and other coccal green algae in paleoecology. Folia Geobotanica 35, 59–82.

Jansen A J M, Schaminée J H J, Schipper P C, Schouten M G C, 2000. Plantengemeenschappen van waterrijke gebieden. In Weeda E J, Schaminée J H J, van Duuren L (eds). Atlas van Plantengemeenschappen in Nederland. Deel 1 Wateren, moerassen en natte heiden. Utrecht: KNNV Uitgeverij. (In Dutch.)

Jansson K N, 2003. Early Holocene glacial lakes and ice marginal retreat pattern in Labrador/Ungava, Canada. Palaeogeography, Palaeoclimatology, Palaeoecology 193, 437–501.

Johansson P W, 1995. The deglaciation in the eastern part of the Weichselian ice divide in Finnish Lapland. Helsinki: Geological Survey of Finland. (Bulletin Vol 383)

Johansson P W, 2007a. Weichselian and Saalian esker systems in north Finland. INQUA 2007 Abstracts. Quaternary International 167–168 (Supplement), 195.

Johansson P W, 2007b. Late Weichselian deglaciation in Finnish Lapland. In Johansson P, Sarala P (eds). Applied Quaternary Research in the Central Part of Glaciated Terrain, 47–54. Espoo: Geological Survey of Finland. (Geological Survey of Finland, Special Paper 46)

Johansson P W, Räsänen M, 1994. Nya preliminära undersökningar av moräntäckta organiska avlagringar i Sokli, Norra Finland. Nordiska geologiska vintermötet Abstracts 21:a, 92. Sweden. (In Swedish)

Johansson P, Lunkka P J, Sarala P, 2011. The glaciation of Finland. In Ehlers J, Gibbard P L, Hughes P D (eds): Quaternary Glaciations – Extent and Chronology: a closer look. Developments in Quaternary Science 15, 105–116.

Johnsen S J, Clausen H B, Dansgaard W, Fuhrer K, Gundestrup N, Hammer C U, Iversen P, Jouzel J, Stauffer B, Steffensen J P, 1992. Irregular glacial interstadials recorded in a new Greenland ice core. Nature 359, 311–313.

Jones V, Birks H, 2004. Lake-sediment records of recent environmental change on Svalbard: results of diatom analysis. Journal of Paleolimnology 31, 445–466.

Jones V J, Solovieva N, Self A E, McGowan S, Rosén P, Salonen J S, Seppä H, Väliranta M, Parrott E, Brooks S J, 2011. The influence of Holocene tree-line advance and retreat on an arctic lake ecosystem; a multi-proxy study from Kharinei Lake, North Eastern European Russia. Journal of Paleolimnology 46, 123–137.

Juggins S, 2013. Quantitative reconstructions in paleolimnology: new paradigm or sick science? Quaternary Science Reviews 64, 20–32.

Juggins S, Birks H J B, 2012. Quantitative environmental reconstructions from biological data. In Birks H J B, Lotter A F, Juggins S, Smol J P (eds), Tracking Environmental Change Using Lake Sediments: Data Handling and Numerical Techniques. Dordrecht: Springer.

Juggins S, Simpson G L, Telford R J, 2015. Taxon selection using statistical learning techniques to improve transfer function prediction. The Holocene 25, 130–136.

Katrantsiotis C, Norström E, Smittenberg R H, Salonen J S, Plikk A, Helmens K, 2021. Seasonal variability in temperature trends and atmospheric circulation systems during the Eemian (Last Interglacial) based on *n*-alkanes hydrogen isotopes from Northern Finland. Quaternary Science Reviews 273, 107250.

Kienast F, Tarasov P, Schirrmeister L, Grosse G, Andreev A A, 2008. Continental climate in the East Siberian Arctic during the last interglacial: Implications from paleobotanical records. Global and Planetary Change 60, 535–562.

Kilham SS, Theriot EC, Fritz SC, 1996. Linking planktonic diatoms and climate change in the large lakes of the Yellowstone ecosystem using resource theory. Limnology and Oceanography 41, 1052–1062.

Kleman J, Hättestrand C, Borgström I, Stroeven A P, 1997. Fennoscandian paleoglaciology reconstructed using a glacial geological inversion model. Journal of Glaciology 43, 283–299.

Kleman J, Hättestrand C, Clarhäll A, 1999. Zooming in on frozen-bed patches: scale-dependent controls on Fennoscandian ice sheet basel thermal zonation. Annals of Glaciology 28, 189–194.

Kleman J, Hättestrand M, Borgström I, Preusser F, Fabel D, 2020. The Idre marginal moraine – an anchorpoint for Middle and late Weichselian ice sheet chronology Quaternary Science Advances 2, 100010.

Klink A, 1989. The lower Rhine: paleoecological analysis. In Petts G E (eds). Historical change of large alluvial rivers: western Europe. Chichester: John Wiley and Sons.

Koff T, Vandel E, 2008. Spatial distribution of macrofossil assemblages in surface sediment of two small lakes in Estonia. Estonian Journal of Ecology 57, 5–20.

Kolstrup E, 1979. Herbs as July temperature indicators for parts of the pleniglacial and late-glacial in the Netherlands. Geologie en Mijnbouw 58, 377–380.

Kolstrup E, 1980. Mededelingen van de Rijks Geologische Dienst. Vol. 32. Climate and stratigraphy in Northwestern Europe between 30,000 BP and 13,000 BP, with special reference to the Netherlands, 181–253.

Komárek J, Jankovská V, 2001. Review of the green algal genus *Pediastrum*: Implication for pollen-analytical research. Berlin: J Cramer. (Bibliotheka Phycologica Band 108)

Krammer K, Lange-Bertalot H, 1986. Bacillariophyceae 1. Teil Naviculaceae. In Ettl H, Gerloff J, Heynig H, Mollenhauser D (eds). Süsswasserflora von Mitteleuropa 2/1. Stuttgart: Gustav Fischer Verlag. (In German.)

Kuhry P, 1997. The palaeoecology of a treed bog in western boreal Canada: a study based on microfossils, macrofossils and physico-chemical properties. Review of Palaeobotany and Palynology 96, 183–224.

Kullman L, 1995. Holocene tree-limit and climate history from the Scandes mountains, Sweden. Ecology 76, 2490–2502.

Kullman L, 1998. Palaeoecological, biogeographical and palaeoclimatological implications of early Holocene immigration of *Larix sibirica* Ledeb. into the Scandes Mountains, Sweden. Global Ecology and Biogeography Letters, 181–188.

Kühl N, Litt T, Schölzel C, Hense A, 2007. Eemian and Early Weichselian temperature and precipitation variability in northern Germany. Quaternary Science Reviews 26, 3311–3317.

Kylander M E, Ampel L, Wohlfarth B, Veres D, 2011. High-resolution X-ray fluorescence core scanning analysis of Les Echets (France) sedimentary sequence: new insights from chemical proxies. Journal of Quaternary Science 26, 109–117.

Kylander M, Plikk A, Rydberg J, Löwemark L, Salonen S J, Fernández-Fernández M, Helmens K F, 2018. Sediment Geochemistry of the Eemian Sequence at Sokli, NE Finland: New insights from XRF core scanning data into boreal lake ontogeny during the Eemian (Marine Isotope Stage 5e) at Sokli, northeast Finland. Quaternary Research 89, 352–364.

Lampinen R, Lahti T, 2012. Kasviatlas 2013 Helsingin Yliopisto. Helsinki: Luonnontieteellinen keskusmuseo.

Lampinen R, Lahti T, 2016. Kasviatlas 2015 – Helsingin Yliopisto, Luonnontieteellinen keskusmuseo, Helsinki. Available at: http://www.luomus.fi/kasviatlas [5 February 2017]. (In Finnish.)

Larocque I, Hall R I, Grahn E, 2001. Chironomids as indicators of climate change: a 100-lake training set from a subarctic region of northern Sweden (Lapland). Journal of Paleolimnology 26, 307–322.

Latałowa M, van der Knaap W O, 2006. Late Quaternary expansion of Norway spruce *Picea abies* (L.) Karst. in Europe according to pollen data. Quaternary Science Reviews 25, 2780–2805.

Lauber K, Wagner G, 1998. Flora Helvetica. 2. edit, Haupt, Bern

Lian OB, Roberts R G, 2006. Dating the Quaternary: progress in luminescence dating of sediments. Quaternary Science Reviews 25, 2449–2468.

Lisiecki L E, Raymo M E, 2005. A Pliocene-Pleistocene stack of 57 globally distributed benthic $\delta^{18}O$ records. Paleoceanography 20, 1–17.

Lotter A F, Bigler C, 2000. Do diatoms in the Swiss Alps reflect the length of ice-cover? Aquatic Sciences 62, 125–141.

Lotter A F, Pienitz R, Schmidt R, 1999. Diatoms as indicators of environmental change near arctic and alpine treeline. In Stoermer E F, Smol J P (eds). The diatoms: application to the environmental and earth sciences. Cambridge: Cambridge University Press, 205–226.

Lundqvist J, 1992. Glacial stratigraphy in Sweden. In Kauranne K (ed). Glacial stratigraphy, engineering geology and earth construction. (Geological Survey of Finland, Special Paper 15), 43–59.

Lunkka J P, Sarala P, Gibbard P L, 2014. The Rautuvaara section, western Finnish Lapland, revisited – new age constraints indicate a complex Scandinavian Ice Sheet history in northern Fennoscandia during the Weichselian Stage. Boreas 44, 68–80.

Luoto T P, 2009. Subfossil Chironomidae (Insecta: Diptera) along a latitudinal gradient in Finland: development of a new temperature inference model. Journal of Quaternary Science 24, 150–158.

Luoto T P, 2010. Hydrological change in lakes inferred from midge assemblages through use of an intralake calibration set. Ecological Monographs 80, 303–329.

Luoto T P, 2011. The relationship between water quality and chironomid distribution in Finland – A new assemblage-based tool for assessments of long-term nutrient dynamics. Ecological Indicators 11, 255–262.

Luoto T P, Sarmaja-Korjonen K, 2011. Midge-inferred Holocene effective moisture fluctuations in a subarctic lake, northern Lapland. Boreas 40, 650–659.

Luoto T P, Ojala A E K, 2016. Meteorological validation of chironomids as a paleotemperature proxy using varved lake sediments. The Holocene 27, 870–878.

Luoto T P, Kultti S, Nevalainen L, Sarmaja-Korjonen K, 2010. Temperature and effective moisture variability in southern Finland during the Holocene quantified with midge-based calibration models. Journal of Quaternary Science 25, 1317–1326.

Luoto T P, Kaukolehto M, Weckström J, Korhola A, Väliranta M, 2014a. New evidence of warm early-Holocene summers in subarctic Finland based on an enhanced regional chironomid-based temperature calibration model. Quaternary Research 81, 50–62.

Luoto T P, Kaukolehto M, Nevalainen L, 2014b. The relationship between water and air temperature in chironomid-based paleoclimate reconstructions: records from boreal and subarctic Finland. The Holocene 24, 1584–1590.

MacDonald G M, Velichko A A, Kremenetski C V, Borisova O K, Goleva A A, Andreev A A, Cwynar L C, Riding R T, Forman S L, Edwards T W D, Aravena R, Hammarlund D, Szeicz J M, Gattaulin V N, 2000. Holocene treeline history and climate change across Northern Eurasia. Quaternary Research 53, 302–311.

Mangerud J, 1991. The Last Interglacial/Glacial cycle in northern Europe. In Shane L C K, Cushing E J (eds). Quaternary Landscapes. Minneapolis: University of Minnesota Press.

Mangerud J, 2004. Ice sheet limits in Norway and on the Norwegian continental shelf. Developments in Quaternary Sciences 2, 271–294.

Mangerud J, 2011. Glacial History of Norway. Developments in Quaternary Sciences 15, 279–298.

Mangerud J, Løvlie R, Gulliksen S, Hufthammer A-K, Larsen E, Valen V, 2003. Paleomagnetic correlations between Scandinavian ice-sheet fluctuations and Greenland Dansgaard-Oeschger events, 45,000–25,000 yrs B.P. Quaternary Research. 59, 213–222.

Mangerud J, Alexanderson H, Birks H H, Paus A, Perić Z M, Svendsen J I, 2023. Did the Eurasian ice sheets melt completely in early Marine Isotope Stage 3? New evidence from Norway and a synthesis for Eurasia. Quaternary Science Reviews 311, 108–136.

McManus J F, Bond G C, Broecker W S, Johnsen S, Labeyrie L, Higgins S, 1994. High-resolution climate records from the North-Atlantic during the Last Interglacial. Nature 371, 326–329.

McMartin I, Campbell J E, Dredge L A, 2019. Middle Wisconsinan marine shells near Repulse Bay, Nunavut, Canada: implications for Marine Isotope Stage 3 ice-free conditions and Laurentide Ice Sheet dynamics in north-West Hudson Bay. Journal of Quaternary Science 34, 64–75.

Michel T J, Saros J E, Interlandi S J, Wolfe A P, 2006. Resource requirements of four freshwater diatom taxa determined by in situ growth bioassays using natural populations from alpine lakes. Hydrobiologia 568, 235–243.

Mikkola E, 1937. Sodankylä. General Geological Map of Finland 1:400,000-Map of Pre-Quaternary Rocks, Sheet C7. Helsinki: Geological Survey of Finland.

Molodkov A N, Bolikhovskaya N S, 2009. Climate change dynamics in Northern Eurasia over the last 200 ka: evidence from mollusc-based ESR-chronostratigraphy and vegetation successions of the loess-palaeosol records. Quaternary International 201, 67–76.

Molodkov A N, Bolikhovskaya N S, 2010. Climato-chronostratigraphic framework of Pleistocene terrestrial and marine deposits of Northern Eurasia based on pollen, electron spin resonance, and infrared optically stimulated luminescence analyses. Estonian Journal of Earth Sciences 59, 49–62.

Miller P A, Giesecke T, Hickler T, Bradshaw R H W, Smith B, Seppä H, Valdes P J, Sykes M T, 2007. Exploring climatic and biotic controls on Holocene vegetation change in Fennoscandia. Journal of Ecology 96, 247–259.

Moller Pillot H K M, 2009. Chironomidae Larvae. Vol. 2. Biology and ecology of the Chironomini. Zeist: KNNV Publishing.

Moss B, 1982. Ecology of Fresh Waters. Hoboken, NJ: Blackwell Scientific Publications, 133–159.

Mossberg B, Stenberg L, 2003. Den nya nordiska floran. Stockholm: Wahlström and Widstrand. (In Swedish.)

Mothes G, 1968. Einige ökologisch interessante Chironomiden aus dem Stechlinseegebiet. Annales Botanici Fennici 5, 92–96. (In German.)

Müller U C, Pross J, Tzedakis P C, Gamble C, Kotthoff, Schmiedl G, Christanis K, 2011. The role of climate in the spread of modern humans into Europe. Quaternary Science Reviews 30, 273–279.

Mäkelä E M, 1996. Size distinctions between Betula pollen types – A review. Grana 35, 248–256.

Mäkinen K, 2005. Dating the Weichselian deposits of southwestern Finnish Lapland. Geological Survey of Finland (Special Paper 40), 67–78.

New M, Lister D, Hulme M, Makin I, 2002. A high-resolution data set of surface climate over global land areas. Climate Research 21, 1–25.

Oksanen P O, Kuhry P, Alekseeva R N, 2001. Holocene development of the Rogovayapeat plateau, east-European Russian Arctic. The Holocene 11, 25–40.

Olander H, Birks H J B, Korhola A, Blom T, 1999. An expanded calibration model for inferring lakewater and air temperatures from fossil chironomid assemblages in northern Fennoscandia. Holocene 9, 279–294.

Olsen L, Grøsfjeld K, Stokland Ø, Lauritzen S-E, Selvik S F, Bergstrøm B, Sveian H, 2001a. Methods and stratigraphies used to reconstruct Mid- and Late Weichselian palaeoenvironmental and paeloclimatic changes in Norway. (Norges Geologisk Undersøgelse Bull. 438), 21–46.

Olsen L, Sveian H, Bergstrøm B, 2001b. Rapid adjustments of the western part of the Scandinavian Ice Sheet during the Mid and Late Weichselian—A new model. Norsk Geologisk Tidsskrift 81, 93–118.

Otvos E G, 2015. The Last Interglacial Stage: definitions and marine highstand, North America and Eurasia. Quaternary International 383, 158–173.

Overpeck J T, Webb T III, Prentice I C, 1985. Quantitative interpretation of fossil pollen spectra: dissimilarity coefficients and the method of modern analogs. Quaternary Research 23, 87–108.

Økland K A, Økland J, 2001. Freshwater bryozoans (Bryozoa) of Norway II: distribution and ecology of two species of Fredericella. Hydrobiologia 459, 103–123.

Økland K A, Økland J, 2005. Freshwater bryozoans (Bryozoa) of Norway V: Review and comparative discussion of the distribution and ecology of the 10 species recorded. Hydrobiologia 534, 31–55.

Pals J P, van Geel B, Delfos A, 1980. Paleoecological studies in the Klokkeweel bog near Hoogkarspel (prov. of Noord Holland). Review of Palaeobotany and Palynology 30, 371–418.

Paus A, 2000. Interpretative problems and sources of error related to pollen-analytical studies of the Holocene on the Timan ridge, western Pechora Basin, northern Russia. AmS-Skrifter 16, 1–16.

Paus A, 2010. Vegetation and environment of the Rødalen alpine area, Central Norway, with emphasis on the early Holocene. Vegetation History and Archaeobotany 19, 29–51.

Paus A, 2013. Human impact, soil erosion, and vegetation response lags to climate change: challenges for the mid-Scandinavian pollen-based transfer-function temperature reconstructions. Vegetation History and Archaeobotany 22, 269–284.

Paus A, Haugland V, 2017. Early- to mid-Holocene forest-line and climate dynamics in southern Scandes mountains inferred from contrasting megafossil and pollen data. The Holocene 27, 361–383.

Pędziszewska A, Tylmann W, Witak M, Piotrowska N, Maciejewska E, Latałowa M, 2015. Holocene environmental changes reflected by pollen, diatoms, and geochemistry of annually laminated sediments of Lake Suminko in the Kashubian Lake District (N Poland). Review of Palaeobotany and Palynology 216, 55–75.

Pennington W, 1980. Modern pollen samples from west Greenland and the interpretation of pollen data from the British Late-Glacial (Late Devensian). New Phytologist 84, 171–201.

Plikk A, 2018. The Eemian Interglacial at Sokli, northern Finland. PhD thesis. Stockholm University, Sweden.

Plikk A, Helmens K F, Fernández-Fernández M, Kylander M, Löwemark L, Risberg J, Salonen J S, Väliranta M, Weckström J, 2016. Development of an Eemian (MIS 5e) Interglacial paleolake at Sokli (N Finland) inferred using multiple proxies. Palaeogeography, Palaeoecology, Palaeoclimatology 463, 11–26.

Plikk A, Engels S, Luoto T P, Nazarova L, Sakari Salonen J, Helmens K F, 2019. Chironomid-based temperature reconstruction for the Eemian Interglacial (MIS 5e) at Sokli, northeast Finland. Journal of Paleolimnology 61, 355–371.

Plikk A, Risberg J, Helmens K F, 2021. Diatom assemblages from an Eemian palaeolake in Northern Europe with morphological observations of rare Aulacoseira sp. resting spores. Diatom Research 36, 313–321.

Prentice I C, 1978. Modern pollen spectra from lake sediments in Finland and Finnmark, north Norway. Boreas 7, 131–153.

Ralska-Jasiewiczowa M, van Geel B, Goslar T, Kuc T, 1992. The record of the Late Glacial/Holocene transition in the varved sediments of lake Gosciaz, central Poland. (Sveriges Geologiska Undersökning Ser. Ca 81), 257–268.

Rantala M V, Luoto T P, Weckström J, Perga M-E, Rautio M, Nevalainen L, 2015. Climate controls on the Holocene development of a subarctic lake in northern Fennoscandia. Quaternary Science Reviews 126, 175–185.

R Core Team, 2022. R: A language and environment for statistical computing. Vienna: R Foundation for Statistical Computing.

Ramsey B C, 2009. Bayesian analysis of radiocarbon dates. Radiocarbon 51, 337–360.

Reimer P J, Baillie M G L, Bard E, Bayliss A, Beck J W, Blackwell P G, Bronk Ramsey C, Buck C E, Burr G S, Edwards R L, Friedrich M, Grootes P M, Guilderson T P, Hajdas I, Heaton T J, Hogg A G, Hughen K A, Kaiser K F, Kromer B, McCormac F G, Manning S W, Reimer R W, Richards D A, Southon J R, Talamo S, Turney C S M, van der Plicht J, Weyhenmeyer C, 2009. IntCal09 and Marine09 radiocarbon age calibration curves, 0–50,000 years cal BP. Radiocarbon 51, 1111–1150.

Renberg I, 1981. Verhandlungen Internationalen Vereinigung für Theoretische und Angewandte Limnologie 21, 94–101.

Rioual P, Andrieu-Ponel V, Rietti-Shati M, Battarbee R W, de Beaulieu J-L, Cheddadi R, Reille M, Svobodova H, Shemesh A, 2001. High-resolution record of climate stability in France during the last interglacial period. Nature 413, 293–296.

Rioual P, Andrieu-Ponel V, de Beaulieu J-L, Reille M, Svobodova H, Battarbee R W, 2007. Diatom responses to limnological and climatic changes at Ribains Maar (French Massif Central) during the Eemian and Early Würm. Quaternary Science Reviews 26, 1557–1609.

Risberg J, Sandgren P, Andrén E, 1996. Early Holocene shore displacement and evidence of irregular isostatic uplift northwest of Lake Vänern, western Sweden. Journal of Paleolimnology 15, 47–63.

Risberg J, Sandgren P, Teller J T, Last W M, 1999. Siliceous microfossils and mineral magnetic characteristics in a sediment core from Lake Manitoba, Canada: a remnant of glacial Lake Agassiz. Canadian Journal of Earth Sciences 36, 1299–1314.

Ritchie J C, Cwynar L C, Spear R W, 1983. Evidence from north-west Canada for an early Holocene Milankovitch thermal maximum. Nature 305, 126–128.

Rosén P, Segerström U, Eriksson L, Renberg I, Birks H J B, 2001. Holocene climatic change reconstructed from diatoms, chironomids, pollen and near-infrared spectroscopy at an alpine lake (Sjuodjljaure) in northern Sweden. The Holocene 11, 551–562.

Rosén P, Vogel H, Cunningham L, Reuss N, Conley J, Persson P, 2010. Fourier transform infrared spectroscopy, a new method for rapid determination of total organic and inorganic carbon and biogenic silica concentration in lake sediments. Journal of Paleolimnology 43, 247–259.

Rørslett B, 1991. Principal determinants of aquatic macrophyte richness in northern European lakes. Aquatic Botany 39, 173–193.

Saarnisto M, Eriksson B, Hirvas H, 1999. Tepsankumpu revisited – pollen evidence of stable Eemian climates in Finnish Lapland. Boreas 28, 12–22.

Sachs J P, Sachse D, Smittenberg R H, Zhang Z, Battisti D S, Golubic S, 2009. Southward movement of the Pacific intertropical convergence zone AD 1400–1850. Nature Geoscience 2, 519–525.

Salgado J, Sayer C D, Brooks S J, Davidson T A, Okamura B, 2018. Eutrophication erodes inter-basin variation in macrophytes and co-occurring invertebrates in a shallow lake: combining ecology and palaeoecology. Journal of Paleolimnology 60, 311–328.

Salonen J S, Seppä H, Väliranta M, Jones V J, Self A, Heikkilä M, Kultti S, Yang H, 2011. The Holocene thermal maximum and late-Holocene cooling in the tundra of NE European Russia. Quaternary Research 75, 501–511.

Salonen J S, Seppä H, Luoto M, Bjune A E, Birks H J B, 2012. A North European pollen–climate calibration set: analyzing the climate response of a biological proxy using novel regression tree methods. Quaternary Science Reviews 45, 95–110.

Salonen J S, Helmens K F, Seppä H, Birks H J B, 2013. Pollen-based paleoclimate reconstructions over long glacial-interglacial timescales: methodological tests based on the Holocene and MIS 5d-c deposits of Sokli, northern Finland. Journal of Quaternary Science 28, 271–282.

Salonen V-P, Moreau J, Hyytinen O, Eskola K O, 2014. Mid-Weichselian interstadial in Kolari, Western Finnish Lapland. Boreas 43, 627–638.

Salonen J S, Helmens K F, Brendryen J, Kuosmanen N, Väliranta M, Goring S, Korpela M, Kylander M, Philip A, Plikk A, Renssen H, Luoto M, 2018. Abrupt high-latitude climate events and decoupled seasonal trends during the Eemian. Nature Communications 9, 2851.

Salonen J S, Korpela M, Williams J W, Luoto M, 2019. Machine-learning based reconstructions of primary and secondary climate variables from North American and European fossil pollen data. Scientific Reports 9, 15805.

Salonen J S, Sánchez-Goñi M F, Renssen H, Plikk A, 2021. Signature of a North Atlantic Oscillation type shift in European winter climate during the Eemian Interglacial. Geology 49: 1220–1224.

Salonen J S, Kuosmanen N, Alsos I G, Heintzman P D, Rijal D P, Schenk F, Bogren F, Luoto M, Philip A, Piilo S, Trasune L, Väliranta M, Helmens K F, 2024. Uncovering Holocene climate fluctuations and ancient conifer populations: Insights from a high-resolution multi-proxy record from Northern Finland. Global and Planetary Change 237, 104462.

Sarala P, Eskola T, 2011. Middle Weichselian interstadial deposit at Petäjäselkä, Northern Finland. E&G Quaternary Science Journal 60, 488–492.

Sarala P, Väliranta M, Eskola T, Vaikutiené G, 2016. First physical evidence for forested environment in the arctic during MIS 3. Scientific Reports 6, 1–9.

Sarmaja-Korjonen K, Seppänen A, Bennike O, 2006. Pediastrum algae from the classic late glacial Bølling Sø site, Denmark: Response of aquatic biota to climate change. Review of Palaeobotany and Palynology 138, 95–107.

Saros J E, Strock K E, Mccue J, Hogan E, Anderson N J, 2014. Response of *Cyclotella* species to nutrients and incubation depth in Arctic lakes. Journal of Plankton Research 36, 450–460.

Self A E, Brooks S J, Birks H J B, Nazarova L, Porinchu D, Odland A, Yang H, Jones V J, 2011. The distribution and abundance of chironomids in high-latitude Eurasian lakes with respect to temperature and continentality: development and application of new chironomid-based climate-inference models in northern Russia. Quaternary Science Reviews 30, 1122–1141.

Seppä H, 1996. Post-glacial dynamics of vegetation and tree-lines in the far north of Fennoscandia. Fennia 174, 1–96.

Seppä H, Birks H J B, 2001. July mean temperature and annual precipitation trends during the Holocene in the Fennoscandian tree-line area: Pollen-based climate reconstructions. The Holocene 11, 527–539.

Seppä H, Hicks S, 2006. Integration of modern and past pollen accumulation rate (PAR) record across the arctic tree-line: a method for more precise vegetation reconstructions. Quaternary Science Reviews 25, 1501–1516.

Seppä H, Birks H J B, Odland A, Poska A, Veski S, 2004. A modern pollen-climate calibration set from northern Europe: developing and testing a tool for paleoclimatological reconstructions. Journal of Biogeography 31, 251–267.

Seppä H, Schurgers G, Miller P A, Bjune A E, Giesecke T, Kühl N, Renssen H, Salonen J S, 2015. Trees tracking a warmer climate: the Holocene range shift of hazel (*Corylus avellana*) in northern Europe. The Holocene 25, 53–63.

Serieyssol C A, Edlund M B, Kallemeyn L W, 2009. Impacts of settlement, damming, and hydro-management in two boreal lakes: a comparative paleolimnological study. Journal of Paleolimnology 42, 497–513.

Shahgedanova M, 2008. The Physical Geography of northern Eurasia. Oxford: Oxford University Press.

Shahgedanova M, Kuznetsov M, 2008. The Arctic Environments. In Shahgedanova M (ed). The Physical Geography of northern Eurasia. Oxford: Oxford University Press, 191–215.

Shala S, 2014. Paleoenvironmental changes in the northern Boreal zone of Finland based on lake sediment analyses: local versus regional drivers. PhD thesis. Stockholm University, Sweden.

Shala S, Helmens K F, Luoto T P, Väliranta M, Weckström J, Salonen J S, Kuhry P, 2014a. Evaluating environmental drivers of Holocene changes in water chemistry and aquatic biota composition at Lake Loitsana, NE Finland. Journal of Paleolimnology 52, 311–329.

Shala S, Helmens K F, Jansson K, Kylander M E, Risberg J, Löwemark l, 2014b. Paleo-environmental record of glacial lake evolution during the early Holocene at Sokli, NE Finland. Boreas 43, 362–376.

Shala S, Helmens K F, Luoto T P, Salonen J S, Väliranta M, Weckström J, 2017. Comparison of quantitative Holocene temperature reconstructions using multiple proxies from a northern boreal lake. The Holocene 27, 1745–1755.

Sánchez Goñi M F, Desprat S, Daniau A-L, Bassinot F C, Polanco-Martínez J M, Harrison S P, Allen J R M, Anderson R S, Behling H, Bonnefille R, Burjachs F, Carrión J S, Cheddadi R, Clark J S, Combourieu-Nebout N, Mustaphi C J C, Debusk G H, Dupont L M, Finch J M, Fletcher W J, Giardini M, González C, Gosling W D, Grigg L D, Grimm E C, Hayashi R, Helmens K F, Heusser L E, Hill T, Hope G, Huntley B, Igarashi Y, Irino T, Jacobs B, Jiménez-Moreno G, Kawai S, Kershaw A P, Kumon F, Lawson I T, Ledru M P, Lézine A M, Liew P M, Magri D, Marchant R, Margari V, Mayle F E, McKenzie G M, Moss P, Müller S, Müller U C, Naughton R M, Oba T, Pérez-Obiol R, Pini R, Vandergoes M J, Vincens A, Whitlock C L, Willard D A, Yamamoto M, 2017. The ACER pollen and charcoal database: a global resource to document vegetation and fire response to abrupt climate changes during the last glacial period. Earth System Science Data 9, 679–695.

SKB, 2020. Post-closure safety for the final repository for spent nuclear fuel at Forsmark. Climate and climate-related issues, PSAR version. SKB TR-20-12, Svensk Kärnbränslehantering AB.

Stančikaitė M, Šeirienė V, Dalia Kisielienė D, Martma T, Gryguc G, Zinkutė R, Mažeika J, Šinkūnas P, 2015. Lateglacial and early Holocene environmental dynamics in northern Lithuania: A multi-proxy record from Ginkūnai Lake. Quaternary International 357, 44–57.

Stoermer E, 1993. Evaluating diatom succession: some pecularities of the Great Lakes case. Journal of Paleolimnology 8, 71–83.

Stroeven A P, Hättestrand C, Kleman J, Heyman J, Fabel D, Fredin O, Goodfellow B W, Harbor J M, Jansen J D, Olsen L, Caffee M W, Fink D, Lunqvist J, Rosqvist G C, Strömberg B, Jansson K N, 2016. Deglaciation of Fennoscandia. Quaternary Science Reviews 147, 91–121.

Sutinen R, 1992. Glacial deposits, their electrical properties and surveying by image interpretation and ground penetrating radar. Helsinki: Geologian tutkimuskeskus. (Geological Survey of Finland, Bulletin 359)

Svendsen J I, Alexanderson H, Astakhov V I, Demidov I, Dowdeswell J A, Funder S, Gataullin V, Henriksen M, Hjort C, Houmark-Nielsen M, Hubberten H W, Ingólfsson Ó, Jakobsson M, Kjær K H, Larsen E, Lokrantz H, Lunkka J P, Lysså A, Mangerud J, Matiouchkov A, Stein R, 2004. Late quaternary ice sheet history of northern Eurasia. Quaternary Science Reviews 23, 1229–1271.

Sweeney C, 2004. A key for the identification of stomata of the native conifers of Scandinavia. Review of Palaeobotany and Palynology 128, 281–290.

Šeirienė V, Kühl, N, Kisielienė D, 2014. Quantitative reconstruction of climate variability during the Eemian (Merkinė) and Weichselian (Nemunas) in Lithuania. Quaternary Research 82, 229–235.

Talvitie J, Lehmuspelto, P, Vuotovesi, T, 1981. Airborne thermal surveying of the ground in Sokli, Finland. Geological Survey of Finland. (Report of investigation 50), 1–13.

Tarasov P E, Webb III T, Andreev A A, Afanas'Eva N B, Berezina N A, Bezusko L G, Blyakharchuk T A, Bolikhovskaya N S, Cheddadi R, Chernavskaya M M, Chernova G M, Dorofeyuk N I, Dirksen V G, Elina G A, Filimonova L V, Glebov F Z, Guiot J, Gunova V S, Harrison S P, Jolly D, Khomutova V I, Kvavadze E V, Osipova I M, Panova N K, Prentice I C, Saarse L, Sevastyanov D V, Volkova V S, Valentina, Zernitskaya P, 1998. Present-day and mid-Holocene biomes reconstructed from pollen and plant macrofossil data from the former Soviet Union and Mongolia. Journal of Biogeography 25, 1029–1053.

Tarkowska-Kukuryk M, 2014. Effects of lake transparency on diversity of microhabitats for chironomid communities. Polish Journal of Ecology 62, 575–588.

Telford R J, Birks H J B, 2011. A novel method for assessing the statistical significance of quantitative reconstructions inferred from biotic assemblages. Quaternary Science Reviews 30, 1272–1278.

Terasmaë J, 1951. On the pollen morphology of Betula nana. Svensk Botanisk Tidskrift 45, 358–361.

ter Braak C J F, Juggins S, 1993. Weighted averaging partial least squares regression (WA-PLS): an improved method for reconstructing environmental variables from species assemblages. Hydrobiologia 269, 485–502.

Thienemann A, 1954. Chironomus. Leben, Verbreitung und wirtschaftliche Bedeutung der Chironomiden. In Die Binnengewässer 20. Stuttgart: Schweizerbart Science Publishers. (In German.)

Tinsley H, Smith RT, 1974. Surface pollen studies across a woodland/heath transition and their application to the interpretation of pollen diagrams. New Phytologist 73, 547–565.

Tishkov A, 2008. Boreal forests. In Shahgedanova M (ed). The Physical Geography of northern Eurasia. Oxford: Oxford University Press, 216–233.

Tumel N, 2008. Permafrost. In Shahgedanova M (ed). The Physical Geography of northern Eurasia. Oxford: Oxford University Press,149–168.

Turner C, 2002. Problems of the duration of the Eemian Interglacial in Europe north of the Alps. Quaternary Research 58, 45–48.

Turon J–L, 1984. Direct land/sea correlations in the last interglacial complex. Nature 309, 673–676.

Tzedakis P C, Drysdale R N, Margari V, Skinner L C, Menviel L, Rhodes R H, Taschetto A S, Hodell D A, Crowhurst S J, Hellstrom J C, Fallick A E, Grimalt J O, McManus J F, Martrat B, Mokeddem Z, Parrenin F, Regattieri E, Roe K, Zanchetta G, 2018. Enhanced climate instability in the North Atlantic and southern Europe during the Last Interglacial. Nature communications 9, 4235.

Ukkonen P, Lunkka J P, Jungner H, Donner J, 1999. New radiocarbon dates from Finnish mammoths indicating large ice-free areas in Fennoscandia during the Middle Weichselain. Journal of Quaternary Science 14, 711–714.

Ulvinen T, Syrjänen K, Anttila S (eds), 2002. Suomen sammalet – levinneisyys, ekologia, uhanalaisuus. Suomen ympäristö 560, Publication of Finnish Environment Institute. (In Finnish.)

Vallenduuk H J, Moller Pillot H K M, 2007. Chironomidae Larvae. Vol 1. General ecology and Tanypodinae. Zeist: KNNV Publishing.

van Dam H, Mertens A, Sinkeldam J, 1994. A coded checklist and ecological indicator values of freshwater diatoms from The Netherlands. Netherlands Journal of Aquatic Ecology 28, 117–133.

van Donk E, van de Bund W J, 2002. Impact of submerged macrophytes including charophytes on phyto and zooplankton communities: Allelopathy versus other mechanisms. Aquatic Botany 72, 261–274.

van Geel B, 1978. A palaeoecological study of Holocene peat bog sections in Germany and The Netherlands, based on the analysis of pollen, spores and macro- and microscopic remains of fungi, algae, cormophytes and animals. Review of Palaeobotany and Palynology 25, 1–120.

van Geel B, 2001. Non-pollen palynomorphs. In Smol J P, Birks, H J B, Last W M (eds). Tracking environmental change using lake sediments. Vol 3. Terrestrial, Algal, and Siliceous indicators. Dordrecht: Kluwer Academic Publishers.

van Geel B, Grenfell H R, 1996. Spores of Zygnemataceae. In Jansonius J, McGregor D C (eds). Palynology: Principles and Applications. Dallas: American Association of Stratigraphic Palynologists Foundation, 173–176.

van Geel B, Hallewas D P, Pals J P, 1983. A Late Holocene deposit under the Westfriese dijk near Enkhuizen (Prov.of Noord-Holland, The Netherlands): paleoecological and archaeological aspects. Review of Palaeobotany and Palynology 38, 269–335.

van Geel B, Coope G R, van der Hammen T, 1989. Paleoecology and stratigraphy of the Lateglacial type section at Usselo (The Netherlands). Amsterdam: Review of Palaeobotany and Palynology 60, 25–129.

van der Hammen T, Wijmstra T A (eds), 1971. The Upper Quaternary of the Dinkel valley (Twente, Eastern Overijssel, The Netherlands). In Mededelingen van de Rijks Geologische Dienst Nieuwe serie. Vol. 22. Harlem: Rijks geologische dienst, 55–214.

van der Wiel A M, 1983. A palaeoecological study of a section from the foot of the Hazendonk (Zuid-Holland, The Netherlands), based on the analysis of pollen, spores and macroscopic plant remains. Review of Palaeobotany and Palynology 38, 35–90.

van Meerbeeck C J, Renssen H, Roche D M, Wohlfarth B, Bohncke S J P, Bos J A A, Engels S, Helmens K F, Sánchez-Goñi M F, Svensson A, Vandenberghe J, 2011. The nature of MIS 3 stadial-interstadial transitions in Europe: new insights from model-data comparisons. Quaternary Science Reviews, 30, 3618–3637.

Vartiainen H, 1980. The petrography, mineralogy and petrochemistry of the Sokli carbonatite massif, northern Finland. Espoo: Geologinen tutkimuslaitos. (Geological Survey of Finland Bulletin 313)

Vartiainen H, 1998. Suomen alkalikivet – apatiitista timanttiin. In Lehtinen M, Nurmi P, Rämo J, T. (eds). 3000 vuosimiljoonnaa, Suomen kallioperä. Helsinki: The Geological Society of Finland, 285–307. (In Finnish.)

Velle G, Larsen J, Eide W, Peglar S M, Birks H J B, 2005. Holocene environmental history and climate of Råtåsjøen, a low-alpine lake in south-central Norway. Journal of Paleolimnology 33, 129–153.

Velle G, Bjune A E, Larsen J, Birks H J B, 2010. Holocene climate and environmental history of Brurskardstjørni, a lake in the catchment of Øvre Heimdalsvatn, south-central Norway. Hydrobiologia 642, 13–34.

Venäläinen A, Tuomenvirta H, Pirinen P, Drebs A, 2005. A basic climate data set 1961–2000 – description and illustrations. Helsinki: Finnish Meteorological Institute. (Finnish Meteorological Institute Reports 5)

Vogel H, Rosén P, Wagner B, Melles M, Persson P, 2008. Fourier transform infrared spectroscopy, a new cost-effective tool for quantitative analysis of biogeochemical properties in long sediment records. Journal of Paleolimnology 40, 689–702.

von Post L, 1930. Norrländska torvmossestudier. II: Några huvudpunkter i skogens och myrarnas postartiska historia inom södra Norrland. Stockholm: Geologiska föreningen. (Geologiska föreningen i Stockholms Förhandlingar 52), 63–90. (In Swedish.)

Väliranta M, 2006a. Terrestrial plant macrofossil records; possible indicators of past lake-level fluctuations in northeastern European Russia and Finnish Lapland? Acta Palaeobotania 46, 235–243.

Väliranta, M. 2006b. Long-term changes in aquatic plant species composition in North-eastern European Russia and Finnish Lapland, as evidenced by plant macrofossil analysis. Aquatic Botany 85, 224–232.

Väliranta M, Birks H H, Helmens K F, Engels S, Piirainen M, 2009. Early Weichselian interstadial (MIS 5c) summer temperatures were higher than today in northern Fennoscandia. Quaternary Science Reviews 28, 777–782.

Väliranta M, Kaakinen A, Kuhry P, Kultti S, Salonen J S, Seppä H, 2011. Scattered late-glacial and early Holocene tree populations as dispersal nuclei for forest development in north-east European Russia. Journal of Biogeography 38, 922–932.

Väliranta M, Sarala P, Eskola T, 2012. Uusia todisteita boreaalisista olosuhteista Veiksel-interstadiaalin aikana (With English summary). Geologi 64, 9–14. (In Finnish.)

Väliranta M, Salonen J S, Heikkilä M, Amon L, Helmens K, Klimaschewski A, Kuhry P, Kultti S, Poska A, Shala S, Veski S, Birks H H, 2015. Plant macrofossil evidence for an early onset of the Holocene summer thermal maximum in Northern Europe. Nature communications 6, 6809.

Walker I R and Cwynar L C, 2006. Midges and palaeotemperature reconstruction – The North American experience. Quaternary Science Reviews 25, 1911–1925.

Walker I R, Mott R J, Smol J P, 1991a. Allerød—Younger Dryas lake temperatures from midge fossils in Atlantic Canada. Science 253, 1010–1012.

Walker I R, Smol J P, Engström D R, Birks H J B, 1991b. An assessment of Chironomidae as quantitative indicators of past climatic change. Canadian Journal of Fisheries and Aquatic Sciences 48, 975–987.

Weckström K, Weckström J, Yliniemi L-M, Korhola A, 2010. The ecology of *Pediastrum* (Chlorophyceae) in subarctic lakes and their potential as paleobioindicators. Journal of Paleolimnology 43, 61–73.

Weckström J, Hanhijärvi S, Forsström L, Kuusisto E, Korhola A, 2014. Reconstructing lake ice cover in subarctic lakes using a diatom-based inference model. Geophysical Research Letters 41, 2026–2032.

Westhoff V, den Held A J, 1975. Plantengemeenschappen in Nederland. 2nd ed. Zutphen: Thieme. (In Dutch.)

Westhoff V, Bakker P A, van Leeuwen C G, van der Voo E E, 1981. Wilde planten: Het lage land. Vol. 2. Deventer: Lange/van Leer. (In Dutch.)

Wetzel R G, 2001. Limnology. Lake and River Ecosystems. 3rd ed. Amsterdam: Elsevier.

Whitlock C, Dean W, Fritz S, Stevens L, Stone J, Power M, Rosenbaum J, Pierce K, Bracht-Flyr B, 2012. Holocene seasonal variability inferred from multiple proxy records from Crevice Lake, Yellowstone National Park, USA. Palaeogeography Palaeoclimatology Palaeoecology 331, 90–103.

Willis K J, van Andel T H, 2004. Trees or no trees? The environments of central and eastern Europe during the Last Glaciation. Quaternary Science Reviews 23, 2369–2387.

Wohlfarth B, 2009. Ice-free conditions in Fennoscandia during Marine Oxygen Isotope Stage 3? SKB TR-09-12, Svensk Kärnbränslehantering AB.

Wohlfarth B, 2010. Ice-free conditions in Sweden during Marine Oxygen Isotope Stage 3? Boreas 39, 377–398.

Wohlfarth B, 2013. A review of Early Weichselian climate (MIS 5d-a) in Europe. SKB TR-13-03, Svensk Kärnbränslehantering AB.

Wohlfarth B, Schwark L, Bennike O, Filimonova L, Tarasov P, Björkmanj L, Brunnberg L, Demidov I, Possnert G, 2004. Unstable early Holocene climatic and environmental conditions in northwestern Russia derived from a multidisciplinary study of a lake sediment sequence from Pichozero, southeastern Russian Karelia. The Holocene 14, 732–746.

Woillard G M, 1978. Grande Pile peat bog: a continuous pollen record for the last 140,000 years. Quaternary Research 9, 1–21.

Woillard G M, Mook W G, 1982. Carbon-14 Dates at Grande Pile: Correlation of land and sea chronologies. Science 215, 159–161.

Wolin J, 1996. Late Holocene lake-level and lake development signals in Lower Herring Lake, Michigan. Journal of Paleolimnology 15, 19–45.

Wood T S, Okamura B, 2005. A new key to the freshwater bryozoans of Britain, Ireland and Continental Europe: with notes on their ecology. Lakeside: Freshwater biological association. (Freshwater biological association scientific publications 63)

Yurtsev B A, 1981. Reliktovye stepnye kompleksy severo-vostochnoi Azii (The Relict Steppes of North-Eastern Asia). Novosibirsk: The USSR Academy of Science Press. (In Russian.)

Zagwijn W H, 1996. An analysis of Eemian climate in Western and Central Europe. Quaternary Science Reviews 15, 451–469.

Zawiska I, Słowiński M, Correa-Metrio A, Obremska M, Luoto T, Nevalainen L, Woszczyk M, Milecka K, 2015. The response of a shallow lake and its catchment to Late Glacial climate changes – A case study from eastern Poland. CATENA 126, 1–10.

Zeng Y, Chen J, Xiao J, Qi L, 2013. Non-residual Sr of the sediments in Daihai Lake as a good indicator of chemical weathering. Quaternary Research 79, 284–291.

Zlotin R, 2008. Biodiversity and Productivity of Ecosystems. In Shahgedanova M (ed). The Physical Geography of northern Eurasia. Oxford: Oxford University Press, 169–190.

Arkitektkopia AB, Bromma, 2024

SKB is responsible for managing spent nuclear fuel and radioactive waste produced by the Swedish nuclear power plants such that man and the environment are protected in the near and distant future.

skb.se